

PDF hosted at the Radboud Repository of the Radboud University Nijmegen

The following full text is a publisher's version.

For additional information about this publication click this link.

<http://hdl.handle.net/2066/18665>

Please be advised that this information was generated on 2017-12-05 and may be subject to change.

Structure and functions of heparan sulfate proteoglycans in the human glomerular basement membrane

Een wetenschappelijke proeve op het gebied
van de Medische Wetenschappen

PROEFSCHRIFT

Ter verkrijging van de graad van doctor
aan de [Katholieke Universiteit Nijmegen](#)
volgens het besluit van het College van Decanen
in het openbaar te verdedigen
op dinsdag 9 februari 1999
des namiddags om 3:30 precies

door

Alexander Jacobus Adrianus Groffen
geboren op 14 maart 1970 te Zevenaar

Promotores:

Prof. Dr. L. A. H. Monnens
Prof. Dr. J. H. Veerkamp

Co-promotor:

Dr. L. P. W. J. van den Heuvel

Manuscriptcommissie:

Prof. Dr. W. van den Berg
Prof. Dr. J. H. M. Berden
Dr. K. J. M. Assmann

This study was financially supported by grant C93.1309 of the Dutch Kidney Foundation.

The investigations described in this thesis were carried out at the Department of Pediatrics, University of Nijmegen, The Netherlands, and at the Department of Biochemistry, University of Oulu, Finland. Both laboratories participated in a concerted action of the European Union entitled "Alterations in extracellular matrix components in diabetic nephropathy and other glomerular diseases" (BIOMED NMH1-CT92-1766)

Publication of this thesis was enabled by a generous gift of the [Dutch Kidney Foundation](#) and the "Fonds ter Bevordering van de Wetenschapsbeoefening" (FBW) of the Department of Pediatrics, University of Nijmegen.

Reproduced by Print Partners Ipskamp, Enschede, The Netherlands

ISBN 90-9011729-6

behorende bij het proefschrift “*Structure and functions of heparan sulfate proteoglycans in the human glomerular basement membrane*”

1. Het “core eiwit” van perlecan speelt waarschijnlijk een rol in de binding van lipoproteïnen aan de extracellulaire matrix.
2. De hoge concentratie agrine in de glomerulaire basaalmembraan suggereert een belangrijke functie in het bepalen van de selectieve doorlaatbaarheid van deze structuur.
3. De affiniteit van agrine voor enerzijds de matrixcomponent laminine en anderzijds de celoppervlakte-eiwitten α -dystroglycan en integrine wijst op een mogelijke functie in signaaltransductie.
4. Aangezien het tripeptide SGD in perlecan en betaglycan als aanhechtingsplaats voor heparansulfaat kan fungeren, dient het heden gebruikte patroon SGxG (waarin voor x elk aminozuur kan worden ingevuld) in de PROSITE database te worden genuanceerd.
López-Casillas et al. (1994), J. Cell Biol. 124:557-568
Costell et al. (1997), Eur. J. Biochem. 243:115-121
5. Moleculaire defecten in de structuur van de glomerulaire filtratieporiën als oorzaak van proteinurie verdienen meer aandacht.
Kestila et al. (1998), Mol. Cell 1:575-82
Matsui et al. (1999), Nephrol. Dial. Transplant. 14:9-11
6. De beschikbaarheid van conditioneel geïmmortaliseerde podocyten is van zeer grote waarde voor het onderzoek naar de invloed van moleculaire processen op hun cellulaire differentiatie.
Mundel et al. (1997), Exp. Cell Res. 236:248-58
7. In de biomedische wetenschappen is vaardigheid in het gebruik van het Internet onontbeerlijk.
8. Het geslacht van een alligator wordt niet door genetica bepaald, maar door de omgevingstemperatuur van het ei.
Ferguson en Joanen (1982), Nature 296:850-853
9. De mens veronderstelt vaak ten onrechte het ultieme doel van de evolutie te zijn geweest.
Richard Dawkins (1986), The Blind Watchmaker
10. Chaperons zijn niet alleen belangrijk in het sociale leven.
Kuznetsov en Nigam (1998), N. Engl. J. Med. 339:1688-1695
11. Asielzoekers mogen blij zijn dat ze niet in een asociale buurt in Vught terecht komen.
12. Met de ontdekking van telomerase is het einde nog niet in zicht.

Aan Jolanda
Aan mijn ouders

ABBREVIATIONS

AChR	acetylcholine receptor
AcNPV	<i>Autographa californica</i> nuclear polyhedrosis virus
apoB	apolipoprotein B
BEV	baculovirus expression vector
bFGF	basic fibroblast growth factor
bp	base pairs
BM	basement membrane
cDNA	complementary DNA
CNS	congenital nephrotic syndrome
CS	chondroitin sulfate
CSPG	chondroitin sulfate proteoglycan
ECM	extracellular matrix
EGF	epidermal growth factor
FGS	focal segmental glomerulosclerosis
GAG	glycosaminoglycan
GBM	glomerular basement membrane
GST	glutathione S-transferase
HDL	high density lipoprotein
HS	heparan sulfate
HSPG	heparan sulfate proteoglycan
IDL	intermediate density lipoprotein
kb	kilobases
kDa	kilodaltons
LDL	low density lipoprotein
Lp(a)	lipoprotein (a)
LPDS	lipoprotein-deficient serum
MAb	monoclonal antibody
MCD	minimal change disease
mRNA	messenger RNA
NMJ	neuromuscular junction
PAb	polyclonal antibody
PCR	polymerase chain reaction
PG	proteoglycan
SDS-PAGE	sodiumdodecylsulfate-polyacrylamide gel electrophoresis
VLDL	very low density lipoprotein

INDEX OF THE THESIS

CHAPTER 1	General Introduction Adapted from <i>Nephrol. Dial. Transplant. (in press)</i>	7
CHAPTER 2	Expression and characterization of human perlecan domains I and II synthesized by baculovirus-infected insect cells <i>Eur. J. Biochem. 241, 827-834 (1996)</i>	37
CHAPTER 3	Lipoprotein binding by the core protein of human perlecan	53
CHAPTER 4	Evidence for the existence of multiple heparan sulfate proteoglycans in the human glomerular basement membrane and mesangial matrix <i>Eur. J. Biochem. 247, 175-182 (1997)</i>	67
CHAPTER 5	Agrin is a major heparan sulfate proteoglycan in the human glomerular basement membrane <i>J. Histochem. Cytochem. 46, 19-27 (1998)</i>	83
CHAPTER 6	Primary structure and high expression of human agrin in basement membranes of adult lung and kidney <i>Eur. J. Biochem. 254, 123-128 (1998)</i>	97
CHAPTER 7	Functional analysis of human renal agrin <i>J. Biol. Chem. (in press)</i>	113
CHAPTER 8	Urinary excretion of basic fibroblast growth factor by nephrotic children with focal segmental glomerulosclerosis <i>Nephrol. Dial. Transplant. (submitted)</i>	129
CHAPTER 9	Survey and Summary	143
	Samenvatting in het Nederlands	149
	List of original papers	153
	Curriculum vitae	154
	Dankwoord	155

CHAPTER ONE

General introduction

Accepted for publication in modified form as: Groffen AJA, Veerkanp JH, Monnens LAH and Van den Heuvel LPWJ (1999) Recent insights in the structure and functions of heparan sulfate proteoglycans in the human glomerular basement membrane. *Nephrol. Dial. Transplant.* (in press)

General introduction

CHAPTER ONE

As the first barrier to be crossed on the way to urinary space, the glomerular basement membrane (GBM) plays a key role in renal function. Besides providing mechanical support to the glomerular capillary wall, the GBM regulates the access of plasma molecules to the tubular system of the nephron. The permeability for a given molecule is highly dependent on its size, shape and charge. As early as in 1980 the charge-selective permeability was demonstrated to relate to the electrostatic properties of covalently bound heparan sulfates within the GBM [1,2]. Since then, the involvement of heparan sulfate proteoglycans in charge-selective ultrafiltration has reached a general consensus. In this section, current insights in the structure of the GBM and especially the role of heparan sulfate proteoglycans are discussed in relation to renal function and pathology. The aim of the study is described.

TO INDEX

THE GLOMERULUS

The role of the glomerulus in renal function

The kidney is made up of a large number of functional units, called the nephrons. Each nephron is composed of a glomerulus, proximal tubule, loop of Henle and distal tubule (see Figure 1). A single nephron traverses all parts of the kidney including the cortex, outer and inner medulla, and connects to the collecting ducts, pelvis and ureter. Each section of the nephron contributes to the specificity of renal clearance. The first step in urinary excretion called ultrafiltration takes place in the glomerulus, and is driven by the high blood pressure within the glomerular capillaries. The specificity of excretion depends upon the selective permeability of the glomerular basement membrane (GBM) that surrounds the capillary wall. Plasma components that traverse the GBM are collected in the primary urine, contained within Bowman's capsule. Subsequently resorption and secretion processes determine the ultimate urine composition. The work described in this thesis focuses on the contribution of the glomerulus to renal function. In this chapter, the up-to-date knowledge of the structural and functional properties of the GBM will be introduced. To illustrate the

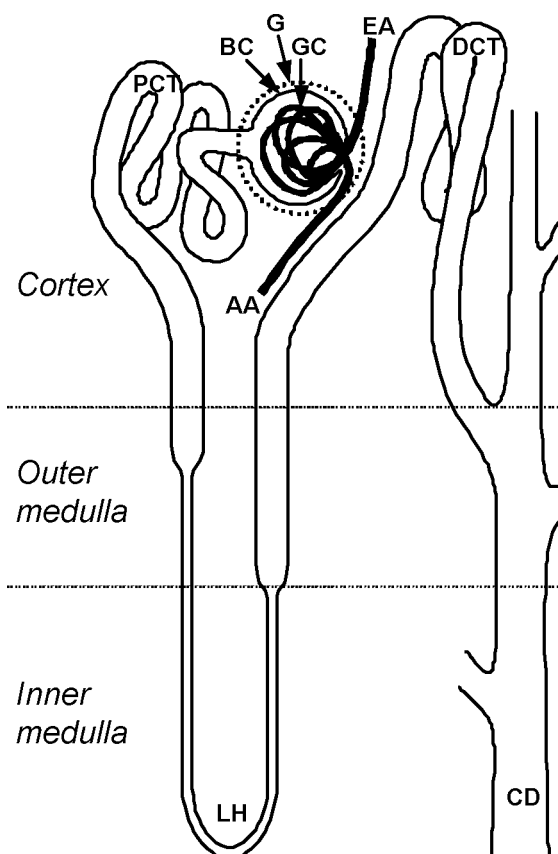


Figure 1: Structure of the nephron. AA: afferent arteriole, BC: Bowman's capsule, CD: collecting duct, DCT: distal convoluted tubule, EA: efferent arteriole, G: glomerulus (dotted circle), GC: glomerular capillaries; LH: loop of Henle; PCT: proximal convoluted tubule.

clinical relevance of these data, various glomerular nephropathies will be described briefly.

Figure 2. A typical glomerular capillary loop with capillary lumen (Cap), endothelial wall (En), GBM, podocyte (P), urinary space (US), mesangial cell (Mes) and mesangial matrix (MM). Electron microscopic view reproduced from [186] with permission by Prof. W. Kriz.

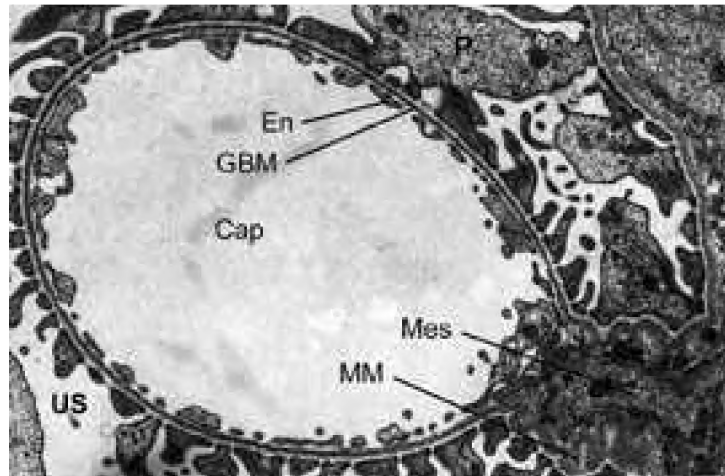
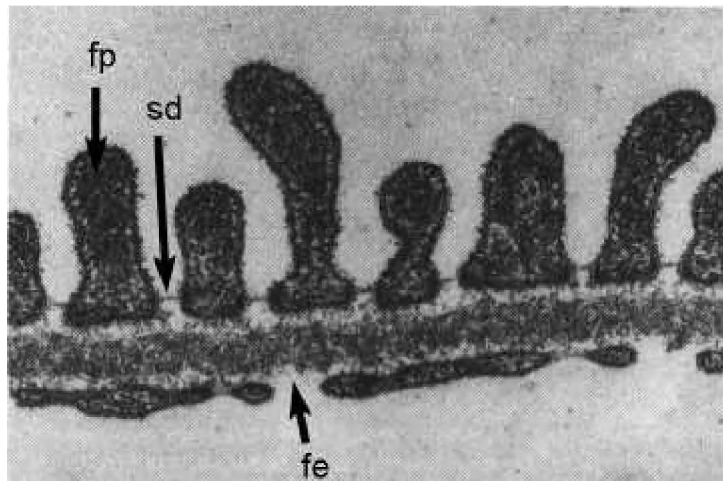


Figure 3. Structure of the filtering membrane. The fenestrae of the capillary endothelium (fe), and the interdigitating foot processes with slit diaphragms (fp, sd) are indicated. Reproduced from [186] with kind permission by Prof. W. Kriz.



Anatomy of the glomerulus

The glomerulus (also designated the Malpighian body) is encapsulated by a layer of parietal epithelial cells, called Bowman's capsule. It contains a large number of blood capillaries that appear in a looped conformation, supported by mesangial cells adhering to the termini of each loop (Figure 2). The wall of the glomerular capillary consists of a single layer of fenestrated endothelial cells. This thin structure is surrounded completely by the GBM, a dense network of extracellular matrix molecules. In various electron microscopic studies, the GBM has been subdivided into three layers of alternating density, the central layer being the most dense. Although the terms "lamina rara interna", "lamina densa", and "lamina rara externa" are still used at present, this subdivision may be based on artifacts introduced during dehydration of tissue sections. The GBM presumably forms a single layer of homogenous density [3]. The outer surface of the GBM, where not associated with the mesangium, is covered with visceral epithelial cells (Figure 3). With reference to their strongly branched appearance, these cells are also called podocytes. Their terminal extremities (called the foot processes) are intervened by slit diaphragms and covered by a

glycocalyx (a layer rich in sialoglycoproteins such as podocalyxin). The association of the foot processes with the glycocalyx may stabilize their shape and maintain the aperture of the slit diaphragms [4].

THE SELECTIVE PERMEABILITY OF THE GLOMERULAR BASEMENT MEMBRANE

The GBM is a molecular scaffold that provides the structural support that the capillary wall needs to endure the high local blood pressure. It also acts as a filter-like membrane that regulates the access of plasma components to the urinary space. Augmented GBM permeability manifests clinically as a nephrotic syndrome, characterized by albuminuria, hypoproteinemia, and edema.

The permeability of the GBM for a given molecule depends strongly on its size, shape and charge. The size- and shape-dependent permeability is ascribed to the strongly cross-linked nature of the BM, giving rise to a dense network with relatively small meshes. The charge-selectivity is associated with the presence of polyanionic charges in the GBM, disabling acidic macromolecules to penetrate by means of electrostatic repulsion. The distribution of anionic sites has been studied by staining the GBM with various cationic probes, including cationized colloidal gold, polyethyleneimine, cuproinic blue, lysozyme, colloidal iron, modified ferritin, poly-L-lysine, protamine sulfate, hexamethrine, ruthenium red, Alcian blue, safranin O and others [5]. Figure 4 shows an example of cationic staining using modified ferritin [6]. Heparan sulfate proteoglycans (HSPGs) are thought to play the leading part in GBM charge-selectivity based on a long history of research. Their significance in renal ultrafiltration became evident when heparan sulfate (HS) was removed from the rat GBM by perfusion with heparitinase, which resulted in an increased permeability for anionic ferritin [1]. Similarly, perfusion with anti-HS antibodies led to selective albuminuria [7]. Despite the crucial role of HSPGs, additional factors may be relevant for charge-selective ultrafiltration [8]. The glycocalyx that decorates the epithelial border also adds polyanionic charge to the GBM. When this structure becomes detached from the GBM, anionic macromolecules were observed to cross the GBM [9]. Finally hyaluronic acid, chondroitin sulfates and carboxyl groups of glutamic and aspartic acid may convey additional anionic charge to the GBM [4].

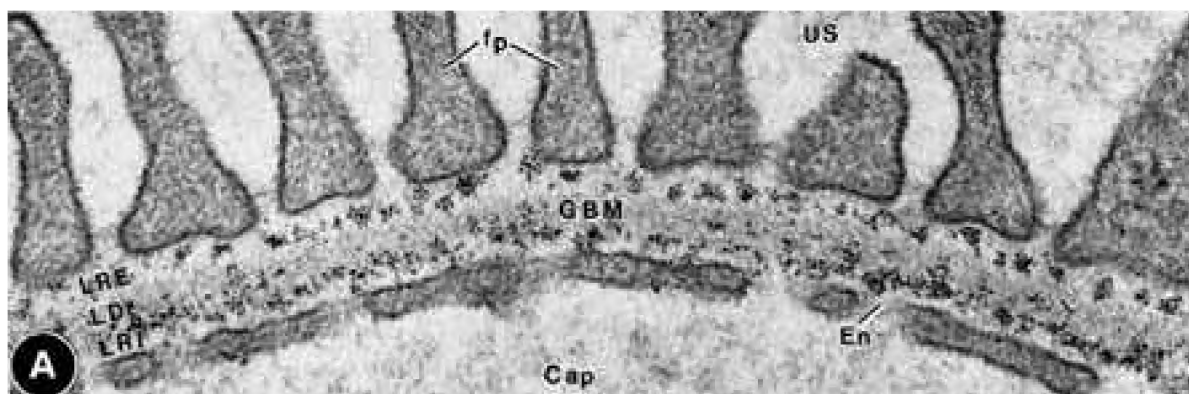


Figure 4: Perfusion of kidney with cationized ferritin shows the regular appearance of HS-associated anionic sites in the GBM. US: urinary space, Cap: capillary lumen, En: endothelium, fp: foot processes, LRI: lamina rara interna, LRE: lamina rara externa, LD: lamina densa. Reproduced from [23] with permission by Prof. Y. Kanwar.

MOLECULAR STRUCTURE OF THE GLOMERULAR BASEMENT MEMBRANE

A major step forward in the investigation of the molecular organization of BMs was the characterization of the Engelbreth-Holm-Swarm (EHS) mouse tumor, that produces high amounts of extracellular matrix [10]. The main molecular components were identified as type IV collagens, laminins, nidogen and proteoglycans [11]. As HSPGs are the main subject of the present study, their characteristics are discussed in a separate section.

Type IV collagen

A basic scaffold of the GBM is formed by collagen type IV, a fibrillar protein that aggregates into a polymeric meshwork. As depicted in Figure 5, each collagen type IV monomer consists of three polypeptide chains folded into a triple-stranded helix [12–14]. The N-terminal domain, named 7S, is composed of the three small globules. The central and largest part of the monomer is formed by the triple-helical, or collagenous domain. The C-terminal globules of the individual chains assemble into the NC1 (non-collagenous) domain. Collagen type IV monomers then aggregate into a large polymer network. This

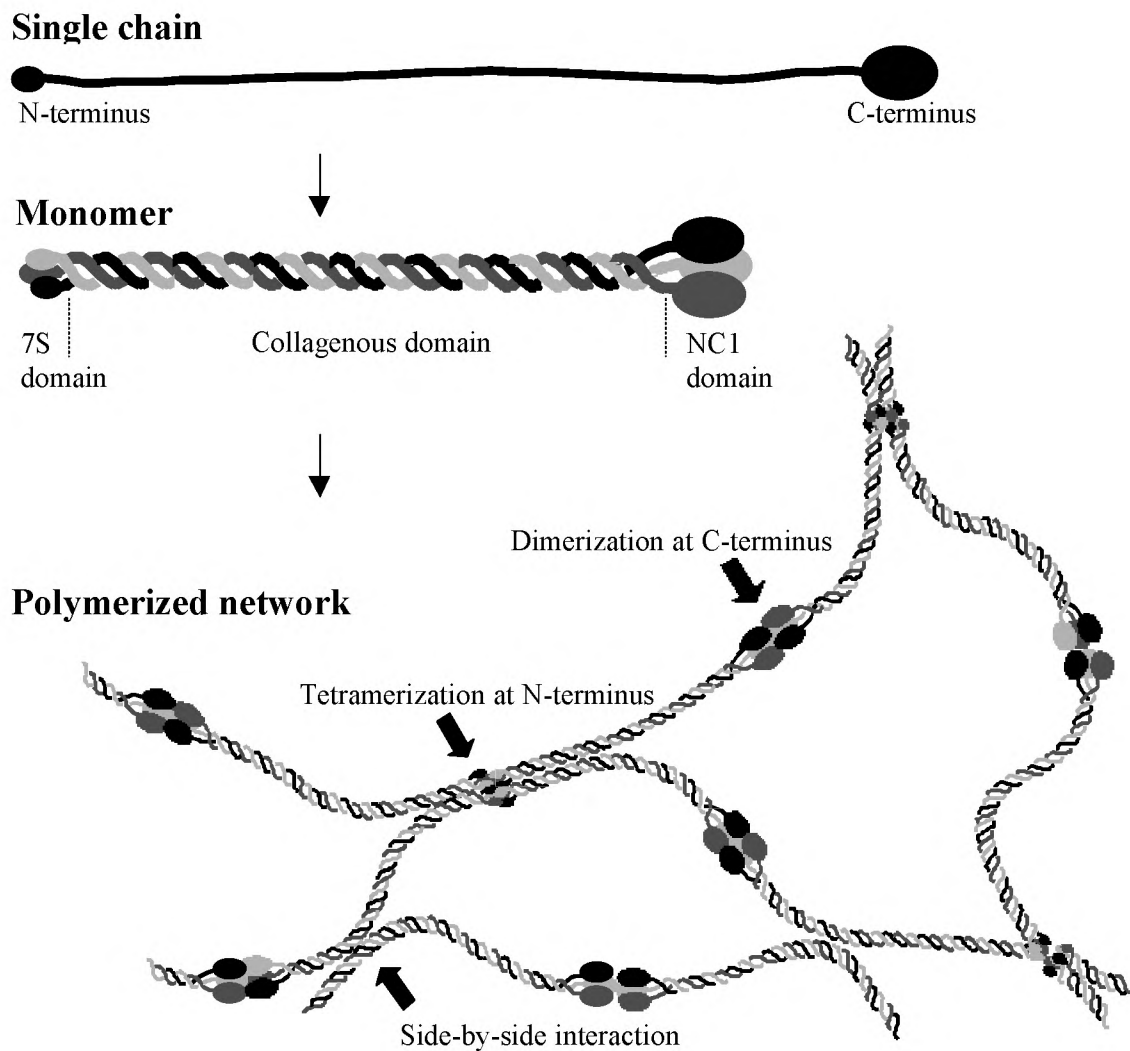


Figure 5: Assembly of a collagen type IV monomer from three polypeptide chains and formation of a polymeric network. Thick arrows indicate three distinct types of interaction that stabilize the network. Drawing based on [12, 14].

structure is stabilized by three types of homotypic interaction (Figure 5): the covalent association of NC1 domains into dimers, the covalent association of 7S domains into tetramers, and the lateral interaction between adjacent collagenous segments [14].

Six genes encoding type IV collagen polypeptide chains have been identified, named $\alpha 1$ through $\alpha 6$. Not all combinations assemble into a functional polymer network. Only two stable collagen IV networks have been characterized; the first composed of only the $\alpha 1$ and $\alpha 2$ chains, and the second containing $\alpha 3$, $\alpha 4$ and $\alpha 5$ [15–17]. The $\alpha 3$ - $\alpha 4$ - $\alpha 5$ network is stronger, presumably because these collagenous triple helices have an increased cross-linking potential [18]. This is illustrated by the progressively disrupted structure of the GBM in Alport syndrome, where the deficiency of $\alpha 3$ - $\alpha 4$ - $\alpha 5$ network assembly is associated with a sustained expression of the $\alpha 1$ and $\alpha 2$ chains [13,19,20]. Whereas the $\alpha 1$ and $\alpha 2$ chains predominate in most BMs, the mature GBM predominantly contains the collagen type IV chains $\alpha 3$, $\alpha 4$ and $\alpha 5$ [21,22].

Laminins

Laminins are assembled by three polypeptide chains designated the laminin α , β and γ chain [24]. Laminins typically resemble a Latin cross, its four arms flexible and with globular domains (Figure 6). Laminin can self-assemble *in vitro* into a large polymer, which may be the main network of collagen-free extracellular matrices known to exist e.g. in embryogenesis [14]. The polymerization of laminin takes place via interaction of the terminal globules of its arms, and is calcium-dependent [26].

For each individual laminin chain, different isoforms were identified designated $\alpha 1$ – $\alpha 5$, $\beta 1$ – $\beta 4$ and $\gamma 1$ – $\gamma 3$. While most variants are encoded by a different gene, truncated chains may also be produced by alternative splicing (e.g. $\alpha 3$) [27] or proteolytic processing (e.g. $\alpha 2$, $\beta 3$ and $\gamma 2$) [28]. Many combinations of α , β and γ chains can form a stable complex, yielding a large variety of laminins (Table 1). The functions of the laminins vary from oligomerization to cell adhesion, migration and differentiation. The laminins that occur in the adult GBM are predominantly composed of the chains $\alpha 5$, $\beta 2$ and $\gamma 1$ (laminin-11) [27,29–32]. This laminin isoform also occurs in the BM of the neuromuscular junction [33]. The laminin $\beta 2$ chain seems to have an important function in the GBM, since mutant mice that lack this chain display (besides abnormalities in the neuromuscular junction) a nephrotic syndrome in the second week after birth. Interestingly, their massive proteinuria is associated with fusion of the foot processes, resembling the phenotype of

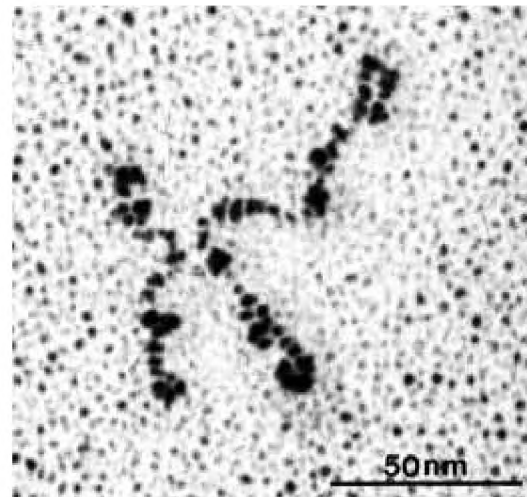


Figure 6. The typical structure of a laminin, shown by rotary shadowing electron microscopy. Reproduced from [25] with permission by Prof. R. Timpl.

Table 1: Laminins and their composition [24, 27].

Name	Composition	Trivial name
Laminin-1	$\alpha 1\beta 1\gamma 1$	EHS laminin
Laminin-2	$\alpha 2\beta 1\gamma 1$	merosin
Laminin-3	$\alpha 1\beta 2\gamma 1$	s-laminin
Laminin-4	$\alpha 2\beta 2\gamma 1$	s-merosin
Laminin-5	$\alpha 3\beta 3\gamma 1$	kalinin
Laminin-6	$\alpha 3\beta 1\gamma 1$	k-laminin
Laminin-7	$\alpha 3\beta 2\gamma 1$	ks-laminin
Laminin-8	$\alpha 4\beta 1\gamma 1$	-
Laminin-9	$\alpha 4\beta 2\gamma 1$	-
Laminin-10	$\alpha 5\beta 1\gamma 1$	-
Laminin-11	$\alpha 5\beta 2\gamma 1$	-

minimal change nephrosis [29,34]. The short arm originating from the $\gamma 1$ chain has a nidogen-binding activity [35], and the long arm of the $\alpha 1$ chain was shown to bind the HSPG agrin [36]. In addition, the long arm was shown to mediate cell attachment [26].

Nidogen

Nidogen, also called entactin, is a 158 kDa large single-chain glycoprotein first purified from the extracellular matrix produced by the EHS tumor. It is composed of three globular domains (G1, G2 and G3) separated by rod-like segments [37]. The carboxy-terminal globule (G3) binds non-covalently and in equimolar amounts to domain III of the laminin $\gamma 1$ chain [35,38]. Domain G2 associates with collagen IV, thus linking the collagen matrix to the laminin network. This domain has also a perlecan-binding function [39,40]. Given these cross-linking properties, nidogen is an important component in the assembly of BMs [11,14,26,41].

Other basement membrane components

BM-40, also called SPARC or osteonectin, is a 33-kDa extracellular glycoprotein with anti-adhesive properties. It is activated by partial proteolysis and binds calcium and collagen type IV [42–44]. Fibronectin is a large dimeric molecule that adheres to many extracellular matrix components including collagens, heparan sulfate and fibrin. In association with certain cell types fibronectin is assembled into a fibrillar network. Fibronectin also binds to the cell surface via integrin, an interaction that is conferred by the Arg-Gly-Asp tripeptide sequence. By these mechanisms, fibronectin has adhesive properties for many cell types and in some cases it induces cell migration. In the glomerulus, fibronectin is mainly found in the mesangial matrix [4]. Another basement membrane molecule is tenascin-C. The incorporation of this molecule was demonstrated to depend on the presence of HSPGs in the extracellular matrix, and tenascin-C colocalized with perlecan and fibronectin [45]. A function for tenascin-C in cell migration on fibronectin-containing matrices was suggested [46]. And finally, fibulins are microfibrillar components of extracellular matrices that consist of three domains, the second containing calcium-binding EGF-like repeats. Two isoforms encoded by different genes were characterized. Both fibulin-1 and -2 were demonstrated to bind laminin, nidogen, fibronectin [47,48] and to form homodimers [47,49]. Fibulin-2 binding to perlecan was also reported [50].

HEPARAN SULFATE PROTEOGLYCAN

Structural characteristics of proteoglycans

Proteoglycans are defined as proteins that carry glycosaminoglycan chains. The polypeptide part is called the core protein. Each glycosaminoglycan chain is a polysaccharide composed of repeating disaccharide units. Different types of glycosaminoglycans exist: hyaluronate, keratan sulfate, dermatan sulfate (DS), chondroitin sulfate (CS), heparin and HS. The structure of the disaccharide repeats differs between the types (Figure 7A). Most glycosaminoglycans are covalently linked to a serine acceptor residue on the core protein of a proteoglycan. In these cases the chain is linked to a serine acceptor residue via a trisaccharide composed of one xylose and two galactose residues (Figure 7C). In exception, hyaluronic acid and heparin are normally present in free form. Heparin is synthesized on a small core protein called serglycin and subsequently split off at secretion. A variety of core proteins exists for HSPGs.

Although the largest proportion of proteoglycans in the BM is formed by HSPGs, other proteoglycan types are certainly present. Chondroitin sulfate proteoglycans (CSPGs) form

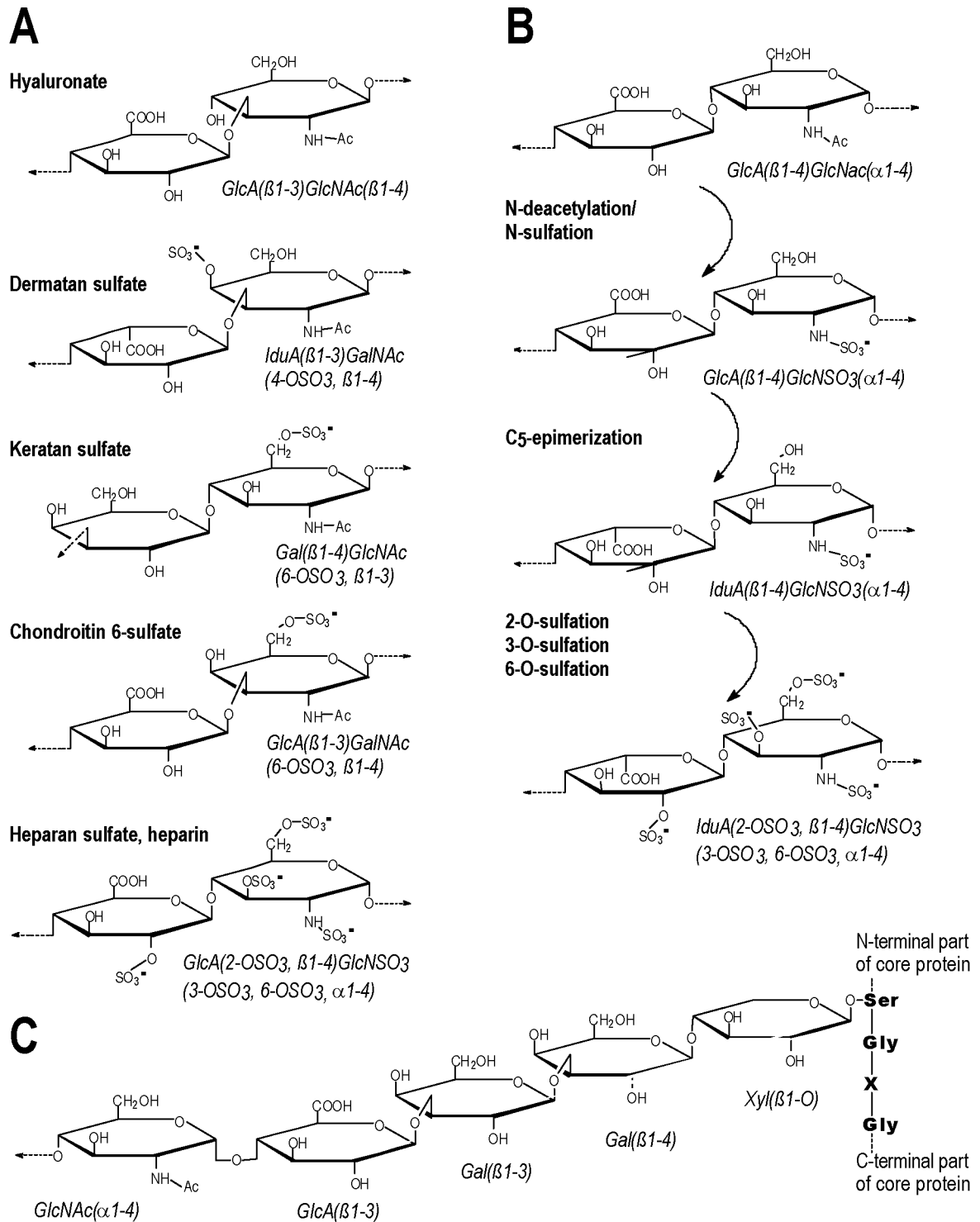


Figure 7. A) The repeating disaccharide units in various types of glycosaminoglycans, B) possible modifications that occur in heparan sulfate and heparin, and C) the attachment of heparan sulfate to a serine residue of the core protein of a proteoglycan. Abbreviated names are shown in italics (Gal: galactose, GalNAc: N-acetylgalactosamine, GlcA: glucuronic acid; GlcNAc: N-acetylglucosamine, GlcNSO₃, N-sulfated glucosamine, IduA: iduronic acid, Xyl: xylose).

the second largest group in most BMs. A CSPG that occurs in the EHS matrix was recently cloned and named bamacan [51,52].

The heterogeneous structure of heparan sulfates

The nascent HS and heparin chains consist of alternating glucuronic acid and N-acetylglucosamine residues (Figure 7C). After extension, the GAG chain may be subjected to various types of modification (Figure 7B) [53]. The first modification is the subsequent deacetylation and sulfation of the amino group of glucuronic acid, catalyzed by the bifunctional enzyme N-deacetylase/N-sulfotransferase [54]. Second, epimerization of these glucuronic acid residues to iduronic acid may take place and finally, the 2-O, 3-O and/or 6-O atoms may be sulfated. Together, the various types of modification enable the disaccharides to assume many different structures. The fine structure of HS chains is highly variable and depends strongly on the type of core protein and the cellular environment. Also within a single chain, sulfate-rich regions alternate with poorly sulfated domains. In heparin more sulfate- and iduronic acid-rich domains are present than in heparan sulfate.

Factors that influence heparan sulfate attachment

The synthesis of glycosaminoglycans attached to a core protein is a post-translational process. The elements required for HS attachment are only partly understood. A first requirement is the presence of a Ser-Gly dipeptide, providing the acceptor site for O-linked glycosylation (Figure 7C). This dipeptide may be part of a tetrapeptide motif, matching the consensus Ser-Gly-X-Gly (where X represents any amino acid) [55,56]. It may also occur in the tripeptide sequence Ser-Gly-Asp [56,62]. A second element that influences glycosylation is the consensus in which the attachment site is located. Clusters of acidic amino acids neighboring the GAG attachment site were shown to promote HS attachment [57]. In addition, the proximal occurrence of multiple Ser-Gly repeats favours glycosylation with HS [58]. Besides these elements of primary structure, a motif of secondary structure has been associated with O-linked glycosylation. This motif was called the SEA module with reference to the molecules in which it was first found: sperm protein, enterokinase, and agrin [59]. The mechanism by which this module promotes GAG attachment is unclear, and experimental evidence for its involvement has not yet been obtained. In each case, the sites of glycosylation were found adjacent to the SEA domain. In addition to the above elements that are included in the core protein structure, the cell type in which proteoglycans are produced also influences the glycosylation process. This is demonstrated by the different types of glycosylation of recombinant perlecan fragments synthesized in different cellular environments [51,60–65].

Heparan sulfate protein interactions

The heterogeneous fine structure of HS leads to a broad variety of functional properties [66–68]. Many proteins with affinity for heparin or HS were described including basic fibroblast growth factor, antithrombin III, lipoprotein lipase, apolipoprotein B-100, apolipoprotein E, hepatic triglyceride lipase, thrombin, β -thromboglobulin, thrombospondin, vitronectin, fibronectin, platelet factor 4, heparin-binding epidermal growth factor, agrin, perlecan, and others [50,69–71]. A consensus motif in the protein ligand was identified as the structure XBBXB, XBBBXXB, where B represents a basic amino acid (arginine, lysine, histidine) and X a nonbasic amino acid. Alternatively, a consensus sequence TXXBXXTBXXXTB was proposed where T represents a turn in the peptide chain [70,72]. The structure within HS that contributes to the binding of proteins is known only in a few cases: basic fibroblast growth factor [73], antithrombin III [74] and lipoprotein lipase [75]. The minimal length of HS fragments required for binding is typically five

to seven disaccharides. The structural analysis of glycosaminoglycan chains is hampered by technical limitations, and the development of systematic techniques for this purpose is of great interest.

PERLECAN: A HSPG PRESENT IN VIRTUALLY ALL BASEMENT MEMBRANES

Many different HSPGs have been identified thus far, most of which are associated with the cell surface. The first molecule identified as a HSPG of basement membranes was perlecan. Later, also the extracellular matrix component agrin was recognized as a HSPG. Here, the structure and functions of perlecan are described. The properties of agrin are introduced in a separate section.

Structure of perlecan

Perlecan, a widely expressed HSPG of BMs, was first isolated from the EHS tumor in 1980 [2]. The name refers to the beads-on-a-string-like appearance observed in rotary shadowing electron microscopy (Figure 8) [76]. Perlecan consists of a large (467 kDa) core protein, carrying three HS chains attached to its N-terminal domain [62,77]. Domain V may also be substituted with glycosaminoglycans [50]. The HS residues contribute to approximately 50% of the total molecular mass of the proteoglycan. It is important to note that the perlecan core protein can alternatively be substituted with CS and/or DS, and in some cases HS is totally absent from the proteoglycan [51,63–65]. Other types of post-translational modifications include palmitoylation, myristoylation and N-glycosylation [78].

The human gene encoding perlecan (named HSPG2) is located on the short arm of chromosome 1 (1p35–p36.1), comprises over 120 kb and contains 94 exons [79–81]. The cDNA sequence of human perlecan (14 kb in length) shows a five-domain organization (Figure 9, roman numbers) [77,82,83]. The N-terminal domain has a primary structure unique for perlecan. Based on secondary structure prediction, this domain was identified as a SEA module [59]. It contains three functional attachment sites for HS [76]. Domain II is composed of four low-density-lipoprotein receptor class A (LA) modules. The similarity with the low-density-lipoprotein receptor includes the ligand-binding domain of the receptor. Immediately downstream lies a single IgG repeat that resembles the 21 more repeats found in the N-CAM-like domain (see below). Domain III shares similarity with the short arms of laminin chains. This domain contains four cysteine-rich LE modules similar to domain III of the laminin short arms, alternated by three cysteine-free (LamB) modules resembling domain IV of the laminin short arms. Domain IV, encoded by 2010 nucleotides, is the largest domain of perlecan. The 21 Ig-like repeats found in this domain are similar to neural cell adhesion molecules (N-CAM), and presumably fold into a globular structure typical for the immunoglobulin superfamily. Domain V, finally, displays similarity to the large globular G domain located on the long arm of the laminin α 1 chain. Domain V also contains several SGXG sequences, but these may not be functional in HS attachment. To fold into the final molecular structure of

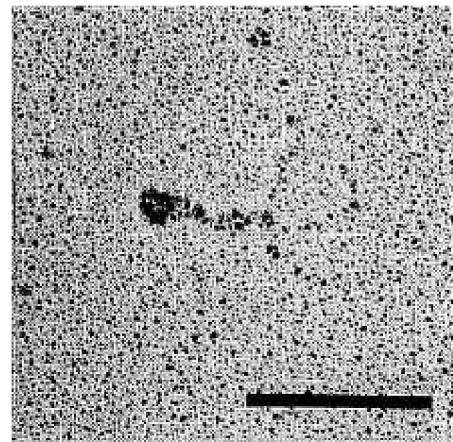


Figure 8. The appearance of perlecan in rotary shadowing electron microscopy. Reproduced from [76] with permission by Prof. M. Paulsson.

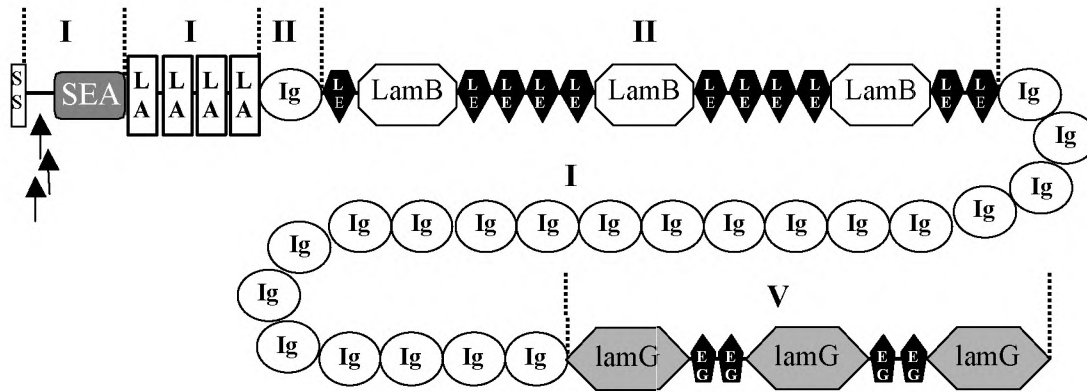


Figure 9. The five-domain organization of human perlecan. SS: signal peptide; SEA: module first found in sperm protein, enterokinase and agrin; LA: LDL-receptor class A module; Ig: Ig-like repeat similar to those of neural cell adhesion molecule; LE: laminin-III-like EGF repeat; LamB: laminin-IV-like domain; EG: EGF-like repeat; lamG: laminin-G-like domain [59, 77, 82, 83]. Arrows indicate glycosaminoglycan attachment sites.

perlecan (Figure 8), domains I and II likely constitute the first globule. Domain III provides the second, third and fourth globule, domain IV the fifth and domain V represents the carboxy-terminal globule [76,77,82–85].

Functions of perlecan

Perlecan is expressed in the BMs of all human tissues analyzed in a thorough study, including skin, lung, colon, liver, heart, connective tissue, thymus, prostate, spleen, pituitary gland, kidney, placenta, skeletal muscle and blood vessels [86]. Many functions are postulated for perlecan. Various interactions superimpose strength on the polymeric BM structure, including self-assembly of the perlecan core protein, nidogen-mediated association with laminins, and binding of collagen IV and fibronectin [87–90]. By virtue of its heavily glycosylated nature, perlecan may confer hydrophilic properties to the matrix, thus increasing its accessibility for plasma and solutes [4]. Perlecan also mediates cell attachment as shown for endothelial cells and fibroblasts, and acts as a repulsive component for other cell types [91–93]. Recombinant domain V was demonstrated to be responsible for integrin $\beta 1$ -mediated cell attachment [50]. This region also binds nidogen, heparin and fibulin-2.

Furthermore, the HS residues of perlecan were shown to participate in mitogenesis and angiogenesis. This activity is mediated by basic fibroblast-growth factor (bFGF). After HS binding, bFGF becomes activated and subsequently presented to its functional receptor located on the cell surface [94,95]. The oligosaccharide structure involved in bFGF binding appears to occur preferentially on perlecan, since the cell surface HSPGs syndecan, fibroglycan and glypican showed no bFGF binding capacity [73,96,97]. The bFGF-mediated mitogenic activity of perlecan explains the strongly mitogenic and angiogenic behavior of perlecan-expressing tumors [98]. Consistently, antisense perlecan cDNA transcription reduces the metastatic potential of human melanoma cells [99–101]. Besides bFGF, also other growth factors were shown to bind to HS. These include heparin-binding epidermal growth factor, acidic FGF, platelet-derived growth factor, granulocyte-macrophage colony stimulating factor, hepatocyte growth factor/scatter factor, interferon- γ and several interleukins [102–104].

In addition perlecan may be involved in lipoprotein metabolism [84]. Lipoprotein lipase was shown to interact with HS [105]. The core protein may contain a binding site for lipoproteins, since the primary structure of domain II is very similar to the ligand-binding

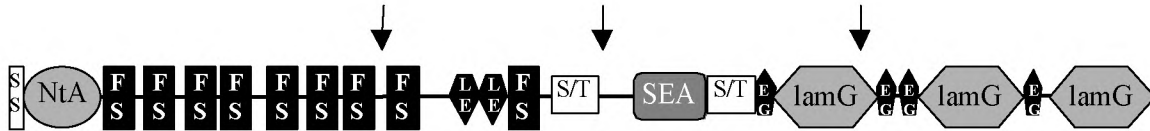


Figure 10. The domain organization of human agrin. SS: signal peptide; NtA: N-terminal Agrin (laminin-binding domain); FS: follistatin-like; LE: laminin-III-like EGF repeat; S/T: serine/threonine-rich; SEA: module first found in sperm protein, enterokinase and agrin; EG: EGF-like repeat; lamG: laminin-G-like domain [119–121]. The arrows indicate glycosaminoglycan attachment sites.

region of the low-density lipoprotein receptor. Thus, a complex would be assembled containing HSPG, lipoprotein lipase and lipoprotein. This resembles the complexes formed on the cell surface, where the complex is internalized prior to metabolic processing [75,105–109]. However, experimental evidence to confirm this hypothesis is still lacking.

In addition to the above mentioned functions, perlecan was initially assumed to play a crucial role in the glomerular permselectivity barrier. For more than a decade, perlecan was the only HSPG known to be associated with basement membranes. The hypothesis that perlecan could be a crucial determinant of GBM-associated polyanionic sites therefore received considerable attention. Despite this, no clear evidence was obtained for such a function of perlecan. Recently, the generation of well-defined monoclonal antibodies against perlecan [86,110] has enabled a more accurate analysis of the identity of the involved proteoglycans. Surprisingly, ultrastructural studies demonstrated the absence of perlecan in large parts of the glomerular capillary loop (chapter 5) [111].

AGRIN: A HSPG WITH SYNAPTOGENIC AND FILTRATION-ASSOCIATED FUNCTIONS

At the interface between an outgrowing axon and the differentiating myotube, a series of molecular events occur that eventually result in the formation of a highly differentiated neuromuscular synapse. Agrin, which proved to be a HSPG [112], is a key factor in this process [113,114]. It has therefore been the subject of extensive investigations in the field of neuroscience, especially in the developing chick, rat and mouse (e.g. [115–117]). Agrin also proved to occur in other tissues, especially kidney and lung [118,119]. In this section the structure and function of agrin is reviewed, together with recent new insights that extend the relevance of agrin expression to glomerular function.

Structure of agrin

The human agrin gene, named *AGRN*, was assigned to the locus 1p36.1–1pter [120]. This is relatively close to the perlecan gene (1p35–1p36). The human agrin mRNA molecule exceeds 7 kb in length and encodes a core protein of 212 kDa, containing three GAG attachment sites [119]. Experimental evidence showed that the core protein is glycosylated with HS. The primary structure shows a multimodular composition containing a globular laminin-binding domain, nine follistatin-like protease inhibitor domains, two laminin-like EGF repeats, two serine/threonine-rich domains, a SEA module, four EGF repeats and three domains sharing homology with globules of laminin α (Figure 10) [119,121–123]. The four globular domains (the laminin-binding and laminin-like domains) can be distinguished by electron microscopy (Figure 11). Also the three HS side chains are visibly attached to the central region of the molecule as demonstrated for recombinant chick agrin [124]. The remainder of the agrin molecule behaves as long flexible rod-like structures. Various isoforms of agrin are expressed through tissue-dependent alternative splicing. The four sites at which splice variants were reported are designated *c*, *x*, *y* and *z* in mammalian

species (C, A and B in chick). A summary of observed amino acid inserts for each site is given in table 2. The composition of the y site is regulated by an intronic enhancer, positioned immediately downstream from this site [125]. The differences between agrin splice variants are restricted to short oligopeptide sequences, and therefore they cannot be distinguished by polyacrylamide gel electrophoresis.

Functions of agrin

Agrin plays a key role in the formation of the neuromuscular junction (NMJ). Neurons and muscle cells produce different splice variants of agrin, each with different functional properties. Neuronal agrin triggers the clustering of acetylcholine receptors (AChRs) on the muscle cell membrane [114,126,127]. This activity requires the presence of an insert at the z splice site [116,128]. The clustering process involves the activation of a muscle-specific kinase (MuSK) [129]. MuSK becomes immobilized in the synaptic region, where it is finally included in a large multimolecular network that traverses the cell membrane. Other components included in this structure are neuregulins, AChRs, rapsyn-associated transmembrane linker, rapsyn, the dystrophin-associated glycoprotein complex and the cytoskeleton [114,130,131]. Adhesion of agrin to integrin $\alpha v \beta 1$ may also play a role in the synaptogenic process [132]. Muscle-specific isoforms of agrin do not have AChR clustering activity. These isoforms induce the differentiation of the nerve terminal, an activity which may take place through the clustering of synaptotagmin in the developing presynaptic densities [133].

Agrin cross-links the assembling supramolecular complex tightly into the synaptic BM through its interaction with laminin. This represents another major function of agrin, for which the N-terminal domain is responsible [36]. The binding to agrin was demonstrated for laminin-1, -2 and -4, and was localized to a central segment of the laminin long arm [124].

Agrin expression is not restricted to the developing NMJ, but also occurs in numerous other embryonal tissues [135]. The highest expression of agrin is seen in BMs of the vascular system, kidney and lung [111,114,118,119,136]. Non-neuronal agrin isoforms have a low AChR-aggregating activity, suggesting distinct functional properties [118]. As far as known, they are devoid of splice inserts at the y and z site, but 9-amino acid insertions in the x site were observed [114,115,119]. The expression pattern of non-neural agrin isoforms suggests a possible function in the selective exchange of molecules between compartments. In the developing blood-brain barrier, the onset of agrin expression coincides with the time at which the BM of capillary vessels becomes impermeable [136]. A possible function of agrin in regulating the molecular access through BMs is especially intriguing with respect to renal function. HSPGs are known to contribute importantly to the polyanionic charge of the GBM, as described elsewhere in this introduction. Renal agrin is expressed primarily along the glomerular capillary loops. In immuno-electron microscopy, anti-agrin antisera decorate the whole width and length of the GBM (Figure 12). These

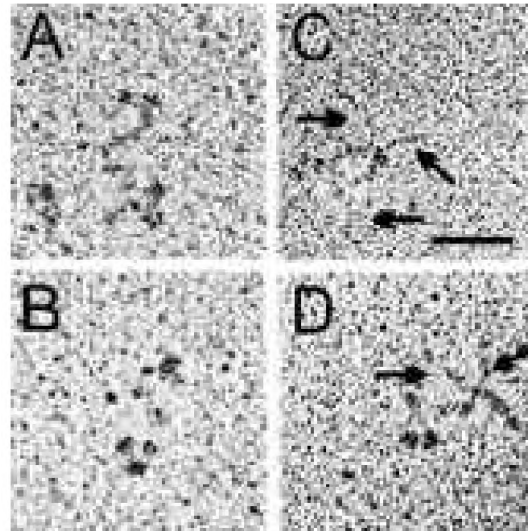


Figure 11. The conformation of agrin in rotary shadowing electron microscopy. This picture shows the conformation of a recombinant chick agrin molecule. Bar, 50 nm. Reproduced from [124] with permission by Prof. M.A. Ruegg.

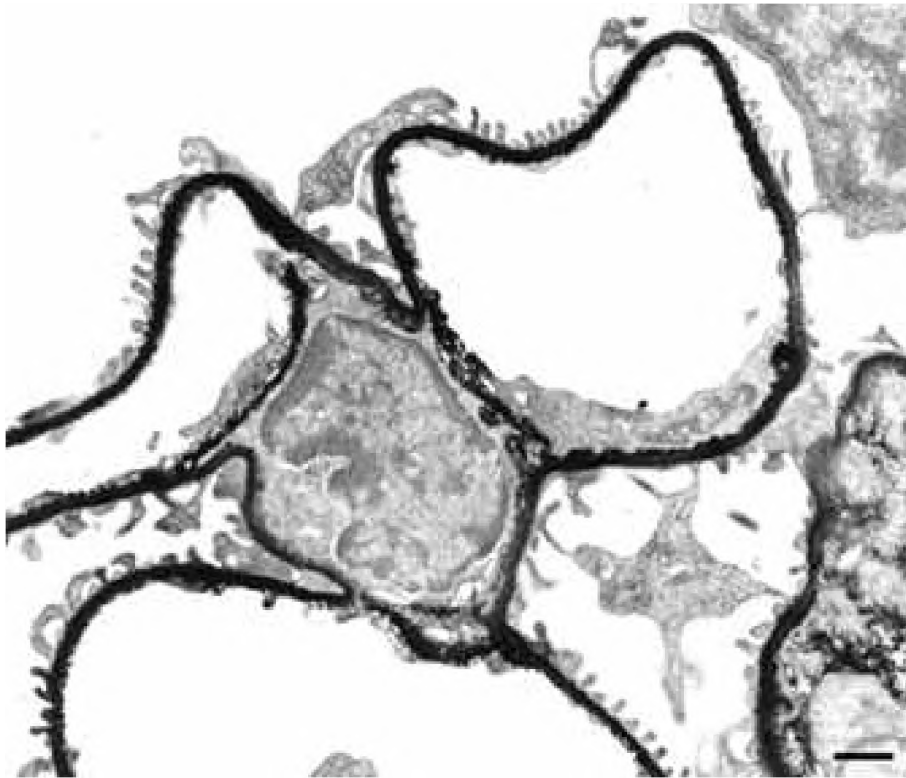


Figure 12. The ultrastructural distribution of agrin in mouse glomeruli analyzed by immuno-electron microscopy. Anti-agrin antiserum strongly stained the GBM in a homogenous linear way. A less intense staining was observed in the mesangial matrix. Used antibodies and procedures are described elsewhere [111]. Bar = 1 μm .

properties suggest that agrin could play a major role in determining glomerular permselectivity.

The peripheral membrane receptor α -dystroglycan was identified as a high-affinity ligand of agrin. α -Dystroglycan also binds laminin and is linked to the dystrophin-associated glycoprotein complex, and thus also to the cytoskeleton. The interaction of agrin with α -dystroglycan is not related to its AChR clustering activity. Carboxy-terminal fragments of agrin that are sufficient for AChR clustering activity do not bind α -dystroglycan [137,138]. Agrin splice variants that lack the y and z inserts (like those that occur in kidney) are inactive in AChR clustering but have a similar capability to bind α -dystroglycan. This was experimentally confirmed by co-immunoprecipitation of agrin from adult kidney with α -dystroglycan [139]. α -Dystroglycan was shown to be present on the membrane of kidney epithelial cells from the moment of mesenchymal-to-epithelial transition. It may play an important role in branching of the nephron during morphogenesis [140–142]. α/β -Dystroglycan is also prominently expressed in the adult human GBM [143]. By binding both α -dystroglycan and laminin, agrin may be one of the components involved in the strong adhesion of the podocyte's foot processes to the GBM.

Finally, another component that interacts with agrin is heparin (a useful property for purification procedures). Not all agrin isoforms show this activity; the binding requires the presence of a basic tetrapeptide cluster at the y splice site [69]. Heparin binding could be a mechanism to modulate the ability of agrin to bind α -dystroglycan. In isoforms containing a four-amino-acid insert at the y site, α -dystroglycan binding is still possible but it can be inhibited in presence of heparin [69,134,144]. Consistently, the α -dystroglycan binding activity of isoforms that lack the y insert is not inhibited by heparin [69,134]. Additional

functions of agrin may be related to protease inhibition [135] or various interactions with growth factors [145].

Table 2. Amino acid composition of agrin splice variants at four sites designated c, x, y and z. The y and z site are named A and B in chicken. Previously reported sequence data are listed for chick, rat, mouse and human agrin.

Site	Species	Symbol	Amino acid composition	Reference/Accession #
c	chick	C ₀	EHCVE ······DKPNS	[36]
		C ₇	EHCVEEHRKLLADKPNS	U35613
	mouse	C ₀	EFCVE ······DKPGI	U84407
		man	C ₀	EFCVE ······DKPGT
x	rat	X ₀	RFLDF ······AATGT	[122]
		X ₉	RFLDFWFPFTFFTGAATGT	M64780
	mouse	X ₀	RFLDF ······AATRT	[120]
		X ₉	RFLDFWFPFTFFTGAATRT	M92657
	man	X ₀	RFMDF ······ATSGA	[119]
		X ₉	RFMDFDWFPFITGATSGA	AF016903
y	chick	A ₀	MGESP ····VPHAF	[121]
		A ₄	MGESPKSRKVPHAF	M94271
	rat	Y ₀	LGESP ····VPHTM	[122]
		Y ₄	LGESPKSRKVPHTM	M64780
	mouse	Y ₀	LGESP ····VPHTM	[120]
		Y ₄	LGESPKSRKVPHTM	M92657
man	Y ₀	LGESP ····VPHTV	[119]	
z	chick	B ₀	AVIKS ······EKKALQ	[121]
		B ₈	AVIKSHLSNEIPA ······EKKALQ	[134]
		B ₁₁	AVIKS ······PDALDYP AEPSEKALQ	M94271
		B ₁₉	AVIKSHLSNEIPAPDALDYP AEPSEKALQ	
	rat	Z ₀	AVIES ······EKKALQ	[122]
		Z ₈	AVIESELTNEIPA ······EKKALQ	[120]
		Z ₁₁	AVIES ······PETLDSRALFSEKALQ	[69]
		Z ₁₉	AVIESELTNEIPAPETLDSRALFSEKALQ	
	mouse	Z ₀	AVTES ······EKKALQ	[120]
		Z ₈	AVTESELTNEIPA ······EKKALQ	M92657
		Z ₁₁	AVTES ······PETLDSRALFSEKALQ	
		Z ₁₉	AVTESELTNEIPAPETLDSRALFSEKALQ	
man	Z ₀	NAVTS ······EKKALQ	[119]	

ADDITIONAL HSPGs IN THE GLOMERULAR BASEMENT MEMBRANE

Although agrin and perlecan are the only identified HSPGs in the GBM, several lines of evidence indicate the existence of an additional species. Fractionation of proteoglycans from GBM extracts yielded distinct classes that could be distinguished by density [146]. In addition to the low-density HSPGs (such as perlecan and agrin), high-density HSPGs were described that contain four HS chains and a relatively small core protein. The immunological relatedness of different HSPGs extracted from the GBM, with core proteins of 250, 150 and 75 kDa, suggested that they could be generated by proteolytic processing of perlecan [147]. This finding however did not rule out the possibility that additional HSPG species exist in the GBM. More recently, the presence of a “unique” high-density HSPG with a core protein of 22 kDa in the human GBM was convincingly demonstrated [204,205]. Tryptic fragments from this basement membrane-associated molecule contained amino acid sequences that do not occur in human perlecan and human agrin. The identity and primary structure of this HSPG are yet unknown.

DEVELOPMENTAL CHANGES IN GBM COMPOSITION

Kidney development starts in early embryogenesis by outgrowth of the ureteric bud into the mesenchyme (Figure 13) [21,27,148,149]. The mesenchyme condenses around the tip of the ureteric bud and induces it to elongate and branch, giving rise to the collecting ducts. This epithelial-mesenchymal interaction requires the expression of HSPGs [150].

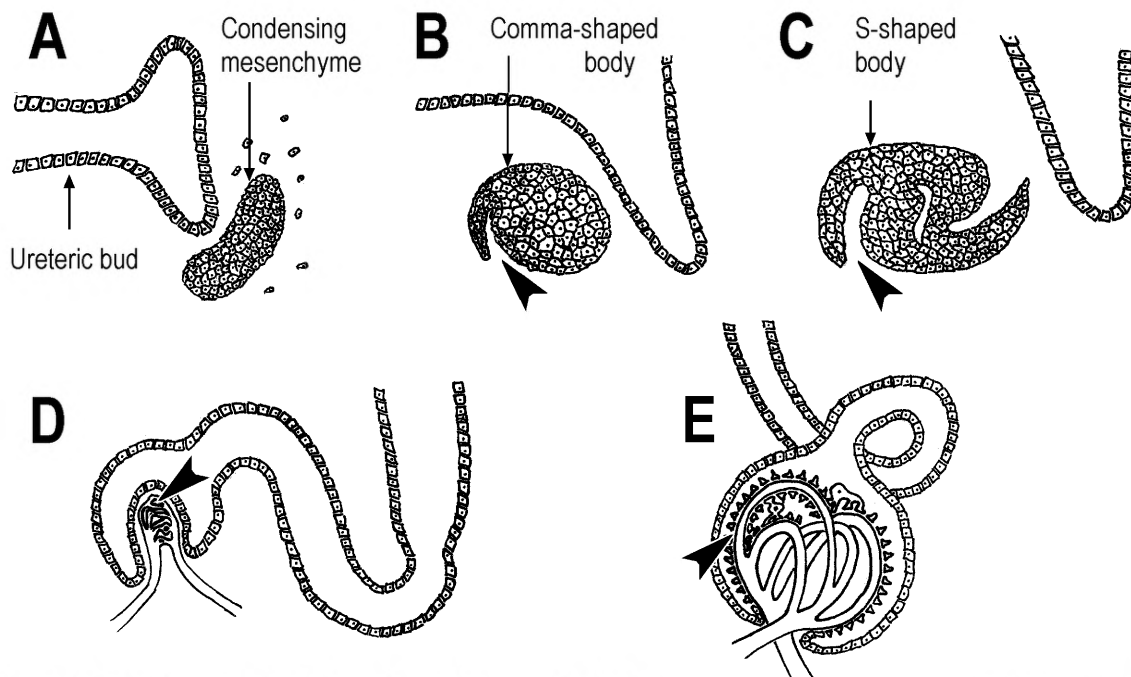


Figure 13. A schematic overview of nephrogenesis. A. Branching of the ureteric bud and aggregation of mesenchymal cells, B. Comma-shaped body stage, C. S-shaped body stage, D. Immature glomerulus stage (formation of capillary loops and tubules), E. Mature glomerulus. Arrowheads indicate the location of the ancestral GBM.

The mesenchymal cells assume epithelial-like characteristics, and start to form vesicles. At this time, collagen IV and laminin are expressed to form an epithelial BM. The laminin chains $\alpha 1$, $\alpha 4$, $\beta 1$ and $\gamma 1$ (laminin-1 and -8) predominate in this ancestral basal lamina [24,27], whereas the collagen network is mainly composed of $\alpha 1$ and $\alpha 2$ chains [151]. Each epithelial vesicle subsequently develops into a comma-shaped and S-shaped body, finally forming a complete nephron including the tubular, glomerular parietal and glomerular visceral epithelium [152,153]. During this process (which is completed postpartum) the $\alpha 1$, $\alpha 4$ and $\beta 1$ laminin chains of the ancestral GBM are gradually substituted by $\alpha 5$ and $\beta 2$ [27,154]. The collagen IV composition alters from $\alpha 1$ - $\alpha 2$ to $\alpha 3$ - $\alpha 4$ - $\alpha 5$ [21,148]. Transient transcription of collagen type II was reported [155]. Also the proteoglycan composition changes between fetal and adult stages, the fetal GBM having a higher CSPG content than the mature GBM. The CSPG bamacan is expressed transiently during the S-shaped body and pre-capillary stage of nephrogenesis, and gradually disappears in the maturing GBM [156]. This is remarkable since bamacan remains present in all other BMs of the nephron [157]. Perlecan transcription and expression was observed from the onset of nephrogenesis [65]. However, it is uncertain how perlecan is glycosylated during different stages of de-

Table 3. Developmental changes in the composition of the GBM

Stage	Collagen IV [21,22,148]	Laminins [27]	Proteoglycans [65,118,139,156-158]
Vesicle	$\alpha 1$, $\alpha 2$	$\alpha_{1,4}$ $\beta 1$ $\gamma 1$	perlecan
Comma-shaped body	$\alpha 1$, $\alpha 2$	$\alpha_{1,4}$ $\beta 1$ $\gamma 1$	perlecan
S-shaped body	$\alpha 1$, $\alpha 2$	$\alpha_{1,4,5}$ $\beta 1$ $\gamma 1$	perlecan, bamacan
Pre-capillary stage	$\alpha 1$, $\alpha 2$	$\alpha_{5,1,4}$ $\beta_{2,1}$ $\gamma 1$	perlecan, agrin, bamacan
Immature glomerulus	$\alpha 1$ - $\alpha 5$	$\alpha_{5,1,4}$ $\beta_{2,1}$ $\gamma 1$	agrin, perlecan, bamacan
Mature glomerulus	$\alpha 3$ - $\alpha 5$	$\alpha 5$ $\beta 2$ $\gamma 1$	agrin >> perlecan

velopment. The time of onset of agrin expression is not known, but agrin mRNA was observed from pre-capillary stages of 15-day old chicken embryos on [118,139,158]. During further kidney development, agrin mRNA is importantly upregulated [119]. Agrin strongly accumulates in the mature GBM, whereas perlecan mainly resides in all other BMs of the nephron [111]. The morphological and compositional changes during nephrogenesis require complex processes of regulation [155,159]. Among the many signaling molecules involved, the transcription factors WT1 and Pax2 play important roles [160,161].

THE ROLE OF GBM HSPGs IN VARIOUS NEPHROPATHIES

The essential role of HSPGs in glomerular ultrafiltration suggested that alterations in their structure or quantity could be a cause of proteinuria under pathogenic conditions. Under experimental conditions this proved indeed possible, as a selective degradation of HS-associated polyanionic sites induced the passage of anionic ferritin [1]. Human diseases marked by a defective permselectivity of the renal ultrafiltration barrier may however originate from more complex mechanisms of pathogenesis. Numerous investigations were performed to investigate the quantity and structure of GBM HSPG in various nephropathies. This section describes both primary renal diseases and secondary nephropathies that are caused by, or lead to, alterations in the structure and composition of GBM HSPGs.

Minimal change disease

Amongst children, minimal change disease (MCD) accounts for 85% of the cases of nephrotic syndrome. Most cases of MCD present before the age of 6 years, typically with edema and a heavy proteinuria of high selectivity. As MCD is successfully treated by steroids the prognosis is good, although multiple relapses of the nephrotic syndrome are common. The glomeruli appear normal by light microscopy but on electron microscopic level, effacement of the epithelial foot processes becomes visible [162,163]. The nephrotic syndrome was shown to be associated with a loss of GBM polyanionic sites [164,165]. Immunological studies showed a reduction of HS in the GBM, while an antibody against the agrin core protein produced undiminished staining [166]. This suggests that the HS chains may be altered in structure or reduced in length or number. The pathogenesis is still elusive [165,167].

Focal segmental glomerulosclerosis

Focal segmental glomerulosclerosis (FSGS) is a histological appearance found in patients with a persistent, steroid-resistant nephrotic syndrome. Progression to end-stage renal failure is common, necessitating kidney transplantation. Recurrence of the disease after renal transplantation can be observed. This suggests the involvement of a circulating factor [162,163]. Morphologic features of FSGS biopsies include sclerotic lesions of focal (i.e. not all glomeruli are affected) and segmental (i.e. not the whole glomerulus is affected) nature. When the affected segments are analysed by electron microscopy, the GBM shows a thickened and laminated morphology. Podocytes, often adhering to the Bowman's capsule, become detached from the GBM. Basic fibroblast growth factor (bFGF) is possibly involved in the mechanism of pathogenesis, since the prolonged exposure of glomeruli to this molecule induced FSGS in rats [168]. Cellular signalling by bFGF requires its activation by binding to a specific structure in HS, indicating a speculative role for HSPGs in the process.

Congenital nephrotic syndrome of the Finnish type

The congenital nephrotic syndrome of the Finnish type (CNS-F) is a rare disorder in most populations, with the highest incidence in Finland (1 per 8000 deliveries) [169]. In line with its autosomal recessive mode of inheritance, the disorder is often associated with a consanguinous familial background. Typical clinical features include a premature delivery with enlarged placenta, proteinuria starting in fetal stages as demonstrated by the increase of α -fetoprotein in the amniotic fluid, and edema observed immediately postpartum or soon after birth [162,163,170]. Morphological abnormalities include enlarged glomeruli and increased mesangial cells and matrix. In electron microscopy the GBM shows a normal width [171], but the epithelial filtration slits are reduced in number [172,173]. Although a causal role of HSPGs in the pathogenesis of CNS-F has been suggested [174,175], several other investigations have contradicted this hypothesis [176–178]. Linkage analysis in both Finnish and non-Finnish pedigrees mapped the responsible gene to the long arm of chromosome 19 (locus 19q13.1) [179,180]. Recently, this novel gene was characterized and named nephrin [181]. The nephrin gene product is a cell surface protein expressed specifically in glomerular slit diaphragms, suggesting an important role in renal ultrafiltration [181]. The possibility that nephrin is a HSPG has not yet been excluded.

Denys Drash Syndrome

Denys-Drash Syndrome (DDS) is a severe congenital disease characterized by renal and gonadal abnormalities, including the appearance of Wilms' tumors and severe nephrotic syndrome [182]. The cause of DDS is a mutation that affects the DNA-binding domains of the WT-1 gene product, a transcription factor that is expressed during the mesenchymal-to-epithelial transition of developing kidney and gonads [183,184]. In the mature nephron, the expression of WT-1 is sustained in the podocytes. To investigate the involvement of HSPG in the development of the nephrotic syndrome, a patient with DDS was analyzed for glycosaminoglycan content. Although the total glycosaminoglycan content was normal, the GBM in DDS showed a reduced HS content, and CS levels appeared to be elevated [185]. Immunoreactivity of the agrin core protein was of normal level [111, 185].

Diabetic glomerulopathy

Diabetic nephropathy is perhaps the most illustrative example of a disease where proteinuria is associated with alterations in HSPG composition of the GBM. Patients with diabetes mellitus are at high risk of developing nephropathy as a secondary effect. About 40% of diabetic patients develop microalbuminuria after 10–15 years, which can subsequently progress into overt proteinuria. Especially in juvenile-onset diabetes end-stage renal failure develops frequently. Most cases of diabetic nephropathy originate from structural alterations in the glomerulus (diabetic glomerulopathy). Glomeruli typically show a substantial widening of the GBM and expansion of the mesangial matrix. This reflects the increased production of matrix components such as collagens, laminin and fibronectin [187–189]. The thickened diabetic GBM was also shown to contain the CSPG biglycan, which is abnormal for the mature GBM [190]. Numerous independent studies have demonstrated a relative decrease of HSPG in the diabetic GBM and in the matrix produced by cultured glomerular epithelial cells in medium containing high glucose levels [189,191–198]. Poorly understood is the interesting finding that heparin administration has a protective effect on the structure and function of diabetic glomeruli. Heparin treatment prevented the thickening of the GBM, the decrease in anionic content and the increase in albumin excretion [188,199–201]. Perlecan transcription is inhibited by high glucose [195], but a major impact of this on GBM permselectivity is not likely. More important, agrin may be down-regulated in diabetes as shown by a reduced staining of its core protein [189,191]. Elucida-

tion of the molecular mechanisms that influence agrin expression in diabetic glomerulopathy will be of great interest to gain insight in its mode of pathogenesis.

Postexercise proteinuria

The induction of proteinuria by maximal exercise is common in healthy subjects [202]. The mechanism that underlies this phenomenon is largely unknown, but data suggest that both increased glomerular permeability and reduced tubular uptake are involved [203]. The proteinuria is associated with a temporary decrease in the electrostatic charge of the GBM [202] and urinary excretion of an unidentified GBM HSPG [204]. This HSPG contains a 22 kDa core protein and is unrelated to perlecan and agrin. Standardized exercise protocols may provide a powerful tool to investigate if altered expression of this small HSPG could be involved in various types of nephropathy, without the need for a kidney biopsy [204,205].

AIM OF THE STUDY AND SCOPE OF THIS THESIS

At the start of this investigation, clear evidence had convincingly demonstrated the importance of heparan sulfate proteoglycans in the GBM for renal ultrafiltration. Perlecan was at that time the only HSPG known to occur in basement membranes. Consistently with this, perlecan was hypothesized to be the major determinant of the polyanionic charge of the GBM. The availability of the complete cDNA structure of human perlecan facilitated several new approaches to study the value of this hypothesis. These approaches include the production of recombinant domains of human perlecan for functional studies, and mutation detection in perlecan mRNA in patients with nephrotic syndromes. Besides these directions of research, the question arose whether additional HSPG species could be present in the GBM.

The production of individual domains of human perlecan as recombinant proteins was performed in three different *in vitro* expression systems. First, the baculovirus expression system was used for expression of perlecan domains I and II (Chapter 2). The host cell line *Spodoptera frugiperda* SF21 supports a wide range of post-translational modifications typical for higher eukaryotes. Consistent with this, the produced recombinant molecule contained glycosaminoglycan side chains, identified as chondroitin sulfate. The results provide experimental evidence for a functional role of the perlecan SEA module in glycosaminoglycan attachment.

Chapter 3 describes the biosynthesis of two perlecan fragments in the *Pichia pastoris* (yeast) expression system. The recombinant proteins include domain II that shares similarity with the low-density-lipoprotein receptor. These proteins were used to investigate the possible role of perlecan in lipoprotein binding.

As described in Chapter 4, a bacterial fusion protein was engineered containing perlecan domains I and II. The hybrid protein was purified and used for immunization of mice. We generated a novel monoclonal antibody 95J10 that recognizes the perlecan core protein. This antibody was used to investigate the spatial distribution of perlecan in the kidney and various other tissues. Using immuno-electron microscopy we found that perlecan is absent from many regions of the GBM (and hence it cannot be the major determinant of its charge-selective permeability). Another monoclonal antibody, that recognizes purified GBM HSPG, produced a clearly different staining suggesting the existence of an unrelated proteoglycan. Given its high expression in the GBM, the identity of this molecule was of great interest to gain insight in the molecular mechanisms of selective ultrafiltration.

Prompted by the detection of agrin-like oligopeptide structures in HSPGs from bovine kidney and the finding that agrin is a HSPG [112], we investigated the possible relationship

between GBM HSPG and agrin. Various experimental approaches, including immunoelectron microscopy, were applied to identify agrin as a HSPG of the GBM. The relative concentrations of agrin and perlecan were compared (Chapter 5).

To gain insight in the structure of this GBM HSPG, we next elucidated the complete cDNA structure of the mature agrin core protein (Chapter 6). The derived protein structure allowed predictions for structure-function relationships in accordance with the structures known for rat and chick agrin. Furthermore we used a cDNA probe to determine transcription levels in multiple human tissues, and compared these data with the accumulation of agrin immunoreactivity in the BM of these organs.

In a previous investigation, our laboratory generated a large panel of monoclonal antibodies against HSPG isolated from the GBM. In Chapter 7 we investigated if these recognize a series of 19 different recombinant fragments of human agrin. Using these recombinant peptides, we localized the epitopes recognised by 25 mAbs on distinct regions of the agrin core protein. The fusion protein containing the N-terminal agrin domain (the laminin-binding domain) showed affinity for immobilised laminin. This activity was exploited to visualize laminin-associated binding sites for agrin in the kidney cortex. Furthermore we analysed the cellular origin of agrin in the GBM.

One function of HSPGs is the binding and activation of basic fibroblast growth factor (bFGF). In Chapter 8 we describe a study to assess the role of bFGF in the pathogenesis of focal segmental glomerulosclerosis (FSGS). Increased concentrations of bFGF in some patients with FSGS suggest a possible role for this growth factor in the development of proteinuria. Chapter 9 concludes this thesis with a survey and indications for future research.

REFERENCES

1. Kanwar YS, Linker A and Farquhar MG (1980) Increased permeability of the glomerular basement membrane to ferritin after removal of glycosaminoglycans (heparan sulfate) by enzyme digestion, *J. Cell Biol.* 86:688–693.
2. Hassell JR, Robey PG, Barrach HJ, Wilczek J, Rennard SI and Martin GR (1980) Isolation of a heparan sulfate-containing proteoglycan from basement membrane, *Proc. Natl. Acad. Sci. USA* 77:4494–4498.
3. Chan FL and Inoue S (1994) Lamina lucida of basement membrane: an artefact, *Microsc. Res. Tech.* 28:48–59.
4. Kanwar YS, Liu ZZ, Kashihara N and Wallner EI (1991) Current status of the structural and functional basis of glomerular filtration and proteinuria, *Semin. Nephrol.* 11:390–413.
5. van Kuppevelt TH and Veerkamp JH (1994) Application of cationic probes for the ultrastructural localization of proteoglycans in basement membranes, *Microsc. Res. Tech.* 28:125–140.
6. Kanwar YS and Farquhar MG (1979) Anionic sites in the glomerular basement membrane. *In vivo* and *in vitro* localization to the laminae rarae by cationic probes, *J. Cell Biol.* 81:137–153.
7. van den Born J, van den Heuvel LP, Bakker MA, Veerkamp JH, Assmann KJ and Berden JH (1992) A monoclonal antibody against GBM heparan sulfate induces an acute selective proteinuria in rats, *Kidney Int.* 41:115–123.
8. Goode NP, Shires M and Davison AM (1996) The glomerular basement membrane charge-selectivity barrier: an oversimplified concept? *Nephrol. Dial. Transplant.* 11:1714–1716.
9. Kanwar YS and Rosenzweig LJ (1982) Altered glomerular permeability as a result of focal detachment of the visceral epithelium, *Kidney Int.* 21:565–574.
10. Orkin RW, Gehron P, McGoodwin EB, Martin GR, Valentine T and Swarm R (1977) A murine tumor producing a matrix of basement membrane, *J. Exp. Med.* 145:204–220.
11. Paulsson M (1992) Basement membrane proteins: structure, assembly, and cellular interactions, *Crit. Rev. Biochem. Mol. Biol.* 27:93–127.
12. Aumailley M (1995) Structure and supra-molecular organization of basement membranes, *Kidney Int.* 47:S4–S7.
13. Hudson BG, Reeders ST and Tryggvason K

- (1993) Type IV collagen: structure, gene organization, and role in human diseases. Molecular basis of Goodpasture and Alport syndromes and diffuse leiomyomatosis, *J. Biol. Chem.* 268:26033–26036.
14. Yurchenco PD and Schittny JC (1990) Molecular architecture of basement membranes, *FASEB J.* 4:1577–1590.
 15. Mariyama M, Leinonen A, Mochizuki T, Tryggvason K and Reeders ST (1994) Complete primary structure of the human $\alpha 3(\text{IV})$ collagen chain. Coexpression of the $\alpha 3(\text{IV})$ and $\alpha 4(\text{IV})$ collagen chains in human tissues, *J. Biol. Chem.* 269:23013–23017.
 16. Leinonen A, Mariyama M, Mochizuki T, Tryggvason K and Reeders ST (1994) Complete primary structure of the human type IV collagen $\alpha 4(\text{IV})$ chain. Comparison with structure and expression of the other $\alpha(\text{IV})$ chains, *J. Biol. Chem.* 269:26172–26177.
 17. Zhou J, Hertz JM, Leinonen A and Tryggvason K (1992) Complete amino acid sequence of the human $\alpha 5(\text{IV})$ collagen chain and identification of a single-base mutation in exon 23 converting glycine 521 in the collagenous domain to cysteine in an Alport syndrome patient, *J. Biol. Chem.* 267:12475–12481.
 18. Hudson BG, Kalluri R and Tryggvason K (1994) Pathology of glomerular basement membrane nephropathy, *Curr. Opin. Nephrol. Hypertens.* 3:334–339.
 19. Tryggvason K, Zhou J, Hostikka SL and Shows TB (1993) Molecular genetics of Alport syndrome, *Kidney Int.* 43:38–44.
 20. Lemmink HH, Schroder CH, Monnens LA and Smeets HJ (1997) The clinical spectrum of type IV collagen mutations, *Hum. Mutat.* 9:477–499.
 21. Miner JH and Sanes JR (1994) Collagen IV $\alpha 3$, $\alpha 4$, and $\alpha 5$ chains in rodent basal laminae: sequence, distribution, association with laminins, and developmental switches, *J. Cell Biol.* 127:879–891.
 22. Kalluri R, Shield CF, Todd P, Hudson BG and Neilson EG (1997) Isoform switching of type IV collagen is developmentally arrested in X-linked Alport syndrome leading to increased susceptibility of renal basement membranes to endoproteolysis, *J. Clin. Invest.* 99:2470–2478.
 23. Kanwar YS (1984) Biophysiology of glomerular filtration and proteinuria, *Lab. Invest.* 51:7–21
 24. Burgeson RE, Chiquet M, Deutzmann R, Ekblom P, Engel J, Kleinman H, Martin GR, Meneguzzi G, Paulsson M and Sanes J (1994) A new nomenclature for the laminins, *Matrix Biol.* 14:209–211.
 25. Timpl R, Rohde H, Risteli L, Ott U, Robey PG and Martin GR (1982) Laminin, *Methods Enzymol.* 82 Pt A: 831–838
 26. Beck K, Hunter I and Engel J (1990) Structure and function of laminin: anatomy of a multidomain glycoprotein, *FASEB J.* 4:148–160.
 27. Miner JH, Patton BL, Lentz SI, Gilbert DJ, Snider WD, Jenkins NA, Copeland NG and Sanes JR (1997) The laminin α chains: expression, developmental transitions, and chromosomal locations of $\alpha 1$ –5, identification of heterotrimeric laminins 8–11, and cloning of a novel $\alpha 3$ isoform, *J. Cell Biol.* 137:685–701.
 28. Timpl R and Brown JC (1994) The laminins, *Matrix Biol.* 14:275–281.
 29. Ryan MC, Christiano AM, Engvall E, Wewer UM, Miner JH, Sanes JR and Burgeson RE (1996) The functions of laminins: lessons from *in vivo* studies, *Matrix Biol.* 15:369–381.
 30. Miner JH, Lewis RM and Sanes JR (1995) Molecular cloning of a novel laminin chain, $\alpha 5$, and widespread expression in adult mouse tissues, *J. Biol. Chem.* 270:28523–28526.
 31. Iivanainen A, Vuolteenaho R, Sainio K, Eddy R, Shows TB, Sariola H and Tryggvason K (1995) The human laminin $\beta 2$ chain (S-laminin): structure, expression in fetal tissues and chromosomal assignment of the LAMB2 gene, *Matrix Biol.* 14:489–497.
 32. Kallunki T, Ikonen J, Chow LT, Kallunki P and Tryggvason K (1991) Structure of the human laminin B2 chain gene reveals extensive divergence from the laminin B1 chain gene, *J. Biol. Chem.* 266:221–228.
 33. Patton BL, Chiu AY and Sanes JR (1998) Synaptic laminin prevents glial entry into the synaptic cleft, *Nature* 393:698–701.
 34. Noakes PG, Miner JH, Gautam M, Cunningham JM, Sanes JR and Merlie JP (1995) The renal glomerulus of mice lacking s-laminin/laminin $\beta 2$: nephrosis despite molecular compensation by laminin $\beta 1$, *Nat. Genet.* 10:400–406.
 35. Paulsson M, Aumailley M, Deutzmann R, Timpl R, Beck K and Engel J (1987) Laminin-nidogen complex. Extraction with chelating agents and structural characteriza-

- tion, *Eur. J. Biochem.* 166:11–19.
36. Denzer AJ, Brandenberger R, Gesemann M, Chiquet M and Rugg MA (1997) Agrin binds to the nerve-muscle basal lamina via laminin, *J. Cell Biol.* 137:671–683.
 37. Olsen DR, Nagayoshi T, Fazio MJ, Mattei MG, Passage E, Weil D, Timpl R, Chu ML and Uitto J (1998) Human nidogen: cDNA cloning, cellular expression, and mapping of the gene to chromosome 1q43, *Am. J. Hum. Genet.* 44:876
 38. Mayer U, Nischt R, Poschl E, Mann K, Fukuda K, Gerl M, Yamada Y and Timpl R (1993) A single EGF-like motif of laminin is responsible for high affinity nidogen binding, *EMBO J.* 12:1879–1885.
 39. Aumailley M, Battaglia C, Mayer U, Reinhardt D, Nischt R, Timpl R and Fox JW (1993) Nidogen mediates the formation of ternary complexes of basement membrane components, *Kidney Int.* 43:7–12.
 40. Mayer U, Mann K, Fessler LI, Fessler JH and Timpl R (1997) Drosophila laminin binds to mammalian nidogen and to heparan sulfate proteoglycan, *Eur. J. Biochem.* 245:745–750.
 41. Yurchenco PD and O'Rear JJ (1994) Basal lamina assembly, *Curr. Opin. Cell Biol.* 6:674–681.
 42. Sasaki T, Gohring W, Mann K, Maurer P, Hohenester E, Knauper V, Murphy G and Timpl R (1997) Limited cleavage of extracellular matrix protein BM-40 by matrix metalloproteinases increases its affinity for collagens, *J. Biol. Chem.* 272:9237–9243.
 43. Maurer P, Gohring W, Sasaki T, Mann K, Timpl R and Nischt R (1997) Recombinant and tissue-derived mouse BM-40 bind to several collagen types and have increased affinities after proteolytic activation, *Cell Mol. Life Sci.* 53:478–484.
 44. Hohenester E, Maurer P and Timpl R (1997) Crystal structure of a pair of follistatin-like and EF-hand calcium-binding domains in BM-40, *EMBO J.* 16:3778–3786.
 45. Chung CY and Erickson HP (1997) Glycosaminoglycans modulate fibronectin matrix assembly and are essential for matrix incorporation of tenascin-C, *J. Cell Sci.* 110:1413–1419.
 46. Deryugina EI and Bourdon MA (1996) Tenascin mediates human glioma cell migration and modulates cell migration on fibronectin, *J. Cell Sci.* 109:643–652.
 47. Tran H, VanDusen WJ and Argraves WS (1997) The self-association and fibronectin-binding sites of fibulin-1 map to calcium-binding epidermal growth factor-like domains, *J. Biol. Chem.* 272:22600–22606.
 48. Sasaki T, Gohring W, Pan TC, Chu ML and Timpl R (1995) Binding of mouse and human fibulin-2 to extracellular matrix ligands, *J. Mol. Biol.* 254:892–899.
 49. Malik KT, Poirier V, Ivins SM and Brown KW (1994) Autoregulation of the human WT1 gene promoter, *FEBS Lett.* 349:75–78.
 50. Brown JC, Sasaki T, Gohring W, Yamada Y and Timpl R (1997) The C-terminal domain V of perlecan promotes beta1 integrin-mediated cell adhesion, binds heparin, nidogen and fibulin-2 and can be modified by glycosaminoglycans, *Eur. J. Biochem.* 250:39–46.
 51. Couchman JR, Kapoor R, Sthanam M and Wu RR (1996) Perlecan and basement membrane-chondroitin sulfate proteoglycan (bamacan) are two basement membrane chondroitin / dermatan sulfate proteoglycans in the Engelbreth-Holm-Swarm tumor matrix, *J. Biol. Chem.* 271:9595–9602.
 52. Wu RR and Couchman JR (1997) cDNA cloning of the basement membrane chondroitin sulfate proteoglycan core protein, bamacan: a five domain structure including coiled-coil motifs, *J. Cell Biol.* 136:433–444.
 53. Salmivirta M, Lidholt K and Lindahl U (1996) Heparan sulfate: a piece of information, *FASEB J.* 10:1270–1279.
 54. Dixon J, Loftus SK, Gladwin AJ, Scambler PJ, Wasmuth JJ and Dixon MJ (1995) Cloning of the human heparan sulfate N-deacetylase/N-sulfotransferase gene from the Treacher Collins Syndrome candidate region at 5q32–q33.1, *Genomics* 26:239–244.
 55. Bourdon MA, Krusius T, Campbell S, Schwartz NB and Ruoslahti E (1987) Identification and synthesis of a recognition signal for the attachment of glycosaminoglycans to proteins, *Proc. Natl. Acad. Sci. USA* 84:3194–3198.
 56. Dolan M, Horchar T, Rigatti B and Hassell JR (1997) Identification of sites in domain I of perlecan that regulate heparan sulfate synthesis, *J. Biol. Chem.* 272:4316–4322.
 57. Zhang L and Esko JD (1994) Amino acid determinants that drive heparan sulfate assembly in a proteoglycan, *J. Biol. Chem.* 269:19295–19299.
 58. Zhang L, David G and Esko JD (1995) Repetitive Ser-Gly sequences enhance heparan sulfate assembly in proteoglycans, *J. Biol. Chem.* 270:27127–27135.
 59. Bork P and Patthy L (1995) The SEA module: a new extracellular domain associated

- with O-glycosylation, *Protein Sci.* 4:1421–1425.
60. Kato M, Koike Y, Ito Y, Suzuki S and Kimata K (1987) Multiple forms of heparan sulfate proteoglycans in the Engelbreth-Holm-Swarm mouse tumor. The occurrence of high-density forms bearing both heparan sulfate and chondroitin sulfate side chains, *J. Biol. Chem.* 262:7180–7188
 61. Groffen AJ, Buskens CA, Tryggvason K, Veerkamp JH, Monnens LA and van den Heuvel LP (1996) Expression and characterization of human perlecan domains I and II synthesized by baculovirus-infected insect cells, *Eur. J. Biochem.* 241:827–834.
 62. Costell M, Mann K, Yamada Y and Timpl R (1997) Characterization of recombinant perlecan domain I and its substitution by glycosaminoglycans and oligosaccharides, *Eur. J. Biochem.* 243:115–121.
 63. Kokenyesi R and Silbert JE (1995) Formation of heparan sulfate or chondroitin/dermatan sulfate on recombinant domain I of mouse perlecan expressed in Chinese hamster ovary cells, *Biochem. Biophys. Res. Commun.* 211:262–267.
 64. SundarRaj N, Fite D, Ledbetter S, Chakravarti S and Hassell JR (1995) Perlecan is a component of cartilage matrix and promotes chondrocyte attachment, *J. Cell Sci.* 108:2663–2672.
 65. Handler M, Yurchenco PD and Iozzo RV (1997) Developmental expression of perlecan during murine embryogenesis, *Dev. Dyn.* 210:130–145.
 66. Gallagher JT, Lyon M and Steward WP (1986) Structure and function of heparan sulphate proteoglycans, *Biochem. J.* 236:313–325.
 67. Witt DP and Lander AD (1994) Differential binding of chemokines to glycosaminoglycan subpopulations, *Curr. Biol.* 4:394–400.
 68. Taipale J and Keski-Oja J (1997) Growth factors in the extracellular matrix, *FASEB J.* 11:51–59.
 69. O'Toole JJ, Deyst KA, Bowe MA, Nastuk MA, McKechnie BA and Fallon JR (1996) Alternative splicing of agrin regulates its binding to heparin α -dystroglycan, and the cell surface, *Proc. Natl. Acad. Sci. USA* 93:7369–7374.
 70. Cardin AD and Weintraub HJ (1989) Molecular modeling of protein-glycosaminoglycan interactions, *Arteriosclerosis* 9:21–32.
 71. Jackson RL, Busch SJ and Cardin AD (1991) Glycosaminoglycans: molecular properties, protein interactions, and role in physiological processes, *Physiol. Rev.* 71:481–539.
 72. Hileman RE, Fromm JR, Weiler JM and Lindhardt RJ (1998) Glycosaminoglycan-protein interactions: definition of consensus sites in glycosaminoglycan binding proteins, *Bioessays* 20:156–167.
 73. Turnbull JE, Fernig DG, Ke Y, Wilkinson MC and Gallagher JT (1992) Identification of the basic fibroblast growth factor binding sequence in fibroblast heparan sulfate, *J. Biol. Chem.* 267:10337–10341.
 74. Pejler G, Backstrom G, Lindahl U, Paulsson M, Dziadek M, Fujiwara S and Timpl R (1987) Structure and affinity for antithrombin of heparan sulfate chains derived from basement membrane proteoglycans, *J. Biol. Chem.* 262:5036–5043.
 75. Parthasarathy N, Goldberg IJ, Sivaram P, Mulloy B, Flory DM and Wagner WD (1994) Oligosaccharide sequences of endothelial cell surface heparan sulfate proteoglycan with affinity for lipoprotein lipase, *J. Biol. Chem.* 269:22391–22396.
 76. Paulsson M, Yurchenco PD, Ruben GC, Engel J and Timpl R (1987) Structure of low density heparan sulfate proteoglycan isolated from a mouse tumor basement membrane, *J. Mol. Biol.* 197:297–313.
 77. Noonan DM, Fulle A, Valente P, Cai S, Horigan E, Sasaki M, Yamada Y and Hassell JR (1991) The complete sequence of perlecan, a basement membrane heparan sulfate proteoglycan, reveals extensive similarity with laminin A chain, low density lipoprotein-receptor, and the neural cell adhesion molecule, *J. Biol. Chem.* 266:22939–22947.
 78. Iozzo RV and Hacopian N (1990) Myristoylation of heparan sulfate proteoglycan and proteins occurs post-translationally in human colon carcinoma cells, *Biochem. Biophys. Res. Commun.* 172:905–912.
 79. Kallunki P, Eddy RL, Byers MG, Kestila M, Shows TB and Tryggvason K (1991) Cloning of human heparan sulfate proteoglycan core protein, assignment of the gene (HSPG2) to 1p36.1–p35 and identification of a BamHI restriction fragment length polymorphism, *Genomics* 11:389–396.
 80. Dodge GR, Kovalszky I, Chu ML, Hassell JR, McBride OW, Yi HF and Iozzo RV (1991) Heparan sulfate proteoglycan of human colon: partial molecular cloning, cellular expression, and mapping of the gene (HSPG2) to the short arm of human chromo-

- some 1, *Genomics* 10:673–680.
81. Cohen IR, Grassel S, Murdoch AD and Iozzo RV (1993) Structural characterization of the complete human perlecan gene and its promoter, *Proc. Natl. Acad. Sci. USA* 90:10404–10408.
 82. Kallunki P and Tryggvason K (1992) Human basement membrane heparan sulfate proteoglycan core protein: a 467-kD protein containing multiple domains resembling elements of the low density lipoprotein receptor, laminin, neural cell adhesion molecules, and epidermal growth factor, *J. Cell Biol.* 116:559–571.
 83. Murdoch AD, Dodge GR, Cohen I, Tuan RS and Iozzo RV (1992) Primary structure of the human heparan sulfate proteoglycan from basement membrane (HSPG2/perlecan). A chimeric molecule with multiple domains homologous to the low density lipoprotein receptor, laminin, neural cell adhesion molecules, and epidermal growth factor, *J. Biol. Chem.* 267:8544–8557.
 84. Iozzo RV, Cohen IR, Grassel S and Murdoch AD (1994) The biology of perlecan: the multifaceted heparan sulphate proteoglycan of basement membranes and pericellular matrices, *Biochem. J.* 302:625–639.
 85. Murdoch AD and Iozzo RV (1993) Perlecan: the multidomain heparan sulphate proteoglycan of basement membrane and extracellular matrix, *Virchows Arch. A. Pathol. Anat. Histochem.* 423:237–242.
 86. Murdoch AD, Liu B, Schwarting R, Tuan RS and Iozzo RV (1994) Widespread expression of perlecan proteoglycan in basement membranes and extracellular matrices of human tissues as detected by a novel monoclonal antibody against domain III and by in situ hybridization, *J. Histochem. Cytochem.* 42:239–249.
 87. Yurchenco PD, Cheng YS and Ruben GC (1987) Self-assembly of a high molecular weight basement membrane heparan sulfate proteoglycan into dimers and oligomers, *J. Biol. Chem.* 262:17668–17676.
 88. Battaglia C, Mayer U, Aumailley M and Timpl R (1992) Basement-membrane heparan sulfate proteoglycan binds to laminin by its heparan sulfate chains and to nidogen by sites in the protein core, *Eur. J. Biochem.* 208:359–366.
 89. heremans A, de Cock B, Cassiman JJ, Van den Berghe H and David G (1990) The core protein of the matrix-associated heparan sulfate proteoglycan binds to fibronectin, *J. Biol. Chem.* 265:8716–8724.
 90. Laurie GW, Bing JT, Kleinman HK, Hassell JR, Aumailley M, Martin GR and Feldmann RJ (1986) Localization of binding sites for laminin, heparan sulfate proteoglycan and fibronectin on basement membrane (type IV) collagen, *J. Mol. Biol.* 189:205–216.
 91. Hayashi K, Madri JA and Yurchenco PD (1992) Endothelial cells interact with the core protein of basement membrane perlecan through β 1 and β 3 integrins: an adhesion modulated by glycosaminoglycan, *J. Cell Biol.* 119:945–959.
 92. Chakravarti S, Horchar T, Jefferson B, Laurie GW and Hassell JR (1995) Recombinant domain III of perlecan promotes cell attachment through its RGDS sequence, *J. Biol. Chem.* 270:404–409.
 93. Klein G, Conzelmann S, Beck S, Timpl R and Muller CA (1994) Perlecan in human bone marrow: a growth-factor-presenting, but anti-adhesive, extracellular matrix component for hematopoietic cells, *Matrix Biol.* 14:457–465.
 94. Aviezer D, Hecht D, Safran M, Eisinger M, David G and Yayon A (1994) Perlecan, basal lamina proteoglycan, promotes basic fibroblast growth factor-receptor binding, mitogenesis, and angiogenesis, *Cell* 79:1005–1013.
 95. Guillonneau X, Tassin J, Berrou E, Bryckaert M, Courtois Y and Mascarelli F (1996) *In vitro* changes in plasma membrane heparan sulfate proteoglycans and in perlecan expression participate in the regulation of fibroblast growth factor 2 mitogenic activity, *J. Cell. Physiol.* 166:170–187.
 96. Vigny M, Ollier-Hartmann MP, Lavigne M, Fayein N, Jeanny JC, Laurent M and Courtois Y (1988) Specific binding of basic fibroblast growth factor to basement membrane-like structures and to purified heparan sulfate proteoglycan of the EHS tumor, *J. Cell. Physiol.* 137:321–328.
 97. Aviezer D, Levy E, Safran M, Svahn C, Buddecke E, Schmidt A, David G, Vlodaysky I and Yayon A (1994) Differential structural requirements of heparin and heparan sulfate proteoglycans that promote binding of basic fibroblast growth factor to its receptor, *J. Biol. Chem.* 269:114–121.
 98. Vlodaysky I, Miao HQ, Medalion B, Danagher P and Ron D (1996) Involvement of heparan sulfate and related molecules in sequestration and growth promoting activity of fibroblast growth factor, *Cancer Metasta-*

- sis Rev.* 15:177–186.
99. Adatia R, Albini A, Carlone S, Giunciuglio D, Benelli R, Santi L and Noonan DM (1997) Suppression of invasive behavior of melanoma cells by stable expression of anti-sense perlecan cDNA, *Ann. Oncol.* 8:1257–1261.
 100. Mathiak M, Yenisey C, Grant DS, Sharma B and Iozzo RV (1997) A role for perlecan in the suppression of growth and invasion in fibrosarcoma cells, *Cancer Res.* 57:2130–2136.
 101. Aviezer D, Iozzo RV, Noonan DM and Yayon A (1997) Suppression of autocrine and paracrine functions of basic fibroblast growth factor by stable expression of perlecan antisense cDNA, *Mol. Cell Biol.* 17:1938–1946.
 102. Thompson SA, Higashiyama S, Wood K, Pollit NS, Damm D, McEnroe G, Garrick B, Ashton N, Lau K, Hancock N, Klagsbrun M and Abraham JA (1994) Characterization of sequences within heparin-binding EGF-like growth factor that mediate interaction with heparin, *J. Biol. Chem.* 269:2541–2549.
 103. Sakata H, Stahl SJ, Taylor WG, Rosenberg JM, Sakaguchi K, Wingfield PT and Rubin JS (1997) Heparin binding and oligomerization of hepatocyte growth factor/scatter factor isoforms. Heparan sulfate glycosaminoglycan requirement for Met binding and signaling, *J. Biol. Chem.* 272:9457–9463.
 104. DiGabriele AD, Lax I, Chen DI, Svahn CM, Jaye M, Schlessinger J and Hendrickson WA (1998) Structure of a heparin-linked biologically active dimer of fibroblast growth factor, *Nature* 396:812–817.
 105. Eisenberg S, Sehayek E, Olivecrona T and Vlodavsky I (1992) Lipoprotein lipase enhances binding of lipoproteins to heparan sulfate on cell surfaces and extracellular matrix, *J. Clin. Invest.* 90:2013–2021.
 106. Mulder M, Lombardi P, Jansen H, van Berkel TJ, Frants RR and Havekes LM (1993) Low density lipoprotein receptor internalizes low density and very low density lipoproteins that are bound to heparan sulfate proteoglycans via lipoprotein lipase, *J. Biol. Chem.* 268:9369–9375.
 107. Misra KB, Kim KC, Cho S, Low MG and Bensadoun A (1994) Purification and characterization of adipocyte heparan sulfate proteoglycans with affinity for lipoprotein lipase, *J. Biol. Chem.* 269:23838–23844.
 108. Berryman DE and Bensadoun A (1995) Heparan sulfate proteoglycans are primarily responsible for the maintenance of enzyme activity, binding, and degradation of lipoprotein lipase in Chinese hamster ovary cells, *J. Biol. Chem.* 270:24525–24531.
 109. Mulder M, Lombardi P, Jansen H, van Berkel TJ, Frants RR and Havekes LM (1992) Heparan sulphate proteoglycans are involved in the lipoprotein lipase-mediated enhancement of the cellular binding of very low density and low density lipoproteins, *Biochem. Biophys. Res. Commun.* 185:582–587.
 110. Groffen AJ, Hop FW, Tryggvason K, Dijkman H, Assmann K, Veerkamp JH, Monnens LA and van den Heuvel LP (1997) Evidence for the existence of multiple heparan sulfate proteoglycans in the human glomerular basement membrane and mesangial matrix, *Eur. J. Biochem.* 247:175–182.
 111. Groffen AJ, Ruegg MA, Dijkman H, van de Velden TJ, Buskens CA, van den Born J, Assmann K, Monnens LA, Veerkamp JH and van den Heuvel LP (1998) Agrin is a major heparan sulfate proteoglycan in the human glomerular basement membrane, *J. Histochem. Cytochem.* 46:19–27.
 112. Tsen G, Halfter W, Kroger S and Cole GJ (1995) Agrin is a heparan sulfate proteoglycan, *J. Biol. Chem.* 270:3392–3399.
 113. Denzer AJ, Gesemann M and Ruegg MA (1996) Diverse functions of the extracellular matrix molecule agrin, *Sem. Neurosci.* 8:357–366.
 114. Ruegg MA and Bixby JL (1998) Agrin orchestrates synaptic differentiation at the vertebrate neuromuscular junction, *Trends. Neurosci.* 21:22–27.
 115. Cohen NA, Kaufmann WE, Worley PF and Rupp F (1997) Expression of agrin in the developing and adult rat brain, *Neuroscience* 76:581–596.
 116. Gautam M, Noakes PG, Moscoso L, Rupp F, Scheller RH, Merlie JP and Sanes JR (1996) Defective neuromuscular synaptogenesis in agrin-deficient mutant mice, *Cell* 85:525–535.
 117. Denzer AJ, Hauser DM, Gesemann M and Ruegg MA (1997) Synaptic differentiation: the role of agrin in the formation and maintenance of the neuromuscular junction, *Cell Tissue Res.* 290:357–365.
 118. Godfrey EW (1991) Comparison of agrin-like proteins from the extracellular matrix of chicken kidney and muscle with neural agrin, a synapse organizing protein, *Exp. Cell Res.* 195:99–109.
 119. Groffen AJ, Buskens CA, van Kuppevelt TH, Veerkamp JH, Monnens LA and van den Heuvel LP (1998) Primary structure and high

- expression of human agrin in basement membranes of adult lung and kidney, *Eur. J. Biochem.* 254:123–128.
120. Rupp F, Ozcelik T, Linial M, Peterson K, Francke U and Scheller R (1992) Structure and chromosomal localization of the mammalian agrin gene, *J. Neurosci.* 12:3535–3544.
 121. Ruegg MA, Tsim KW, Horton SE, Kroger S, Escher G, Gensch EM and McMahan UJ (1992) The agrin gene codes for a family of basal lamina proteins that differ in function and distribution, *Neuron* 8:691–699.
 122. Rupp F, Payan DG, Magill-Solc C, Cowan DM and Scheller RH (1991) Structure and expression of a rat agrin, *Neuron* 6:811–823.
 123. Denzer AJ, Gesemann M, Schumacher B and Ruegg MA (1995) An amino-terminal extension is required for the secretion of chick agrin and its binding to extracellular matrix, *J. Cell Biol.* 131:1547–1560.
 124. Denzer AJ, Schulthess T, Fauser C, Schumacher B, Kammerer RA, Engel J and Ruegg MA (1998) Electron microscopic structure of agrin and mapping of its binding site in laminin-1, *EMBO J.* 17:335–343.
 125. Wei N, Lin CQ, Modafferi EF, Gomes WA and Black DL (1997) A unique intronic splicing enhancer controls the inclusion of the agrin Y exon, *RNA.* 3:1275–1288.
 126. Denzer AJ, Hauser DM, Gesemann M and Ruegg MA (1997) Synaptic differentiation: the role of agrin in the formation and maintenance of the neuromuscular junction, *Cell Tissue Res.* 290:357–365.
 127. Cole GJ and Halfter W (1996) Agrin: an extracellular matrix heparan sulfate proteoglycan involved in cell interactions and synaptogenesis, *Perspect. Dev. Neurobiol.* 3:359–371.
 128. Gesemann M, Denzer AJ and Ruegg MA (1995) Acetylcholine receptor-aggregating activity of agrin isoforms and mapping of the active site, *J. Cell Biol.* 128:625–636.
 129. Hopf C and Hoch W (1998) Tyrosine phosphorylation of the muscle-specific kinase is exclusively induced by acetylcholine receptor-aggregating agrin fragments, *Eur. J. Biochem.* 253:382–389.
 130. Glass DJ, Bowen DC, Stitt TN, Radziejewski C, Bruno J, Ryan TE, Gies DR, Shah S, Mattsson K, Burden SJ, DiStefano PS, Valenzuela DM, DeChiara TM and Yancopoulos GD (1996) Agrin acts via a MuSK receptor complex, *Cell* 85:513–523.
 131. Meier T, Masciulli F, Moore C, Schoumacher F, Eppenberger U, Denzer AJ, Jones G and Brenner HR (1998) Agrin can mediate acetylcholine receptor gene expression in muscle by aggregation of muscle-derived neuregulins, *J. Cell Biol.* 141:715–726.
 132. Martin PT and Sanes JR (1997) Integrins mediate adhesion to agrin and modulate agrin signaling, *Development* 124:3909–3917.
 133. Campagna JA, Ruegg MA and Bixby JL (1997) Evidence that agrin directly influences presynaptic differentiation at neuromuscular junctions *in vitro*, *Eur. J. Neurosci.* 9:2269–2283.
 134. Gesemann M, Cavalli V, Denzer AJ, Brancaccio A, Schumacher B and Ruegg MA (1996) Alternative splicing of agrin alters its binding to heparin, dystroglycan, and the putative agrin receptor, *Neuron* 16:755–767.
 135. Biroc SL, Payan DG and Fisher JM (1993) Isoforms of agrin are widely expressed in the developing rat and may function as protease inhibitors, *Brain Res. Dev. Brain Res.* 75:119–129.
 136. Barber AJ and Lieth E (1997) Agrin accumulates in the brain microvascular basal lamina during development of the blood-brain barrier, *Dev. Dyn.* 208:62–74.
 137. Hopf C and Hoch W (1996) Agrin binding to α -dystroglycan. Domains of agrin necessary to induce acetylcholine receptor clustering are overlapping but not identical to the α -dystroglycan-binding region, *J. Biol. Chem.* 271:5231–5236.
 138. Meier T, Gesemann M, Cavalli V, Ruegg MA and Wallace BG (1996) AChR phosphorylation and aggregation induced by an agrin fragment that lacks the binding domain for α -dystroglycan, *EMBO J.* 15:2625–2631.
 139. Gesemann M, Brancaccio A, Schumacher B and Ruegg MA (1998) Agrin is a high-affinity binding protein of dystroglycan in non-muscle tissue, *J. Biol. Chem.* 273:600–605.
 140. Durbeej M and Ekblom P (1997) Dystroglycan and laminins: glycoconjugates involved in branching epithelial morphogenesis, *Exp. Lung Res.* 23:109–118.
 141. Durbeej M, Larsson E, Ibraghimov-Beskrovnaya O, Roberds SL, Campbell KP and Ekblom P (1995) Non-muscle α -dystroglycan is involved in epithelial development, *J. Cell Biol.* 130:79–91.
 142. Matsumura K, Yamada H, Saito F, Sunada Y and Shimizu T (1997) The role of dystroglycan, a novel receptor of laminin and agrin,

- in cell differentiation, *Histol. Histopathol.* 12:195–203.
143. Durbeej M, Henry MD, Ferletta M, Campbell KP and Ekblom P (1998) Distribution of dystroglycan in normal adult mouse tissues, *J. Histochem. Cytochem.* 46:449–457.
 144. Campanelli JT, Gayer GG and Scheller RH (1996) Alternative RNA splicing that determines agrin activity regulates binding to heparin and α -dystroglycan, *Development* 122:1663–1672.
 145. Patthy L and Nikolics K (1993) Functions of agrin and agrin-related proteins, *Trends. Neurosci.* 16:76–81.
 146. Hassell JR, Leyshon WC, Ledbetter SR, Tyree B, Suzuki S, Kato M, Kimata K and Kleinman HK (1985) Isolation of two forms of basement membrane proteoglycans. *J. Biol. Chem.* 260:8098–8105.
 147. Klein DJ, Brown DM, Oegema TR, Brenchley PE, Anderson JC, Dickinson MA, Horigan EA and Hassell JR (1988) Glomerular basement membrane proteoglycans are derived from a large precursor. *J. Cell Biol.* 106:963–970.
 148. Miner JH (1998) Developmental biology of glomerular basement membrane components, *Curr. Opin. Nephrol. Hypertens.* 7:13–19.
 149. Wallner EI, Carone FA, Abrahamson DR, Kumar A and Kanwar YS (1997) Diverse aspects of metanephric development, *Microsc. Res. Tech.* 39:261–284.
 150. Kanwar YS, Liu ZZ, Kumar A, Usman MI, Wada J and Wallner EI (1996) D-glucose-induced dysmorphogenesis of embryonic kidney, *J. Clin. Invest.* 98:2478–2488.
 151. Miner JH and Sanes JR (1996) Molecular and functional defects in kidneys of mice lacking collagen $\alpha 3(\text{IV})$: implications for Alport syndrome, *J. Cell Biol.* 135:1403–1413.
 152. Rauscher FJ, 3d (1993) The WT1 Wilms tumor gene product: a developmentally regulated transcription factor in the kidney that functions as a tumor suppressor, *FASEB J.* 7:896–903.
 153. Gilbert SF (1994) *Developmental biology.* 4th ed. Sinauer Associates, Inc. Sunderland, Massachusetts:
 154. Durbeej M, Fecker L, Hjalt T, Zhang HY, Salmivirta K, Klein G, Timpl R, Sorokin L, Ebendal T, Ekblom P and Ekblom M (1996) Expression of laminin $\alpha 1$, $\alpha 5$ and $\beta 2$ chains during embryogenesis of the kidney and vasculature, *Matrix Biol.* 15:397–413.
 155. Wada J, Kumar A, Ota K, Wallner EI, Battle DC and Kanwar YS (1997) Representational difference analysis of cDNA of genes expressed in embryonic kidney, *Kidney Int.* 51:1629–1638.
 156. Couchman JR, Abrahamson DR and McCarthy KJ (1993) Basement membrane proteoglycans and development, *Kidney Int.* 43:79–84.
 157. McCarthy KJ, Bynum K, St. John PL, Abrahamson DR and Couchman JR (1993) Basement membrane proteoglycans in glomerular morphogenesis: chondroitin sulfate proteoglycan is temporally and spatially restricted during development, *J. Histochem. Cytochem.* 41:401–414.
 158. Stone DM and Nikolics K (1995) Tissue- and age-specific expression patterns of alternatively spliced agrin mRNA transcripts in embryonic rat suggest novel developmental roles, *J. Neurosci.* 15:6767–6778.
 159. Haltia A, Solin ML, Muramatsu T, Jalanko H, Holmberg C, Miettinen A and Holthofer H (1997) Expression of nine developmental stage-specific genes in human kidney and cultured renal cells, *Exp. Nephrol.* 5:457–464.
 160. Hewitt JA, Kessler PM, Campbell CE and Williams BR (1996) Tissue-specific regulation of the WT1 locus, *Med. Pediatr. Oncol.* 27:456–461.
 161. McConnell MJ, Cunliffe HE, Chua LJ, Ward TA and Eccles MR (1997) Differential regulation of the human Wilms tumour suppressor gene (WT1) promoter by two isoforms of PAX2, *Oncogene* 14:2689–2700.
 162. Churg J, Bernstein J and Glasscock RJ (1995) *Renal disease: Classification and atlas of glomerular diseases.* 2nd ed. Igaku-Shoin, Tokyo.
 163. Jenis EH and Lowenthal DT (1977) *Kidney biopsy interpretation.* F. A. Davis Company; Philadelphia:
 164. Bakker WW, van Luijk WH, Hene RJ, Desmit EM, van der Hem GK and Vos JT (1986) Loss of glomerular polyanion *in vitro* induced by mononuclear blood cells from patients with minimal-change nephrotic syndrome, *Am. J. Nephrol.* 6:107–111.
 165. Maruyama K, Tomizawa S, Shimabukuro N, Fukuda T, Johshita T and Kuroume T (1989) Effect of supernatants derived from T lymphocyte culture in minimal change nephrotic syndrome on rat kidney capillaries, *Nephron* 51:73–76.
 166. van den Born J, van den Heuvel LP, Bakker MA, Veerkamp JH, Assmann KJ, Weening JJ

- and Berden JH (1993) Distribution of GBM heparan sulfate proteoglycan core protein and side chains in human glomerular diseases, *Kidney Int.* 43:454–463.
167. Cheung PK, Klok PA and Bakker WW (1996) Minimal change-like glomerular alterations induced by a human plasma factor, *Nephron* 74:586–593.
 168. Kriz W, Hahnel B, Rosener S and Elger M (1995) Long-term treatment of rats with FGF-2 results in focal segmental glomerulosclerosis, *Kidney Int.* 48:1435–1450.
 169. Mannikko M, Lenkkeri U, Kashtan CE, Kestila M, Holmberg C and Tryggvason K (1996) Haplotype analysis of congenital nephrotic syndrome of the Finnish type in non-Finnish families, *J. Am. Soc. Nephrol.* 7:2700–2703.
 170. Hallman N, Norio R and Kouvalainen K (1967) Main features of the congenital nephrotic syndrome, *Acta Paediatr. Scand. Suppl* 172:75–78.
 171. Autio-Harmanen H and Rapola J (1983) The thickness of the glomerular basement membrane in congenital nephrotic syndrome of the Finnish type, *Nephron* 34:48–50.
 172. Autio-Harmanen H, Vaananen R and Rapola J (1981) Scanning electron microscopic study of normal human glomerulogenesis and of fetal glomeruli in congenital nephrotic syndrome of the Finnish type, *Kidney Int.* 20:747–752.
 173. Haltia A, Solin ML, Holmberg C, Reivinen J, Miettinen A and Holthofer H (1998) Morphologic changes suggesting abnormal renal differentiation in congenital nephrotic syndrome, *Pediatr. Res.* 43:410–414.
 174. Vermeylen C, Levin M, Mossman J and Barratt TM (1989) Glomerular and urinary heparan sulphate in congenital nephrotic syndrome, *Pediatr. Nephrol.* 3:122–129.
 175. Vernier RL, Klein DJ, Sisson SP, Mahan JD, Oegema TR and Brown DM (1983) Heparan sulfate-rich anionic sites in the human glomerular basement membrane. Decreased concentration in congenital nephrotic syndrome, *N. Engl. J. Med.* 309:1001–1009.
 176. van den Heuvel LP, van den Born J, Jalanko H, Schroder CH, Veerkamp JH, Assmann KJ, Berden JH, Holmberg C, Rapola J and Monnens LA (1992) The glycosaminoglycan content of renal basement membranes in the congenital nephrotic syndrome of the Finnish type, *Pediatr. Nephrol.* 6:10–15.
 177. Ljungberg P, Rapola J, Holmberg C, Holthofer H and Jalanko H (1995) Glomerular anionic charge in congenital nephrotic syndrome of the Finnish type, *Histochem. J.* 27:536–546.
 178. Ljungberg P (1994) Glycosaminoglycans in urine and amniotic fluid in congenital nephrotic syndrome of the Finnish type, *Pediatr. Nephrol.* 8:531–536.
 179. Mannikko M, Kestaila M, Holmberg C, Norio R, Ryyanen M, Olsen A, Peltonen L and Tryggvason K (1995) Fine mapping and haplotype analysis of the locus for congenital nephrotic syndrome on chromosome 19q13.1, *Am. J. Hum. Genet.* 57:1377–1383.
 180. Fuchshuber A, Niaudet P, Gribouval O, Jean G, Gubler MC, Broyer M and Antignac C (1996) Congenital nephrotic syndrome of the Finnish type: linkage to the locus in a non-Finnish population, *Pediatr. Nephrol.* 10:135–138.
 181. Kestila M, Lenkkeri U, Mannikko M, Lamerdin J, McCready P, Putaala H, Ruotsalainen V, Morita T, Nissinen M, Herva R, Kashtan CE, Peltonen L, Holmberg C, Olsen A and Tryggvason K (1998) Positionally cloned gene for a novel glomerular protein - nephrin- is mutated in congenital nephrotic syndrome, *Mol. Cell* 1:575–582.
 182. Little M, Holmes G, Bickmore W, van Heyningen V, Hastie N and Wainwright B (1995) DNA binding capacity of the WT1 protein is abolished by Denys-Drash syndrome WT1 point mutations, *Hum. Mol. Genet.* 4:351–358.
 183. Holmes G, Boterashvili S, English M, Wainwright B, Licht J and Little M (1997) Two N-terminal self-association domains are required for the dominant negative transcriptional activity of WT1 Denys-Drash mutant proteins, *Biochem. Biophys. Res. Commun.* 233:723–728.
 184. Borel F, Barilla KC, Hamilton TB, Iskandar M and Romaniuk PJ (1996) Effects of Denys-Drash syndrome point mutations on the DNA binding activity of the Wilms' tumor suppressor protein WT1, *Biochemistry* 35:12070–12076.
 185. van den Heuvel LP, Westenend PJ, van den Born J, Assmann KJ, Knoers N and Monnens LA (1995) Aberrant proteoglycan composition of the glomerular basement membrane in a patient with Denys-Drash syndrome, *Nephrol. Dial. Transplant.* 10:2205–2211.
 186. Williams JD, Asscher AW, Moffat DB, Sanders E (1991) Clinical atlas of the kidney, Gower Medical Publishing, London.

187. Brees DK, Hutchison FN, Cole GJ and Williams JC, Jr (1996) Differential effects of diabetes and glomerulonephritis on glomerular basement membrane composition, *Proc. Soc. Exp. Biol. Med.* 212:69–77.
188. Ceol M, Nerlich A, Baggio B, Anglani F, Sauer U, Schleicher E and Gambaro G (1996) Increased glomerular $\alpha 1$ (IV) collagen expression and deposition in long-term diabetic rats is prevented by chronic glycosaminoglycan treatment, *Lab. Invest.* 74:484–495.
189. van den Born J, van Kraats AA, Bakker MA, Assmann KJ, van den Heuvel LP, Veerkamp JH and Berden JH (1995) Selective proteinuria in diabetic nephropathy in the rat is associated with a relative decrease in glomerular basement membrane heparan sulphate, *Diabetologia* 38:161–172.
190. McCarthy KJ, Abrahamson DR, Bynum KR, St. John PL and Couchman JR (1994) Basement membrane-specific chondroitin sulfate proteoglycan is abnormally associated with the glomerular capillary basement membrane of diabetic rats, *J. Histochem. Cytochem.* 42:473–484.
191. Tamsma JT, van den Born J, Bruijn JA, Assmann KJ, Weening JJ, Berden JH, Wieslander J, Schrama E, Hermans J and Veerkamp JH (1994) Expression of glomerular extracellular matrix components in human diabetic nephropathy: decrease of heparan sulphate in the glomerular basement membrane, *Diabetologia* 37:313–320.
192. van den Born J, van Kraats AA, Bakker MA, Assmann KJ, Dijkman HB, van der Laak JA and Berden JH (1995) Reduction of heparan sulphate-associated anionic sites in the glomerular basement membrane of rats with streptozotocin-induced diabetic nephropathy, *Diabetologia* 38:1169–1175.
193. Goode NP, Shires M, Crellin DM, Aparicio SR and Davison AM (1995) Alterations of glomerular basement membrane charge and structure in diabetic nephropathy, *Diabetologia* 38:1455–1465.
194. van Det NF, van den Born J, Tamsma JT, Verhagen NA, Berden JH, Bruijn JA, Daha MR and van der Woude FJ (1996) Effects of high glucose on the production of heparan sulfate proteoglycan by mesangial and epithelial cells, *Kidney Int.* 49:1079–1089.
195. Kasinath BS, Grellier P, Choudhury GG and Abboud SL (1996) Regulation of basement membrane heparan sulfate proteoglycan, perlecan, gene expression in glomerular epithelial cells by high glucose medium, *J. Cell. Physiol.* 167:131–136.
196. van der Woude FJ and van Det NF (1997) Heparan sulphate proteoglycans and diabetic nephropathy, *Exp. Nephrol.* 5:180–188.
197. Bollineni JS, Alluru I and Reddi AS (1997) Heparan sulfate proteoglycan synthesis and its expression are decreased in the retina of diabetic rats, *Curr. Eye Res.* 16:127–130.
198. Jensen T (1997) Pathogenesis of diabetic vascular disease: evidence for the role of reduced heparan sulfate proteoglycan, *Diabetes* 46 Suppl 2:S98–100.
199. Myrup B, Hansen PM, Jensen T, Kofoed-Enevoldsen A, Feldt-Rasmussen B, Gram J, Klufft C, Jespersen J and Deckert T (1995) Effect of low-dose heparin on urinary albumin excretion in insulin-dependent diabetes mellitus, *Lancet* 345:421–422.
200. Oturai PS, Rasch R, Hasselager E, Johansen PB, Yokoyama H, Thomsen MK, Myrup B, Kofoed-Enevoldsen A and Deckert T (1996) Effects of heparin and aminoguanidine on glomerular basement membrane thickening in diabetic rats, *APMIS* 104:259–264.
201. Yokoyama H, Myrup B, Oturai P and Deckert T (1995) Heparin, a possible therapy for diabetic complications: the effect on mesangial and myomedial cells *in vivo* and *in vitro*, especially in relation to extracellular matrix, *J. Diabetes Complications* 9:97–103.
202. Poortmans JR and Vanderstraeten J (1994) Kidney function during exercise in healthy and diseased humans. An update. *Sports Med.* 18:419–437.
203. Poortmans JR, Brauman H, Staroukine M, Verniory A, Decaestecker C and Leclercq R (1988) Indirect evidence of glomerular/tubular mixed-type postexercise proteinuria in healthy humans. *Am. J. Physiol.* 254:F277–F283.
204. Heintz B, Stocker G, Mrowka C, Rentz U, Melzer H, Stickeler E, Sieberth HG, Greiling H and Haubeck HD (1995) Decreased glomerular basement membrane heparan sulfate proteoglycan in essential hypertension, *Hypertension* 25:399–407.
205. Stocker G, Stickeler E, Switalla S, Fischer DC, Greiling H and Haubeck HD (1997) Development of an enzyme assay specific for a core protein epitope of a novel small basement membrane associated heparan sulfate proteoglycan from human kidney, *Eur. J. Clin. Chem. Clin. Biochem.* 35:95–99.

CHAPTER TWO

Expression and characterization of human perlecan domains I and II synthesized by baculovirus-infected insect cells

Expression and characterization of human perlecan domains I and II synthesized by baculovirus-infected insect cells

CHAPTER TWO

SUMMARY We present the *in vitro* expression and purification of N-terminal fragments of human perlecan in insect cells. Three “tailored” fragments of human perlecan cDNA were introduced into the polyhedrin locus of baculovirus expression vectors (BEVs) encoding amino acids 1–196 (domain I), 1–404 (domain I and II^a) and 1–506 (domain I, II^a and II^b). The integrity of the BEVs was checked by DNA sequencing, polymerase chain reaction, restriction enzyme analysis and Southern blotting. Northern hybridization and metabolic labeling with [³⁵S]methionine showed that expression of the perlecan-(1–404)-fragment and the perlecan-(1–506)-fragment was successful, but in the case of the perlecan-(1–196)-fragment no recombinant protein was produced. Immunoblotting showed that both the (1–404)-fragment and the (1–506)-fragment are recognized by 95J10, a monoclonal antibody that was previously raised against perlecan-(24–404)-fragment expressed in *Escherichia coli*. Gel permeation and anion exchange chromatography were applied to purify the recombinant proteins. Glycosaminoglycans were demonstrated to be present. Deglycosylation with chondroitinase ABC showed that the (1–404)-fragment was glycosylated with chondroitin sulfate residues. Consistent with these results, glycosaminoglycans isolated from the (1–404)-fragment were identified as chondroitin sulfate by agarose gel electrophoresis. Furthermore the (1–404)-fragment showed affinity to immobilized basic fibroblast growth factor. The availability of baculovirus-derived recombinant perlecan fragments will facilitate domain-specific investigation of the structural and functional properties of perlecan in the future.

TO INDEX

INTRODUCTION

Heparan sulfate proteoglycans are essential components of cell surface and basement membranes serving a diversity of functions. Perlecan (HSPG2) is a large proteoglycan of basement membranes consisting of a 467 kDa core protein with three heparan sulfate chains attached to its N-terminal domain. The other domains share homology with the LDL-receptor (domain II), laminin $\alpha 1$, $\beta 1$ and $\gamma 1$ short arms (domain III), neural cell-adhesion molecule (domain IV) and the globular end of laminin $\alpha 1$ (domain V) [1-3]. The perlecan gene is mapped to the short arm of chromosome 1 and comprises over 120 kb, consisting of 94 exons [4, 5]. Consistent with its multidomain structure, the core protein of perlecan serves multiple functions. The proteoglycan is anchored within the basement membrane through binding to laminins (an interaction that is enhanced in presence of nidogen/entactin), fibronectin and collagen types IV and VI($\alpha 2$) [6-8]. These interactions may increase the rigidity of the basement membrane and immobilize perlecan within the matrix. Up to date, little information is available regarding the functionality of the individual domains of the core protein. However, some insight into the roles of domain III and I has been gained by previous *in vitro* expression studies. Domain III of mouse perlecan was produced by HT1080 cells [9]. The recombinant protein binds to the cell surface through interaction of RGD peptide sequences with integrins [10]. Although this tripeptide is not conserved in human perlecan an alternative

cell binding mechanism may exist. In another study, domain III of human perlecan was expressed successfully in *Escherichia coli*. A monoclonal antibody was raised and used to demonstrate the ubiquity of perlecan in human basement membranes [3]. Furthermore, expression of murine domain I in chinese hamster ovary cells provided evidence for the location of the glycosaminoglycan attachment sites near the N-terminus of perlecan [11].

The presence of the strongly anionic heparan sulfate is essential for the charge-selective permeability of the glomerular basement membrane [12]. Heparan sulfate has also been shown to bind a wide range of growth factors like heparin-binding epidermal growth factor, interferon- γ , granulocyte-macrophage colony stimulating factor, interleukins IL-3, IL-8 and bFGF [13-16]. The biological activity of bFGF requires the presence of a specific oligosaccharide sequence within heparan sulfate or heparin [14, 17]. Binding to this oligosaccharide is essential for the growth factor to trigger its cell surface receptor. It was demonstrated that bFGF activation *in vivo* is solely dependent on the heparan sulfate chains of perlecan [13].

Together with cell surface HSPGs of the vascular endothelium, perlecan also plays a role in the regulation of coagulation. Antithrombin III binding to heparan sulfate increases its anti-coagulant activity [18, 19]. Finally, perlecan may be involved in lipoprotein metabolism. Heparan sulfate chains are known to bind lipoprotein lipase, a key enzyme in lipoprotein metabolism [20, 21]. Regarding the strong similarity between domain II and the low-density lipoprotein receptor it can be speculated that the heparan sulfate residues, lipoprotein lipase, low-density lipoprotein and domain II might associate somehow into a large complex [22]. However, no experimental evidence was obtained thus far to support this hypothesis.

In the present study we have used recombinant baculovirus expression vectors (BEVs) to produce truncated perlecan fragments that are both glycosylated and expressed at high level. The baculovirus expression system utilizes the extremely strong polyhedrin promoter by substituting the polyhedrin gene for a cDNA sequence encoding the protein of interest [23, 24]. Many post-translational modifications are well-described in insect cells, including O-glycosylation [25], N-glycosylation, palmitoylation and myristoylation. Although chondroitin sulfate and heparan sulfate proteoglycans have been observed in the fruit fly *Drosophila melanogaster* [26], no evidence is available yet for the correct synthesis of HSPGs during late stages of baculovirus infection.

MATERIALS AND METHODS

Materials

Vent[®] polymerase, T4 polynucleotide kinase, *XcmI* and *DraIII* endonuclease (New England Biolabs), *BamHI*, *NotI*, *PstI* endonuclease, T4 DNA ligase, bFGF, methionine-deficient Grace's medium, fetal bovine serum (Life Technologies), *SrfI* endonuclease, pCR-Script plasmid (Stratagene Cloning Systems), pVL1393 plasmid (Invitrogen), *Spodoptera frugiperda* SF21 cells, wildtype AcNPV strain C6, transfection reagent, BacPAK6 linearized viral DNA (Clontech Laboratories), "SDS-6B" biotinylated marker, Brij35, TNM-FH insect culture medium (Sigma Chemical), RNazol (Biotecx Laboratories), [³⁵S]methionine (ICN Biomedicals), [α -³²P]ATP, Hybond N⁺, photographic film (Amersham), EN₃HANCE (NEN), SDS (Fluka Chemie), PhastSystem, FPLC system, MonoQ, Superose 12 column, DEAE Sepharose CL-4B (Pharmacia Biotech), secondary antibody conjugates (Dakopatts), Immobilon-P membrane (Millipore), MultiMark prestained marker (Novex) and chondroitinase ABC from *Proteus vulgaris* (Seikagaku).

Construction of transfer vectors

Three transfer vectors were constructed designated pVL1393-P1 (encoding amino acids 1–196 of human perlecan), pVL1393-P12^a (amino acids 1–404) and pVL1393-P12^{ab} (1–506). The initiation codon is supplied by the insert, and the open reading frame is placed out of the original polyhedrin reading frame to avoid aberrant initiation. To introduce translation termination codons, mutagenic primers (Table 1) were used with clones Hpe2 and P5 [1] as template and Vent[®] polymerase. The PCR products were inserted into the *SrfI* cloning site of pCR-Script according to the suppliers protocol. Transformants (prepared according to [27]) were screened to contain the unique *Bam*HI-site at the 5'-, and the *Not*I-site at the 3'-orientation from the cDNA fragments. The cDNA sequences were checked completely by sequencing (ABI apparatus type 37717) The *Bam*HI-*Not*I fragment containing PCR product 1 (Table 1) was subcloned into pVL1393, yielding pVL1393-P1. The *Xcm*I-*Not*I fragment containing the major 3' part of PCR product 2 (Table 1) was subcloned into pVL1393-P1, yielding pVL1393-P12^a. The *Dra*III-*Not*I fragment containing the major 3' part of PCR product 3 (Table 1) was subcloned into pVL1393-P12^a, yielding pVL1393-P12^{ab}.

Table 1. Primers used for introduction of translation stop codons into sequences of human perlecan. All sequences are in 5' to 3' direction; underlined residue indicates mismatch in mutagenic primer. Nucleotide numbering corresponds to the cDNA sequence available from GenBank by accession number X62515 [1].

Product	Nucleotides	Primer set
1	41-628	atgggggtggcgggcgccgg (f) tc <u>at</u> gggaactggggcactgtgc (r)
2	543-1252	tc <u>at</u> ctccagcggctctgt (f) <u>tt</u> acatgcagcaaactcgtc (r)
3	985-1560	tgagctagactgtggccccc (f) <u>tc</u> aggggcctgctcgttgg (r)

The PCR products were inserted into the *SrfI* cloning site of pCR-Script according to the suppliers protocol. Transformants (prepared according to [27]) were screened to contain the unique *Bam*HI-site at the 5'-, and the *Not*I-site at the 3'-orientation from the cDNA fragments. The cDNA sequences were checked completely by sequencing (ABI apparatus type 37717) The *Bam*HI-*Not*I fragment containing PCR product 1 (Table 1) was subcloned into pVL1393, yielding pVL1393-P1. The *Xcm*I-*Not*I fragment containing the major 3' part of PCR product 2 (Table 1) was subcloned into pVL1393-P1, yielding pVL1393-P12^a. The *Dra*III-*Not*I fragment containing the major 3' part of PCR product 3 (Table 1) was subcloned into pVL1393-P12^a, yielding pVL1393-P12^{ab}.

Tissue culture and isolation of recombinant baculoviruses

The general tissue culture methods were adapted from [23]. *Spodoptera frugiperda* SF21 cells were cultured at 27°C in TNM-FH medium supplemented with 10% fetal bovine serum. Except where otherwise stated, monolayer cultures were used. Recombinant viruses were derived from BacPAK6 by liposome-mediated cotransfection. The culture supernatant was harvested 4 days after cotransfection and individual plaques were obtained by a soft-agar overlay method. Well-isolated plaques were picked and left to diffuse overnight in 500 µl normal medium at 4°C. Pure plaques were propagated by infecting 5·10⁵ SF21 cells in a 35 mm dish with 100 µl of the plaque pick and harvesting the medium 4 days after infection. For further propagation of baculovirus strains during a maximum of two passages, suspension cultures of 50 ml were inoculated with 5·10⁵ cells/ml and incubated until logarithmic growth. Cells were then infected with a multiplicity of 0.1 and harvested 96 h post infection, at which time the cell densities had reached a plateau of about 2·10⁶ cells/ml. Cell densities were monitored in a hemocytometer (Bürker). Virus stocks were titrated by plaque assays. For expression of recombinant proteins, cells were infected at semiconfluence with a multiplicity of 5 and harvested at 50-60 h post infection.

Genome analysis of baculovirus expression vectors

Independently isolated baculovirus strains were analyzed for correct integration locus and purity. Baculovirus genomic DNA was isolated from non-occluded virions as described [28]. Shortly, the medium was cleared from cells (15 min at 300x g) and non-occluded virions were collected by ultracentrifugation for 1 h at 100,000x g. The virions were incubated overnight at 37°C in presence of 0.1 mg/ml proteinase K and 1% SDS. The DNA was further purified following standard procedures [29] and stored at 4°C. After endonuclease *Pst*I digestion, 1 µg of fragmented virus DNA was applied to each lane of a 0.35% agarose gel and separated overnight at 4°C. Southern blot transfer to a Hybond N⁺ membrane was performed overnight by capillary force. The filter was hybridized at 42°C with a 520 bp cDNA fragment homologous to domain I of human perlecan (domain I), and washed under medium stringent

conditions (75 mM NaCl containing 7.5 mM sodium citrate and 0.1% SDS, pH 7.0 at 42°C). For autoradiography, a photographic film was developed after 4 days exposure.

[³⁵S]methionine incorporation and autoradiography

This procedure was adapted from ref. [23]. A suspension culture of insect cells was grown to a cell density of $5 \cdot 10^5$ cells/ml and infected with recombinant baculovirus with a multiplicity of 10. Forty-eight h after infection, 1.5 ml of cell suspension was centrifuged (5 min at 500x g, 24°C) and the cells were resuspended in 1.5 ml of methionine-deficient Grace's medium. The cells were further incubated for 60 min; all incubations were at 27°C under frequent inversion. The cells were collected and incubated for 60 min in 1.5 ml of methionine-deficient Grace's medium supplemented with 50 µCi/ml [³⁵S]methionine (specific activity >1000 Ci/mmol). The labeling mixture was removed and cells were washed twice with NaCl/P_i (140 mM NaCl, 2.7 mM KCl, 10 mM Na₂HPO₄, 1.8 mM KH₂PO₄, pH 7.5). Finally, the cells were incubated for 90 min in 200 µl NaCl/P_i and centrifuged (5 min 500x g). The supernatant was stored at -80°C. Due to the host shut-off in the baculovirus infection cycle, the supernatant contains a limited set of extracellular proteins, synthesized at 50 h post infection and labeled with [³⁵S]methionine. Proteins were analyzed by SDS-PAGE (12.5 %) and processed for autoradiography with EN₃HANCE according to the manufacturer's instructions.

Size exclusion and ion exchange chromatography

For size exclusion chromatography, a Superose 12 column (height 30 cm, V_i =23.7 ml, V₀= 7.6 ml as determined for blue dextran-2000) was calibrated with molecular weight marker proteins and contained 208 plates average in the range of 14 to 440 kDa. Sample volume was 200 µl, flow rate 0.5 ml/min and elution was performed in NaCl/P_i containing 0.01% Brij35 and 0.01% NaN₃.

For ion exchange chromatography, sample volumes varying from 200 µl to 10 ml were applied to a MonoQ column with a bed volume of 1 ml. A linear gradient from 0 to 1 M NaCl in 10 mM Tris (pH 6.8), 0.1% Zwittergent 3-12 and 0.01% NaN₃ was used for elution with a flow rate of 0.5 ml/min. Aliquots of each sample were dissolved in UltimaGold scintillation mix (Packard) and counted for 4 min in a liquid scintillation analyzer.

Chondroitinase ABC treatment

Samples were incubated with 0.5 U/ml chondroitinase ABC (protease-free) for 16 h at 37°C in 0.1 M Tris (pH 8.0) containing 0.025% NaN₃. Control reactions were included containing 0.1 mg/ml chondroitin sulfate in presence and absence of chondroitinase ABC. The efficiency of the deglycosylation was measured by a 1,9-dimethyl-methylene blue assay [30].

Immunological methods

For immunoblotting and ELISA procedures we followed standard methods [31] using 95J10, a perlecan-specific mAb that was previously raised in recombinant *E. coli* (paper in preparation). In summary, recombinant perlecan-(24-404)-fragment was produced in the bacterial pGEX expression system [32] and treated with thrombin. The recombinant fragment was used for production of mAbs in mice according to previously described procedures [33]. Hybridoma cell lines were screened in ELISA against the recombinant fusion protein and in indirect immunofluorescence studies on human kidney cortex sections. The glomerular staining pattern observed with 95J10 matched the results obtained with the anti-perlecan mAb 7B5 [3]. Immunological detection was based on chemiluminescent (immunoblotting) or chromogenic (ELISA) reactions driven by horse radish peroxidase.

Basic FGF binding assay

Quantities of 24, 100, 250 and 500 ng bFGF and BSA were dissolved in 100 μ l 50 mM carbonate buffer (pH 9.6) and transferred into 96-wells plates incubated overnight at 4°C for coating. After thorough washing, the wells were incubated with 2.5 μ g of the perlecan-(1–404)-fragment in NaCl/P_i containing 3% BSA, partially purified by exchange chromatography (fractions eluted between 0.4 and 0.6 M NaCl from MonoQ). After thorough washing with NaCl/P_i, bound (1–404)-fragment was detected as in the above described ELISA.

Additional methods

Glycosaminoglycan electrophoresis was performed according to [34]. Protein concentrations were measured by the Bradford method as BSA.

RESULTS

Isolation of recombinant baculovirus strains

To allow expression of perlecan fragments in *Spodoptera frugiperda* SF21 insect cells, three recombinant baculovirus strains were generated as follows. Truncated cDNA fragments were prepared encoding amino acids (1–196), (1–404) and (1–506) of human perlecan. The cDNA fragments were inserted into the transfer vector pVL1393. The integrity of the cDNA constructs was confirmed by restriction enzyme analysis and the complete coding regions and non-translated borders were verified by sequence analysis.

In the pVL1393-derived transfer vectors, the cDNA inserts are flanked by regions that are homologous to AcNPV sequences surrounding the polyhedrin gene. These flanking sequences allow homologous recombination, resulting in substitution of the wildtype polyhedrin gene by the cDNA constructs of interest. To counterselect against non-recombinant virus replication, we employed a parental virus specially designed for this purpose, BacPAK6. A soft-agar overlay plaque assay yielded only polyhedrin-negative plaques. Well-isolated plaques were picked to isolate recombinant baculovirus strains. PCR amplification techniques were used for a primary screening of the virus strains (data not shown).

For more thorough investigation, the baculovirus isolates were propagated and genomic DNA (134 kb circular) was purified and digested with *Pst*I endonuclease (Figure 1A). The *Pst*I digestion pattern can discriminate between different loci of integration because an additional restriction site is introduced juxtaposing the inserted cDNA sequence. Consequently, the polyhedrin-containing *Pst*I fragment (arrow a in Figure 1A) of wildtype AcNPV is further degraded into smaller products in recombinant strains (arrow b in Figure 1A). The observed fragment sizes were in full concordance with the expected values, calculated from the nucleotide sequences of AcNPV (GenBank #L22858) and of the introduced cDNA constructs. Furthermore, the presence of perlecan cDNA in these subfragments was demonstrated by Southern blotting with a probe homologous to an internal fragment of domain I (arrow b in Figure 1B). From these data we conclude that perlecan cDNA constructs encoding (1–196)-, (1–404)- and (1–506)-fragment were successfully introduced into the polyhedrin locus of the baculovirus genome.

Transcription and expression of perlecan fragments

To confirm the presence of recombinant mRNA, a Northern hybridization was performed with a cDNA probe specific for domain I of human perlecan (data not shown). No mRNA was detected in wildtype, whereas high levels were produced in recombinant baculovirus-infected SF21 cells. As discussed below, the size of the mRNA observed for the perlecan-(1–196)-fragment was substantially larger than expected (approximately 4 kb). Transcription was observed at 36 and 64 h post infection but not at 0 or 12 h, which corresponds with the

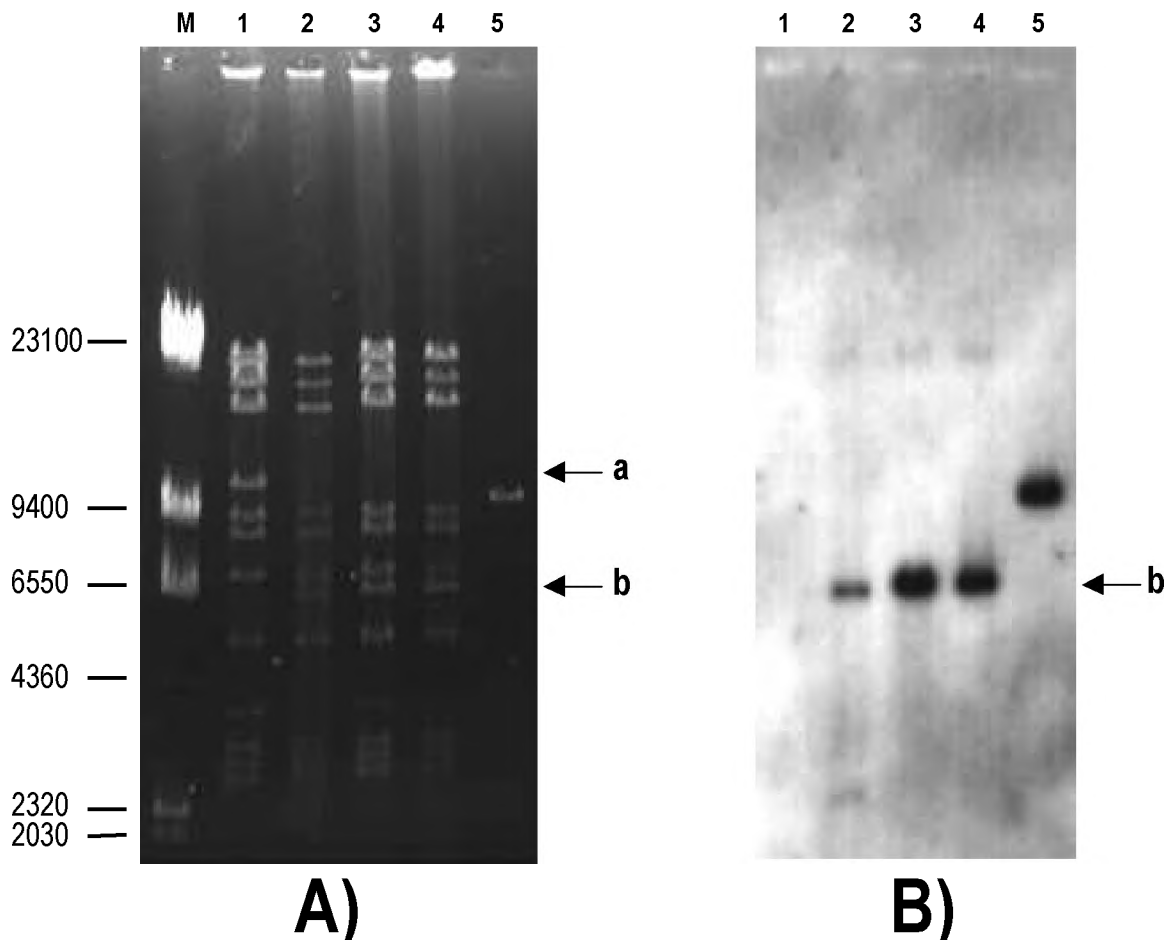


Figure 1 A) Restriction enzyme analysis of wildtype (lane 1) and recombinant (lanes 2-4) baculovirus strains and B) Southern hybridization confirming the insertion of perlecan cDNA constructs into the polyhedrin locus of the baculovirus genome. Lane 1: wildtype AcNPV; lane 2: recombinant AcNPV encoding perlecan-(1-196)-polypeptide; lane 3: AcNPV encoding perlecan-(1-404)-polypeptide; lane 4: AcNPV encoding perlecan-(1-506)-polypeptide; lane 5: linearized pVL1393-P1 plasmid DNA as positive control for hybridization. Genomic DNA was digested with *Pst*I and fragments were separated by electrophoresis on a 0.35% agarose gel (A). The same gel was used for Southern blot transfer and hybridization with a domain I-specific probe against human perlecan (B). Arrows indicate (a) wildtype *Pst*I-D fragment carrying the polyhedrin-locus; (b) recombinant *Pst*I fragments carrying the inserted cDNA constructs.

characteristics of late-phase baculovirus promoters.

Production of the recombinant perlecan fragments was studied by metabolic labeling with [³⁵S]methionine. Best results were obtained by labeling at 50 h post infection, when only a limited set of virus-encoded proteins is secreted from baculovirus-infected cell cultures. The supernatant was harvested and analyzed without further manipulation by SDS-PAGE and autoradiography (Figure 2). Comparison of recombinant and wildtype baculovirus-encoded proteins revealed the presence of recombinant perlecan-(1-404)-fragment and -(1-506)-fragment. In contrast, no additional band was visible in case of the (1-196)-fragment. The (1-404)- and (1-506)-fragment migrate in SDS-PAGE as molecules of approximately 53 and 62 kDa respectively, as estimated by standard curve interpolation. Based on the primary amino acid sequences, molecular masses of the core proteins are predicted as 42 and 53 kDa respectively, taking removal of the signal peptides into account. To investigate the integrity of the two produced proteins, immunological studies were performed with the mAb 95J10 (raised against domain I and II^a of human perlecan expressed in *E. coli*). Western blot analysis

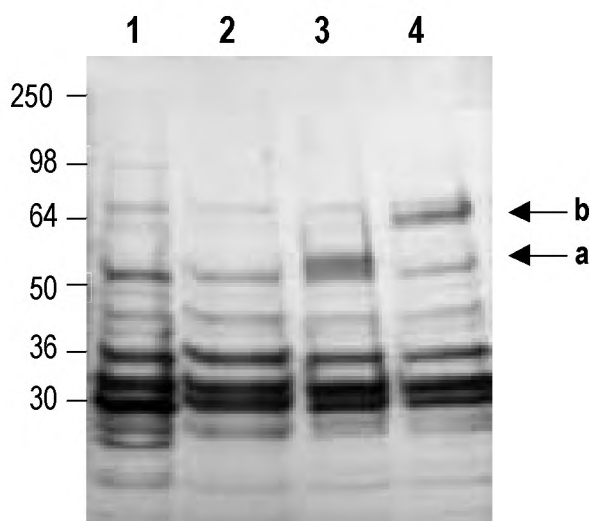


Figure 2. Extracellular protein production by baculovirus-infected insect cells after metabolic labeling with [³⁵S]methionine. *Spodoptera frugiperda* SF21 cells were infected with wildtype AcNPV (lane 1), AcNPV encoding perlecan-(1 196)-fragment (lane 2), (1 404)-fragment (lane 3), or (1 506)-fragment (lane 4). Arrows a and b indicate (1 506)- and (1 404)-fragment respectively. Molecular mass markers are indicated on the left. The labeled supernatants were harvested and analyzed by SDS-PAGE (12.5%) and autoradiography.

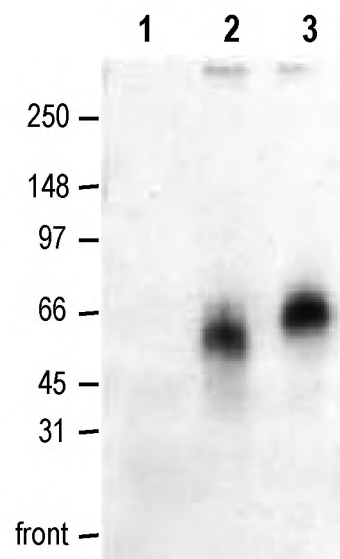


Figure 3. Western blot detection of recombinant perlecan fragments using mAb 95J10. SF21 cells were infected with wildtype AcNPV (lane 1), AcNPV encoding perlecan-(1 404)-fragment (lane 2) or (1 506)-fragment (lane 3). Marker proteins are indicated on the left.

showed that the (1–404)- and (1–506)-fragment are immunologically related to human perlecan (Figure 3). As a control, the 95J10 epitope was not detected in insect cells infected with wildtype AcNPV (lane 1) or recombinant AcNPV encoding the (1–196)-fragment (not shown). Consistent results were found in ELISA (data not shown). The obtained yield was between 1 and 5 mg of recombinant protein per 10^9 cells.

Purification of recombinant perlecan fragments

[³⁵S]methionine labeled supernatants (Figure 2, lane 3 and 4) were used to investigate the behavior of the (1–404)- and (1–506)-fragment on chromatographic media. For size exclusion chromatography, a Superose 12 column was utilized. Individual fractions were collected and aliquots were separated by SDS-PAGE. Radioactive proteins were visualized by autoradiography (Figure 4). Both the (1–404)- and (1–506)-fragment (not shown) eluted at $K_{av} = 0.23$ – 0.29 , whereas these bands did not appear in case of the (1–196)-fragment or after infection with wildtype AcNPV (data not shown).

An essentially pure fraction of [³⁵S]methionine labeled (1–404)-fragment obtained by gel permeation (Figure 4, lane 2) was applied onto a MonoQ anion exchange column to study its binding characteristics. The recombinant protein strongly bound to the matrix at pH 6.8. A linear salt gradient was used for elution and radioactivity of the fractions was quantified by liquid scintillation counting (Figure 5). The protein eluted from the column at a concentration of 0.4 to 0.5 M NaCl. A similar procedure was followed with non-radioactive (1–404)-fragment, using immunological detection procedures (Figure 6). In this case, the (1–404)-fragment was incubated with DEAE Sepharose (a matrix carrying the same active groups as MonoQ). After elution with a NaCl gradient increasing stepwise from 0.0 to 1.0 M, all fractions were analyzed by an ELISA procedure using 95J10. Consistent with the previous results, the majority of the protein was detected in the fraction containing 0.4 M NaCl.

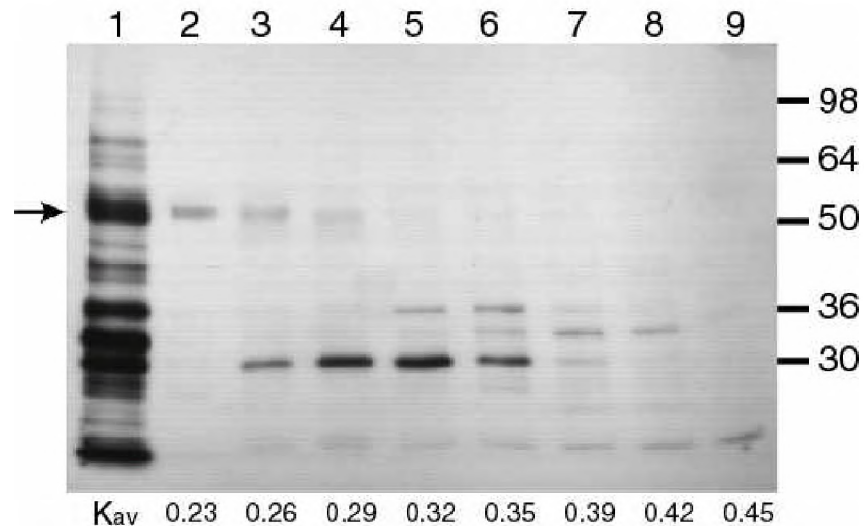


Figure 4. Purification of the perlecan-(1-404)-fragment by size exclusion chromatography. Crude culture supernatant obtained after metabolic labeling with [^{35}S]methionine (lane 1) was applied onto a Superose 12 column under non-denaturing conditions. Individual fractions (lanes 2–9) were analyzed by 12.5% SDS-PAGE and autoradiography. K_{av} values are noted for each fraction. The arrow indicates the (1–404)-fragment. Molecular mass markers are indicated on the right (MultiMark prestained marker).

Characterization of glycosaminoglycan residues

The binding characteristics of the (1–404)-fragment to anion exchange beads suggest that exposed negative charges are present on the molecule. We therefore studied the glycosylation characteristics of the (1–404)-fragment produced by baculovirus-infected insect cells. After treatment with chondroitinase ABC (protease-free), its binding capacity to DEAE Sepharose was abolished (Figure 6) and the protein was found in the flow-through. Further evidence for

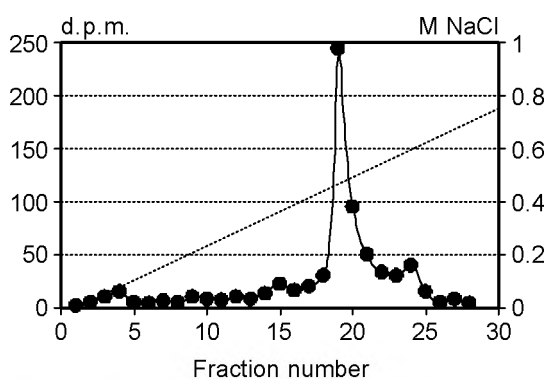


Figure 5. Anion exchange chromatography of perlecan-(1–404)-fragment. [^{35}S]methionine labeled (1–404)-fragment, purified by size exclusion chromatography as shown in Figure 4 (lane 2), was applied onto a MonoQ anion exchange column. The radioactive protein strongly bound to the matrix at pH 6.8 and eluted in a linear NaCl gradient at a concentration of 0.4–0.5 M.

the presence of chondroitin sulfate residues on the (1–404)-fragment is shown in Figure 7. Glycosaminoglycans were extracted from the recombinant proteoglycan by alkaline borohydride treatment and analyzed by agarose gel electrophoresis. A single band was visible that co-migrated with chondroitin sulfate. The above data suggest that the (1–404)-fragment produced by recombinant AcNPV, is glycosylated with one or more chondroitin sulfate residues. The proteoglycan-like properties of the (1–404)-fragment conform with its ability to bind basic fibroblast growth factor (Table 2). This was demonstrated by coating increasing quantities of bFGF on ELISA plates, incubating with culture supernatant of baculovirus-infected insect cells, and determining the amount of immobilized (1–404)-fragment in an ELISA-like procedure with mAb 95J10. This interaction between the

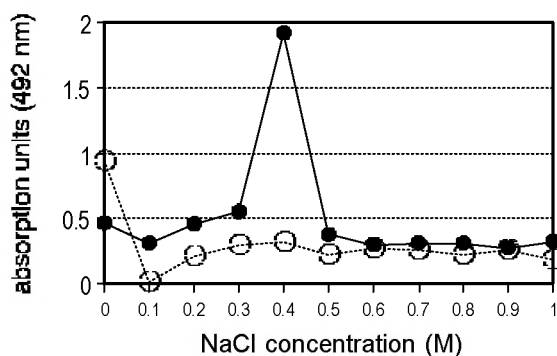


Figure 6. Ion exchange chromatography of intact and chondroitinase ABC-digested perlecan-(1 404)-fragment. Closed circles: intact (1 404)-fragment; open circles: (1 404)-fragment digested with protease-free chondroitinase ABC. The proteins were eluted from DEAE-Sepharose beads using a stepwise NaCl gradient. Aliquots of each fraction were analyzed *in duplo* by an ELISA using the perlecan-specific mAb 95J10. The relative concentrations of (1 404)-fragment are given in absorbance units at 492 nm.

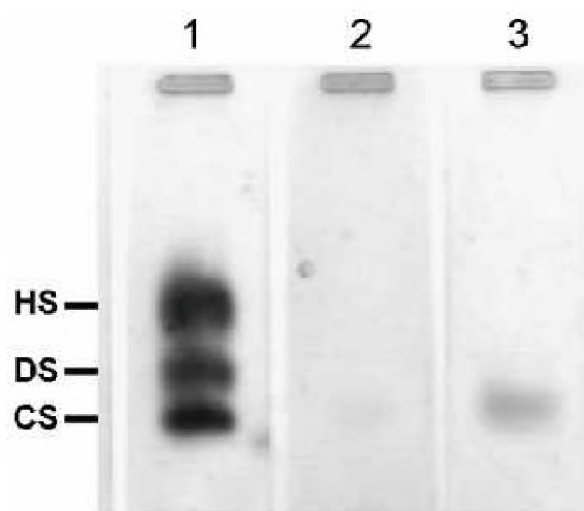


Figure 7. Characterization of glycosaminoglycans extracted from recombinant perlecan-(1 404)-fragment. Lanes 1: 5 ng marker glycosaminoglycans containing heparan sulfate (HS), dermatan sulfate (DS) and chondroitin sulfate (CS). Lanes 2 and 3: glycosaminoglycans extracted from recombinant (1 404)-fragment (five-fold diluted and undiluted, respectively). Glycosaminoglycans were separated by agarose gel electrophoresis and stained with combined Azure A / silver [34].

(1–404)-fragment and bFGF is inhibited in presence of free glycosaminoglycans, heparan sulfate being a stronger competitor than chondroitin sulfate (Table 3). This is not surprising since bFGF has been reported to have a higher affinity for heparan sulfate than for chondroitin sulfate. The results indicate that the binding of the (1–404)-fragment to immobilized bFGF is mediated by the glycosaminoglycan moieties of the recombinant proteoglycan.

DISCUSSION

No recombinant protein is synthesized by BEVs encoding the perlecan-(1 196)-fragment

The inability of AcNPV-infected insect cells to produce the recombinant perlecan-(1–196)-fragment is poorly understood. The possibility of a frame shift or point mutation in the cDNA construct was excluded by sequence analysis. Baculoviruses carrying the cDNA construct encoding the (1–196)-fragment were convincingly shown to contain the insert correctly in the polyhedrin locus, and the size of the cDNA fragment was confirmed by PCR. These results clearly indicate that the recombinant virus offers an intact open reading frame. Transcription analysis by Northern blotting showed that an unexpectedly long mRNA (approx. 4 kb) was present, induced between 12 and 36 h post-infection. However, no recombinant protein was produced.

One possible explanation for the deficiency in recombinant (1–196)-fragment production is the inefficient use of the polyadenylation signal. In late phases of baculovirus infection, transcription is mediated by a virus-encoded RNA polymerase [35], and not all factors that influence termination of transcription by this enzyme are known [36]. For the AcNPV polyhedrin gene, multiple transcripts (1.2, 3.4 and 4.9 kb in size) have been observed with a common 5' end [37, 38]. Therefore the elongated mRNA might result from “read-through” transcription, and we speculate that this may cause instability of the mRNA.

Table 2. The recombinant perlecan-(1-404)-fragment binds to immobilized bFGF. Increasing quantities of bFGF or BSA were coated on ELISA plates. Wells were incubated with supernatant from (1-404)-fragment-producing cells, washed, and bound fragment was measured by ELISA with mAb 95J10, given in absorption units at 492 nm.

Amount coated (ng)	BSA (A_{492})	bFGF (A_{492})
0	0.225	0.225
24	0.226	0.202
100	0.225	0.639
250	0.225	1.690
500	0.226	3.254

Table 3. Free glycosaminoglycans compete for binding of perlecan-(1-404)-fragment to bFGF. A constant amount of bFGF (250 ng) was coated on ELISA plates. Binding of (1-404)-fragment was assayed in presence of increasing concentrations of free HS or CS. Bound fragment was measured as absorbance units at 492 nm.

Competitor ($\mu\text{g/ml}$)	HS (A_{492})	CS (A_{492})
0	1.690	1.690
0.25	0.675	1.564
1	0.159	1.149
5	0.058	0.573
25	0.066	0.159
100	0.023	0.213

Another reason for the lack of (1–196)-expression could be the activity of an additional late-phase promoter positioned approximately 2 kb downstream of the polyhedrin coding sequence [37]. This promoter drives the transcription of a 3.2 kb mRNA in the opposite orientation, comprising the antisense strand of the inserted cDNA. Since the probe used for Northern hybridization was double-stranded, the observed signal may represent the “antisense” transcript. In wildtype AcNPV, the level of this transcript is down-regulated by transcription from the polyhedrin promoter [37]. Possibly the consensus generated in this BEV influences the balance between sense and antisense transcription, in favor of the antisense product.

Successful expression and purification of (1 404)- and (1 506)-fragment

The recombinant perlecan-(1–404)-fragment and (1–506)-fragment, comprising domains I and II of human perlecan, were successfully synthesized in the baculovirus expression system. This was shown by metabolic labeling (Figure 2) and immunological assays with the mAb 95J10 (Figure 3). The signal peptide (originating from human perlecan cDNA) was recognized and the proteins were transported to the extracellular compartment. During electrophoresis on a 12.5% SDS-polyacrylamide gel, the [^{35}S]methionine labeled recombinant proteins migrate as 53 and 62 kDa

respectively, which is 10 kDa larger than the calculated mass of their core proteins. As argued below, this difference can be explained by post-translational modifications, since the electrophoretic mobility of glycosylated proteins does not correlate to molecular mass in a linear logarithmic manner. In contrast, elution on a gel permeation column calibrated with globular marker proteins takes place at $K_{av} = 0.23\text{--}0.26$ which coincides with an apparent mass of 180–250 kDa. This discrepancy illustrates that molecular weight determinations based on relative mobility should be considered very carefully, especially when proteoglycans are involved. The yield of between 1 and 5 mg recombinant protein per 10^9 cells is in agreement with the results obtained with other recombinant proteins [23].

Identification of glycosaminoglycans as chondroitin sulfate

The presence of chondroitin sulfate glycosaminoglycans on baculovirus-derived perlecan-(1–404)-fragment is supported by the following findings. Firstly, the (1–404)-fragment strongly binds to the anion exchange matrices DEAE-Sepharose CL-4B and MonoQ. The observed elution pattern resembles the characteristic behavior of proteoglycans previously isolated from basement membranes [39, 40]. Secondly, the binding capacity of the (1–404)-fragment to anion exchange columns is abolished by chondroitinase ABC treatment. Furthermore, glycosaminoglycans isolated from the (1–404)-fragment were convincingly identified as chondroitin sulfate (Figure 7) by agarose gel electrophoresis. Finally, the (1–404)-fragment

binds to immobilized bFGF (Table 2). This interaction is inhibited in presence of free glycosaminoglycans (Table 3), suggesting that binding of the (1–404)-fragment is mediated through its side chains.

Although the interaction between bFGF and the (1–404)-fragment provides evidence for attachment of glycosaminoglycans, it can hardly be compared to the binding event that occurs in the basement membrane. The binding of bFGF *in vivo* is known to require specific oligosaccharide sequences that are present solely in heparan sulfate and heparin [13, 41], involving a dissociation constant of 10^{-8} to 10^{-9} M [16]. In our ELISA-based binding assay the affinity must be lower, since free chondroitin sulfate acts as a potent competitor. We therefore conclude that baculovirus-derived (1–404)-fragment binds to immobilized bFGF with relatively low affinity through its chondroitin sulfate chains.

The appearance of chondroitin sulfate residues on the perlecan-(1–404)-fragment is unexpected since the predominant *in vivo* form of perlecan carries heparan sulfate chains. Some efforts have been made to elucidate the factors influencing glycosylation of proteoglycans. The composition of glycosaminoglycan chains has been found to depend firstly on the amino acid sequence of the core protein [42]. The primary structure of perlecan domain I permits both attachment of heparan sulfate and chondroitin sulfate [11]. A second determinant for glycosylation is the cell type in which the proteoglycan is synthesized. Hybrid heparan/chondroitin sulfate forms of perlecan have been observed in Engelbreth-Holm-Swarm tumor cells [43], in cultured human glomerular visceral epithelial cells [44] and chinese hamster ovary cells [11]. Despite these data, the exact determinants for the type of glycosylation remain unclear.

Application of recombinant fragments of human perlecan

Expression of perlecan fragments in the baculovirus system provides an important tool to study the functions of this proteoglycan in a domain-specific manner. In the present study we described the expression and purification of perlecan-(1–404)- and -(1–506)-fragment, comprising the two N-terminal domains of perlecan. Given the spatial separation of the structural domains as visualized by electron microscopy [45], it is likely that the (1–506)-fragment will have identical properties as the corresponding globule in the whole perlecan molecule. The included domains are likely candidates to play a role in lipoprotein metabolism. Domain II of perlecan shows strong homology with the ligand binding domain of the low-density lipoprotein receptor [1, 2]. A synergic action has been proposed for the combined binding of lipoprotein together with lipoprotein lipase, a complex that could be stabilized by a favorable configuration of heparan sulfate in the proximity of the low-density lipoprotein receptor like domain [20, 22]. These and other hypothetical functions of the N-terminal core domains of perlecan will be assessed in the future.

ACKNOWLEDGEMENTS

The authors wish to acknowledge Elly M.M. Versteeg and Toin H.M.S.M. van Kuppevelt for Glycosaminoglycan gel electrophoresis. This study was supported by grant C93.1309 of the Dutch Kidney Foundation. The laboratory participates in a concerted action “Alterations in extracellular matrix components in diabetic nephropathy and other glomerular diseases”, which is financially supported by the EC with the Biomed I program (BMH1-CT92-1766)

REFERENCES

1. Kallunki P and Tryggvason K (1992) Human basement membrane heparan sulfate proteoglycan core protein: a 467-kD protein containing multiple domains resembling elements of the low density lipoprotein receptor, laminin, neural cell adhesion

- molecules, and epidermal growth factor, *J. Cell. Biol.* 116: 559-571
2. Murdoch AD, Dodge GR, Cohen I, Tuan RS and Iozzo RV (1992) Primary structure of the human heparan sulfate proteoglycan from basement membrane (HSPG2/perlecan). A chimeric molecule with multiple domains homologous to the low density lipoprotein receptor, laminin, neural cell adhesion molecules, and epidermal growth factor, *J. Biol. Chem.* 267: 8544-8557
 3. Murdoch AD, Liu B, Schwarting R, Tuan RS and Iozzo RV (1994) Widespread expression of perlecan proteoglycan in basement membranes and extracellular matrices of human tissues as detected by a novel monoclonal antibody against domain III and by in situ hybridization, *J. Histochem. Cytochem.* 42: 239-249
 4. Dodge GR, Kovalszky I, Chu ML, Hassell JR, McBride OW, Yi HF and Iozzo RV (1991) Heparan sulfate proteoglycan of human colon: partial molecular cloning, cellular expression, and mapping of the gene (HSPG2) to the short arm of human chromosome 1, *Genomics* 10: 673-680
 5. Cohen IR, Grassel S, Murdoch AD and Iozzo RV (1993) Structural characterization of the complete human perlecan gene and its promoter, *Proc. Natl. Acad. Sci. USA* 90: 10404-10408
 6. Battaglia C, Mayer U, Aumailley M and Timpl R (1992) Basement-membrane heparan sulfate proteoglycan binds to laminin by its heparan sulfate chains and to nidogen by sites in the protein core, *Eur. J. Biochem.* 208: 359-366
 7. Heremans A, de Cock B, Cassiman JJ, van den Berghe H and David G (1990) The core protein of the matrix-associated heparan sulfate proteoglycan binds to fibronectin, *J. Biol. Chem.* 265: 8716-8724
 8. Laurie GW, Bing JT, Kleinman HK, Hassell JR, Aumailley M, Martin GR and Feldmann RJ (1986) Localization of binding sites for laminin, heparan sulfate proteoglycan and fibronectin on basement membrane (type IV) collagen, *J. Mol. Biol.* 189: 205-216
 9. Chakravarti S, Horchar T, Jefferson B, Laurie GW and Hassell JR (1995) Recombinant domain III of perlecan promotes cell attachment through its RGDS sequence, *J. Biol. Chem.* 270: 404-409
 10. Hayashi K, Madri JA and Yurchenco PD (1992) Endothelial cells interact with the core protein of basement membrane perlecan through $\beta 1$ and $\beta 3$ integrins: an adhesion modulated by glycosaminoglycan, *J. Cell. Biol.* 119: 945-959
 11. Kokenyesi R and Silbert JE (1995) Formation of heparan sulfate or chondroitin/dermatan sulfate on recombinant domain I of mouse perlecan expressed in Chinese hamster ovary cells, *Biochem. Biophys. Res. Commun.* 211: 262-267
 12. Kanwar YS, Linker A and Farquhar MG (1980) Increased permeability of the glomerular basement membrane to ferritin after removal of glycosaminoglycans (heparan sulfate) by enzyme digestion, *J. Cell. Biol.* 86: 688-693
 13. Aviezer D, Hecht D, Safran M, Eisinger M, David G and Yayon A (1994) Perlecan, basal lamina proteoglycan, promotes basic fibroblast growth factor-receptor binding, mitogenesis, and angiogenesis, *Cell* 79: 1005-1013
 14. Gallagher JT (1994) Heparan sulphates as membrane receptors for the fibroblast growth factors, *Eur. J. Clin. Chem. Clin. Biochem.* 32: 239-247
 15. Schlessinger J, Lax I and Lemmon M (1995) Regulation of growth factor activation by proteoglycans: What is the role of the low affinity receptors? *Cell* 83: 357-360
 16. Guillonneau X, Tassin J, Berrou E, Bryckaert M, Courtois Y and Mascarelli F (1996) In vitro changes in plasma membrane heparan sulfate proteoglycans and in perlecan expression participate in the regulation of fibroblast growth factor 2 mitogenic activity, *J. Cell. Physiol.* 166: 170-187
 17. Turnbull JE, Fernig DG, Ke Y, Wilkinson MC and Gallagher JT (1992) Identification of the basic fibroblast growth factor binding sequence in fibroblast heparan sulfate, *J. Biol. Chem.* 267: 10337-10341
 18. Pejler G, Backstrom G, Lindahl U, Paulsson M, Dziadek M, Fujiwara S and Timpl R (1987) Structure and affinity for antithrombin of heparan sulfate chains derived from basement membrane proteoglycans, *J. Biol. Chem.* 262: 5036-5043
 19. Mertens G, Cassiman JJ, van den Berghe H, Vermeylen J and David G (1992) Cell surface heparan sulfate proteoglycans from human vascular endothelial cells. Core protein characterization and antithrombin III binding properties, *J. Biol. Chem.* 267: 20435-20443
 20. Eisenberg S, Sehayek E, Olivecrona T and Vlodaysky I (1992) Lipoprotein lipase enhances binding of lipoproteins to heparan

- sulfate on cell surfaces and extracellular matrix, *J. Clin. Invest.* 90: 2013-2021
21. Olivecrona G and Olivecrona T (1995) Triglyceride lipases and atherosclerosis, *Curr. Opin. Lipidol.* 6: 291-305
 22. Iozzo RV (1994) Perlecan: a gem of a proteoglycan, *Matrix. Biol.* 14: 203-208
 23. O'Reilly DR, Miller LK and Luckow VA (1992) *Baculovirus expression vectors: a laboratory manual*, Freeman and Company, New York
 24. Miller LK (1993) Baculoviruses: high-level expression in insect cells, *Curr. Opin. Genet. Dev.* 3: 97-101
 25. Thomsen DR, Post LE and Elhammer AP (1990) Structure of O-glycosidically linked oligosaccharides synthesized by the insect cell line Sf9, *J. Cell Biochem.* 43: 67-79
 26. Graner M, Stupka K and Karr TL (1994) Biochemical and cytological characterization of DROP-1: a widely distributed proteoglycan in *Drosophila*, *Insect. Biochem. Mol. Biol.* 24: 557-567
 27. Inoue H, Nojima H and Okayama H (1990) High efficiency transformation of *Escherichia coli* with plasmids, *Gene.* 96: 23-28
 28. Smith GE and Summers MD (1978) Analysis of baculovirus genomes with restriction endonucleases, *Virology.* 89: 517-527
 29. Sambrook J, Fritsch EF and Maniatis T (1989) *Molecular cloning, a laboratory manual*, 2nd Edn, Cold Spring Harbor Laboratory Press, Cold Spring Harbor, NY
 30. Reubsact FA, Langeveld JP and Veerkamp JH (1985) Glycosaminoglycan content of glomerular and tubular basement membranes of various mammalian species, *Biochim. Biophys. Acta* 838: 144-150
 31. Harlow E and Lane D (1988) *Antibodies, a laboratory manual*, Cold Spring Harbor Laboratory Press, Cold Spring Harbor, NY.
 32. Smith DB and Johnson KS (1988) Single-step purification of polypeptides expressed in *Escherichia coli* as fusions with glutathione-S-transferase, *Gene* 67: 31-40
 33. Van den Heuvel LP, van den Born J, Veerkamp JH, van der Velden TJ, Schenkels L, Monnens LA, Schröder CH and Berden JH (1990) Heparan sulfate proteoglycan from human tubular basement membrane. Comparison with this component from the glomerular basement membrane, *Biochim. Biophys. Acta* 1025: 67-76
 34. Van de Lest CH, Versteeg EM, Veerkamp JH and Van Kuppevelt TH (1994) Quantification and characterization of glycosaminoglycans at the nanogram level by a combined azure A-silver staining in agarose gels, *Anal. Biochem.* 221: 356-361
 35. Huh NE and Weaver RF (1990) Identifying the RNA polymerases that synthesize specific transcripts of the *Autographa californica* nuclear polyhedrosis virus, *J. Gen. Virol.* 71: 195-201
 36. Westwood JA, Jones IM and Bishop DH (1993) Analyses of alternative poly(A) signals for use in baculovirus expression vectors, *Virology.* 195: 90-99
 37. Ooi BG and Miller LK (1990) Transcription of the baculovirus polyhedrin gene reduces the levels of an antisense transcript initiated downstream, *J. Virol.* 64: 3126-3129
 38. Pham DQ and Sivasubramanian N (1992) *In vivo* transcriptional analysis of three baculovirus genes: evidence of homology between viral and host transcripts, *Virology* 190: 288-297
 39. Van den Heuvel LP, van den Born J, van der Velden TJ, Veerkamp JH, Monnens LA, Schroder CH and Berden JH (1989) Isolation and partial characterization of heparan sulfate proteoglycan from the human glomerular basement membrane, *Biochem. J.* 264: 457-465
 40. Van de Lest CH, Versteeg EM, Veerkamp JH and van Kuppevelt TH (1995) Digestion of proteoglycans in porcine pancreatic elastase-induced emphysema in rats, *Eur. Respir. J.* 8: 238-245
 41. Aviezer D, Levy E, Safran M, Svahn C, Buddecke E, Schmidt A, David G, Vlodavsky I and Yayon A (1994) Differential structural requirements of heparin and heparan sulfate proteoglycans that promote binding of basic fibroblast growth factor to its receptor, *J. Biol. Chem.* 269:114-121
 42. Zhang L, David G and Esko JD (1995) Repetitive Ser-Gly sequences enhance heparan sulfate assembly in proteoglycans, *J. Biol. Chem.* 270:27127-27135
 43. Danielson KG, Martinez-Hernandez A, Hassell JR and Iozzo RV (1992) Establishment of a cell line from the EHS tumor: biosynthesis of basement membrane constituents and characterization of a hybrid proteoglycan containing heparan and chondroitin sulfate chains, *Matrix.* 12: 22-35
 44. Van Det NF, van den Born J, Tamsma JT, Verhagen NA, van den Heuvel LP, Berden JH, Bruijn JA, Daha MR and van der Woude FJ (1995) Proteoglycan production by human glomerular visceral epithelial cells and

mesangial cells in vitro, *Biochem. J.* 307:
759-768

45. Paulsson M, Yurchenco PD, Ruben GC,
Engel J and Timpl R (1987) Structure of low

density heparan sulfate proteoglycan isolated
from a mouse tumor basement membrane, *J.*
Mol. Biol. 197: 297-313

CHAPTER THREE

Lipoprotein binding by the core protein of human perlecan

Lipoprotein binding by the core protein of human perlecan

CHAPTER THREE

SUMMARY Perlecan is a proteoglycan of virtually all extracellular matrices including those of the vascular system. Domain I of perlecan may be glycosylated with heparan sulfate (HS), chondroitin sulfate or dermatan sulfate. The primary structure of domain II is similar to that of the low-density lipoprotein receptor. In this study we present *in vitro* evidence for a possible role of perlecan in lipoprotein adhesion to the extracellular matrix. Two recombinant fragments of human perlecan (one comprising domain I and II^a, the other domain I, II^a and II^b) were produced in the yeast *Pichia pastoris* at high level (0.5 and 2.4 g/l respectively). The fragments were devoid of glycosaminoglycans as shown by anion exchange chromatography and insensitivity to heparitinase and chondroitinase ABC. Both fragments and a similar recombinant protein produced in *E. coli* showed affinity for the human lipoproteins VLDL and IDL (together in one fraction), LDL and Lp(a), whereas HDL was not bound. Addition of exogenous HS did not significantly influence the interaction. In contrast to the glycosaminoglycan-free perlecan fragments, a similar fragment produced as a chondroitin sulfate proteoglycan by insect cells was not functional in lipoprotein binding. The results suggest that the core protein of human perlecan functions as a lipoprotein binding site in the extracellular matrix, and that this activity may be modulated by its glycosylation characteristics.

TO INDEX

INTRODUCTION

Heparan sulfate proteoglycans of the cell surface are essential factors in receptor-mediated internalization of lipoprotein particles. Internalization by the low-density lipoprotein (LDL) receptor requires a dual interaction of apolipoprotein B-100 (apoB-100) with HS and the receptor. Both interactions were localized to site B of apoB-100 (residues 3359-3369), which is not present in apo-B48 [1,2]. In analogy, the internalization of remnant lipoproteins requires a dual binding of apolipoprotein E to HS and the LDL receptor related protein (LRP) [3]. Lipoproteins also bind to the extracellular matrix, where they also associate with glycosaminoglycans [4-6]. However, the participation of core protein structures in this process has not been described yet.

Perlecan is a widely expressed extracellular proteoglycan that is present in all vascular basement membranes [7]. The core protein of human perlecan has a molecular mass of 467 kDa and is composed of five functional domains [8,9]. Domain I (residues 24-196) offers three sites for glycosaminoglycan attachment [10]. Despite the designation of perlecan as a heparan sulfate (HS) proteoglycan, this domain may also be glycosylated with other glycosaminoglycans such as chondroitin sulfate and dermatan sulfate [11-14]. The type of glycosylation may importantly alter the functional properties of perlecan. For example, the angiogenic and mitogenic activity of perlecan depends on the activation of fibroblast growth factors by interaction with HS residues [15,16]. Also lipoprotein lipase was shown to bind HS [17,18]. For a more complete survey of the many functions of HS, several excellent reviews are available [19-22]. Domain II^a (residues 197-404) is similar in primary structure to the apoB-100 binding site of the low-density lipoprotein (LDL) receptor [8,9]. The LDL receptor-like

domain is flanked on the C-terminal side by a single Ig-like loop, designated domain II^b (residues 405–506). This loop is similar to the 21 Ig-like repeats that occur in domain IV. The presence of the LDL receptor-like domain led us to hypothesize that the lipoprotein binding sites in the extracellular matrix might reside on perlecan. Here, we tested this hypothesis using recombinant proteins comprising domains I and II of human perlecan. To take a possible contribution of domain II^b into account, we produced different recombinant constructs that either excluded or included this Ig-like loop. In addition, we compare recombinant proteins produced by different expression systems to reveal functional differences induced by post-translational modifications. The results suggest that perlecan may be a functional binding site for lipoproteins in the extracellular matrix.

MATERIALS AND METHODS

Antibodies

Monoclonal antibody 95J10 was raised against human perlecan-(24–404)-fragment produced as a fusion protein with glutathione-S-transferase in *Escherichia coli* [23]. This antibody does not cross-react with perlecan from other species, other basement membrane components, glycosaminoglycans, glutathione-S-transferase or proteins from *E. coli* cell lysate [24].

Generation of recombinant *Pichia pastoris* clones

Recombinant yeast clones expressing perlecan fragments were generated following procedures supplied with the *Pichia pastoris* expression kit (Invitrogen, Leek, The Netherlands). Perlecan cDNA fragments were excised from the plasmids pVL1393-P12a and pVL1393-P12ab [25]. The plasmids were digested with *Nco*I, treated with the Klenow fragment of DNA polymerase I, purified and subsequently *Not*I-digested. The two fragments (1.2 and 1.5 kb) were ligated into the *Sna*BI and *Not*I sites of the pPIC9K vector (Invitrogen) [26]. The resulting vectors pPIC9K-P12a and pPIC9K-P12ab were transformed into the *E. coli* strain DH5 α for propagation. The integrity of the plasmids was confirmed by restriction enzyme analysis and by sequencing on a ABI377-type automated sequence analyzer (ABI Prism). The plasmids were linearized by digestion with *Sal*II and electroporated into *P. pastoris* GS115 spheroblasts. After integration of the expression cassette into the *P. pastoris* genome, recombinant colonies were selected by growth on histidine-deficient media. Clones containing multiple copies of the expression cassette were identified by determining the maximum concentration of G418 allowing growth [26].

Characterization of recombinant fragments produced in *P. pastoris*

For expression of recombinant perlecan-(24–404)-fragment and perlecan-(24–506)-fragment the selected clones were grown at 30°C in BMMY medium (86.8 mM KH₂PO₄, 13.2 mM K₂HPO₄, 20 g/l peptone, 13.4 g/l yeast nitrogen base, 10 g/l yeast extract, 0.5 % methanol and 0.4 mg/l biotin, pH 6.0) while shaking at 225 rpm. Alternative media used for optimization were BMM (86.8 mM KH₂PO₄, 13.2 mM K₂HPO₄, 13.4 g/l yeast nitrogen base, 0.5 % methanol, 0.4 mg/l biotin, pH 6.0) and MM (13.4 g/l yeast nitrogen base, 0.5 % methanol, 0.4 mg/l biotin, pH 6.0). Medium was harvested after 0, 5, 20, 28, 44, 51, 72 or 100 h, centrifuged for 3 min at 10,000 x g and stored at –80°C until analysis.

Ion exchange chromatography was performed using 1-ml columns of DEAE Sepharose (Pharmacia) with 50 mM Tris pH 7.0 as equilibration and wash buffer. For elution, a gradual increase of NaCl to a final concentration of 2 M was applied. All fractions were analyzed for presence of recombinant fragments by dot blotting. To this end, 1 μ l of each supernatant was spotted onto a nitrocellulose membrane and allowed to air-dry. After blocking for 1 h with 3%

BSA in PBS containing 0.1% Tween-20, the membrane was incubated for 1 h at 22°C with MAb 95J10 (10 µg IgG/ml in PBS containing 1.5% BSA and 0.2% Tween-20), washed, and incubated for 1 h at 22°C with alkaline phosphatase-conjugated goat-anti-mouse serum (diluted 1:1000 in PBS containing 1.5% BSA and 0.2% Tween-20). The membrane was washed again and incubated in a solution of 0.33 mg/ml p-nitro blue tetrazolium, 0.165 mg/ml bromo-chloro-indolylphosphate, 100 mM NaCl, 5 mM MgCl₂ and 100 mM Tris·HCl pH 9.5 for 20 min at 22°C.

To estimate produced yields, quantitative ELISA was performed as described elsewhere [24] except that serial two-fold dilutions of the yeast culture medium were coated for 16 h at 4°C, starting from a 20-fold dilution as the highest concentration of supernatant. A calibration curve with standard amounts of affinity purified bacterial fusion protein was taken on the same plate and all samples were analyzed in duplicate.

Recombinant perlecan fragments from other expression systems

Recombinant human perlecan-(24–404)-fragment was expressed as a fusion protein in *E. coli* and purified by affinity chromatography as described previously [23]. This protein did not contain glycosaminoglycan residues. The expression, characterization and purification of perlecan-(1–404)-fragment by baculovirus-infected insect cells was also described previously [25]. This fragment was secreted into the cell culture medium and contained chondroitin sulfate residues. For this study we harvested the culture medium at 64 h after infection of the insect cells.

Isolation of lipoproteins from human plasma

Lipoprotein fractions and lipoprotein-deficient serum (LPDS) were isolated by density-gradient ultracentrifugation as described [27]. In short, 2.0 ml of fresh human plasma was transferred to a SW40 polycarbonate ultracentrifuge tube and mixed with 0.770 g KBr. Subsequently, 2 ml of high-density buffer (2.65 M KBr, 195 mM NaCl and 0.27 mM EDTA, $d=1.225$ g/ml), 4 ml of medium-density buffer (1.14 M KBr, 84 mM NaCl and 0.27 mM EDTA, $d=1.100$ g/ml) and 4 ml of low-density buffer (0.27 mM EDTA; $d=1.006$ g/ml) were layered on top of the surface without mixing. After centrifugation for 22 h at 40,000 rpm and 20°C in a SW40 swing-out rotor and a Beckmann L7-55 ultracentrifuge, individual lipoprotein fractions were aspirated: VLDL/IDL (together on the surface), LDL, Lp(a) and HDL/LPDS (together at the bottom). The bottom fraction was desalted by size exclusion chromatography using Sephadex G-10 resin (Pharmacia Biotech, Roosendaal, The Netherlands), the density adjusted to 1.21 g/ml, and HDL ($d<1.21$) and LPDS ($d>1.21$) were separated by ultracentrifugation for 24 h at 20°C in a fixed-angle TFT 45.6 rotor. All lipoproteins except the VLDL/IDL fraction were dialyzed against 160 mM NaCl, 10 mM EDTA and 10 mM NaHPO₄ (pH 7.4) during 24 h at 4°C. The samples were supplemented with 5% saccharose for cryoprotection and stored at –20°C until use. Protein content was assayed by the Lowry method with BSA as standard. Cholesterol was determined using the CHOD-PAP reagent (Boehringer Mannheim, Germany) following the manufacturer's instructions.

Glycosidase digestion

For chondroitinase treatment, culture media containing recombinant proteins from *P. pastoris* were added to two volumes of a 0.2 M Tris·HCl buffer containing 0.05% NaN₃ at pH 8.0. This mixture was incubated for 2 h at 37°C in presence of 0.3 U/ml chondroitinase ABC (Seikagaku Corp., Tokyo, Japan). For heparitinase digestion, the recombinant proteins were dialyzed for 20 h at 4°C against heparitinase-buffer (0.1 M sodium acetate, 10 mM CaCl₂, pH 7.0). Heparitinase (Seikagaku) was added to a final concentration of 0.05 U/ml and the mixture was incubated for 3 h at 43°C. To monitor the reaction progress, 2 mg/ml HS (from

bovine kidney, Sigma) was added to the dialysate and treated the same way. For application in lipoprotein binding studies, perlecan-(24–404)-fragment and perlecan-(24–506)-fragment were diluted in PBS to 60 and 80 µg/ml respectively. The absence of proteolytic activity in these mixtures was ascertained by SDS-PAGE analysis before and after the incubation. Lipoproteins and LPDS were diluted to 125 µg/ml protein in 0.1 M sodium acetate and 20 mM CaCl₂ (pH 7.0). One ml was incubated for 3 h at 43 °C with 10 mU heparitinase.

Determination of glycosaminoglycan content

To measure the glycosaminoglycan content, 400 µl of samples were mixed with 1 ml of Farndale's reagent (0.2% (w/v) sodium formiate, 0.2% (v/v) formic acid and 0.0016% (w/v) 1,9-dimethyl-methylene blue in water, pH 3.5) [28]. The optical density was measured at 525 nm. A calibration curve was constructed using 400 µl of HS standard dilutions (range 2.5 to 25 µg/ml in heparitinase-buffer). Glycosaminoglycan concentrations were calculated by interpolation of a linear regression curve (correlation coefficient >0.998; n=20).

Lipoprotein binding studies

Lipoproteins were diluted to 25 µg/ml on protein basis in coating buffer (50 mM carbonate, pH 9.6) and 100 µl was incubated for 16 h at 4°C in ELISA wells (Nunc maxisorp). The wells were then blocked for 30 min at 22°C with 10 mg/ml bovine serum albumin in coating buffer, washed twice with PBS, and incubated for 1 h at 37°C with 100 µl culture supernatant from the selected *P. pastoris* clone diluted in PBS to a final concentration of 60 µg/ml (perlecan-(24–404)-fragment) and 80 µg/ml (perlecan-(24–506)-fragment). In some cases heparitinase was added as described above. After washing 5 times with PBS, the wells were incubated for 1 h at 22°C with 95J10 (10 µg IgG/ml in PBS), washed again 5 times, and further processed according to standard protocols [29] using a peroxidase-conjugated goat-anti-mouse antiserum (1:2500 in PBS containing 1%BSA, Dakopatts). The produced optical density was read at 492 nm.

RESULTS

Optimization of expression of perlecan fragments in *P. pastoris*

Two fragments of human perlecan were expressed as recombinant proteins in the yeast *P. pastoris*. The first fragment comprised domain I and II^a of perlecan, including amino acids 24–404. The second fragment comprised domain II^b in addition, including amino acids 24–506. We will refer to these constructs as perlecan-(24–404)-fragment and perlecan-(24–506)-fragment respectively. The original signal sequence of human perlecan (amino acids 1–21) was replaced by a yeast signal sequence to induce secretion of the recombinant proteins into the culture medium.

To optimize the expression levels of both constructs, we characterized the recombinant yeast clones for the number of expression cassettes per cell. The cassette also contains a G418 resistance marker, and the resistance towards increasing concentrations of G418 was previously demonstrated to correlate in a linear way with the amount of integrations. For 118 clones containing the expression cassette for perlecan-(24–404)-fragment, 119 clones containing that for perlecan-(24–506)-fragment, and 48 clones containing the empty expression cassette, we measured the maximum concentration of G418 at which growth occurred. The results are listed in Table 1. Growth of the host strain was observed at a maximum concentration of 0.25 g/l G418. Five clones encoding the (24–404)-fragment and seven clones encoding the (24–506)-fragment that were able to grow in presence of 4.0 g/l G418 were selected for further examination.

Table 1. Screening of *P. pastoris* clones for the number of integrated copies of the expression cassettes encoding A) perlecan-(24 404)-fragment, B) perlecan-(24 506)-fragment or C) the empty cassette as a control. The induced resistance towards G418 was used as a marker. For each concentration of G418 tested, the number of clones for which this was the maximal level allowing growth is given.

G418 (g/l)	Number of resistant clones		
	A	B	C
0.25	21	21	9
0.50	1	3	0
0.75	0	3	1
1.00	2	7	1
1.50	42	12	11
2.00	47	58	23
4.00	5	15	3
total	118	119	48

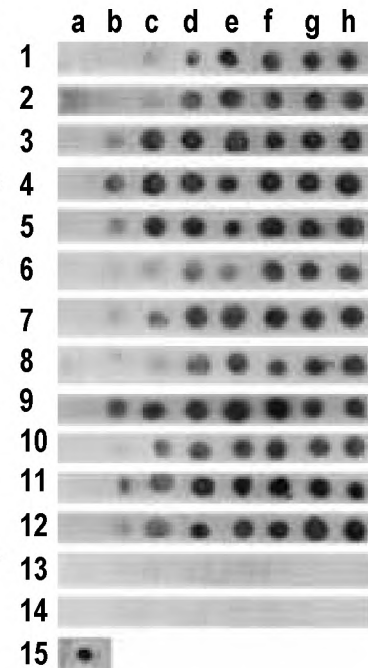


Figure 1. Influence of the time of harvest on the yield of recombinant perlecan fragments produced by *P. pastoris*. Perlecan-like immunoreactivity was detected in 1- μ l aliquots of supernatant from recombinant clones spotted onto nitrocellulose membrane. Clones 1–5 encode the (24–404)-fragment, clones 6–12 encode the (24–506)-fragment, and clones 13–14 carry the empty expression cassette as a negative control. On the bottom, supernatant containing perlecan-(1–404)-fragment from baculovirus-infected insect cells was spotted as a positive control (nr. 15). The time of harvest was 0, 5, 20, 28, 44, 51, 72, and 99 h (a–h).

For optimal results we also determined how the yield of the recombinant proteins was influenced by the time of harvest. At various time points after inoculation, we measured the presence of recombinant proteins by immunoblotting with a monoclonal antibody directed to the N-terminal region of human perlecan [23]. Perlecan-(24–404)-fragment and perlecan-(24–506)-fragment became readily detectable from 5 h incubation on (Figure 1). The immunoreactivity increased markedly during the first 28 to 44 h. As a control, recombinant *P. pastoris* clones that contain the empty expression cassette produced no detectable perlecan-like immunoreactivity.

Next, we compared the expression levels obtained by use of various growth media. A single yeast clone was cultured in three different media (named MM, BMM and BMMY medium) for expression of perlecan-(24–404)-fragment. The culture media were analyzed after 40 h by western blotting with an anti-perlecan monoclonal antibody. The use of BMMY medium gave clearly the highest yields (approximately 5-fold higher than MM and BMM; data not shown).

Characterization of the recombinant fragments

Culture media of five *P. pastoris* clones expressing perlecan-(24–404)-fragment and seven clones expressing perlecan-(24–506)-fragment were analyzed by western blotting (Figure 2). All analyzed clones produced perlecan-like immunoreactivity, whereas no detectable staining was observed for clones that carried the empty expression cassette. For the (24–404)-fragment multiple bands were stained, of which the major band corresponded with the predicted molecular mass, 42 kDa. The other band displayed a lower electrophoretic mobility, suggesting different post-translational modification characteristics or a higher molecular mass (e.g. by read-through translation in a percentage of cases). As expected for the (24–506)-fragment the major band corresponded with the predicted molecular mass (53 kDa) and no prominent additional bands were visible. The yields were 2.4 g/l for perlecan-(24–404)-fragment and 0.5 g/l for perlecan-(24–506)-fragment, respectively.

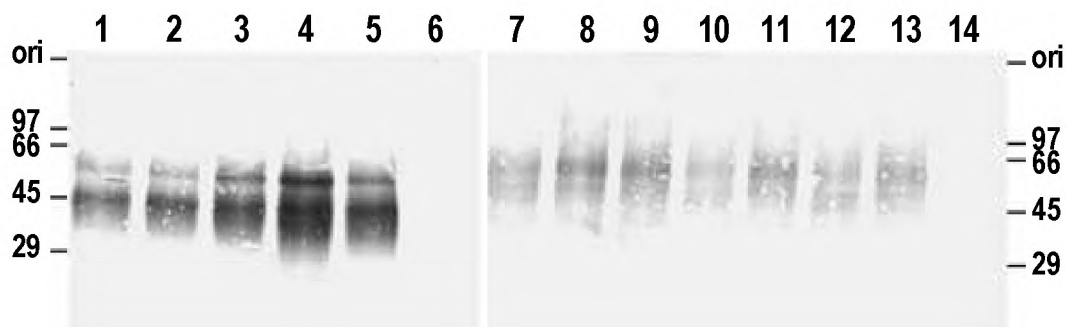


Figure 2. Characterization of recombinant perlecan-(24 404)-fragment and perlecan-(24 506)-fragment by western blotting with an anti-perlecan monoclonal antibody. Eight μ l of culture medium was applied in each lane. Lanes 1 5: different *P. pastoris* clones expressing perlecan-(24 404)-fragment. Lanes 7 13: different clones expressing perlecan-(24 506)-fragment. Lanes 6 and 14: supernatant from two *P. pastoris* clones with multiple insertions of the empty expression cassette as a negative control.

The smeared appearance of the (24–404)-fragment and the (24–506)-fragment on western blots suggested that some type of glycosylation of the recombinant proteins occurred. However, smears observed for glycosaminoglycan-containing proteoglycans are normally more prominent. The mobility of both recombinant proteins was not altered after heparitinase or chondroitinase ABC digestion. Furthermore, the fragments did not bind to DEAE Sepharose in anion exchange chromatography. As proteoglycans are known to firmly bind to this matrix under the used conditions (up to 2.0 M NaCl is required for elution), this indicates that glycosaminoglycan chains are absent.

Interaction of lipoproteins with recombinant domain I and II of human perlecan

To investigate the functionality of perlecan domain II as a lipoprotein receptor, lipoproteins were isolated from human plasma. The preparations were analyzed for protein and cholesterol content (Table 2). Standard amounts were coated into ELISA wells. Subsequently, binding of perlecan fragments to these preparations was analyzed by incubating the wells with culture medium, followed by immunodetection. The results are summarized in Figure 3.

Both the perlecan-(24–404)-fragment and the (24–506)-fragment produced by *P. pastoris* showed affinity for VLDL/IDL, LDL and Lp(a) (Figure 3A, B). The highest signal was observed for LDL. When the fragments were incubated in LDL-coated wells, the generated absorbance exceeded that of directly coated fragment. In contrast to this, no binding to HDL or LPDS was observed. Also perlecan-(24–404)-fragment expressed as a fusion protein in *E. coli* had affinity for VLDL/IDL, LDL and Lp(a) (Figure 3C). Also in this case, the highest absorbance levels were observed in LDL-coated wells.

In contrast to the adhesive properties of recombinant fragments from *P. pastoris* and *E. coli*, perlecan-(1–404)-fragment produced by the baculovirus expression system did not bind to any of the analyzed lipoprotein

Table 2. Protein and cholesterol content of lipoprotein fractions isolated from human plasma.

Fraction	Protein (mg/ml)	Cholesterol (mM)
VLDL/IDL	1.08	3.6
LDL	0.25	0.6
Lp(a)	0.64	0.8
HDL	2.08	1.0
LPDS	51.2	0.1

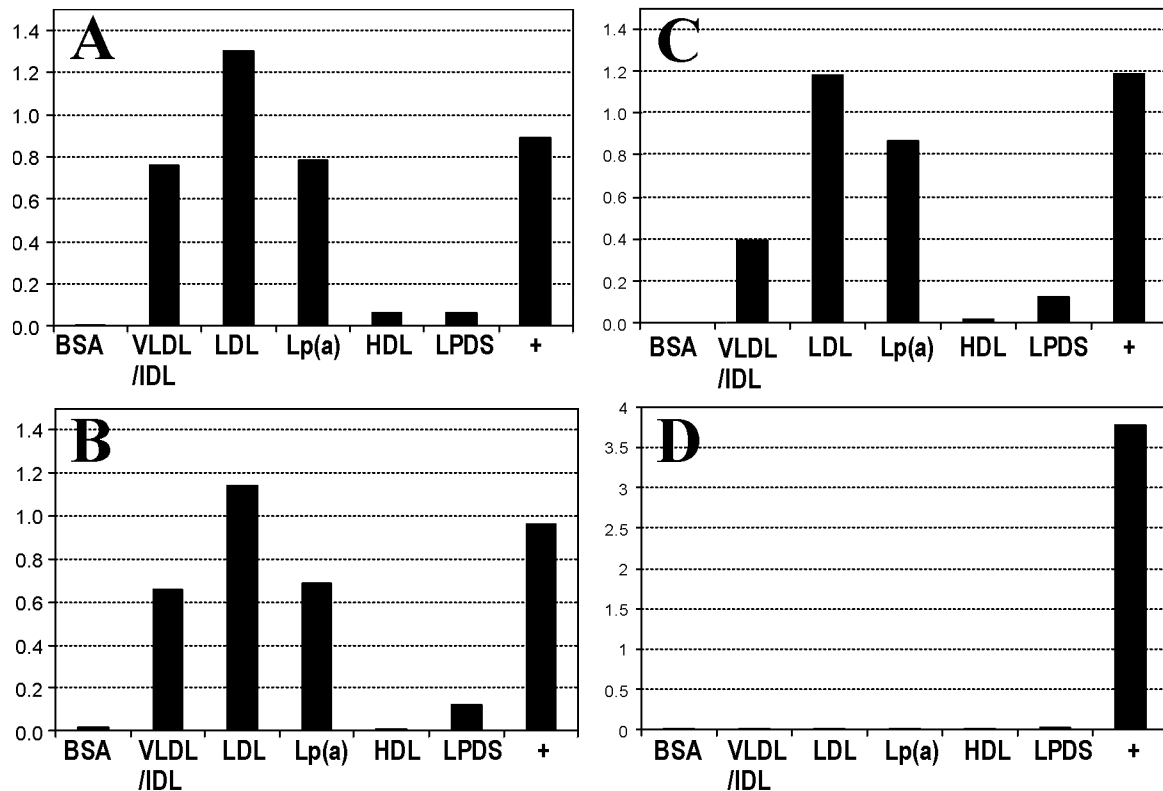


Figure 3. Binding of recombinant fragments of human perlecan to lipoproteins isolated from human plasma. (A) Perlecan-(24 404)-fragment produced in *P. pastoris*, (B) perlecan-(24 506)-fragment produced in *P. pastoris*, (C) perlecan-(24 404)-fragment produced as bacterial fusion protein, and (D) perlecan-(1 404)-fragment produced by baculovirus-infected insect cells were incubated in ELISA wells coated with 2.5 μ g BSA, VLDL/IDL, LDL, Lp(a), HDL or LPDS. The mean value of two independent measurements is shown. As a positive control (+), the used concentration of each recombinant fragment was directly coated into the wells.

fractions (Figure 3D). The same concentration of this recombinant protein produced a full-scale detection signal when directly coated into the wells. These results suggest that domains I and II of perlecan may bind lipoproteins when the fragment is devoid of glycosaminoglycans, but this affinity is absent when it is associated with chondroitin sulfate. For this reason, we investigated the influence of glycosaminoglycan interactions in more detail.

Influence of glycosaminoglycans on lipoprotein binding

Since the apoB-100 component of lipoproteins is known to contain glycosaminoglycan binding sites, we analyzed the lipoprotein fractions for glycosaminoglycan content (Table 3). The VLDL/IDL, LDL and Lp(a) preparations contained significant amounts of glycosaminoglycan (approximately 21, 26 and 54 ng per μ g of protein, respectively). HDL and LPDS were free of glycosaminoglycans. To differentiate between different types of glycosaminoglycan, the lipoproteins were treated with heparitinase. This enzyme

Table 3: Glycosaminoglycan content of the lipoprotein fractions before and after treatment with heparitinase (HT). Two individual measurements are given.

Fraction	Glycosaminoglycan (ng/ μ g protein)			
	- HT		+ HT	
VLDL/IDL	21.0	21.0	15.0	16.5
LDL	25.5	27.7	0.7	0.7
Lp(a)	53.2	54.0	0.0	1.5
HDL	0.0	1.5	0.0	0.7
LPDS	0.0	0.0	0.0	0.7

Table 4. Reduced binding of recombinant perlecan fragments produced in *P. pastoris* to lipoprotein fractions VLDL/IDL, LDL and Lp(a) as coated substrates after heparitinase (HT) treatment. Binding activities are given as optical density units.

Substrate	Perlecan-(24-404)-fragment		Perlecan-(24-506)-fragment	
	- HT	+ HT	- HT	+ HT
	A ₄₉₂	A ₄₉₂	A ₄₉₂	A ₄₉₂
BSA	0.06	0.06	0.07	0.06
VLDL/IDL	0.48	0.18	1.14	0.40
LDL	0.78	0.42	1.80	0.85
Lp(a)	0.69	0.29	1.46	0.66

recognizes and hydrolyzes specific disaccharide structures in the HS chain, which are not present in chondroitin sulfate, dermatan sulfate, keratan sulfate or hyaluronate. A HS chain may be degraded completely or in part, depending on the frequency of occurrence of these structures. Glycosaminoglycans in LDL and Lp(a) were completely degraded by heparitinase, demonstrating that they contain HS as the only glycosaminoglycan type (Table 3). The glycosaminoglycan content of VLDL/IDL was reduced partially by heparitinase, leaving 77% of the material intact. This fraction therefore contains HS, which may be of a different composition, partly inaccessible for the enzyme, or accompanied by other glycosaminoglycan types.

To reveal a possible involvement of HS in the interaction of lipoproteins with the perlecan core protein fragments, we analyzed the effect of heparitinase on binding. When recombinant fragments were applied to the lipoprotein-coated wells in the presence of heparitinase, the observed binding was importantly reduced (Table 4). This was demonstrated for both recombinant proteins from *P. pastoris*. Thus, binding of lipoproteins to the perlecan core protein fragment is potentiated by the presence of endogenous HS. When the concentration of HS was increased by exogenous addition, the binding of perlecan-(24-404)-fragment to VLDL/IDL, LDL and Lp(a) was not influenced significantly (Figure 4). The perlecan fragment still did not bind to HDL or LPDS, indicating that their inability to bind the perlecan

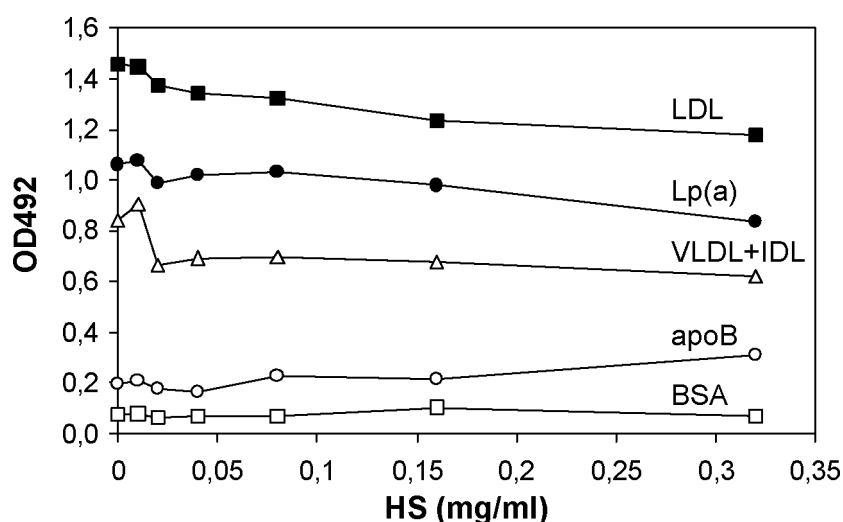


Figure 4. Influence of exogenous HS on the binding of perlecan-(24 404)-fragment to different lipoprotein fractions. After coating the native lipoproteins or BSA as control, wells were incubated with the perlecan-(24 404)-fragment from *P. pastoris* in presence of increasing concentrations of HS. Binding of the fragment was quantitated by ELISA as optical density units at 492 nm.

fragments is not due to the lack of HS in these fractions.

DISCUSSION

The availability of recombinant fragments containing domains I and II of human perlecan offers opportunities to study their functions in a well-defined way. Extraction of perlecan from tissues is complicated due to the strong interactions with many other components of the basement membrane, implicating a high risk for contamination. The purification procedure is time-consuming and therefore prone to proteolytic degradation and low recovery. The use of recombinant protein fragments circumvents these problems. The *P. pastoris* expression system allows the stable and high-level eukaryotic expression of proteins. In contrast to the baculovirus expression system [25], glycosaminoglycan synthesis on the recombinant fragments was not supported by *P. pastoris*. None of the three used host systems produced the perlecan fragments as a HS proteoglycan.

The lipoprotein-binding activity of perlecan can be assigned to the core protein, since the binding was observed for recombinant fragments from *P. pastoris* and *E. coli*, both devoid of glycosaminoglycan residues. The involvement of the core protein is also confirmed by the inability of soluble HS to compete with the fragments for binding. The binding site is located within domains I and II^a. The subdomain II^b is apparently not essential for lipoprotein binding. Given the high similarity of domain II with the LDL receptor it can be speculated, that this domain is most likely responsible for the interaction.

Comparing the perlecan-binding activity among individual lipoproteins, the results suggests that apoB-100 may be the involved ligand. All lipoprotein fractions that bound the recombinant perlecan fragments contain apoB-100, whereas the non-binding fractions lack this component. The highest binding activity was observed for LDL, that contains apoB-100 as the only protein component. However the differences cannot be merely explained by apoB content: VLDL/IDL (that contains relatively little apoB) showed a high affinity in this respect. Neither was a direct correlation with the HS content of the lipoproteins apparent. To confirm if apoB-100 acts as a ligand and to localize the involved binding site, further experimental evidence is required.

Glycosaminoglycans appear to play a modulating role in the binding of lipoproteins to the core protein of perlecan. HS or HSPG binds to lipoproteins *in vivo*, as shown by the co-purification of HS with VLDL/IDL, LDL and Lp(a) from human plasma. ApoB could be involved, since this apoprotein has HS affinity [1, 2]. We also showed that treatment of these lipoproteins with heparitinase reduced binding activity to the perlecan fragments. This suggests that endogenous HS potentiates binding, assuming that the lipoproteins remained native during the heparitinase treatment. The presence of endogenous HS explains that extra HS does not influence binding of lipoproteins. But how is lipoprotein binding affected when HS is covalently attached to domain I of perlecan? When glycosylated with chondroitin sulfate, the perlecan-(1–404)-fragment showed no affinity for lipoproteins. HS attachment may act synergistic and enhance lipoprotein binding to the core protein. Alternatively, the presence of HS residues on domain I could inhibit lipoprotein binding if the supramolecular conformation required for such a dual binding is unfavorable.

In conclusion, we demonstrated that the core protein of human perlecan has lipoprotein binding activity *in vitro*. This phenomenon may contribute to regulate the retention of lipoproteins in the extracellular matrix in a glycosylation-dependent way. As increased lipoprotein adhesion to the subendothelial matrix is considered to be a causal event in the development of atherosclerosis, these data may contribute to a better understanding of the mechanism involved.

ACKNOWLEDGEMENTS

This study was supported by grant C93.1309 from the Dutch Kidney Foundation. The laboratory participated in the Concerted Action "Alterations in extracellular matrix components in diabetic nephropathy and other glomerular diseases", which was financially supported by the European Community with the Biomed I program (BMH1-CT92-1766).

REFERENCES

- Boren J, Olin K, Lee I, Chait A, Wight TN and Innerarity TL (1998) Identification of the principal proteoglycan-binding site in LDL. A single-point mutation in apo-B100 severely affects proteoglycan interaction without affecting LDL receptor binding, *J. Clin. Invest.* 101: 2658-2664.
- Boren J, Lee I, Zhu W, Arnold K, Taylor S and Innerarity TL (1998) Identification of the low density lipoprotein receptor-binding site in apolipoprotein B100 and the modulation of its binding activity by the carboxyl terminus in familial defective apo-B100, *J. Clin. Invest.* 101: 1084-1093.
- Mahley RW, Ji ZS, Brecht WJ, Miranda RD and He D (1994) Role of heparan sulfate proteoglycans and the LDL receptor-related protein in remnant lipoprotein metabolism, *Ann. N. Y. Acad. Sci.* 737: 39-52.
- Saxena U and Goldberg IJ (1994) Endothelial cells and atherosclerosis: lipoprotein metabolism, matrix interactions, and monocyte recruitment, *Curr. Opin. Lipidol.* 5: 316-322.
- Williams KJ and Fuki IV (1997) Cell-surface heparan sulfate proteoglycans: dynamic molecules mediating ligand catabolism, *Curr. Opin. Lipidol.* 8: 253-262.
- Camejo G, Hurt-Camejo E, Wiklund O and Bondjers G (1998) Association of apo B lipoproteins with arterial proteoglycans: pathological significance and molecular basis, *Atherosclerosis* 139: 205-222.
- Murdoch AD, Liu B, Schwarting R, Tuan RS and Iozzo RV (1994) Widespread expression of perlecan proteoglycan in basement membranes and extracellular matrices of human tissues as detected by a novel monoclonal antibody against domain III and by in situ hybridization, *J. Histochem. Cytochem.* 42: 239-249.
- Kallunki P and Tryggvason K (1992) Human basement membrane heparan sulfate proteoglycan core protein: a 467-kD protein containing multiple domains resembling elements of the low density lipoprotein receptor, laminin, neural cell adhesion molecules, and epidermal growth factor, *J. Cell Biol.* 116: 559-571.
- Murdoch AD, Dodge GR, Cohen I, Tuan RS and Iozzo RV (1992) Primary structure of the human heparan sulfate proteoglycan from basement membrane (HSPG2/perlecan). A chimeric molecule with multiple domains homologous to the low density lipoprotein receptor, laminin, neural cell adhesion molecules, and epidermal growth factor, *J. Biol. Chem.* 267: 8544-8557.
- Bork P and Patthy L (1995) The SEA module: a new extracellular domain associated with O-glycosylation, *Protein Sci.* 4: 1421-1425.
- Couchman JR, Kapoor R, Sthanam M and Wu RR (1996) Perlecan and basement membrane-chondroitin sulfate proteoglycan (bamacan) are two basement membrane chondroitin/dermatan sulfate proteoglycans in the Engelbreth-Holm-Swarm tumor matrix, *J. Biol. Chem.* 271: 9595-9602.
- Costell M, Mann K, Yamada Y and Timpl R (1997) Characterization of recombinant perlecan domain I and its substitution by glycosaminoglycans and oligosaccharides, *Eur. J. Biochem.* 243: 115-121.
- Kokenyesi R and Silbert JE (1995) Formation of heparan sulfate or chondroitin/dermatan sulfate on recombinant domain I of mouse perlecan expressed in Chinese hamster ovary cells, *Biochem. Biophys. Res. Commun.* 211: 262-267.
- SundarRaj N, Fite D, Ledbetter S, Chakravarti S and Hassell JR (1995) Perlecan is a component of cartilage matrix and promotes chondrocyte attachment, *J. Cell Sci.* 108: 2663-2672.
- Aviezer D, Hecht D, Safran M, Eisinger M, David G and Yayon A (1994) Perlecan, basal lamina proteoglycan, promotes basic fibroblast growth factor-receptor binding, mitogenesis, and angiogenesis, *Cell* 79: 1005-1013.
- Turnbull JE, Fernig DG, Ke Y, Wilkinson MC and Gallagher JT (1992) Identification of the basic fibroblast growth factor binding

- sequence in fibroblast heparan sulfate, *J. Biol. Chem.* 267: 10337-10341.
17. Berryman DE and Bensadoun A (1995) Heparan sulfate proteoglycans are primarily responsible for the maintenance of enzyme activity, binding, and degradation of lipoprotein lipase in Chinese hamster ovary cells, *J. Biol. Chem.* 270: 24525-24531.
 18. Parthasarathy N, Goldberg IJ, Sivaram P, Mulloy B, Flory DM and Wagner WD (1994) Oligosaccharide sequences of endothelial cell surface heparan sulfate proteoglycan with affinity for lipoprotein lipase, *J. Biol. Chem.* 269: 22391-22396.
 19. Salmivirta M, Lidholt K and Lindahl U (1996) Heparan sulfate: a piece of information, *FASEB J.* 10: 1270-1279.
 20. Jackson RL, Busch SJ and Cardin AD (1991) Glycosaminoglycans: molecular properties, protein interactions, and role in physiological processes, *Physiol. Rev.* 71: 481-539.
 21. Gallagher JT, Lyon M and Steward WP (1986) Structure and function of heparan sulphate proteoglycans, *Biochem. J.* 236: 313-325.
 22. Hardingham TE and Fosang AJ (1992) Proteoglycans: many forms and many functions, *FASEB J.* 6: 861-870.
 23. Groffen AJ, Hop FW, Tryggvason K, Dijkman H, Assmann K, Veerkamp JH, Monnens LA and Van den Heuvel LP (1997) Evidence for the existence of multiple heparan sulfate proteoglycans in the human glomerular basement membrane and mesangial matrix, *Eur. J. Biochem.* 247: 175-182.
 24. Groffen AJ, Ruegg MA, Dijkman H, Van de Velden TJ, Buskens CA, Van den Born J, Assmann K, Monnens LA, Veerkamp JH and Van den Heuvel LP (1998) Agrin is a major heparan sulfate proteoglycan in the human glomerular basement membrane, *J. Histochem. Cytochem.* 46: 19-27.
 25. Groffen AJ, Buskens CA, Tryggvason K, Veerkamp JH, Monnens LA and Van den Heuvel LP (1996) Expression and characterization of human perlecan domains I and II synthesized by baculovirus-infected insect cells, *Eur. J. Biochem.* 241: 827-834.
 26. Scorer CA, Clare JJ, McCombie WR, Romanos MA and Sreekrishna K (1994) Rapid selection using G418 of high copy number transformants of *Pichia pastoris* for high-level foreign gene expression, *Biotechnology (N. Y.)* 12: 181-184.
 27. Demacker PN, Van Sommeren-Zondag DF, Stalenhoef AF, Stuyt PM, Van 't Laar A (1983) Ultracentrifugation in swinging-bucket and fixed-angle rotors evaluated for isolation and determination of high-density lipoprotein subfractions HDL₂ and HDL₃, *Clin. Chem.* 29: 656-663.
 28. Farndale RW, Buttle DJ and Barrett AJ (1986) Improved quantitation and discrimination of sulphated glycosaminoglycans by use of dimethylene blue, *Biochim. Biophys. Acta* 883: 173-177.
 29. Harlow E and Lane D (1988) Antibodies, a laboratory manual. Cold Spring Harbor Laboratory Press; Cold Spring Harbor, NY.

CHAPTER FOUR

Evidence for the existence of multiple heparan sulfate proteoglycans in the human glomerular basement membrane and mesangial matrix

Evidence for the existence of multiple heparan sulfate proteoglycans in the human glomerular basement membrane and mesangial matrix

CHAPTER FOUR

SUMMARY Heparan sulfate proteoglycans (HSPGs) are essential components of the glomerular basement membrane (GBM) that carry a strong anionic charge. A well-characterized extracellular HSPG is perlecan, ubiquitously expressed in basement membranes. A cDNA construct encoding domain I and II of human perlecan was expressed as a fusion protein with glutathione S-transferase. This fusion protein was used to generate the novel monoclonal antibody 95J10. We compared the staining pattern of 95J10 with that of M215, a previously prepared mAb that recognizes HSPG isolated from human GBM. In kidney cortex, the anti-perlecan mAb 95J10 showed a strong staining of the mesangium, Bowman's capsule, the tubular basement membrane and stained the GBM only slightly. In contrast, M215 predominantly stained the GBM in a linear fashion. Immunoelectron microscopy supported these results showing concentrations of perlecan in some regions of the GBM, whereas the yet unidentified M215-antigen was homogeneously distributed throughout the GBM. Also in other human tissues, both antibodies also produced a clearly different staining pattern. Furthermore a polyclonal antiserum recognizing HSPG isolated from the GBM did not recognize perlecan from the EHS tumor. These results provide evidence for the presence of another HSPG in the GBM that is immunologically distinct from perlecan. The absence of perlecan splice variants in the kidney suggests that this component is encoded by a different gene than perlecan. Given its marked expression in the GBM, this component could be a determining factor in the maintenance of selective glomerular permeability.

TO INDEX

INTRODUCTION

The glomerular basement membrane (GBM) is a specialized extracellular matrix located at the interface of the glomerular visceral epithelium and the vascular endothelium. The GBM provides a rigid structure that supports the tissue to withstand high local blood pressure, its mechanical strength being enhanced by the highly organized interplay of its biopolymer components [e.g. collagen IV, laminin, nidogen and heparan sulfate proteoglycans (HSPGs)] [1]. Another crucial function of the GBM is to regulate the passage of proteins depending on their molecular size and charge [2]. The impermeability of the GBM for anionic macromolecules is assigned to the presence of HSPGs anchored within it. The electrostatic charge of these HSPGs can be visualized by electron microscopy using cationic ferritin [2] or heparan sulfate (HS)-specific mAbs [3]. The significance of this mechanism was demonstrated by perfusing rat kidney with heparitinase, which resulted in leakage of anionic tracer proteins [4]. A similar effect was observed when the kidney was perfused with anti-HS mAbs [5]. Alterations in the HS content of the GBM causing nephrotic syndrome are involved in, for example, minimal change nephropathy, glomerulonephritis, diabetic nephropathy, and Denys-Drash syndrome [6–8].

For biochemical characterization, HSPGs were extracted from isolated glomeruli [9], from epithelial cell lines [10] or from the mouse Engelbreth-Holm-Swarm sarcoma [11–13]. Extraction of HSPG from basement membranes is complicated due to its strong interactions with other components. In addition, their analysis is confused by their smeared appearance on protein gels and their sensitivity to proteolysis. The first basement membrane proteoglycan characterized was termed perlecan, with reference to its beads-on-a-string-like appearance in rotary shadowing electron microscopy [14]. It consists of a 467 kDa core protein carrying five functional domains and three HS chains attached in close proximity to its N-terminus [15–17]. Human perlecan is expressed by a single gene, named *HSPG2* and located on the short arm of chromosome 1 [18–20]. Several observations have suggested the presence of additional basement membrane HSPGs: low-density forms (representing perlecan) and high-density forms characterized by relatively small core proteins (18–143 kDa) [21, 22]. However, it was demonstrated that these high-density proteoglycans are immunologically related to perlecan, suggesting that they are generated by proteolytic processing [23].

Previous immunofluorescence studies performed with various polyclonal and monoclonal antibodies yielded inconsistent results, with particular differences in the staining intensity of the GBM [3, 9, 11, 24, 25]. For the generation of mAbs, prokaryotic expression offers a large advantage over proteoglycan extraction from basement membranes, because the risk of co-immunization with contaminating HSPG species is eliminated. Furthermore, recombinant protein expression allows the development of domain-specific antibodies. We have synthesized domains I and II of human perlecan as a bacterial fusion protein and generated the monoclonal antibody 95J10. In this study, we compare the expression pattern in human tissues for 95J10 and M215, a mAb that was previously raised against isolated human GBM-HSPG [3]. The results provide evidence for the presence of a yet unidentified HSPG in the GBM, which appears to be immunologically distinct from perlecan.

EXPERIMENTAL PROCEDURES

Materials

The following were obtained from the indicated sources: pGEX4T-3 expression vector, glutathione-conjugated Sepharose 4B (Pharmacia Biotech); reduced glutathione (Boehringer Mannheim), pCR-Script cloning vector, *SrfI* (Stratagene Cloning Systems); isopropyl- β -D-thiogalactoside, T4 DNA ligase, *NcoI*, *BamHI* (Life Technologies); Vent polymerase, *NotI*, *XcmI* (New England Biolabs); thermal cycler apparatus (Perkin Elmer); automated sequencer (Applied Biosystems); thrombin, phenylmethylsulfonyl fluoride, ribonuclease A (Sigma Chemical Co.), 2-iodoacetamide (Merck); N-ethylenemaleimide, EDTA (Fluka Chemie); benzamidine hydrochloride (Janssen Chimica); 6-aminohexanoic acid (Aldrich Chemical); Tween-20 (ICN Biomedicals); Immobilon-P, ultrafiltration units (Millipore); goat-anti-mouse peroxidase conjugate (Dakopatts); sheep-anti-mouse fluorescein isothiocyanate conjugate (Cappel, Oss, The Netherlands); [γ - 32 P]ATP, ECL detection kit (Amersham).

Construction of the expression vector pGEX4T3-P12a

A prokaryotic expression vector encoding amino acids 24–404 of human perlecan was prepared as follows. Two PCR products were generated from cDNA clone Hpe2 [16] using Vent polymerase for proofreading activity. The primer sets were: 5'-TCATCTCCAGCGGCTCTGT-3' (forward P1), 5'-TCATGGGAACTGGGGCACTGTGC-3' (reverse P1), 5'-TCATCTCCAGCGGCTCTGT-3' (forward P2) and 5'-TTACATGCAGCC-AAACTCGTC-3' (reverse P2, this primer introduces an in-frame stop codon immediately behind amino acid 404). The two PCR products were inserted into the *SrfI* cloning site of pCR-Script [26, 27] and screened to detect the unique *NotI*-site at the 3'-end of the cDNA

fragments. The P2 fragment was then ligated to the P1 fragment by use of the *XcmI* restriction site, and introduced into pGEX4T-3 [28] using the *NcoI* and *NotI* cloning sites. The fidelity of amplification and ligation procedures was checked by sequence analysis. The resulting expression vector was named pGEX4T3-P12a.

Expression and purification of recombinant perlecan-(24–404)-fragment

Expression of the recombinant perlecan-(24–404)-fragment was performed as described [28], except that the cell pellet was resuspended in 125 ml ice-cold NaCl/P_i (140 mM NaCl, 2.7 mM KCl, 10 mM Na₂HPO₄, 2 mM KH₂PO₄, pH 7.5), 1% Triton-X100, 10 mM N-ethylmaleimide, 5 mM EDTA, 10 mM 6-amino-hexanoic acid, 5 mM 2-iodoacetamide, 1 mM phenylmethylsulfonyl fluoride and 1 mM benzamidinium-HCl. Cell lysis and affinity purification of the recombinant fusion protein were performed in the presence of 1% Triton-X100, which was essential for optimal yields. In contrast, the yield could not be improved by other modifications of the procedure such as the use of sarkosyl for solubilization [29], growth at 30°C [30] or treatment with Mg²⁺ and ATP prior to affinity chromatography [31]. Affinity-purified fusion protein was incubated with 1.7 NIH U/ml human thrombin (specific activity approximately 4000 NIH U/mg) and incubated for 60 min at 22°C. To exhaustively remove the glutathione-S-transferase (GST) fragment from the thrombin-digested mixture, the mixture was dialysed against NaCl/P_i to remove free glutathione and passed through a glutathione-conjugated Sepharose 4B column (1 ml) at room temperature. The flow-through was concentrated by ultrafiltration against a 10-kDa cutoff membrane to a final concentration of 0.63 mg/ml (determined by the Bradford method with BSA as reference) [32].

Antibodies

The anti-perlecan mAb 95J10 was prepared as follows. Mice were immunized and boosted with 20 µg purified perlecan-(24–404)-fragment per injection (this preparation was completely devoid of GST). Hybridoma cell lines were screened by ELISA with an independently isolated batch of recombinant fusion protein. Twelve positive clones were examined in indirect immunofluorescence studies for their capacity to stain human renal basement membranes. A mAb designated 95J10 was selected that showed strong glomerular staining. The mAb also reacted in western blot analysis with the fusion protein and with perlecan-(1–404)-fragment expressed by baculovirus-infected insect cells [33], which indicated that it also recognizes the antigen in a denatured conformation. No cross-reactivity of mAb 95J10 with *Escherichia coli* proteins or GST was observed by ELISA and western blotting. Experimental animal care, cell fusion, and generation of the monoclonal hybridoma cell line 95J10 were performed by Diabor Ltd., Oulu, Finland.

Other antibodies used were R254 (a rat mAb against mouse perlecan; a generous gift of Dr. J. van den Born), M215 (a mouse mAb against the core protein of HSPG isolated from human GBM [3]), and K42 (a rabbit antiserum recognizing HSPG from the human and murine GBM [9]).

Immunological methods

SDS-PAGE and immunoblot analyses were carried out following standard procedures [30]. All samples were denatured by boiling in presence of 2-mercaptoethanol prior to loading onto a homogeneous 5% polyacrylamide gel. Immunofluorescence and tissue distribution studies were performed with adult human tissue specimens obtained during autopsy, snap-frozen in liquid nitrogen, and stored at –80°C until use. Cryostat sections of 2 µm were attached to glass slides and treated with acetone for 10 min at 4°C for fixation. mAb M215 or 95J10 were applied as undiluted hybridoma supernatant. After 1 h incubation at 22°C, specimens were submerged five times in fresh NaCl/P_i for washing. Bound primary antibody was detected by

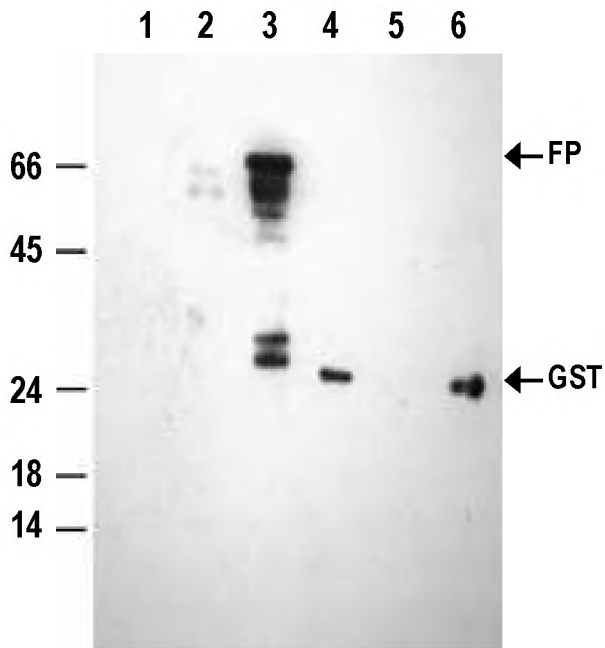


Figure 1. Western blot detection of recombinant fusion protein with a GST-specific monoclonal antibody. Lane 1, crude cell extract of bacteria carrying the plasmid pGEX4t3; lane 2, crude cell extract of bacteria carrying the plasmid pGEX4t3-P12a; lane 3, affinity purified preparation of the fusion protein; lane 4: thrombin-digested fusion protein; lane 5: perlecan-(24-404)-fragment obtained from thrombin-digested fusion protein; lane 6, GST fragment obtained from thrombin-digested fusion protein. The positions of marker proteins are given on the left. Arrows on the right indicate the fusion protein in lane 2 and 3 (FP) and the GST fragment in lane 4 and 6.

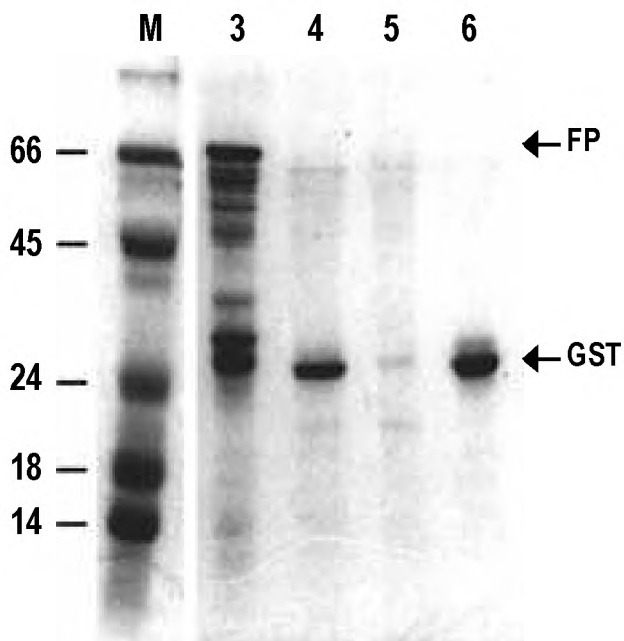


Figure 2. SDS-PAGE analysis of recombinant protein produced by recombinant *E. coli*. Recombinant protein was extracted from *E. coli*, purified by glutathione affinity chromatography and digested with thrombin. Proteins were separated by SDS-PAGE (12.5% polyacrylamide) and stained with Coomassie brilliant blue. M, marker lane; molecular mass indications are given on the left (kDa). The contents of lanes 3-6 are as described in Figure 1.

incubating with fluorescein-isothiocyanate-conjugated sheep-anti-mouse immunoglobulins (30 min at 22°C in the dark). After thorough washing with fresh NaCl/P_i, the preparations were examined with a Leitz fluorescence microscope. For immunoelectron microscopy, kidney cortex slices were fixed with periodate-lysine and paraformaldehyde, immersed in 2.3 M sucrose for cryprotection and snap-frozen in liquid nitrogen. Staining of peroxidase-conjugated antibody complexes was performed following standard protocols [34] and the sections were postfixed in Epon 812. Thin sections were examined with a Jeol 1200 EX electron microscope.

Northern hybridization

A multiple human tissue northern blot (Clontech Laboratories Inc.) was treated according to the supplier's protocol with an antisense probe homologous to exon 3 of perlecan (5'-AAGTCCCCGCTGCCAGGTCCTCCACTGCCAGGTCGT-3') [20]. This exon is a prerequisite for the presence of the HS chains. After hybridization, the filter was washed 3 x 15 min under stringent conditions (15 mM NaCl, 1.5 mM sodium citrate, 0.1% SDS, pH 7.0 at 50°C) and exposed for autoradiography for 91 h.

RESULTS

Expression of perlecan domains I and II as a fusion protein with GST

A cDNA construct was prepared encoding domain I and II of human perlecan, fused to the carboxyl end of GST from *Schistosoma japonicum* [28]. For localization of the recombinant protein, we tested the cell lysate, the culture supernatant, and the inclusion bodies isolated from the bacteria. The recombinant protein was found exclusively in the cell lysate. Crude cell extracts were analyzed by SDS-PAGE and immunoblotting with an anti-GST mAb (Figure 1), confirming the presence of a recombinant fusion protein. Although the fusion protein was expressed at a level of 1.3 ± 0.3 mg/l crude culture (mean \pm SD, n=4), only 120 μ g/l could be recovered by affinity chromatography. The affinity-purified fraction did not appear as a single band on SDS-PAGE, but contained multiple proteins as shown in lane 3 (Figure 1). The largest of these proteins appeared as a strong band, which corresponded to the predicted molecular mass of 68 kDa. The observed additional bands and the low final yield suggest sensitivity of the fusion protein to proteolysis.

The GST fragment was removed from the hybrid protein utilizing an engineered recognition site for thrombin cleavage, and an additional round of affinity chromatography. Coomassie brilliant blue staining of the recombinant perlecan-(24–404)-fragment identified two bands of 26 and 19 kDa in size respectively (Figure 2, lane 5). The staining signal is weak compared to the GST fraction (Figure 2, lane 6), which indicated a relatively low protein concentration. These results likely reflect proteolytic degradation of the fusion protein, also observed in lane 3 (Figure 1 and 2). The final preparation, completely devoid of GST as shown in Figure 1 (lane 5), was used to generate the monoclonal antibody mAb 95J10.

HSPG distribution in the human kidney

In indirect immunofluorescence studies on human kidney cortex, mAb 95J10 displayed a bright staining of the mesangium, Bowman's capsule, the tubular basement membrane, and peritubular capillaries (Figure 3B). The overall staining of the GBM was weak and visible only along fragments of the glomerular capillaries. In the arteriole, an intense staining was observed in intima, media and adventitia (Figure 3A). The staining was especially pronounced at the luminal border. The staining was compared with that of another mAb designated M215. This mAb was obtained by immunization with HSPG purified from isolated human GBM, and is directed against an epitope of the core protein [3]. mAb M215 showed a strong linear

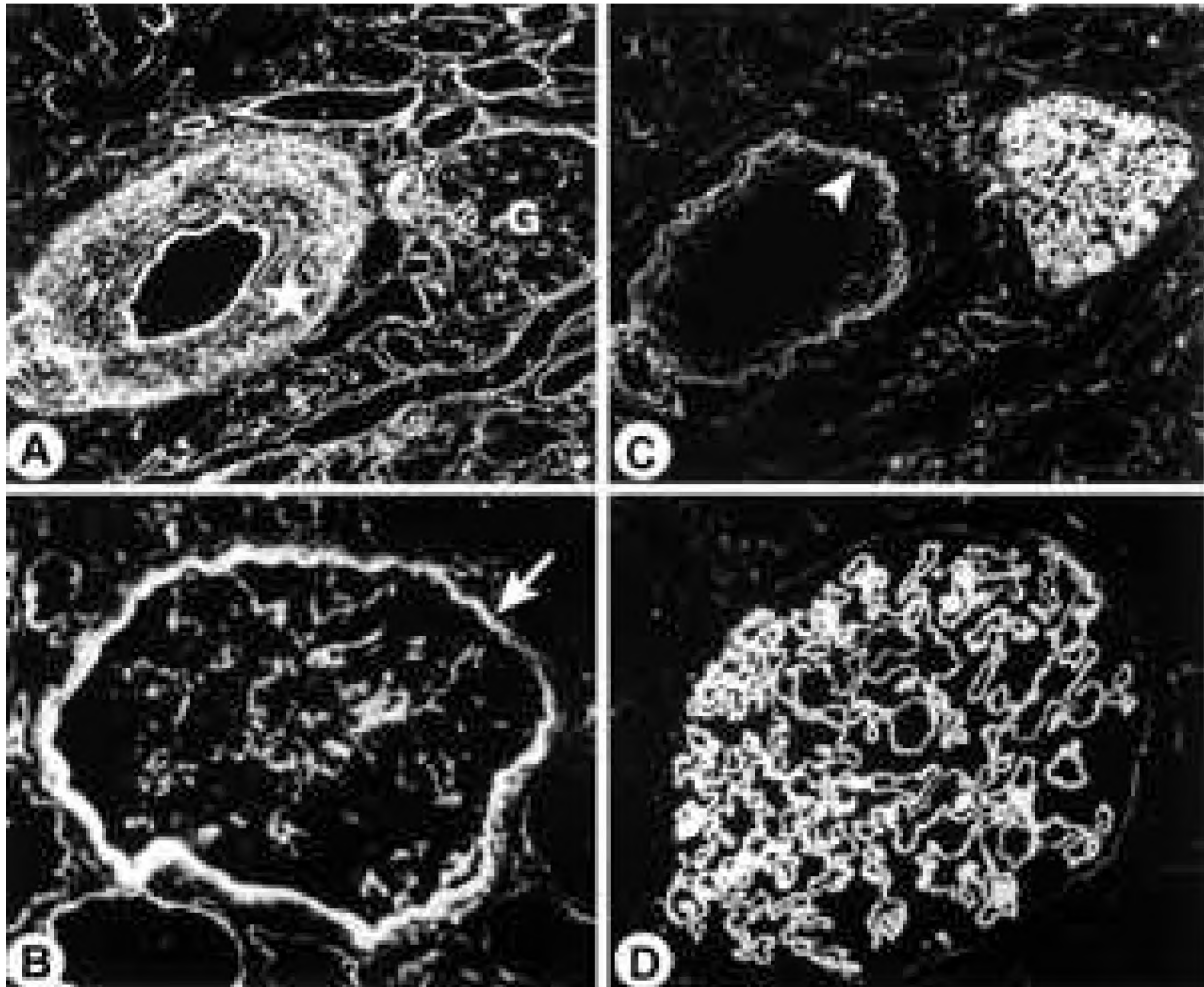


Figure 3. Immunofluorescence detection of heparan sulfate proteoglycans in the human renal cortex. Cryosections were stained for perlecan (A, B) and non-perlecan GBM-HSPG (C, D) using the mAbs 95J10 and M215, respectively. The asterisk in A indicates the tunica media of the arteriole; the arrow in B indicates Bowman's capsule; the arrowhead in C indicates autofluorescence typically originating from the elastica interna of the arteriole. Magnifications are 150x (A,C) and 400x (B, D).

staining of the GBM in immunofluorescence studies (Figure 3D), along with a less intense but also linear staining of all other renal basement membranes (Bowman's capsule, the tubular basement membrane and the basement membranes of the peritubular capillaries). mAb M215 did not stain the mesangial matrix. In contrast to 95J10, vascular staining of M215 was restricted to the endothelial border (Figure 3C).

The ultrastructural distribution of HSPGs in the GBM was analyzed by immunoelectron microscopy with both mAbs (Figure 4). The anti-perlecan mAb 95J10 stained the GBM along some fragments of the capillary wall, whereas other regions were not stained at all (Figure 4A). In all cases, the staining was clustered at the endothelial side of the basal lamina (Figure 4C). Besides the local accumulation of perlecan in the GBM, an elevated expression was seen in the mesangial matrix (Figure 4A). M215, however, produced a homogenous staining along the entire length of the GBM (Figure 4B and D). The clustered appearance of perlecan, and the linear distribution of non-perlecan GBM-HSPG, agree with the results from immunofluorescence studies.

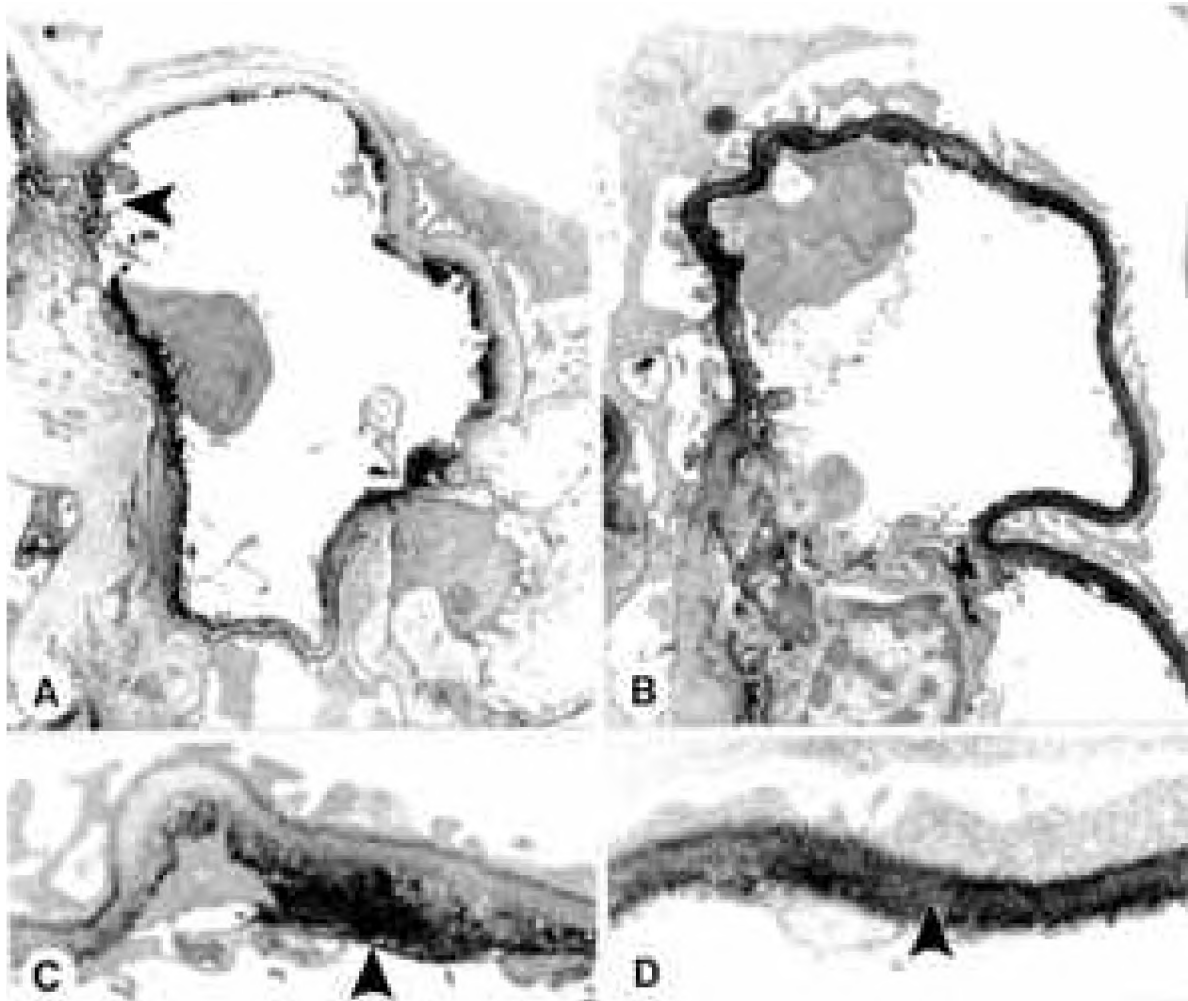


Figure 4. The ultrastructural localization of HSPGs in the glomerular basement membrane. Human kidney cortex was stained for perlecan (A, C) and non-perlecan GBM-HSPG (B, D) using mAbs 95J10 and M215 and was examined by immunoelectron microscopy. The arrowhead in A shows elevated levels of perlecan in the mesangial matrix. The arrowhead in C shows a typical condensation of perlecan on the endothelial side of the GBM. The arrowhead in D shows the homogenous linear distribution of non-perlecan GBM-HSPG. Magnifications 5000x (A, B) and 15 000x (C, D).

HSPG distribution in human tissues

Adjacent sections of human tissues were stained for perlecan (mAb 95J10) and non-perlecan GBM-HSPG (mAb M215). We especially focused on tissues that clearly displayed different staining patterns in indirect immunofluorescence studies using both mAbs. Figure 5 shows typical results in skin, pancreas, artery, tongue, and cerebrum. Both antibodies stained the epidermal basement membrane in the skin (Figure 5A and F). In addition, mAb 95J10 stained the capillaries more intensely than M215. In the pancreas, mAb 95J10 (Figure 5B) displayed a strong staining of the sinusoids, the islets of Langerhans, and the capillaries whereas mAb M215 (Figure 5G) only stained the capillaries. In arteries, 95J10 (Figure 5C) stained the media and adventitia with vasa vasorum, reflecting the basement membrane distribution surrounding the smooth muscle cells. In contrast, the staining by mAb M215 was confined to the vasa vasorum (Figure 5 H). In cryosections from human tongue, mAb 95J10 (Figure 5D) strongly recognized the endomysium that surrounds the skeletal muscle fibers, the capillaries, an artery, nerve fibers with a myelin sheath, and perineurium (bundles are surrounded by connective tissue). In contrast, mAb M215 stained only the capillaries (Figure 5I). In cerebrum, 95J10 strongly stains veins in the cerebral cortex, the arteries, and the capillaries.

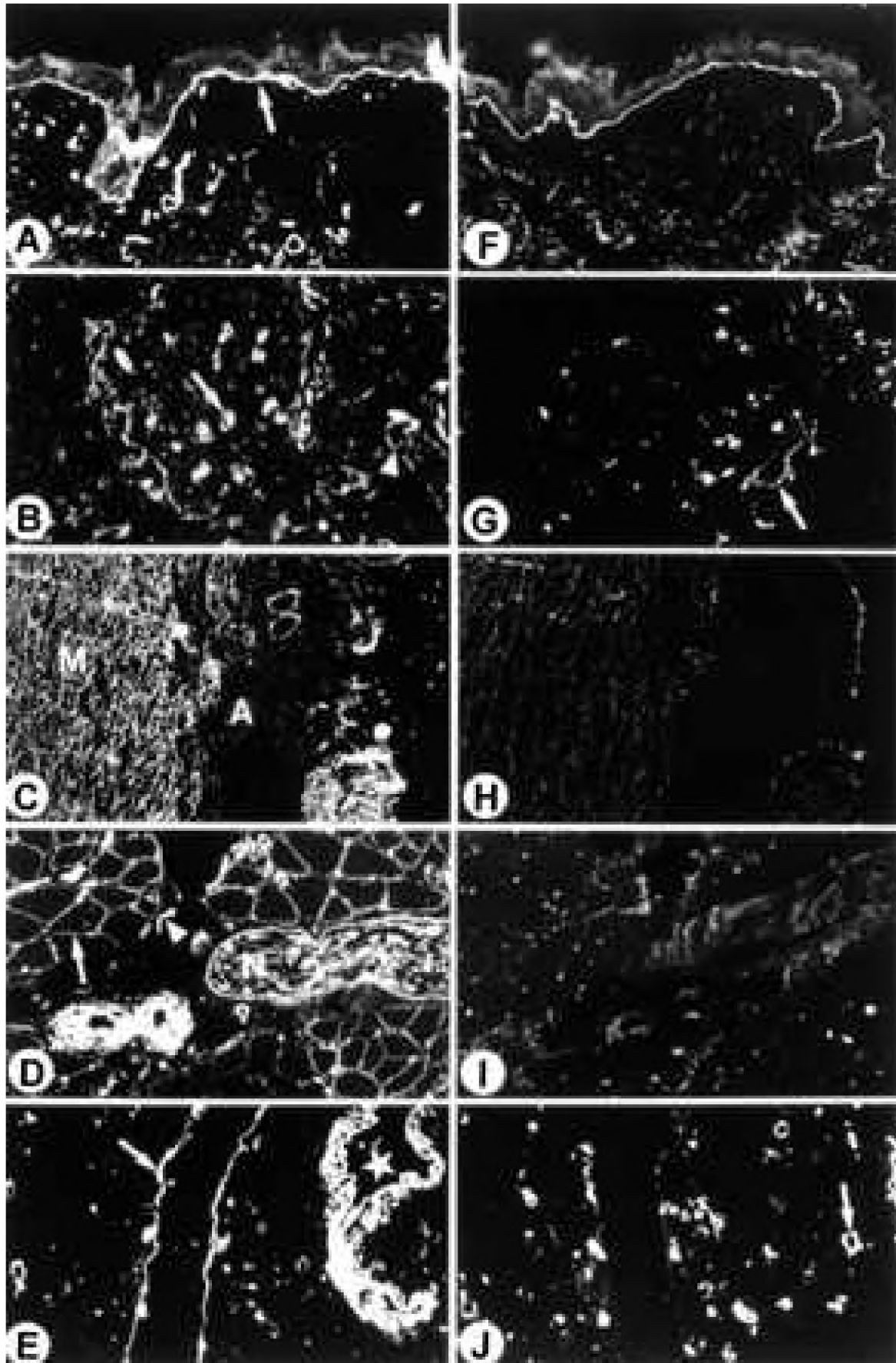


Figure 5. Indirect immunofluorescence staining of HSPGs in various human tissues. Cryosections were stained with mAb 95J10 (A E) or mAb M215 (F J). A and F, skin (arrow indicates epidermal basement membrane). B and G, pancreas (in B arrow indicates sinusoids and arrowhead indicates capillary. In G, arrow indicates capillary). C and H, artery (M, media; A, adventitia). D and I, tongue (arrow indicates skeletal muscle fibers; arrowhead indicates capillary; N, nerve fibers). E and J, cerebrum (in E arrow indicates vein and asterisk indicates artery; in J, arrow indicates capillary). Magnifications were 100x (C, E, H, J), 150x (A, D, F, I) and 400x (B, G).

In the same tissue, mAb M215 only stains the capillaries (Figure 5J). In all cases, the specificity of the staining was checked by parallel incubations without the primary antibody. The results obtained by immunohistochemistry suggest the occurrence of two different GBM-associated HSPG species. Could the observed differences be based on different epitope accessibilities *in vivo*? To exclude this possibility, preparations of HSPG isolated from the human GBM and from the mouse EHS tumor were analyzed by western blotting (Figure 6). The EHS tumor is known to produce large amounts of perlecan. Using a rabbit polyclonal antiserum (K42) that recognizes both murine and human GBM-HSPG [9], no staining of EHS-HSPG was detected. Staining with mAb M215 gave identical results (data not shown). As a control for the transfer of EHS-HSPG to the blot, an identical treatment with a rat mAb against mouse perlecan resulted in a marked staining of EHS-HSPG. mAb 95J10 could not be

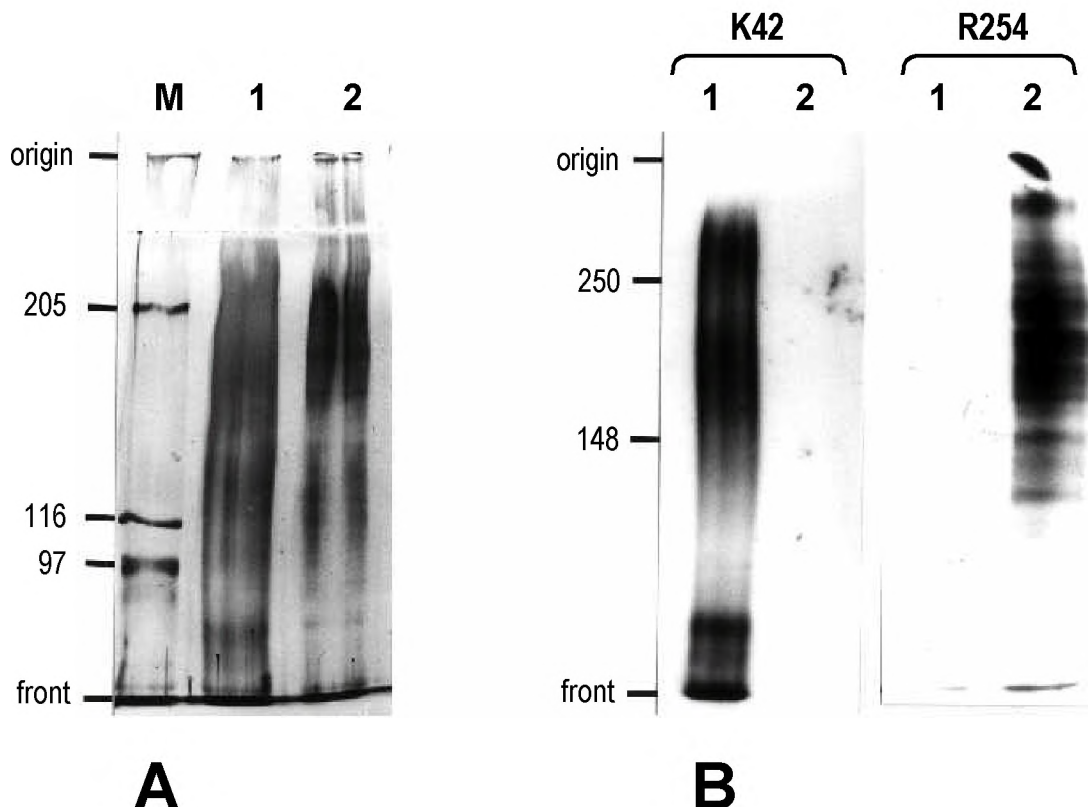


Figure 6. Comparative immunoblot analysis of HSPGs from glomerular basement membrane and EHS tumor. Equal quantities of HSPG isolated from the human GBM (lanes 1) and from the mouse EHS tumor (lanes 2) were separated by SDS-PAGE (5% polyacrylamide). Both HSPGs were analyzed by silver staining (A) and immunoblotting (B). For immunoblotting, we used K42 (a rabbit pAb that recognizes GBM-HSPG from mouse and man; left part of B) and R254 (a rat mAb that recognizes mouse perlecan; right part of B).

used for this purpose, since it is specific for human perlecan. The specificity of antiserum K42 for GBM-HSPG, without any cross-reaction with perlecan, confirms that the two HSPG species are immunologically unrelated.

Perlecan splice variants occur in brain, placenta and skeletal muscle but not in kidney

Elucidation of the perlecan gene structure showed the theoretical possibility of alternative splicing [16, 17, 20]. Interestingly, the occurrence of splice variants would result in the expression of perlecan isoforms. We therefore investigated the occurrence of perlecan splice variants by northern blotting (Figure 7). The full size messenger RNA (approximately 14 kb) was detected in heart, placenta, skeletal muscle, kidney and pancreas, but was hardly or not at all present in brain, lung, and liver. Interestingly, a smaller size mRNA species was detected in brain (2.5–2.6 kb), placenta (1.9 kb and 6.4–6.7 kb) and skeletal muscle (3.1–3.3 kb). The significance of these molecules is not clear. In the kidney however, we could not distinguish any splice variants.

DISCUSSION

As the presence of strongly anionic HSPGs is important to maintain the selective permeability of the GBM, the identification of perlecan as a basement membrane-associated HSPG has provoked many investigators to study perlecan expression levels during nephropathy. We used a novel mAb designated 95J10, directed against amino acids 22–404 of human perlecan, to analyze the distribution of perlecan in the glomerulus in more detail. The staining pattern of 95J10 in indirect immunofluorescence is in agreement with other studies performed with mAbs raised against recombinant fragments from domain III of perlecan [24, 25], and with a polyclonal antiserum against perlecan from the EHS-tumor [11]. However, the exact localization of perlecan in the GBM can hardly be deduced from immunofluorescence microscopy studies. Our results from immunoelectron microscopy indicate that perlecan is present in the GBM, but only on the endothelial side. Moreover, perlecan is distributed in a non-homogenous pattern and many segments of the GBM were not stained by 95J10. Therefore, charge-selective properties of the GBM can not be ascribed to the anionic charge of perlecan alone.

The expression pattern of perlecan is in marked contrast to that observed with M215, a previously described mAb against HSPG isolated from the GBM [3]. This HSPG is less widely distributed than perlecan, as shown by indirect immunofluorescence on multiple human tissues. In the kidney, this antibody predominantly stained the GBM in a linear manner. Similar results were obtained with other monoclonal and polyclonal antibodies raised

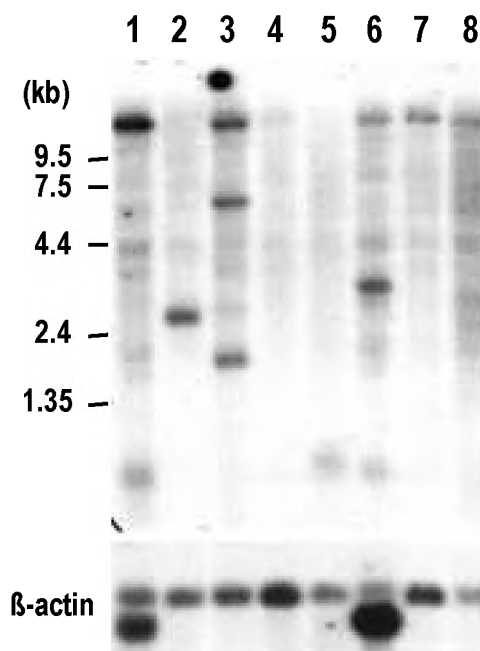


Figure 7. Northern blot analysis of mRNA from various human tissues. PolyA-rich mRNA isolated from heart (1), brain (2), placenta (3), lung (4), liver (5), skeletal muscle (6), kidney (7), and pancreas (8) was hybridized with a perlecan-specific probe and washed stringently. The bottom panel shows a control hybridization with a β -actin-specific probe to indicate differences in total mRNA content.

against GBM-HSPG, and with a mAb that recognizes an epitope on the HS chain [5, 8, 9]. The homogenous distribution of this HSPG within the GBM was confirmed by immunoelectron microscopy.

Our results indicate that two immunologically unrelated HSPG species are present in the GBM. This conclusion is based on the following considerations. Firstly, the anti-HSPG antibodies 95J10 and M215 show a clearly different distribution in human tissues. Comparing the staining patterns of 95J10 and M215, it is of importance that both antibodies are directed against the core proteins. The exact composition of the glycosaminoglycan residues is not solely dependent on the nature of the core protein but is also influenced by the cellular environment in which they are synthesized and modified. Secondly, we demonstrated that a polyclonal antiserum against GBM-HSPG does not cross-react with perlecan. Thirdly, observations from other groups also support the presence of multiple extracellular HSPG species in the glomerulus. In one of these investigations, proteoglycan synthesis was studied in cultures of three cell types from calf glomeruli. Epithelial cells excreted immunologically distinct HSPG components (M_r approximately 300 kDa) as compared to endothelial and mesangial cells which produced a perlecan-type HSPG (molecular weight 500 kDa) [35]. Another study supported the synthesis of perlecan-like HSPG by cultured rat mesangial cells [36]. And finally, partial amino acid sequences of HSPG isolated from bovine and human kidney also supported the presence of HSPG species that are unrelated to perlecan [37, 38].

After hybridization of kidney mRNA, only the full length perlecan transcript could be distinguished (Figure 7). Although minor differences in mRNA length cannot be detected by this method, such small rearrangements could not explain the altered immunoreactivity towards mAbs with different domain specificities (this study and [24, 25]). Heparan sulfate-carrying splice isoforms of perlecan could not be missed through the choice of the probe, because the corresponding exon is required for the presence of HS chains [20]. Therefore, the production of multiple HSPGs in the GBM is not mediated by alternative splicing of perlecan. This indicates that a different gene is involved.

The availability of the recombinant perlecan-(24–404)-fragment and the novel mAb 95J10 could be of value in determining the functional properties of the individual domains of the perlecan core protein. The ultrastructural localization of perlecan in the GBM suggests that its role in the maintenance of selective glomerular permeability is more modest than was initially assumed. The presence of an additional HSPG, that is unrelated to perlecan, may indicate a new direction for investigating the structural basis of charge-selective GBM permeability. The unidentified HSPG that is highly expressed in the GBM may play an important role in renal function.

ACKNOWLEDGMENTS

This study was supported by grant C93.1309 of the Dutch Kidney Foundation. The laboratory participates in a Concerted Action "Alterations in extracellular matrix components in diabetic nephropathy and other glomerular diseases", which is financially supported by the EC and the Biomed I program (BMH1-CT92-1766). The authors wish to acknowledge J. van den Born and L. Uitto for kindly providing mAbs against HSPG and GST, respectively.

REFERENCES

1. Paulsson M (1992) Basement membrane proteins: structure, assembly, and cellular interactions, *Crit. Rev. Biochem. Mol. Biol.* 27: 93–127.

2. Kanwar YS (1984) Biology of disease: Biophysiology of glomerular filtration and proteinuria, *Lab. Invest.* 51: 7–21.
3. Van den Born J, Van den Heuvel LP, Bakker MA, Veerkamp JH, Assmann KJ, and Berden JH (1994) Monoclonal antibodies against the protein core and glycosaminoglycan side chain of glomerular basement membrane heparan sulfate proteoglycan: characterization and immunohistological application in human tissues, *J. Histochem. Cytochem.* 42: 89–102.
4. Rosenzweig LJ and Kanwar YS (1982) Removal of sulfated (heparan sulfate) or unsulfated (hyaluronic acid) glycosaminoglycans results in increased permeability of the glomerular basement membrane to ¹²⁵I-bovine serum albumin, *Lab. Invest.* 47: 177–184.
5. Van den Born J, Van den Heuvel LP, Bakker MA, Veerkamp JH, Assmann KJ and Berden JH (1992) A monoclonal antibody against GBM heparan sulfate induces an acute selective proteinuria in rats, *Kidney Int.* 41: 115–123.
6. Vernier RL, Steffes MW, Sisson-Ross S and Mauer SM (1992) Heparan sulfate proteoglycan in the glomerular basement membrane in type I diabetes mellitus, *Kidney Int.* 41: 1070–1080.
7. Wilkinson AH, Gillespie C, Hartley B and Williams GD (1989) Increase in proteinuria and reduction in number of anionic sites in the glomerular basement membrane in rabbits by infusion of human nephrotic plasma in vivo, *Clin. Sci.* 77: 43–48.
8. Van den Heuvel LP, Westenend PJ, Van den Born J, Assmann KJ, Knoers N and Monnens LAH (1995) Aberrant proteoglycan composition of the glomerular basement membrane in a patient with Denys-Drash syndrome, *Nephrol. Dial. Transplant.* 10: 2205–2211.
9. Van den Heuvel LP, Van den Born J, Van de Velden TJ, Veerkamp JH, Monnens LA, Schroder CH and Berden JH (1989) Isolation and partial characterization of heparan sulfate proteoglycan from the human glomerular basement membrane, *Biochem. J.* 264: 457–465.
10. Gowda DC, Bhavanandan VP and Davidson EA (1986) Isolation and characterization of proteoglycans secreted by normal and malignant human mammary epithelial cells. *J. Biol. Chem.* 261: 4926–4934.
11. Hassell JR, Gehron-Robey P, Barrach HJ, Wilczek J, Rennard SI and Martin GR (1980) Isolation of a heparan sulfate-containing proteoglycan from basement membrane, *Proc. Natl. Acad. Sci. U. S. A.* 77: 4494–4498.
12. Danielson KG, Martinez-Hernandez A, Hassell JR and Iozzo RV (1992) Establishment of a cell line from the EHS tumor: biosynthesis of basement membrane constituents and characterization of a hybrid proteoglycan containing heparan and chondroitin sulfate chains, *Matrix* 12: 22–35.
13. Timpl R (1993) Proteoglycans of basement membranes, *Experientia* 49: 417–428.
14. Paulsson M, Yurchenco PD, Ruben GC, Engel J and Timpl R (1987) Structure of low density heparan sulfate proteoglycan from a mouse tumor basement membrane, *J. Mol. Biol.* 197: 297–313.
15. Noonan DM, Fulle A, Valente P, Cai S, Horigan E, Sasaki M, Yamada Y and Hassell JR (1991) The complete sequence of perlecan a basement membrane heparan sulfate proteoglycan reveals extensive similarity with laminin A chain low density lipoprotein-receptor and the neural cell adhesion molecule, *J. Biol. Chem.* 266: 22939–22947.
16. Kallunki P and Tryggvason K (1992) Human basement membrane heparan sulfate proteoglycan core protein: a 467-kD protein containing multiple domains resembling elements of the low density lipoprotein receptor laminin neural cell adhesion molecules and epidermal growth factor, *J. Cell. Biol.* 116: 559–571.
17. Murdoch AD, Dodge GR, Cohen I, Tuan RS and Iozzo RV (1992) Primary structure of the human heparan sulfate proteoglycan from basement membrane (HSPG2/perlecan). A chimeric molecule with multiple domains homologous to the low density lipoprotein receptor, laminin, neural cell adhesion molecules, and epidermal growth factor, *J. Biol. Chem.* 267: 8544–8557.
18. Kallunki P, Eddy RL, Byers MG, Kestila M, Shows TB and Tryggvason K (1991) Cloning of human heparan sulfate proteoglycan core protein, assignment of the gene (HSPG2) to 1p36.1–p35 and identification of a BamHI restriction fragment length polymorphism, *Genomics* 11: 389–396.
19. Dodge GR, Kovalszky I, Chu ML, Hassell JR, McBride OW, Yi HF and Iozzo RV (1991) Heparan sulfate proteoglycan of human colon: partial molecular cloning, cellular expression, and mapping of the gene (HSPG2) to the short arm of human chromosome 1, *Genomics* 10: 673–680.

20. Cohen IR, Grassel S, Murdoch AD and Iozzo RV (1993) Structural characterization of the complete human perlecan gene and its promoter, *Proc. Natl. Acad. Sci. U. S. A.* 90: 10404–10408.
21. Hassell JR, Leyshon WC, Ledbetter SR, Tyree B, Suzuki S, Kato M, Kimata K and Kleinman HK (1985) Isolation of two forms of basement membrane proteoglycan, *J. Biol. Chem.* 260: 8098–8105.
22. Kato M, Koike Y, Ito Y, Suzuki S and Kimata K (1987) Multiple forms of heparan sulfate proteoglycans in the Engelbreth-Holm-Swarm mouse tumor. The occurrence of high-density forms bearing both heparan sulfate and chondroitin sulfate side chains, *J. Biol. Chem.* 262: 7180–7188.
23. Klein DJ, Brown DM, Oegema TR, Brenchley PE, Anderson JC, Dickinson MA, Horigan EA and Hassell JR (1988) Glomerular basement membrane proteoglycans are derived from a large precursor, *J. Cell. Biol.* 106: 963–970.
24. Murdoch AD, Liu B, Schwarting R, Tuan RS and Iozzo RV (1994) Widespread expression of perlecan proteoglycan in basement membranes and extracellular matrices of human tissues as detected by a novel monoclonal antibody against domain III and by in situ hybridization, *J. Histochem. Cytochem.* 42: 239–249.
25. Couchman JR, Ljubimov AV, Sthanam M, Horchar T and Hassell JR (1995) Antibody mapping and tissue localization of globular and cysteine-rich regions of perlecan domain III, *J. Histochem. Cytochem.* 43: 955–963.
26. Liu ZG and Schwartz LM (1992) An efficient method for blunt-end ligation of PCR products, *Biotechniques* 12: 28–30.
27. Inoue H, Nojima H and Okayama H (1990) High efficiency transformation of *Escherichia coli* with plasmids, *Gene* 96: 23–28.
28. Smith DB and Johnson KS (1988) Single-step purification of polypeptides expressed in *Escherichia coli* as fusions with glutathione S-transferase, *Gene* 67: 31–40.
29. Frankel S, Sohn R and Leinwand L (1991) The use of sarkosyl in generating soluble protein after bacterial expression, *Proc. Natl. Acad. Sci. U. S. A.* 88: 1192–1196.
30. Schein CH and Noteborn MH (1988) Formation of soluble recombinant proteins in *Escherichia coli* is favored by lower growth temperature, *Biotechnology* 6: 291–294.
31. Yu-Sherman M and Goldberg AL (1992) Involvement of the chaperonin dnaK in the rapid degradation of a mutant protein in *Escherichia coli*, *EMBO J.* 11: 71–77.
32. Harlow E and Lane D (1988) *Antibodies, a laboratory manual*. Cold Spring Harbor Laboratory Press, Cold Spring Harbor NY
33. Groffen AJ, Buskens CA, Tryggvason K, Veerkamp JA, Monnens LA and Van den Heuvel LP (1996) Expression and characterization of human perlecan domains I and II synthesized by baculovirus-infected insect cells, *Eur. J. Biochem.* 241: 827–834.
34. Mentzel S, Van Son JP, Dijkman HB, Koene RA and Assmann KJ (1996) Organ distribution of aminopeptidase A and dipeptidyl peptidase IV in mice. *J. Histochem. Cytochem.* 44: 445–461.
35. Shen GQ, Kresbach G, Spiro MJ and Spiro RG (1995) Evaluation of the cell specificity and sulfate dependence of glomerular extracellular matrix proteoglycan synthesis, *Arch. Biochem. Biophys.* 321: 83–93.
36. Thomas GJ, Shewring L, McCarthy KJ, Couchman JR, Mason RM and Davies M (1995) Rat mesangial cells in vitro synthesize a spectrum of proteoglycan species including those of the basement membrane and interstitium, *Kidney Int.* 48: 1278–1289.
37. Hagen SG, Michael AF and Butkowski RJ (1993) Immunochemical and biochemical evidence for distinct basement membrane heparan sulfate proteoglycans, *J. Biol. Chem.* 268: 7261–7269.
38. Heintz B, Stocker G, Mrowka C, Rentz U, Melzer H, Stickeler E, Sieberth HG, Greiling H and Haubeck HD (1995) Decreased glomerular basement membrane heparan sulfate proteoglycan in essential hypertension, *Hypertension* 25: 399–407.

CHAPTER FIVE

Agrin is a major heparan sulfate proteoglycan in the human glomerular basement membrane

Agrin is a major heparan sulfate proteoglycan in the human glomerular basement membrane

CHAPTER FIVE

SUMMARY Agrin is a heparan sulfate proteoglycan (HSPG) that is highly concentrated in the synaptic basal lamina at the neuromuscular junction (NMJ). Agrin-like immunoreactivity is also detected outside the NMJ. Here, we show that agrin is a major HSPG component of the human glomerular basement membrane (GBM). This in addition to perlecan, a previously characterized HSPG of basement membranes. Antibodies against agrin and against an unidentified GBM-HSPG produced a strong staining of the GBM and the NMJ, different from that observed with anti-perlecan antibodies. In addition, anti-agrin antisera recognized purified GBM-HSPG and competed with an anti-GBM-HSPG monoclonal antibody (mAb) in ELISA. Furthermore, both antibodies recognized a molecule that migrated in SDS-PAGE as a smear and had a molecular mass of approximately 200–210 kDa after deglycosylation. In immunoelectron microscopy agrin showed a linear distribution along the GBM and was present throughout the width of the GBM. This was again different from perlecan, which was exclusively present on the endothelial side of the GBM and distributed in a nonlinear manner. Quantitative ELISA showed that, compared with perlecan, the agrin-like GBM-HSPG showed a sixfold higher molarity in crude glomerular extract. These results show that agrin is a major component of the GBM, indicating that it may play a role in renal ultrafiltration and cell-matrix interaction.

To INDEX

INTRODUCTION

The glomerular basement membrane (GBM) is a highly organized network of extracellular proteins such as collagen IV ($\alpha 3$, $\alpha 4$ and $\alpha 5$), laminins ($\alpha 5$, $\alpha 1$, $\beta 2$, $\gamma 1$), nidogen/entactin and heparan sulfate proteoglycans (HSPGs) [1]. Closely associated with the vascular endothelium and the podocyte it provides mechanical support to both cell layers, and modulates the access of plasma molecules to the primary urine depending on their molecular size, shape and charge. The charge-selectivity is partly ascribed to the presence of HSPGs which provide the GBM with an electrostatic charge, resulting in a decreased permeability for anionic macromolecules such as albumin [2].

Since the characterization of perlecan as a HSPG component of basement membranes [3], this compound has been studied extensively as a candidate factor in the development of albuminuria. Perlecan consists of five functional domains composing a core protein of 467 kDa, carrying three heparan sulfate chains attached to the unique N-terminal domain [3,4]. To date however, the involvement of perlecan in renal ultrafiltration is questionable. Well-defined monoclonal antibodies (mAbs) against the perlecan core protein [3,5,6] showed a clearly different distribution from antibodies directed against isolated GBM-HSPG and epitopes on the heparan sulfate chains [7–9], indicating the presence of additional HSPG species in the GBM. A possible role for agrin in the kidney was suggested by the possibility to stain neuromuscular junctions (NMJs) with anti-GBM-HSPG antibodies [10], the identification of agrin as a HSPG [11] and the production of tryptic peptides from bovine tubular basement membrane HSPGs with a high sequence similarity compared with rat agrin [12].

In rat and mouse, the agrin core protein has an approximate molecular mass of 210 kDa [13,14]. Agrin induces the clustering of acetylcholine receptors (AChRs) and aggregation of sodium channels during the development of the neuromuscular junction [15–17]. The AChR clustering activity varies for different isoforms that are produced by the use of alternative splice sites [18–20]. Agrin isoforms active in AChR clustering are expressed by neurons, while muscle cells and many other tissues appear to express isoforms inactive in this process [21–23]. In this study we show that agrin is a major HSPG of the human GBM. This finding may give new clues for investigating the structure of the GBM in the normal and diseased kidney.

EXPERIMENTAL PROCEDURES

Antibodies

Characteristics of the used antibodies are as follows. Anti-agrin pAb 707 was raised in rabbit against full-length chick agrin from recombinant source [24]. Mouse mAb M215, mAb M138 and rabbit polyclonal antibody (pAb) K42 were raised against human HSPG isolated from the GBM [7,9]. These three antibodies identically stain human tissues in immunofluorescence. pAb K42 crossreacts with this antigen in rat and mouse tissues. The mouse mAb 95J10 is directed against a core protein epitope within domains I and II of human perlecan [6]. Crossreactivity with various human basement membrane components was negligible, as determined by ELISA (Table 1), including collagen type I from human placenta, collagen type IV from human placenta, heparan sulfate, chondroitin sulfate B (Sigma, St. Louis, MO, USA), and fibronectin from human plasma (Boehringer Mannheim, Germany). The mouse mAbs Agr-33 and Agr-131 (StressGen Biotechnologies, Victoria, Canada) are directed against spatially separated epitopes on the core protein of rat agrin [25]. They do not crossreact in immunofluorescence on human tissues (unpublished observations).

Table 1. Crossreactivity of antibodies 95J10, M215 and K42 with human basement membrane components as determined by ELISA. One μg of each component was coated. Immunoreactivity was measured as absorption units at 492 nm.

Component	mAb 95J10	mAb M215	pAb K42
Collagen I	0.05	0.05	0.04
Collagen IV	0.04	0.04	0.05
Fibronectin	0.04	0.04	0.04
Albumin	0.04	0.04	0.19
Heparan sulfate	0.04	0.04	0.05
Chondroitin sulfate	0.04	0.04	0.05
Heparin	0.04	0.04	0.04
Purified GBM-HSPG	0.16	2.41	1.40
Purified GST-P12a	2.07	0.05	0.05
Blanco	0.04	0.04	0.04

Indirect immunofluorescence

Adult human kidney cortex tissue obtained from post-trauma donors was snap-frozen in polybrene, cooled with liquid nitrogen. Two- μm sections were stored at -80°C until use. Skeletal muscle tissue was obtained from adult rat hamstrings and frozen in polybrene immediately after dissection. Six- μm sections were prepared as above. Immunohistochemistry was performed as described elsewhere [10], using FITC-conjugated goat-anti-mouse and goat-anti-rabbit as the secondary antibodies (Dakopatts, Copenhagen, Denmark). For identification of neuromuscular synapses in skeletal muscle sections, rhodamine-conjugated α -bungarotoxin was added to the secondary antibody mixture at a final dilution of 1:400. In double immunofluorescence studies, mAbs were detected by goat-anti-mouse immunoglobulins coupled to Texas Red (Sanbio, Uden, The Netherlands).

Immuno-electron microscopy

Incubations were performed at 22°C, unless otherwise indicated. Kidney cortex slices were immersed for 3 h with PLP fixative (a mixture of periodate-lysine and 2% paraformaldehyde), rinsed with PBS (pH 7.4), cryoprotected in 2.3 M sucrose for 45 min and snap-frozen in liquid nitrogen. Twenty-five- μ m cryostat sections were incubated with pAb 707 diluted 1:100 in PBS containing 1% BSA for 18 h at 4°C and then washed three times for 30 min with PBS. This was also done with mAb 95J10 (diluted 1:5) and mAb M215 (diluted 1:10). After rinsing, the sections were incubated for 90 min with the appropriate peroxidase-conjugated secondary antibody (goat-anti-rabbit immunoglobulins: Dakopatts; rabbit-anti-mouse immunoglobulins: BioSys) diluted 1:70 in PBS containing 1% BSA. After three 30-min washes in PBS, the sections were preincubated for 10 min in PBS containing 0.05% diaminobenzidine. Subsequently, the sections were stained for 10 min with the same medium containing 0.03 % hydrogen peroxide. For immunogold labeling, goat-anti-rabbit and goat-anti-mouse immunoglobulins coupled to colloidal gold of 1 nm (Nanoprobes, Stony Brook, NY) were diluted 50-fold in PBS containing 1 % BSA. The sections were incubated for 90 min at 22°C, then washed three times for 30 min in distilled water, and the gold signal was enhanced using HQ silver (Nanoprobes) for 5 min. After washing in distilled water for 18 h at 4°C the sections were postfixed in 1% osmium for 20 min at 22°C, dehydrated and embedded in Epon 812. Thin sections were prepared on a Reichert ultratome and examined in a Jeol 1200 EX electron microscope.

Preparation of glomerular extract

Glomeruli were isolated from human kidney cortex by the sieving method [26] and resuspended in 20 volumes 4 M guanidine HCl, 0.2% (w/v) Zwittergent 3–12, 50 mM sodium acetate, 10 mM EDTA, 10 mM N-ethylmaleimide, 10 mM 6-aminohexanoic acid, 5 mM 2-iodoacetamide, 1 mM phenylmethylsulfonyl fluoride and 1 mM benzamidinium HCl (pH 6.0). The suspension was incubated for 16 h at 4°C for extraction, and centrifuged for 25 min at 10,000 \times g to remove insoluble material.

Enzyme-linked immunosorbent assay

For quantitative determination of HSPGs by ELISA, crude glomerular extract was diluted 40-fold in coating buffer [27]. Perlecan levels were measured with 95J10 as the primary antibody, using a recombinant fragment comprising domains I and II of human perlecan [6] as standard. In the case of M215, purified GBM-HSPG [7] was used as standard. To correct for the efficiency of coating, known amounts of the standards were added to the diluted extract before coating. Regression lines were computed for the calibration curves, which were linear functions of the amount of internal standard. The concentration of each HSPG in the crude glomerular extract was calculated as the average of five individual measurements.

For semi-quantitative ELISA, wells were uniformly coated with 0.5 μ g/well purified GBM-HSPG. Protein concentrations were determined according to the Bradford method with BSA as standard [28]. Competition ELISA was performed by using a mixture of pAb 707 (serial dilution) and mAb M138 (0.2 μ g/ml) as the primary antibody. Subsequently, bound mAb was measured using a peroxidase-conjugated goat-anti-mouse serum (1:2000, Dakopatts) as above.

Nitrous acid treatment and immunoblotting

Five μ g GBM-HSPG [7] was dissolved in 100 μ l nitrous acid solution, freshly prepared by dissolving 5% (w/v) NaNO₂ in 1.5 M hydrochloric acid. This mixture was incubated for 80 min at 22°C. Subsequently, the core proteins were precipitated in the presence of 75 % ethanol. SDS-PAGE and immunoblotting were carried out according to described procedures

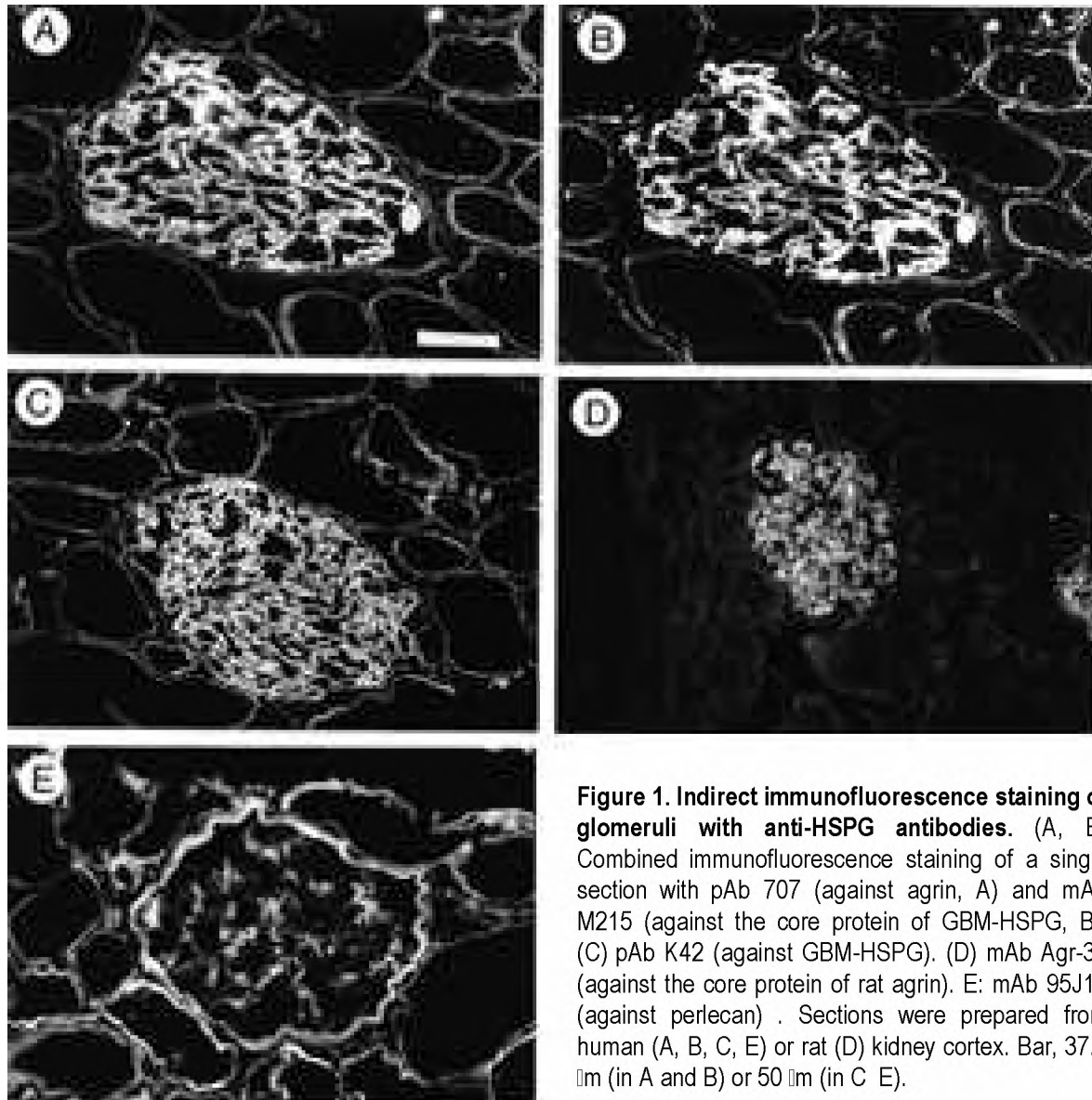


Figure 1. Indirect immunofluorescence staining of glomeruli with anti-HSPG antibodies. (A, B) Combined immunofluorescence staining of a single section with pAb 707 (against agrin, A) and mAb M215 (against the core protein of GBM-HSPG, B). (C) pAb K42 (against GBM-HSPG). (D) mAb Agr-33 (against the core protein of rat agrin). E: mAb 95J10 (against perlecan). Sections were prepared from human (A, B, C, E) or rat (D) kidney cortex. Bar, 37.5 μm (in A and B) or 50 μm (in C, E).

[27]. All samples were denatured prior to electrophoresis through 3–20% polyacrylamide, using Multimark as a molecular size marker (Novex, San Diego, USA).

RESULTS

Immunofluorescence microscopy

The presence of agrin in the glomerulus was investigated by indirect immunofluorescence. Cryosections of human renal cortex were stained with antibodies against agrin, perlecan and “GBM-HSPG”, a previously described HSPG isolated from the human GBM [7]. Combined staining with anti-agrin pAb 707 (Figure 1A) and mAb M215 against GBM-HSPG (Figure 1B) gave identical results. This consisted of a strong linear staining of the GBM, together with a weak linear staining of tubular basement membranes. Similar results were obtained with four independent anti-agrin antisera, and all corresponding pre-immune sera were negative (not shown). The observed staining pattern closely resembled that observed with the pAb

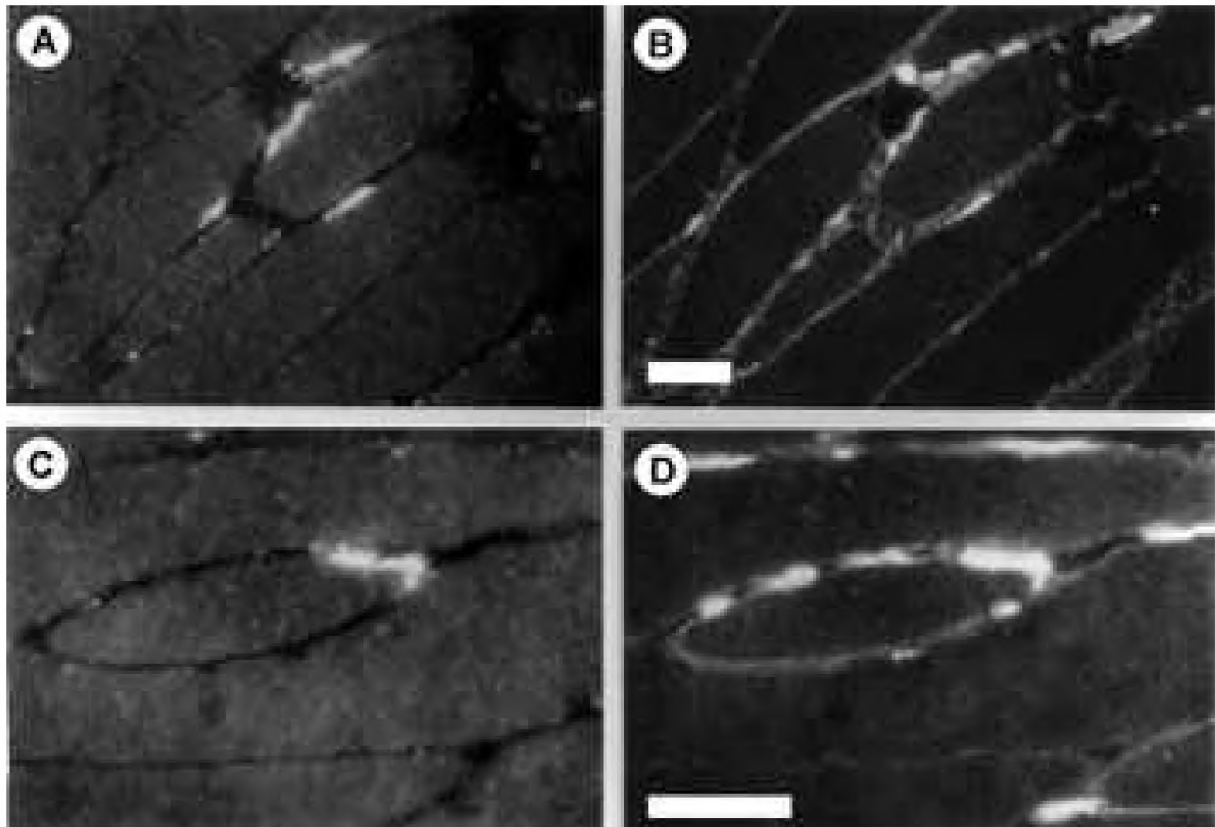
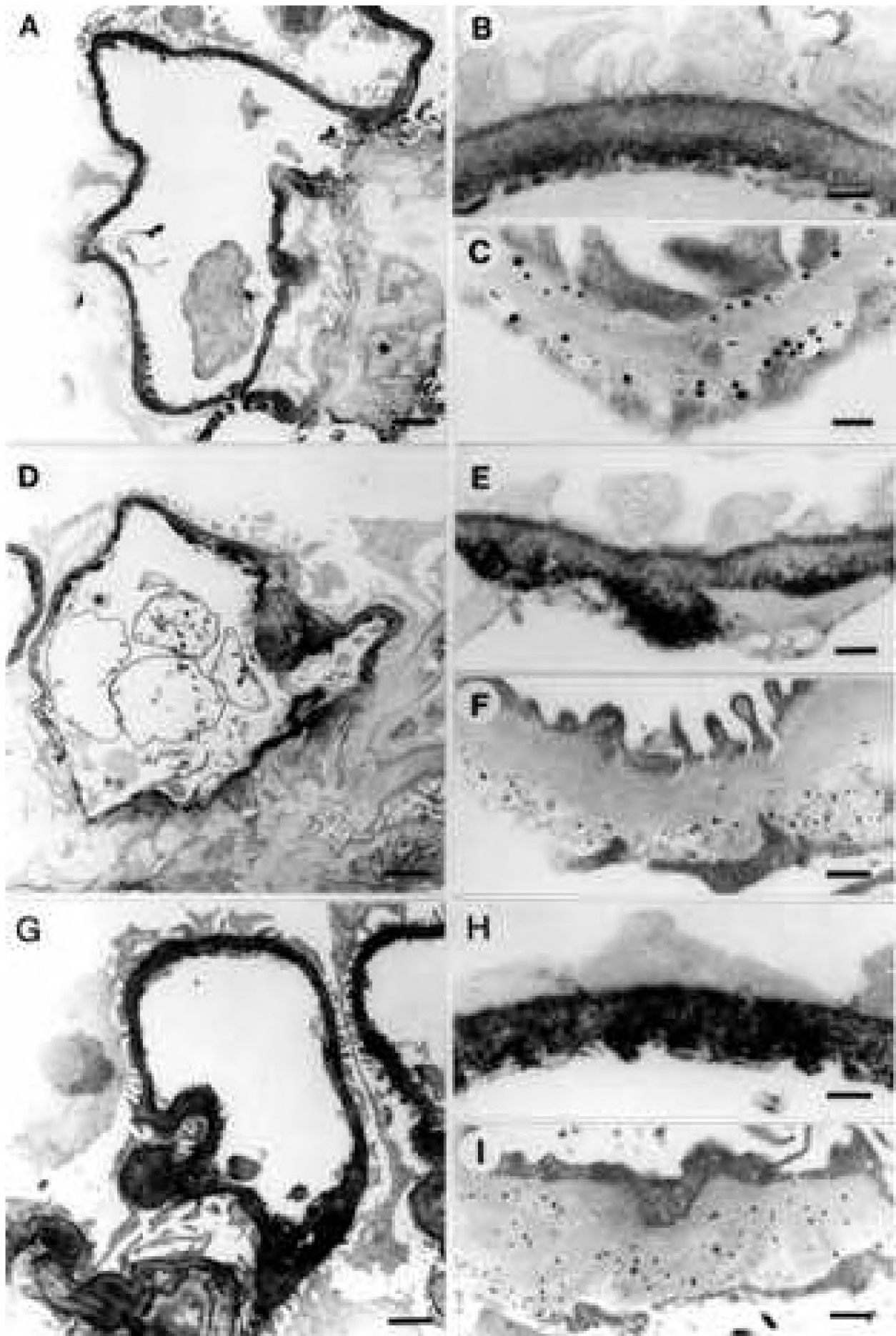


Figure 2. Distribution of agrin (top panel) and GBM-HSPG (bottom panel) in rat skeletal muscle. (A, C) Staining by rhodamine- α -bungarotoxin indicates the acetylcholine receptor clusters in the neuromuscular junction. (B, D) Indirect immunofluorescence using the anti-agrin mAb Agr-33 (B) and anti-GBM-HSPG pAb K42 (D). Bars, 50 μ m.

K42, directed against HSPG isolated from the GBM (Figure 1C). To confirm that the glomerular staining was not an artifact due to crossreactivity of the pAb, two mAbs Agr-33 (Figure 1D) and Agr-131 (not shown) against rat agrin were used to stain rat kidney cortex. Both antibodies produced a strong staining of the GBM, and a very weak staining of the tubular basement membrane. In comparison with anti-agrin and anti-GBM-HSPG staining, the anti-perlecan antibody produced a clearly different staining pattern (Figure 1E). The above results indicate that agrin is present in the GBM.

Because agrin is concentrated at the NMJ, we next compared staining patterns of anti-agrin and anti-GBM-HSPG antibodies in rat skeletal muscle sections. Junctions were identified by staining with rhodamine- α -bungarotoxin, recognizing the acetylcholine receptor clusters on the postsynaptic membrane (Figure 2A). Staining of the same section with mAb Agr-33 (directed against rat agrin) resulted in a strong signal localized at the synaptic cleft of the neuromuscular junction (Figure 2B). All junctions identified by rhodamine- α -bungarotoxin staining showed a strong immunofluorescence. In addition, extrajunctional patches were



observed that were strongly stained by Agr-33 but not by rhodamine- α -bungarotoxin. Furthermore, a weak staining of basement membranes surrounding the muscle fibers was present. Comparably, sections stained by rhodamine- α -bungarotoxin (Figure 2C) were immunostained with anti-GBM-HSPG pAb K42 (Figure 2D). In agreement with Agr-33, K42 stained all neuromuscular junctions together with some focal accumulations outside the junction and the weak staining of the basement membrane that surrounds the muscle fibers.

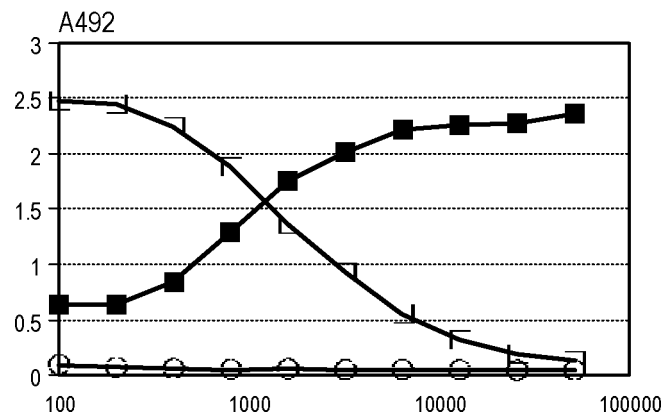


Figure 4. Recognition of GBM-HSPG by serially diluted anti-agrin antiserum (open squares) or pre-immune serum (open circles) in ELISA. Similarly, binding of a mouse mAb M138 was measured in presence of serially diluted anti-agrin antiserum as a competitor (solid squares).

Immuno-electron microscopy

To study the distribution of basement membrane HSPGs at the ultrastructural level, immuno-electron microscopy was performed on human kidney cortex. The distribution of agrin (top panel), perlecan (middle panel) and the GBM-HSPG recognized by M215 (bottom panel) is shown in Fig. 3. Using anti-agrin pAb 707, a strong linear staining was seen along the full length of the GBM (Fig. 3A–C). The whole width of the GBM was stained, but the signal was markedly stronger at both edges of the GBM. This localization at both the endothelial and epithelial side of the GBM was confirmed by immunogold labeling (Fig. 3C). We could also observe a faint staining of the mesangial matrix. The anti-perlecan mAb 95J10 produced a strong staining at the interface of the mesangium and the capillary endothelium (Fig. 3D–F). The overall GBM staining was mild, and restricted to the endothelial side in a non-linear pattern. Also by immunogold labeling, perlecan staining was found exclusively on the endothelial side of the GBM. With mAb M215, a strong linear staining was observed throughout the whole length and width of the GBM (Fig. 3 G–I). Immunogold labeling also demonstrated that the M215-epitope was present throughout the GBM. Occasionally, a mild staining of the mesangial matrix was observed. The linear distribution of the agrin-like HSPG along the GBM corresponds with the homogenous linear staining by immunofluorescence in this and previous studies (Figure 1B) [7–9,29]. Also the ultrastructural distribution of perlecan corresponds with the staining observed in immunofluorescence, characterized by a discontinuous staining of the capillaries and a relatively strong staining of the mesangium and Bowman's capsule (Figure 1E) [3,5,30].

Immunoreactivity of anti-agrin pAb 707 with purified GBM-HSPG

The described results show a colocalization of agrin-like and GBM-HSPG-like immunoreactivity in both the GBM and the neuromuscular junction. Given the unknown identity of the purified GBM-HSPG and the identification of agrin as a HSPG, we asked

← **Figure 3. Immuno-electron microscopy of human glomeruli with anti-agrin antiserum 707 (A C); anti-perlecan mAb 95J10 (D F) and anti-GBM-HSPG mAb M215 (G I).** Immunolocalization was visualized by peroxidase staining (A, B, D, E, G and H) or by colloidal gold particles (C, F and I). Standard bar sizes are 2 μ m (A, D, G) and 0.25 μ m (B, C, E, F, H, I) respectively.

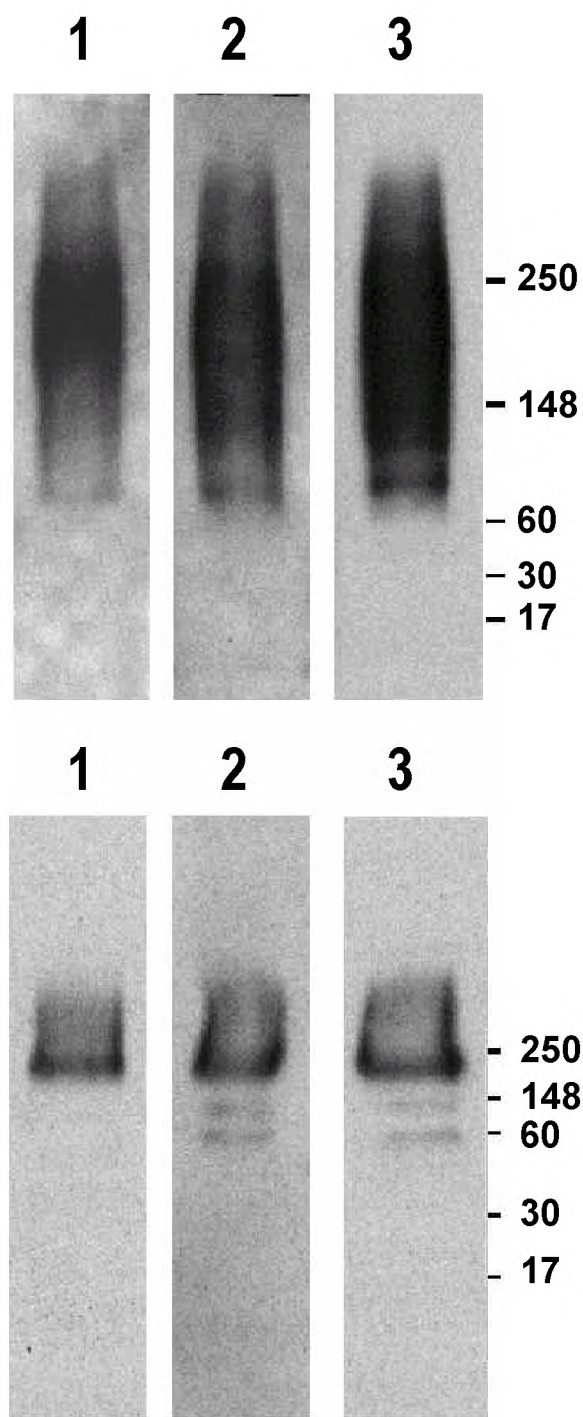


Figure 5. Western blot analysis of intact (top) and nitrous acid treated GBM-HSPG (bottom). Proteoglycans were denatured and separated by SDS-PAGE (3-20%). Antibodies used were pAb 707 (lane 1), mAb M215 (lane 2) and mAb M138 (lane 3). Positions of marker proteins are indicated on the right.

prominent band, two additional bands were weakly stained by M215 and M138. These bands are presumably degradation products, and could also be visualized with pAb 707 after prolonged exposure (not shown).

whether both proteoglycans could be identical. To address this, isolated GBM-HSPG was coated into microtiter wells. Antisera raised against agrin showed a strong reaction with this proteoglycan, whereas the corresponding pre-immune sera were negative (Figure 4, open squares and circles). In addition we tested the capability of anti-agrin antiserum to compete in ELISA with four different mAbs against human GBM-HSPG (including M215 and M138, all recognizing the same core protein). The binding of three mAbs was not blocked. Since the anti-agrin antiserum was raised against chick agrin, this suggests that the corresponding epitopes of human agrin are not immunogenic or absent in chick agrin. However, the binding of M138 to native GBM-HSPG was inhibited by anti-agrin (Figure 4, solid squares). These results show that the isolated GBM-HSPG is recognized by both anti-GBM-HSPG and anti-agrin antibodies.

Western blot analysis of isolated GBM-HSPG was performed with antibodies against agrin and GBM-HSPG (Figure 5). All antibodies recognized a large proteoglycan with a characteristically smeared appearance and similar molecular mass. The antigen was sensitive to nitrous acid treatment, indicating the presence of heparan sulfate residues. The nitrous acid-treated core protein was recognized by all antibodies and displayed a molecular mass of approximately 200–210 kDa. Besides this

Quantitative detection of HSPGs in isolated glomeruli

The strong staining of agrin in immunofluorescence and immuno-electron microscopy suggests that it is highly concentrated in the GBM. To determine the relative contribution of each molecule to the total HSPG content of the glomerulus, quantitative ELISA was performed with 95J10 and M215. A standard curve for 95J10 was constructed using an affinity-purified recombinant fragment comprising domains I and II of human perlecan [6]. For M215, the purified GBM-HSPG preparation was used as standard. The results (Table 2) show that the agrin-like HSPG is present in sixfold molar excess over perlecan.

Table 2. HSPG levels in extract from isolated human glomeruli, determined by quantitative ELISA with mAbs 95J10 and M215 (n=5).

Antibody used	HSPG concentration
95J10	0.46 ± 0.08 μM
M215	2.86 ± 0.14 μM

DISCUSSION

In this study we have used pAb 707 against chick agrin [24] to investigate the presence of agrin in the human glomerulus. To this end, we first confirmed that the pAb retains a high specificity for agrin in mouse, rat and human tissues. Comparing the distribution of agrin and GBM-HSPG by immunofluorescence, we found an exact colocalization in both the glomerulus and the neuromuscular junction. Consistently, the pAb 707 recognized the HSPG isolated from the human GBM in a direct ELISA assay. The antiserum could also inhibit the binding of mAb M138 to GBM-HSPG in a competition ELISA assay. This demonstrates that one of the epitopes recognised by pAb 707 is identical or proximate to the M138 epitope, known to be located on the core protein [9]. Finally, the estimated molecular mass of the core protein (200–210 kDa) corresponds to that of rat agrin [11, 13] as shown by immunoblot analysis. These data suggest that the unidentified HSPG component of the GBM is identical to agrin. Nevertheless, small differences are seen by immuno-electron microscopy with pAb 707 and mAb M215. The anti-agrin antibody is particularly bound to the endothelial and epithelial side of the GBM, whereas M215 binding was observed throughout the width of the GBM. This difference, also confirmed by immunogold labeling, might be related to different access of both antibodies to the lamina densa. Alternatively, the corresponding epitopes may be shielded by interactions of agrin in the lamina densa.

The quantitation of the agrin-like GBM-HSPG and perlecan in extract from isolated glomeruli could be misleading in two ways. Firstly, the standard used for quantitation by M215 cannot be considered absolutely contaminant-free, even though it was extensively purified. Although no contaminants were observed by visual inspection of SDS-PAGE analyses, a trace amount of perlecan was detected by ELISA (Table 1). Likewise, the presence of trace amounts of hypothetical other HSPG species can not be excluded. And secondly, the relative concentrations of both HSPGs in whole glomeruli are not necessarily identical to those in the GBM. Considering that perlecan is also present in Bowman's capsule (Figure 1E), the relative abundance of the agrin-like HSPG within the GBM is presumably even higher.

Which functions could agrin serve in the human GBM? Although many aspects of the structure and function of agrin isoforms have been studied in detail, the presence of agrin in the mammalian kidney and GBM was not yet described. One study reported the occurrence of agrin-like proteins in the tubular structures of chick kidney, and showed that these molecules have only little AChR-clustering activity [21]. This suggests a distinct function for agrin in the GBM. We speculate on three possible functions. First, the presence of agrin contributes to the incorporation of polyanions into the GBM. The ultrastructural localization of the different

HSPGs within the GBM does not support a key role for perlecan in determining selective permeability. The contribution of agrin may be crucial regarding its homogenous presence in the GBM (Figure 3) and its abundance in isolated glomeruli (Table 2). Hence, agrin could be essential to maintain charge-selectivity during ultrafiltration.

Second, agrin may provide a cytoskeletal link for the GBM through its interaction with α -dystroglycan [33] and laminin [34]. While α -dystroglycan appears not to be the receptor involved in AChR clustering [18, 35], it has been shown to be important for the development of kidney epithelial cells [36, 37]. Whereas the α -dystroglycan-binding region of agrin is mapped to the C-terminal half of the molecule, an N-terminal fragment of 130 amino acids was shown to bind to laminin-1, -2 and -4 [34]. Binding of agrin to laminin can also be expected in the GBM since its laminin composition resembles that of the NMJ, including the chains $\alpha 1$, $\beta 2$ and $\gamma 1$ [38, 39].

A third possible function of agrin in the GBM is suggested by the presence of nine Kazal-type protease inhibitor domains [13]. Agrin inhibits the proteases trypsin, chymotrypsin and plasmin [23], and therefore it may stabilize the structure of the extracellular matrix.

In contrast to the early expression of agrin in synaptogenesis, the onset of expression in the GBM may be delayed to later stages of development. Agrin-deficient mutant mice show aberrations in the development of neuromuscular junctions and die short before birth. At this stage, no prominent kidney malformations were mentioned [40]. This relates to the abundance of agrin mRNA in the early development of the rat nervous system, in later stages (E15–P1) accompanied by lower but significant mRNA levels in the kidney [41]. Important alterations in proteoglycan composition are known to occur during development and maturation of the GBM [8, 42]. Agrin is likely to be one of the components involved in these changes.

From this study we conclude that agrin is a major HSPG component of the human GBM. This finding has drastic implications for the investigation of structural and functional properties of the GBM. Changes in agrin structure and content may be important for glomerular function and play a role in various types of glomerulopathy. The structure of the agrin isoform which is present in the GBM and its relevance for cell-matrix interactions are subjects for further investigation.

ACKNOWLEDGMENTS

This study was supported by grant C93.1309 of the Dutch Kidney Foundation and grant #31–33697.92 of the Swiss National Science Foundation. The laboratory participates in a concerted action project entitled “Alterations in extracellular matrix components in diabetic nephropathy and other glomerular diseases”, which is financially supported by the EC and the Biomed I program (BMH1-CT92-1766).

REFERENCES

1. Paulsson M (1992) Basement membrane proteins: structure, assembly, and cellular interactions, *Crit. Rev. Biochem. Mol. Biol.* 27, 93–127.
2. Kanwar YS, Liu ZZ, Kashihara N and Wallner EI (1991) Current status of the structural and functional basis of glomerular filtration and proteinuria, *Semin. Nephrol.* 11, 390–413.
3. Murdoch AD, Liu B, Schwarting R, Tuan RS and Iozzo RV (1994) Widespread expression of perlecan proteoglycan in basement membranes and extracellular matrices of human tissues as detected by a novel monoclonal antibody against domain III and by in situ hybridization, *J. Histochem. Cytochem.* 42, 239–249.

4. Kallunki P and Tryggvason K (1992) Human basement membrane heparan sulfate proteoglycan core protein: a 467-kD protein containing multiple domains resembling elements of the low density lipoprotein receptor laminin neural cell adhesion molecules and epidermal growth factor, *J. Cell. Biol.* 116, 559–571.
5. Couchman JR, Ljubimov AV, Sthanam M, Horchar T and Hassel JR (1995) Antibody mapping and tissue localization of globular and cysteine-rich regions of perlecan domain III, *J. Histochem. Cytochem.* 43, 955–963.
6. Groffen AJ, Hop FW, Tryggvason K, Dijkman H, Assmann KJ, Veerkamp JH, Monnens LA and van den Heuvel LP (1997) Evidence for the existence of multiple heparan sulfate proteoglycans in the human glomerular basement membrane and mesangial matrix, *Eur. J. Biochem.* 247, 175–182.
7. Van den Heuvel LP, van den Born J, van de Velden TJ, Veerkamp JH, Monnens LA, Schröder CH and Berden JH (1989) Isolation and partial characterization of heparan sulfate proteoglycan from the human glomerular basement membrane, *Biochem. J.* 264, 457–465.
8. Van den Heuvel LP, Westenend PJ, van den Born J, Assmann KJ, Knoers N and Monnens LA (1995) Aberrant proteoglycan composition of the glomerular basement membrane in a patient with Denys-Drash syndrome, *Nephrol. Dial. Transplant.* 10, 2205–2211.
9. Van den Born J, van den Heuvel LP, Bakker MA, Veerkamp JH, Assmann KJ and Berden JH (1994) Monoclonal antibodies against the protein core and glycosaminoglycan side chain of glomerular basement membrane heparan sulfate proteoglycan: characterization and immunohistochemical application in human tissues, *J. Histochem. Cytochem.* 42, 89–102.
10. Van Kuppevelt TH, Benders AA, Versteeg EM and Veerkamp JH (1992) Ultrosor G and brain extract induce a continuous basement membrane with specific synaptic elements in aneurally cultured human skeletal muscle cells, *Exp. Cell Res.* 200, 306–315.
11. Tsen G, Halfter W, Kröger S and Cole GJ (1995) Agrin is a heparan sulfate proteoglycan, *J. Biol. Chem.* 270, 3392–3399.
12. Hagen SG, Michael AF and Butkowski RJ (1993) Immunochemical and biochemical evidence for distinct basement membrane heparan sulfate proteoglycans, *J. Biol. Chem.* 268, 7261–7269.
13. Rupp F, Payan DG, Magill-Solc C, Cowan DM and Scheller RH (1991) Structure and expression of a rat agrin, *Neuron* 6, 811–823.
14. Rupp F, Özçelik T, Linial M, Peterson K, Francke U and Scheller RH (1992) Structure and chromosomal localization of the mammalian agrin gene, *J. Neurosci.* 12, 3535–3544.
15. Glass DJ, Bowen DC, Stitt TN, Radziejewski C, Bruno J, Ryan TE, Gies DR, Shah S, Mattson K, Burden SJ, DiStefano PS, Valenzuela DM, DeChiara TM and Yancopoulos GD (1996) Agrin acts via a MuSK receptor complex, *Cell* 85, 513–523.
16. Kleiman RJ and Reichardt LF (1996) Testing the agrin hypothesis, *Cell* 85, 461–464.
17. Sharp AA and Caldwell JH (1996) Aggregation of sodium channels induced by a postnatally upregulated isoform of agrin, *J. Neurosci.* 15, 6767–6778.
18. Gesemann M, Cavalli V, Denzer AJ, Brancaccio A, Schumacher B and Ruegg MA (1996) Alternative splicing of agrin alters its binding to heparin, dystroglycan, and the putative agrin receptor, *Neuron* 16, 755–767.
19. O'Toole JJ, Deyst KA, Bowe MA, Nastuk MA, McKechnie BA and Fallon JR (1996) Alternative splicing of agrin regulates its binding to heparin, α -dystroglycan, and the cell surface, *Proc. Natl. Acad. Sci. USA* 93, 7369–7374.
20. Ruegg MA, Tsim KWK, Horton SE, Kröger S, Escher G, Gensch EM and McMahan UJ (1992) The agrin gene codes for a family of basal lamina proteins that differ in function and distribution, *Neuron* 8, 691–699.
21. Godfrey EW (1991) Comparison of agrin-like proteins from the extracellular matrix of chicken kidney and muscle with neural agrin, a synapse organizing protein, *Exp. Cell Res.* 195, 99–109.
22. McMahan UJ, Horton SE, Werle MJ, Honig LS, Kroger S, Ruegg MA and Escher G (1992) Agrin isoforms and their role in synaptogenesis, *Curr. Opin. Cell Biol.* 4, 869–874.
23. Biroc SL, Payan DG and Fisher JM (1993) Isoforms of agrin are widely expressed in the developing rat and may function as protease inhibitors, *Exp. Brain Res.* 75, 119–129.
24. Denzer AJ, Gesemann M, Schumacher B and Ruegg MA (1995) An amino-terminal extension is required for the secretion of

- chick agrin and its binding to extracellular matrix, *J. Cell Biol.* 131, 1547–1560.
25. Hoch W, Campanelli JT, Harrison S and Scheller RH (1994) Structural domains of agrin are required for clustering of nicotinic acetylcholine receptors, *EMBO J.* 13, 2814–2821.
 26. Langeveld PJ and Veerkamp JH (1981) Chemical characterization of glomerular and tubular basement membranes of various mammalian species, *Comp. Biochem. Physiol.* 68B, 31–40.
 27. Harlow E and Lane D (1988) *Antibodies: a laboratory manual*. Cold Spring Harbor Laboratory Press, Cold Spring Harbor, NY.
 28. Ausubel F (1989) *Current protocols in molecular biology*. New York, John Wiley and Sons.
 29. Van den Born J, van den Heuvel LP, Bakker MA, Veerkamp JH, Assmann KJ and Berden JH (1992) A monoclonal antibody against GBM heparan sulfate induces an acute selective proteinuria in rats, *Kidney Int.* 41, 115–123.
 30. Hassell JR, Gehron-Robey P, Barrach HJ, Wilczek J, Rennard SI and Martin GR (1980) Isolation of a heparan sulfate-containing proteoglycan from basement membrane, *Proc. Natl. Acad. Sci. USA* 77, 4494–4498.
 31. Vernier RL, Steffes MW, Sisson-Ross S and Mauer SM (1992) Heparan sulfate proteoglycan in the glomerular basement membrane in type I diabetes mellitus, *Kidney Int.* 41, 1070–1080.
 32. Wilkinson AH, Gillespie C, Hartley B and Williams GD (1989) Increase in proteinuria and reduction in number of anionic sites in the glomerular basement membrane in rabbits by infusion of human nephrotic plasma *in vivo*, *Clin. Sci.* 77, 43–48.
 33. Deyst KA, Bowe MA, Leszyk JD and Fallon JR (1995) The α -dystroglycan- β -dystroglycan complex: membrane organization and relationship to an agrin receptor, *J. Biol. Chem.* 270, 25956–25959.
 34. Denzer AJ, Brandenberger R, Gesemann M, Chiquet M and Rugg MA (1997) Agrin binds to nerve-muscle basal lamina via laminin, *J. Cell Biol.* 137, 671–683.
 35. Meier T, Gesemann M, Cavalli V, Rugg MA and Wallace BG (1996) AChR phosphorylation and aggregation induced by an agrin fragment that lacks the binding domain for α -dystroglycan, *EMBO J.* 15, 2625–2631.
 36. Durbeej M, Larsson E, Ibraghimov-Beskrovnaya O, Roberds SL, Campbell KP and Ekblom P (1995) Non-muscle α -dystroglycan is involved in epithelial development, *J. Cell Biol.* 130, 79–91.
 37. Matsumura K, Yamada H, Saito F, Sunada Y and Shimizu T (1997) The role of dystroglycan, a novel receptor of laminin and agrin, in cell differentiation, *Histol. Histopathol.* 12, 195–203.
 38. Miner JH, Lewis RM and Sanes JR (1995) Molecular cloning of a novel laminin chain, $\alpha 5$, and widespread expression in adult mouse tissues, *J. Biol. Chem.* 270, 28523–28526.
 39. Miner JH and Sanes JR (1996) Molecular and functional defects in kidneys of mice lacking collagen $\alpha 3(\text{IV})$: implications for Alport syndrome, *J. Cell Biol.* 135, 1403–1413.
 40. Gautam M, Noakes PG, Moscoso L, Rupp F, Scheller RH, Merlie JP and Sanes, JR (1996) Defective neuromuscular synaptogenesis in agrin-deficient mutant mice, *Cell* 85, 525–535.
 41. Stone D and Nikolics K (1995) Tissue- and age-specific expression patterns of alternatively spliced agrin mRNA transcripts in embryonic rat suggest novel developmental roles, *J. Neurosci.* 15, 6767–6778.
 42. Couchman JR, McCarthy KJ, Abrahamson DR, Fine JD and Parry G (1990) Immunological and molecular approaches to the study of basement membrane proteoglycan diversity, *Biochem. Soc. Trans.* 18, 819–820.

CHAPTER SIX

Primary structure and high expression of human agrin in basement membranes of adult lung and kidney

Primary structure and high expression of human agrin in basement membranes of adult lung and kidney

CHAPTER SIX

SUMMARY Agrin is a heparan sulfate proteoglycan involved in the development of the neuromuscular junction during embryogenesis. In addition to this well-characterized function, agrin may have functions in other tissues, and during other stages in development. In this study we present the cDNA sequence that encodes human agrin, and demonstrate a high agrin content in adult basement membranes. The N-terminal domain of human agrin is highly similar to that of chick agrin, suggesting a similar function in laminin binding. The presence of four SGXG tetrapeptide sequences supports serine-linked glycosylation of the core protein, two sites being particularly favorable for heparan sulfate attachment. The SEA module (previously associated with O-glycosylation) is also strongly conserved between species. Comparison of agrin mRNA levels in fetal and adult human tissues showed a remarkable upregulation in adult kidney and lung. These high transcription levels corresponded with the accumulation of agrin in the alveolar and glomerular basement membranes. The data provide new directions for investigating the role of agrin in its different physiological environments, including the basement membranes of the neuromuscular junction, kidney and lung.

TO INDEX

INTRODUCTION

Agrin is a heparan sulfate proteoglycan (HSPG) of basement membranes (BMs). It induces aggregation of acetylcholine receptors (AChRs) at the neuromuscular junction (NMJ) [1, 2]. Its primary structure was previously reported for electric ray, rat, mouse and chick [3–6]. The agrin gene was shown to encode multiple isoforms through alternative splicing at three sites, designated *x*, *y* and *z*. These splice variants differ greatly in function [6–9]. During the formation of the NMJ (the contact site of a motoneuron and a skeletal muscle cell), agrin isoforms expressed by motoneurons induce the clustering of AChRs within the postsynaptic membrane. Isoforms expressed by the muscle cell do not have a clustering activity [6, 10–12]. Agrin-related proteins are also expressed in non-neural tissues, suggesting functions in addition to neuromuscular synapse development [1, 13–16]. The many molecular interactions described for agrin make this feasible. Agrin was shown to bind laminin [17, 18] and α -dystroglycan [19, 20]. α -Dystroglycan is a peripheral membrane receptor associated with the dystrophin glycoprotein complex [20]. Thus, agrin may anchor the BM to the cytoskeleton and be involved in signal transduction. Furthermore, agrin was recently identified as a major HSPG of the glomerular BM [21]. Here it could participate in the charge-selective ultrafiltration process. Agrin could be involved in the storage, activation, inhibition or presentation of various growth factors, and modulate their effect in a tissue-dependent manner.

The human agrin gene was previously mapped to chromosome 1 [5], but the cDNA structure is unknown. To obtain cDNA clones encoding full-length agrin, we used expressed sequence tag information from public databases [18, 22]. Here, we report the cDNA sequence of human agrin, and provide data concerning its distribution in human tissues.

EXPERIMENTAL PROCEDURES

Materials

Human skeletal muscle poly(A)-rich RNA was purchased from Clontech (Palo Alto, CA, USA). RNazolB was from Campro Scientific (Veenendaal, The Netherlands). Oligo(dT) cellulose columns were from New England Biolabs (Beverly, MA, USA). Superscript II, oligonucleotides and biochemicals for RACE procedures (rapid amplification of cDNA ends) were from Life Technologies (Breda, The Netherlands). Long-distance polymerase chain reactions were performed using the Expand PCR system (Boehringer Mannheim, Mannheim, Germany) according to the manufacturer's instructions. This system uses a mixture of Taq and Pwo polymerase [23]. For subcloning of the PCR products the pGEM-T vector was used (Promega, Madison, USA).

Molecular cloning of human agrin cDNA

Human glomerular RNA was isolated from kidney cortex tissue using established sieving methods [24] and extraction in RNazolB. Poly(A)-rich RNA was obtained by standard procedures [25]. In addition to this RNA preparation, commercially available poly(A)-rich RNA from human skeletal muscle was used. Full length cDNA synthesis was performed using SuperscriptII with both oligo(dT) and random primers. This reaction mixture was incubated for 60 min at 42°C. The resulting cDNA preparations were used as template for long-distance PCR reactions.

The oligonucleotides used to amplify each cDNA clone (designated Cs1 through Cs4) are listed in Table 1. The position of each clone is indicated in Figure 1A. Clones Cs1 and Cs2 were derived from human glomerular cDNA; Cs3 and Cs4 from skeletal muscle cDNA. The design of the primers was based on sequence information from public databases. Relevant accession numbers are M64780 (rat cDNA), M94271, U35613 (chick cDNA), M92654 (mouse genomic DNA), L01423 (marine ray cDNA), S44195, H11951 and U84406 (human expressed sequence tags) [3–6, 16, 18, 22]. The procedures used for RACE experiments are described elsewhere [26]. The resulting PCR products were cloned into the pGEM-T vector and propagated in *E. coli* strain JM109.

Sequence analysis

Automated sequence analysis was carried out using an ABI377-type apparatus (ABI Prism, Warrington, Great Britain). The reported cDNA structure is based on high-quality double-stranded sequence information. Labeling reactions were performed with Amplitaq polymerase using the Dye Terminator Sequencing system (ABI Prism) in a GeneAmp 9600 thermal cycler (Perkin Elmer Cetus, Gouda, The Netherlands). Multiple independent clones were sequenced

Table 1: Oligonucleotides used for amplification of cDNA clones encoding human agrin. The clones Cs1 and Cs2 were amplified by a single PCR, whereas clones Cs3 and Cs4 were generated using a second reaction with nested primers. Universal primers for RACE procedures used were according to the supplier's protocol [26]. All primers are listed in 5' to 3' direction.

Clone (size)	forward primer	reverse primer
Cs1 (4.1 kb)	cgagacctgtggagatgccgtg	gttggtgtgacgggacggtggaacgcagc
Cs2 (1.3 kb)	gccgcgtgcgtcctgcccg	ctggtcacacgggccctg
Cs3 (1.5 kb)	gagaaggcactgcagagcaaccactttgaactgagc gctgcgttcaccgtgccgtcaacaccaac	3'-RACE anchored d(T) primer 3'-RACE anchor primer
Cs4 (1.7 kb)	5'-RACE anchored d(G) primer 5'-RACE anchor primer	ctgccgggctcctcgtac cacggcatctccacaggtctcg

from purified plasmid DNA as template. PCR products from RACE experiments were sequenced from purified PCR product as template, isolated using the Qiaquick protocol (Qiagen, Hilden, Germany).

Computational chemistry was performed on the CAOS/CAMM network (University of Nijmegen, The Netherlands) by using the following programs. Signal sequence and cleavage site predictions were calculated with the SignalP program [27]. MOTIFS was used to identify amino acid sequence patterns described in the PROSITE dictionary. PEPSTATS was used to calculate the molecular mass of the core protein. The BLASTP algorithm was used to detect similarity with known amino acid sequences [28].

Hybridization procedures

A master blot, containing poly(A)-rich RNA isolated from various human tissues, and a human multiple tissue northern blot were purchased from Clontech. The quantity of mRNA spotted for each tissue onto the master blot was normalized using eight different housekeeping gene transcripts as probes (ribosomal protein S9, ubiquitin, 23-kDa highly basic protein, hypoxanthine guanine phosphoribosyl transferase, tubulin, β -actin, phospholipase and glyceraldehyde-3-phosphate dehydrogenase). A probe homologous to human agrin was prepared by random primed labeling [25]. The filters were washed under stringent conditions ($0.1 \times$ SSPE, 0.5% SDS at 55°C) and analyzed by autoradiography. The signals on the master blot were quantified with a phosphorimager (BioRad, Veenendaal, The Netherlands), subtracted with the average background density, and integrated over the spot area with the Molecular Analyst software package (BioRad Laboratories, Veenendaal, The Netherlands).

Immunofluorescence

Cryosections from inflated human lung tissue and kidney cortex were prepared as previously described [29, 30]. Skeletal muscle cryosections were prepared from human diaphragm. To stain agrin we used a rabbit antiserum raised against full-length recombinant chick agrin [16], a kind gift of Dr. M.A. Ruegg, Dept. of Anatomy, University of Basel, Switzerland. We previously showed that this antibody retains specificity for human agrin [21]. Immunofluorescence staining and microscopic analysis were performed as described previously [21].

RESULTS

Molecular cloning and domain structure of human agrin

Using long-distance polymerase chain reactions in conjunction with 5'- and 3'- RACE strategies [26], we obtained four cDNA clones encoding human agrin. The positions of the clones are indicated in Figure 1A. The clones together comprise a cDNA sequence of 7032 nucleotides (Figure 2), providing an open reading frame ending at position 6081. The extreme 5' terminus of the cDNA sequence is incomplete, and starts 30 nucleotides upstream from the predicted signal peptide cleavage site [18, 27]. The mature core protein comprises 2016 amino acids (212 kDa). The agrin core protein is composed of multiple modules, depicted in Figure 1B. The degree of similarity with agrins from other species is given for each domain in Figure 1C. The overall conservation is strong, with high similarities observed especially for the laminin-binding domain and the SEA module. Since the core protein structure was previously reviewed in detail for other species, we will discuss the domain organization only briefly.

The N-terminus of the mature polypeptide is formed by a module named NtA, that was experimentally shown to have a laminin-binding function in chick agrin [18]. Nine follistatin-like domains are present, sharing similarity with many other Kazal-type protease inhibitors including pancreatic trypsin inhibitor, follistatin, ovinhibitor, thrombin inhibitor and elastase

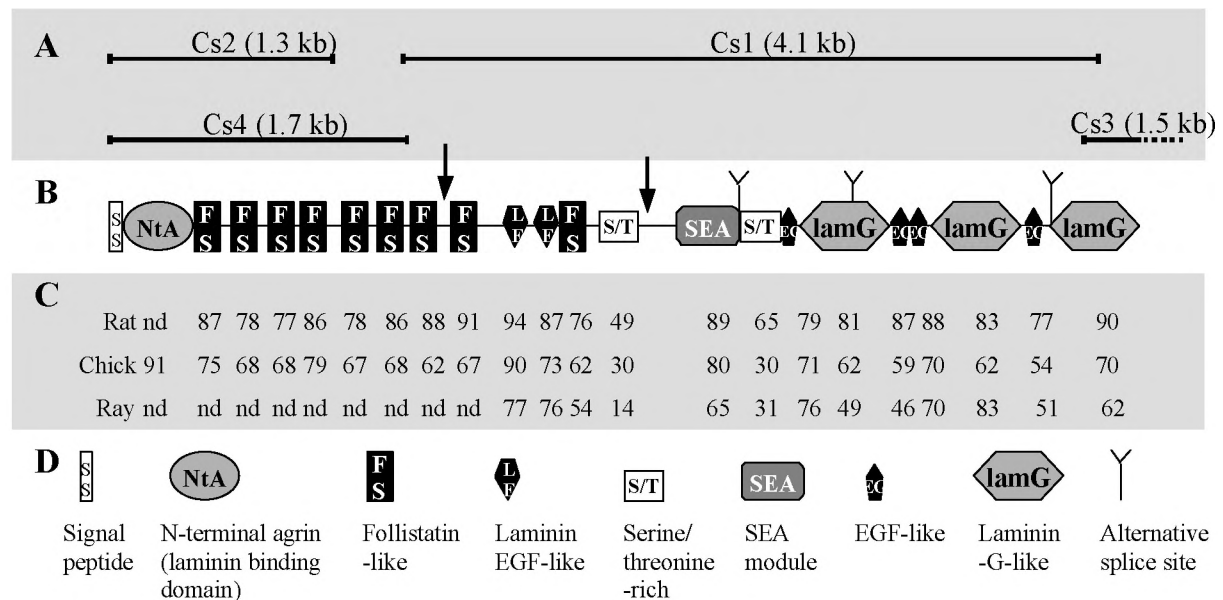


Figure 1. A) Position of individual cDNA clones encoding human agrin. B) Schematic representation of the domain structure of agrin. Arrows indicate putative glycosaminoglycan attachment sites. C) The degree of similarity between human agrin and agrins from other species, calculated as the percentage of identical amino acids (nd: no data). D) Symbols and nomenclature for individual domains are as described by [37].

inhibitor. In most cases the similarity was limited to the conserved PVCGSDGVTY pattern (underlined in Figure 2). In the case of the elastase inhibitor, a high similarity with the fifth follistatin-like domain extended to the specificity-determining region just upstream from this conserved pattern. However, the functionality of the protease inhibitor-like domains is still unclear, and the value of these predictions remains to be investigated. The 8th and 9th follistatin-like domains are separated by two LE repeats with similarity to the laminin-type epidermal growth factor (EGF) repeats. These elements most likely form a rod-like structure comparable to those observed on the short arms of laminins [31].

The central part of the agrin molecule is composed of two S/T-rich domains, characterized by their extremely high proline, threonine and serine content. The first domain contains 25% proline, 18% threonine and 16% serine; the second domain 22%, 16% and 9% respectively. Both domains are devoid of cysteine residues. The degree of conservation of the S/T-rich domains between human and rat agrin is relatively low (49% and 65% amino acid identity), but the prolines are particularly conserved. The SEA module is a pattern of secondary structure found in sperm protein, enterokinase, agrin, MUC1 (a mucin-like glycoprotein) and perlecan. Since all these molecules are components of the extracellular matrix and occur in heavily glycosylated environments, the SEA module is suggested to be involved in O-glycosylation [32]. Four potential attachment sites for glycosaminoglycans (double underlined in Figure 2) were detected by ProSite analysis, matching the consensus sequence SGXG [33]. Finally, the C-terminal region of agrin contains four EGF-like repeats and three laminin-G-like domains.

Figure 2. Primary structure of human agrin. First line, cDNA sequence with nucleotide numbering at the right and left. Second line, deduced amino acid sequence. Domain borders are indicated by arrowheads below the amino acid sequence. The conserved regions of follistatin-like domains are underlined. To indicate possible sites for glycosaminoglycan attachment, SGXG motifs are bold-underlined and SG dipeptides are boxed. Putative sites for alternative splicing (x, y and z) are indicated in parentheses, and the 9-amino acid insert in splice site x is dotted-underlined. This sequence is available from GenBank under accession number [AF016903](https://www.ncbi.nlm.nih.gov/nuccore/AF016903).

1	gcgcggtgcgtcctgcccggagccggcgggacatgcccgagcgcgcgctggagcggcgcgaggaggogaaogtggtg	81
1	a a c v l p g a g g ▲ T C P E R A L E R R E E E A N V V	27
	signal peptide (partial) laminin-binding domain	
82	ctcaaccgggacggtggaggagatcctcaacgtggaccgggtgcagcacagctactcctgcaaggttogggtctggcggtac	162
28	L T G T V E E I L N V D P V Q H T Y S C K V R V W R Y	54
163	ttgaaggcacaagacctggtggcccgggagagcctgctggacggcggcaacaaggtggtgatcagcggtttggagacccc	243
55	L K G K D L V A R E S L L D G G N K V V I [S G] F G D P	81
244	ctcatctgtgacaaccagggtgtccactggggacaccaggatcttctttgtgaacctgcacccccatacctgtggcagcc	324
82	L I C D N Q V S T G D T R I F F V N P A P P Y L W P A	108
325	cacaagaacagactgatgtcactccagcctcatgcggatcaccctgcggaacctggaggaggtggagtctgtgtggaa	405
109	H K N E L M L N S S L M R I T L R N L E E V E F C V E	135
406	gataaacccgggaccacttcaactcagctgctccgagcctcctgatgcgtgcccggggaatgctgtgcccgttggcgcc	486
136	D K P G T H F T P V P P T P P D ▲ C R G M L C G F G A	162
	follistatin-like domain 1	
487	gtgtgagagcccaacggaggggcggggcgggctcctgcgtctgcaagaagagcccggtgccccagcgtggtggcgcct	567
163	V C E P N A E G P G R A S C V C K K S P C P S V V A P	189
568	gtgtgtgggtggagcgcctccacctacagcaacgaatgcgagctgcagcgggcagtgccagcagcgcgcgcctccgc	648
190	V C G S D A S T Y S N E C E L Q R A Q C S Q Q R R I R	216
649	ctgtcagcggcggcggcgtgcccgggacccctgctccaacgtgacctgcagcttggcagcacctgtgcccgtctgc	729
217	L L S R G P C G S R D P ▲ C S N V T C S F G S T C A R S	243
	follistatin-like domain 2	
730	gccagcgggtgacggcctcgtgctgtgccccgcagcctgcccgtggcggccccggagggaacctgtgcccagcagcggc	810
244	A D G L T A S C L C P A T C R G A P E G T V C G S D G	270
811	gccgactacccggcagtgccagttcctgcccgcgcctgcgcgccagagagaatgtcttcaagaagttcagcggccct	891
271	A D Y P G E C Q F L R R A C A R Q E N V F K K F D G P	297
892	tgtgacctgtcagggcgcctccctgaccggagcgcagctgcccgtgtgaacctggcagcagcggcgcctgagatgctc	972
298	C D P ▲ C Q G A L P D P S R S C R V N P R T R R P E M L	324
	follistatin-like domain 3	
973	ctacggccccagagctgccctgcccggcagggcagctgtgtggggcagcagtgctacactcagaaaacgactgtgtcatg	1053
325	L R P E S C P A R Q A P V C G D D G V T Y E N D C V M	351
1054	ggccgatccggggcgcgcgggggtctcctcctgcagaaagtgcgctccggcagtgccagggctgagaccagtgcccggag	1134
352	G R [S G] A A R G L L L Q K V R [S G] Q C Q G R D Q C ▲ P E	378
1135	ccctgcccgttcaatgcccgtgtgctgtcccgcgtggcgtcccgcgtgctcctgcgacccgctcacctgtgacggggcc	1215
379	P C R F N A V C L S R R G R P R C S C D R V T C D G A	405
	follistatin-like domain 4	
1216	tacagggccgtgtgtgcccaggacggggcagcagctatgacagtgatgtgtggcggcagcaggtgagtgcccggcagcagct	1296
406	Y R P V C A Q D G R T Y D S D C W R Q Q A E C R Q Q R	432
1297	gccatccccagcaagcaccaggcccgtgtgaccaggcccgcctcccctgcctcggggtgcaagtgtgcatttggggcgacg	1377
433	A I P S K H Q G P C D Q A P S ▲ C L G V Q C A F G A T	459
	follistatin-like domain 5	
1378	tgtgtgtgaagaacgggcagggcagcagctgtgaatgcctgcagggcgtgctcagagcctctacgatcctgtgtgcccagcagc	1458
460	C A V K N G Q A A C E C L Q A C S S L Y D P V C G S D	486
1459	ggcgtcacatacggcagcgcgtgcgagctggaggccacggcctgtaccctcggggcggagatccagggtggcgcgcaaaagga	1539
487	G V T Y G S A C E L E A T A C T L G R E I Q V A R K G	513
1540	ccctgtgaccgtgcccggcagtgcccgtttggagccctgtgcgagggccgagaccggggcgtcgtgtgcccctctgaatgc	1620
514	P C D R ▲ C G Q C R F G A L C E A E T G R C V C P S E C	540
	follistatin-like domain 6	
1621	gtggtttggcccagcccgtgtgtggtccgacgggcacacgtaccccagcagtgcatgctgcagctgcacgctgcaca	1701
541	V A L A Q P V C G S D G H T Y P S E C M L H V H A C T	569
1702	caccagatcagcctgcagctggcctcagctggaccctgcgagacctgtggagatgcccgtgtgtgctttggggctgtgtgc	1782
568	H Q I S L H V A S A G P C E T ▲ C G D A V C A F G A V C	594
	follistatin-like domain 7	
1783	tcgcagggcagtggtgtgtccccgggtgtgagcacccccgcggcccccgtgtgtggcagcagcgggtgcacctacggc	1863
595	S A G Q C V C P R C E H P P P G P V C G S D G V T Y G	621
1864	agtgcctgcgagctacgggaagccgcctgcctccagcagacacagatcgaggaggcccgggcagggccgtgcccagcagcc	1944
622	S A C E L R E A A C L Q Q T Q I E E A R A G P C E Q A	648
1945	gagtgcgggtccggaggtcttggctctggggaggacgggtgactgtgagcaggagctgtgcccggcagcgggtgcatctgg	2025
649	E C G [S G] G [S G] [S G] E D G D ▲ C E Q E L C R Q R G G I W	675
	follistatin-like domain 8	
2026	gaagaggactcggaggacggcggcgtgtgtctgtgacttcagctgccagagtgctccagggcagcccgggtgtgcccgtcagat	2106
676	D E D S E D G P C V C D F S C Q S V P G S P V C G S D	702
2107	ggggtcacctacagcaccagtggtgagctgaagaagccaggtgtgagtcacagcagggctctacgttagcggcccagggga	2187
703	G V T Y S T E C E L K K A R C E S Q R G L Y V A A Q G	729
2188	gcctgcggagggccccaccttcgcccgcgtgcgcctgtgccccttacactgtgcccagacgcctacggctgctgcccag	2268
730	A C R G P T F A P L P ▲ V A P L H C A Q T P Y G C C Q	756
	LE domains	

2269	gacaatatcaccgcagcccgggctgggctggctgccccagtgccctgcaacccccatggctcttacggc	2349
757	D N I T A A R G V G L A G C P S A C Q C N P H G S Y G	783
2350	ggcactgtgaccagccacaggccagtgctcctgcccaggtgtgggggctcaggtgtgaccgctgtgagcctggc	2430
784	G T C D P A T G Q C S C R P G V G G L R C D R C E P G	810
2431	ttctggaactttcagggcatcgtcaccgatggccggagtggtgtacacctgcaactgtgatccccaaaggcgcgtgogg	2511
811	F W N F R G I V T D G R <u>[S G]</u> C T P C S C D P Q G A V R	837
2512	gatgactgtgagcagatgacggggctgtgctcgtgtaagccgggggtggctggacccaagtgtgggcagtgccagacggc	2592
838	D D C E Q M T G L C S C K P G V A G P K C G Q C P D G	864
2593	cgtgccctgggccccgggctgtgaagctgacgcttctgcccctgcaactgtgaggagatgctggtgagttcgggtgog	2673
865	R A L G P A G C E A D A S A \blacktriangle P A T S A S V T V T T P G L	891
	follistatin-like domain 9	
2674	cggtgcgtggaggagtctggctcagcccactgtgtctgcccagatgctcactgtccagaggccaaogctaccaaggtctgt	2754
892	R C V E E <u>[S G]</u> S A H C V C P M L T C P E A N A T <u>K V C</u>	918
2755	gggtcagatggagtcacatacggcaacagtgctcagctgaagaccatgcctgcccagggcctgcaaatctctatccag	2835
919	<u>G S D G V T Y</u> G N E C Q L K T I A C R Q G L Q I S I Q	945
2836	agcctgggcccctgcccaggaggtgttgctcccagcactcaccggacatctgcctccgtgactgtgaccaccccagggtcc	2916
946	S L G P C Q E A V A P S \blacktriangle T H P T S A S V T V T T P G L	972
	S/T-rich domain 1	
2917	ctcctgagccaggcactgcccggccccccgggcccctcccctggctcccagcagtagccgcacacagccagaccacccct	2997
973	L L S Q A L P A P P G A L P L A P S S T A H S Q T T P	999
2998	ccgcctcatcgcagcctcggaccactgcccagcgtcccagaccaccgtgtggcccgtgtgacgggtgcccccaaggca	3078
1000	P P S S R P R T T A S V P R T T V W P V L T V P P T A	1026
3079	ccctcccctgcaaccagcctgggtggcgtcgcctttggtgaatctggcagcactgatggaagcagcagatgaggaactgagc	3159
1027	P S P A P S L V A S A F G E <u>[S G]</u> S T D G S S D E E L <u>[S]</u>	1053
3160	ggggaccaggaggccagtggggggtgctctgggggctcagcccctggaggggcagcagcgtggccaccccctggccacct	3240
1054	<u>[G]</u> D Q E A <u>[S G]</u> <u>[G G]</u> <u>[S G]</u> G L E P L E G S S V A T P G P P	1080
3241	gtcagagagggcttctcgtctacaactccgcttgggctgctgctctgatgggaagcgcctcgtggacgcagagggctcc	3321
1081	V E R A S C Y N S A L G C C S D G K T P S L D A E G S	1107
3322	aactgcccgcaccacaaggtgtccagggcgtcctggagctggaggggcgtcagggccaggagctgttctacacgcccag	3402
1108	N C \blacktriangle P A T K V F Q G V L E L E G V E G Q E L F Y T P E	1134
	SEA module	
3403	atggctgaccccagtcagaactgttcggggagacagccaggagcattgagagcaccctggacgacctctccggaattca	3483
1135	M A D P K S E L F G E T A R S I E S T L D D L F R N S	1161
3484	gacgtcaagaaggtttccggagtgctcgccttgcgggacctggggcccggcaaatccgtccgcgacctgtggatgtgcac	3564
1162	D V K K D F R S V R L R D L G P G K S V R A I V D V H	1188
3565	tttgaccccaccagccttcaggggcaccgcagctggcccggcccctgctccggcagatccagggtgcccagggcggctcc	3645
1189	F D P T T A F R A P D V A R A L L R Q I Q V S R R R S	1215
3646	ttgggggtgaggcggcgcctgcccaggacagtgccgatttatggactttgactggtttctcgtgttatcagggggccacg	3726
1216	L G V R R P L Q E H V R F M D F D \blacktriangle D W F P A F I T G A T	1242
	(site x)	
3727	tcaggagccattgctgcccggaccagggccagagccaccactgcatcgcgcctgcccctcctctgctgtgaccccctgggcc	3807
1243	<u>[S G]</u> A I A A G A T A R A T T A S R L P S S A V T P R A	1269
	S/T-rich domain 2	
3808	ccgcaccccagtcacacaagccagcccgttgccaagaccagggcagccccaccacaagctcggccccccaccactgcccc	3888
1270	P H P S H T S Q P V A K T T A A P T T R R P P T T A P	1296
3889	agcctgtgcccggacgtcggccccggccccccagcagcctccaagccctgtgactcacagccctgctccacgggggg	3969
1297	S R V P G R R P P A P Q Q P P K P \blacktriangle C D S Q P C F H G G	1323
	EGF-like repeat 1	
3970	acctgccaggactgggcattggggcggggcttcacctgcagctgcccggcaggcaggggagggcgcctctgtgagaaggtg	4050
1324	T C Q D W A L G G G F T C S C P A G R G G A V C \blacktriangle E K V	1350
	laminin-	
4051	cttgcccccctgtgcccgccttcaggggcccgcctcctcctggccttccccaccctccgcgctaccacaagctgcccctg	4131
1351	L G A P V P A F E G R S F L A F P T L R A Y H T L R L	1377
	G-like domain 1	
4132	gcactggaattccgggcgctggagcctcaggggctgctgctgtacaatggcaacggccggggcaaggacttccctggcattg	4212
1378	A L E F R A L E P Q G L L L Y N G N A R G K D F L A L	1404
4213	gcgctgctagatggccgctgacagctcaggtttgacacaggttcggggcggggcgtgctgaccagtgccgctgcccgttagag	4293
1405	A L L D G R V Q L R F D T G <u>[S G]</u> P A V L T S A V P V E	1431
4294	ccgggacagtgccaccgctggagctgtcccggcactggcggcggggcaccctctcggtggatgggtgagaccccctgtctg	4374
1432	P G Q W H R L E L S R H W R R G T L S V D G E T P V L	1458
4375	ggcgagagtcccagtgccaccgacggcctcaacctggacacagacctctttgtggggcggcgtaccggaggaccaggtgcc	4455
1459	G E S P <u>[S G]</u> T D G L N L D T D L F V G G V P E D Q A A	1485
	(site y)	
4456	gtggcgtggagcggacctcgtggggcggcctgaggggggtgcatcogtttctggagctcaacaaccagcgcctggag	4536
1486	V A L E R T F V G A G L R G C I R L L D V N N Q R L E	1512

4537	cttggcattgggcccggggctgccaccagagctctggcgtgggagtgcggggaccaccctgctgcccaccctgc	4617
1513	L G I G P G A A T R G <u>[S G]</u> V G E C G D H P \blacktriangle C L P N P C	1539
		EGF-like repeat 2
4618	catggcggggccccatgccagaacctggaggctggaaggttccattgccagtccccgccggcgcgaccacaacctgt	4698
1540	H G G A P C Q N L E A G R F H C Q C P P G R V G P T C	1566
4699	gccgatgagaagagcccctgccagcccaaccctgccatggggcggcgccctgcccgtgtgctgccaggggtggtgctcag	4779
1567	A D E K S P C Q P N P \blacktriangle C H G A A P C R V L P E G G A Q	1593
		EGF-like repeat 3
4780	tgcgagtccccctggggcgtgaggcacccttctgccagacagcctcggggcaggacggctctggcccttctggtgac	4860
1594	C E C P L G R E G T F C \blacktriangle Q T A <u>[S G]</u> Q D G <u>[S G]</u> P F L A D	1620
		laminin-G-like domain 2
4861	ttcaacggcttctcccacctggagctgagaggcctgcacacctttgcaogggacctgggggagaagatggcgctggaggtc	4941
1621	F N G F S H L E L R G L H T F A R D L G E K M A L E V	1647
4942	gtgttctggcagggcccagcggcctcctgctctacaacgggcagaagacggacggcaagggggacttctgtgctg	5022
1648	V F L A R G P <u>[S G]</u> L L L Y N G Q K T D G K G D F V S L	1674
5023	gcactgcccggaccgcccctggagttccgctacgacctggcaagggggcagcggatcagggagcagggagccagtcacc	5103
1675	A L R D R R L E F R Y D L G K G A A V I R S R E P V T	1701
5104	ctgggagcctggaccagggctctcactggagcgaacggccgcaaggggtgccctgctgtggcgacggccccctgtgtt	5184
1702	L G A W T R V S L E R N G R K G A L R V G D G P R V L	1728
5185	ggggagtccccggttccgcacacogtcccaacctgaaggagccgctctacgtagggggcgctcccgacttcagcaagctg	5265
1729	G E S P V P H T V L N L K E P L Y V G G A P D F S K L	1755
5266	gccctgctgctgcccgtgtcctctggtcttcagcgggtccatccagctggtctcctcggagggccagctgctgacccc	5346
1756	A R A A A V S <u>[S G]</u> F D G A I Q L V S L G G R Q L L T P	1782
5347	gagcagctgctgcccaggtggaogtcaogtccctttgacggtaaccctgcacccggcctcaggccaccctgctcaat	5427
1783	E H V L R Q V D V T S F A G H P \blacktriangle C T R A <u>[S G]</u> H P C L N	1809
		EGF-like repeat 4
5428	ggggcctcctgctcccagggaggtgctcctatgtgtgctgctccgggggattctcaggaccgcaactgcgagaagggg	5508
1810	G A S C V P R E A A Y V C L C P G G F <u>[S G]</u> P H C \blacktriangle E K G	1836
		laminin-G-like domain 3
5509	ctggtggagaagtcagcgggggagctggataccttggcctttgacggggggacctttgtcgagtaacctcaacgctgtgacc	5589
1837	L V E K S A G D V D T L A F D G R T F V E Y L N A V T	1863
5590	gagagcagaagggcactgcagagcaaccctttgaactgagcctgcccactgagggccacgaggggctggtgctctggag	5670
1864	E S E K A L Q S N H F E L S L R T E A T Q G L V L W <u>[S G]</u>	1890
	(site z)	
5671	ggcaaggccacggagcggggcagactatgtggcactggccattgtggacggggcaacctgcaactgagctacaacctgggctcc	5751
1891	<u>[G]</u> K A T E R A D Y V A L A I V D G H L Q L S Y N L G S	1917
5752	cagcccgtggtgctgctgctccacogtgcocgtcaacaccaaccgctggttgcgggtcgtggcacaataggagcagagggaa	5832
1918	Q P V V L R S T V P V N T N R W L R V V A H R E Q R E	1944
5833	ggttccctgcaggtgggcaatgagggcccctgtgaccggctcctcccctggtggcggcagcagctggacactgatggagcc	5913
1945	G S L Q V G N E A P V T G S S P L G A T Q L D T D G A	1971
5914	ctgtggcttggggcctgcccggagctgcccgtgggcccagcactgcccaggcctaaggcaaggctttgtggctgctt	5994
1972	L W L G G L P E L P V G P A L P K A Y G T G F V G C L	1998
5995	cgggatggtggtggggcggcaccogctgcacctgctggaggaogccgtcacaagccagagctgcccctgccccacc	6075
1999	R D V V V G R H P L H L L E D A V T K P E L R P C P T	2025
6076	ccatgagctggcaccagagccccgcggcogctgtaattatcttctatcttttgtaaaactgttgccttttgatattgtttc	6156
2026	P .	
6157	ttgctgagtgtggcgggagggactgctggcccggcctccctccgtccaggcagcogtctgcagacagacctagtgt	6237
6238	gagggatggacagggcaggtggcagcgtggagggctcggcgtggatggcagcctcaggacacacaccctgctcaaggtg	6318
6319	ctgagcccccgcttgcactgcccctgccccacgggtgctcccgcggggaagcagccccggctcctgaataccctcgtccc	6399
6400	gtcaggggggactcgtgtccccaaaagggaaggggctgctgaggtctgatggggccctcctccgggtgacccccacagggcc	6480
6481	ttccaagcccctatttgagctgctcctcctgtgtgtgctctggacctgctcggcctcctgcgccaactgtgactt	6561
6562	ccaaacaatgttactgctgggcacagctctgctgttgcctccogtgcctgctgcccagccccaggtgctgaggagcagagg	6642
6643	ccagaccagggccgatctgggtgtcctgacctcagctggccctgcccagccacctggacatgacogtatccctctgcca	6723
6724	caccccagggcctgaggggctatcgagaggactcactgtggatggggttgacctctgcccctgctgggtatctgg	6804
6805	gctggccatggctgtgttctcatgtgttattttatggacctggaggtgggtctcatcttccatctcgcctg	6885
6886	agagcggctgagggctcctcactgcaaatcctcccacagcgtcagtgaaagctcctgtctcagaatgaccagggggc	6966
6967	cagccagtgctgaccaaggtcaaggggaggtgcagaggtggcagggatggctccgaagccagaa	7032

Transcription of human agrin in fetal and adult tissues

Although many studies involving agrin are related to neuromuscular development, the expression of agrin is more widespread [1, 13, 14, 21]. We compared the transcription levels of agrin mRNA in fetal and adult human tissues, using the 4.1 kb cDNA clone Cs1 as a homologous probe. For quantitation, we used a dot blot containing carefully normalized quantities of poly(A)-rich RNA from a wide range of human tissues. The most prominent hybridization signals originated from adult kidney and lung (Figure 3). Agrin mRNA levels were also higher than average in adult liver and the thyroid gland. Besides this, low amounts of agrin

mRNA were detected in all other tissues. These signals are likely specific, since they were identical after hybridization with a different probe (clone Cs2). Most likely, the detected mRNA originates from the vascularization of these tissues. This possibility is supported by the detection of agrin-like immunoreactivity in capillaries of many tissues [30, 34]. In fetal stages, agrin mRNA was detected at low levels in all tissues tested, but slightly higher amounts were observed in kidney and lung (Figure 3). To analyze the lengths of agrin mRNAs in kidney and lung, northern blot analyses were performed. Hybridization with clone Cs2 visualized only a single mRNA band, 7.6 – 7.8 kb in size. In addition to this full length transcript, a relatively short transcript was identified when clone Cs1 was used as probe. The approximate length of this transcript was 5 kb. The fact that this molecule does not hybridize to Cs2 indicates that it is truncated at the 5' end.

heart 0.04	aorta 0.02	skeletal muscle 0.03	colon 0.07	bladder 0.01	uterus 0.02	prostate 0.04	stomach 0.05
testis 0.01	ovary 0.06	pancreas 0.05	pituitary gland 0.04	adrenal gland 0.02	thyroid gland 0.12	salivary gland 0.06	mammary gland 0.03
kidney 2.31	liver 0.41	small intestine 0.09	spleen 0.03	thymus 0.04	peripheral leukocyte 0.01	lymph node 0.03	bone marrow 0.01
appendix 0.10	lung 2.69	trachea 0.10	placenta 0.04				
fetal brain 0.03	fetal heart 0.03	fetal kidney 0.18	fetal liver 0.07	fetal spleen 0.03	fetal thymus 0.04	fetal lung 0.15	

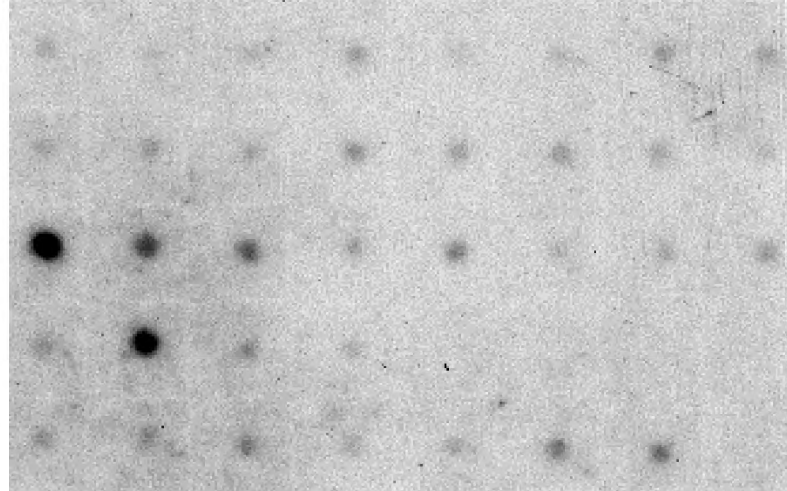


Figure 3. Comparison of agrin mRNA levels in human tissues. RNA isolated from various fetal and adult human tissues was hybridized with clone Cs1. Relative agrin mRNA levels were calculated in arbitrary units (A). The corresponding autoradiograph is shown (B). The quantity of RNA spotted onto this commercial blot (Clontech) was normalized by hybridization with probes for eight different housekeeping mRNAs. Adult kidney RNA was pooled from 3 male/female Caucasian donors, ages 42–63. Adult lung RNA was pooled from 2 male/female Caucasians, ages 23 and 42. Fetal RNA was pooled from 14 or more Caucasians, ages 17–28 weeks.

Expression of human agrin in kidney, lung and skeletal muscle

To compare the different agrin mRNA levels with protein expression, we analyzed the distribution of agrin immunoreactivity in adult human tissues by indirect immunofluorescence. Consistent with their high mRNA levels, a strong staining was observed in lung and kidney. In lung, agrin immunoreactivity was located in the alveolar as well as the capillary BMs (Figure 5A). Between the alveolar epithelium and the capillary endothelium, both BMs fuse. Also the capillaries of fetal and adult brain contained agrin-like immunoreactivity (data not shown). In the kidney (Figure 5B), anti-agrin immunostaining was prominent in the glomerular BM, together with a less intense staining of the tubular BM, Bowman's capsule and vascular walls. In skeletal muscle, clusters of agrin-like antigenicity were observed in the NMJ (Figure 5D). To identify junctions, a combined staining with rhodamine-conjugated α -bungarotoxin was performed (Figure 5C). Besides this intense

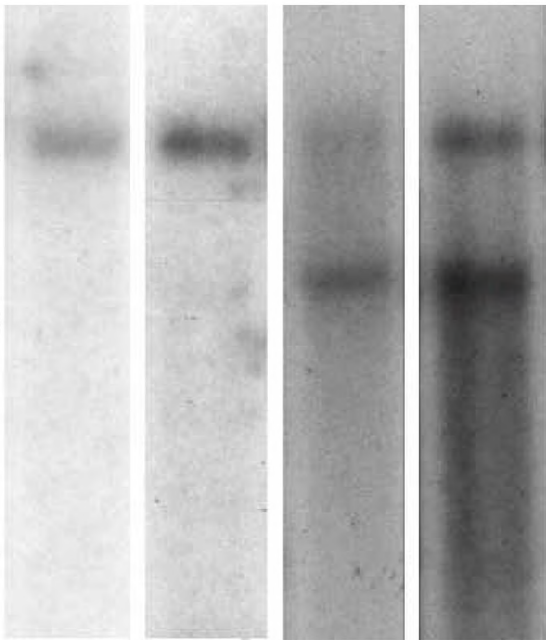


Figure 4. Northern blot analysis of human agrin mRNA in adult lung and kidney. After hybridization with clone Cs2 as a probe, a single band was observed in lung (lane 1) and kidney (lane 2) corresponding with an mRNA length of 7.6-7.8 kb. In addition, a relatively short transcript was observed in both tissues after hybridization with clone Cs1 (lane 3: lung; lane 4: kidney). The positions of molecular mass markers are indicated on the left.

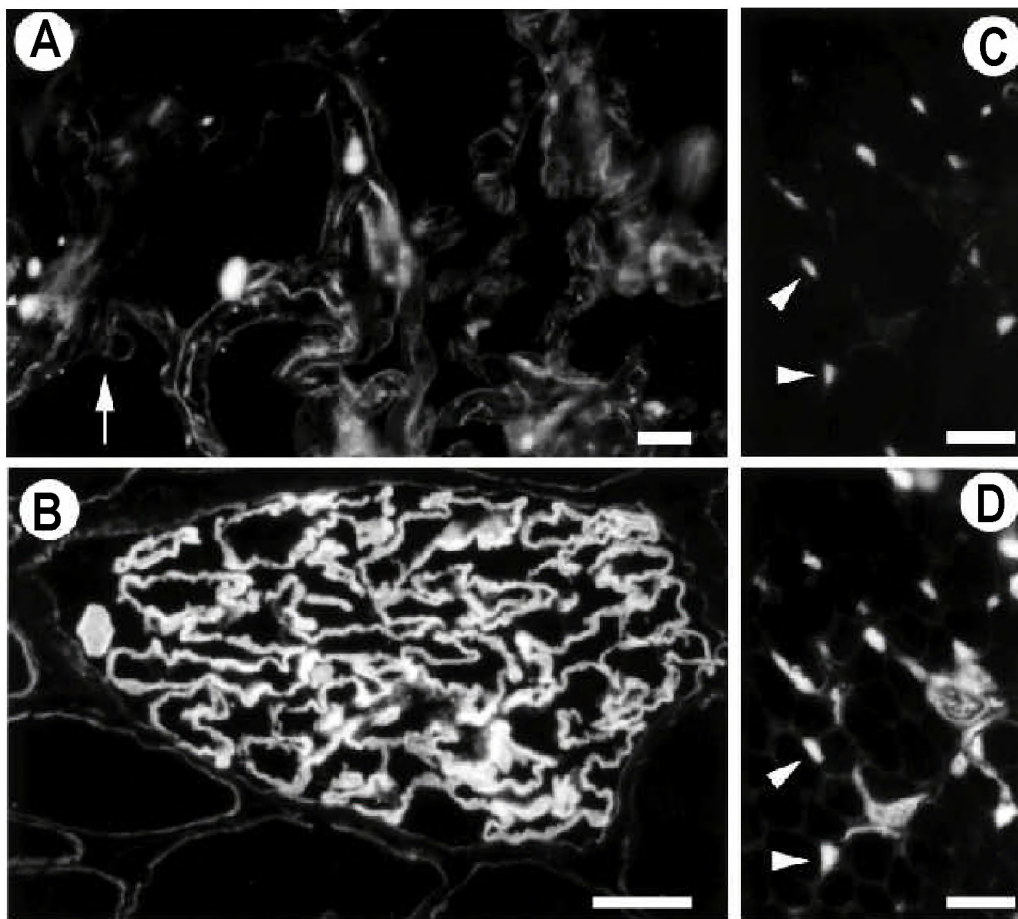


Figure 5. Immunofluorescence detection of agrin in cryosections of human lung (A), kidney (B), and skeletal muscle (D). To identify neuromuscular junctions, in (C), the same section as shown in (D) was stained with α -bungarotoxin. The arrow in (A) indicates a capillary. Arrowheads in (C) and (D) indicate two typical neuromuscular junctions. Bar, 25 μ m.

staining, a weak staining of the BM surrounding the skeletal muscle cells was observed. These staining characteristics agree with previously reported data on rat, chick and mouse skeletal muscle [4, 13]. In summary, the results indicate that the high transcription levels in lung and kidney result in the accumulation of agrin in the alveolar and glomerular BM.

DISCUSSION

Size and composition of human agrin

The cDNA sequence presented in this study lacks approximately 42 nucleotides of the signal sequence, assuming a similar signal peptide length compared to chick agrin. Thus, the predicted size of human agrin mRNA is 7.1 kb or larger, depending on the size of the 5' non-coding region. This corresponds with the largest transcripts present in lung and kidney, as shown in Figure 4. After cleavage of the signal peptide, the calculated molecular mass of the human agrin core protein is 212 kDa. This agrees with previous estimations of 220–250 kDa, based on SDS-PAGE experiments after removal of the glycosaminoglycan chains [1, 7, 15].

The agrin core protein is substituted with heparan sulfate chains [1]. In previous studies on chick agrin, it was demonstrated that the proteoglycan comigrates with proteins of approximately 400 kDa as a diffuse band, characteristic for heavily glycosylated proteins [1]. As shown in Figure 2, the presented primary structure offers several sites for glycosaminoglycan attachment. The first potential O-glycosylation site is located near the N-terminal boundary of the fifth follistatin-like domain. This site contains a SGGSGSG sequence, of which the SGSG repeat unit was identified as a site that strongly supports glycosaminoglycan attachment, with preference for heparan sulfate rather than chondroitin sulfate [35]. The second possible attachment site that precedes the SEA module is most favorable, as far as the requirements for glycosaminoglycan attachment are known, for modification with heparan sulfate residues [1, 33, 35, 36]. This site is located in a strongly acidic cluster with acidic residues at –2 and –4 relative to the putative serine acceptor site (see Figure 2). Three additional SG dipeptides are present in this cluster and could also be glycosylated, given their position relative to acidic residues. Other SGXG patterns are placed in a less favorable context for substitution with HS chains, and therefore a function of these sites in glycosaminoglycan attachment is less likely as far as can be predicted. Thus, glycosaminoglycan attachment may be confined to the central region of the human agrin core protein (arrows in Figure 1B).

Age- and tissue-dependence of agrin expression

The role of neuronal agrin in embryogenesis is evident from numerous studies, and it is known that concentrations of agrin remain present in the adult NMJ. This correlates with the minor hybridization signals in skeletal muscle (Figure 3), because NMJs comprise only a minute part of the total tissue mass. However, the significance of agrin in non-neural tissues is not yet clear. In this study, we found a strong upregulation of agrin transcription in adult kidney and lung. This leads to the accumulation of agrin-like immunoreactivity in the BMs of these tissues, as shown by indirect immunofluorescence. In adult lung, the localization of agrin was primarily confined to the capillary and alveolar BM. In kidney most immunoreactivity was located in the glomerular BM, but the tubular BM was also stained. Our results from northern blotting suggest that the agrin gene may produce a 5'-truncated transcript, encoding an isoform that carries heparan sulfates, but lacks the laminin-binding domain. In line with these ideas, relatively small agrin-like molecules were previously reported to occur [13, 37].

The composition of the reported cDNA at the known splice sites was as follows. At site *x*, located near the SEA module, a 9 amino acids insert (DWFPAFITG) was found as indicated

in Figure 2. At the *y* and *z* site, all analyzed clones were devoid of any inserts. The absence of a basic tetrapeptide at the *y* site indicates that this agrin isoform has a low heparin-binding activity [9, 19]. At the *z* site, an insert is required for the acetylcholine receptor-clustering activity of neuronal agrin isoforms. The presented primary structure thus predicts a low acetylcholine receptor clustering activity for agrin from kidney and skeletal muscle, which is in agreement with previous experiments [13]. In a recent review, Ruegg and Bixby demonstrated high amounts of agrin-like protein in adult kidney and lung, which lack inserts at the *y* and *z* site [38]. All findings indicate that agrin isoforms are not only involved in embryonic development, but may exert additional functions in mature tissues.

Significance of agrin expression for renal and pulmonary function

The glomerular, alveolar and neuromuscular BMs have in common that they are fused BMs assembled by two different cell types, located on opposite sides of the BM. The collagen fibril network in these matrices is mainly composed of collagen IV chains $\alpha 3$, $\alpha 4$ and $\alpha 5$, whereas the $\alpha 1$ and $\alpha 2$ chains predominate in most other BMs [39]. Also the laminin composition is mutually comparable and different from other BMs, with the presence of the laminin $\beta 2$ chain (S-laminin) as the most distinct characteristic [39–42].

In the glomerular BM, agrin likely acts as a permselectivity modulator. The importance of HSPGs in this structure was demonstrated by perfusing rat kidney with heparitinase, resulting in an increased permeability for anionic macromolecules, and hence albuminuria [43]. The contribution of agrin to the polyanionic charge of the glomerular BM may be essential for this mechanism [44]. A filtration-associated function was also suggested for agrin expressed in capillaries, especially those that act as a blood-brain barrier [34].

In the alveolar BM, the relevance of HSPGs was established by previous studies. Intratracheal instillation of elastase induced a decrease in alveolar HSPG content, followed by pulmonary emphysema [45]. A similar effect was observed after instillation of β -D-xyloside, an inhibitor of proteoglycan synthesis [30]. The function of agrin isoforms in the alveolar BM could be related to the inhibition of proteases [14]. The anti-proteolytic activity of agrin is particularly interesting because the disruption of the balance between proteolysis and protease inhibition is considered a causal factor in the pathogenesis of pulmonary emphysema [46].

Future directions

Up to date, agrin and perlecan are the only identified HSPGs associated with BMs. Both genes are clustered on the short arm of human chromosome 1 [5, 47, 48]. The presence of additional BM HSPG species is not unlikely [49]. The molecular cloning of cDNA encoding human agrin offers new starting points for the investigation of its functional properties. The high expression of agrin in the differentiated alveolar and glomerular BM suggests that agrin may be a mediator in pulmonary and renal function. Since HSPGs are known to play an important role in pulmonary emphysema and nephrotic syndrome, agrin may be involved in the pathogenesis of these disorders. In future research, we intend to focus on the role of agrin in various types of nephrotic syndrome. In addition, we will investigate the exact composition of agrin splice variants present in the human glomerular and alveolar BM.

ACKNOWLEDGEMENTS

The authors wish to thank Dr. Markus Ruegg for providing anti-agrin antisera. This study was supported by grant C93.1309 of the Dutch Kidney Foundation. The laboratory participates in a BIOMED I concerted action “Alterations in extracellular matrix composition in diabetes and other glomerular diseases”, which is financially supported by the EC and the Biomed I program (BMH1-CT92-1766).

REFERENCES

1. Tsen G, Napier A, Halfter W and Cole GJ (1995) Agrin is a heparan sulfate proteoglycan, *J. Biol. Chem.* 270:15934–15937.
2. Bowe MA and Fallon JR (1995) The role of agrin in synapse formation, *Annu. Rev. Neurosci.* 18:443–462.
3. Smith MA, Magill-Solc C, Rupp F, Yao YM, Schilling JW, Snow P and McMahan UJ (1992) Isolation and characterization of an agrin homologue in the marine ray, *Mol. Cell Neurosci.* 3:406–417.
4. Rupp F, Payan DG, Magill-Solc C, Cowam DM and Scheller RH (1991) Structure and distribution of a rat agrin, *Neuron* 6:811–823.
5. Rupp F, Özçelik T, Linial M, Peterson K, Francke U and Scheller RH (1992) Structure and chromosomal localization of the mammalian agrin gene, *J. Neurosci.* 12:3535–3544.
6. Ruegg MA, Tsim KW, Horton SE, Kröger S, Escher G, Gensch EM and McMahan UJ (1992) The agrin gene codes for a family of basal lamina proteins that differ in function and distribution, *Neuron* 8:691–699.
7. Hoch W, Campanelli JT and Scheller RH (1994) Structural domains of agrin are required for clustering of nicotinic acetylcholine receptors, *J. Cell Biol.* 126:1–4.
8. Denzer AJ, Gesemann M and Ruegg MA (1996) Diverse functions of the extracellular matrix molecule agrin, *Semin. Neurosci.* 8:357–366.
9. O'Toole JJ, Deyst KA, Bowe MA, Nastuk MA, McKechnie BA and Fallon JR (1996) Alternative splicing of agrin regulates its binding to heparin, α -dystroglycan, and the cell surface, *Proc. Natl. Acad. Sci. USA* 93:7369–7374.
10. Meier T, Gesemann M, Cavalli V, Ruegg MA and Wallace BG (1996) AChR phosphorylation and aggregation induced by an agrin fragment that lacks the binding domain for α -dystroglycan, *EMBO J.* 15:2625–2631.
11. Bowen DC, Sugiyama J, Ferns M and Hall ZW (1996) Neural agrin activates a high-affinity receptor in C2 muscle cells that is unresponsive to muscle agrin, *J. Neurosci.* 16:3791–3797.
12. McMahan UJ, Horton SE, Werle MJ, Honig LS, Kröger S, Ruegg MA and Escher G (1992) Agrin isoforms and their role in synaptogenesis, *Curr. Opin. Cell Biol.* 4:869–874.
13. Godfrey EW (1991) Comparison of agrin-like proteins from the extracellular matrix of chicken kidney and muscle with neural agrin, a synapse organizing protein, *Exp. Cell Res.* 195:99–109.
14. Biroc SL, Payan DG and Fischer JM (1993) Isoforms of agrin are widely expressed in the developing rat and may function as protease inhibitors, *Brain Res.* 75:119–129.
15. Cole GJ and Halfter W (1996) Agrin: an extracellular matrix heparan sulfate proteoglycan involved in cell interactions and synaptogenesis, *Perspectives Dev. Neurobiol.* 3:359–371.
16. Denzer AJ, Gesemann M, Schumacher B and Ruegg MA (1995) An amino-terminal extension is required for the secretion of chick agrin and its binding to extracellular matrix, *J. Cell Biol.* 131:1547–1560.
17. Patthy L and Nikolics K (1993) Functions of agrin and agrin-related proteins, *Trends Neurosci.* 16:76–81.
18. Denzer AJ, Brandenberger R, Gesemann M, Chiquet M and Ruegg MA (1997) Agrin binds to nerve-muscle basal lamina via laminin, *J. Cell Biol.* 137:671–683.
19. Gesemann M, Cavalli V, Denzer AJ, Brancaccio A, Schumacher B and Ruegg MA (1996) Alternative splicing of agrin alters its binding to heparin, dystroglycan, and the putative agrin receptor, *Neuron* 16:755–767.
20. Matsumura K, Yamada H, Saito F, Sunada Y and Shimizu T (1997) The role of dystroglycan, a novel receptor of laminin and agrin, in cell differentiation, *Histol. Histopathol.* 12:195–203.
21. Groffen AJ, Ruegg MA, Dijkman H, Van der Velden TJ, Buskens CA, Van den Born J, Assmann KJ, Monnens LA, Veerkamp JH and Van den Heuvel LP (1998) Agrin is a major heparan sulfate proteoglycan in the human glomerular basement membrane, *J. Histochem. Cytochem.* 46:19–27.
22. Hillier LD, Lennon G, Becker M, Bonaldo MF, Chiapeli B, Chissoe S, Dietrich N, DuBoque T, Favello A, Gish W, Hawkins M, Hultman M, Kucaba T, Lacy M, Le N, Mardis E, Moore B, Morris M, Parsons J, Prange C, Rifkin L, Rohlfing T, Schellenberg K, Marra M, et al. (1996) The WashU-Merck EST project, *Genome Res.* 6:807–828.

23. Cheng S, Fockler C, Barnes WM and Higuchi R (1994) Effective amplification of long targets from cloned inserts and human genomic DNA, *Proc. Natl. Acad. Sci. USA* 91:5695–5699.
24. Langeveld PJ and Veerkamp JH (1981) Chemical characterization of glomerular and tubular basement membranes of various mammalian species, *Comp. Biochem. Physiol.* 68B:31–40.
25. Sambrook J, Fritsch EF and Maniatis T (1989) *Molecular cloning: a laboratory manual*, 2nd edn, Cold Spring Harbor Laboratory Press, Cold Spring Harbor, NY, USA.
26. Frohman MA (1993) Rapid amplification of complementary DNA ends for generation of full-length complementary DNAs: thermal RACE, *Methods Enzymol.* 218:340–356.
27. Nielsen H, Engelbrecht J, Brunak S and Von Heijne G (1997) Identification of prokaryotic and eukaryotic signal peptides and prediction of their cleavage sites, *Protein Engineering* 10:1–6.
28. Altschul SF, Gish W, Miller W, Myers EW and Lipman DJ (1990) Basic local alignment search tool, *J. Mol. Biol.* 215:403–410.
29. Van Kuppevelt TH, Van de Lest CH, Versteeg EM, Dekhuijzen PN and Veerkamp JH (1997) Induction of emphysematous lesions in rat lung by β -D-xyloside, an inhibitor of proteoglycan synthesis, *Am. J. Respir. Cell. Mol. Biol.* 16:75–84.
30. Groffen AJ, Hop FW, Tryggvason K, Dijkman H, Assmann KJ, Veerkamp JH, Monnens LA and Van den Heuvel LP (1997) Evidence for the existence of multiple heparan sulfate proteoglycans in the human glomerular basement membrane and mesangial matrix, *Eur. J. Biochem.* 247:175–182.
31. Engel J, Efimov VP and Maurer P (1994) Domain organizations of extracellular matrix proteins and their evolution, *Development* 1994 Suppl., 35–42.
32. Bork P and Patthy L (1995) The SEA module: a new extracellular domain associated with O-glycosylation, *Protein Sci.* 4:1421–1425.
33. Bourdon MA, Krusius T, Campbell S, Schwartz NB and Ruoslahti E (1987) Identification and synthesis of a recognition signal for the attachment of glycosaminoglycans to proteins, *Proc. Natl. Acad. Sci. USA* 84:3194–3198.
34. Barber AJ and Lieth E (1997) Agrin accumulates in the brain microvascular basal lamina during development of the blood-brain barrier, *Dev. Dyn.* 208:62–74.
35. Zhang L, David G and Esko JD (1995) Repetitive Ser-Gly sequences enhance heparan sulfate assembly in proteoglycans, *J. Biol. Chem.* 270:27127–27135.
36. Zhang L and Esko JD (1994) Amino acid determinants that drive heparan sulfate assembly in a proteoglycan, *J. Biol. Chem.* 269:19295–19299.
37. Hagen SG, Michael AF and Butkowski RJ (1993) Immunochemical and biochemical evidence for distinct basement membrane heparan sulfate proteoglycans, *J. Biol. Chem.* 268:7261–7269.
38. Ruegg MA and Bixby JL (1998) Agrin orchestrates synaptic differentiation at the vertebrate neuromuscular junction, *Trends Neurosci.* 21:22–27.
39. Sanes JR, Engvall E, Butkowski R and Hunter DD (1990) Molecular heterogeneity of basal laminae: isoforms of laminin and collagen IV at the neuromuscular junction and elsewhere, *J. Cell Biol.* 111:1685–1699.
40. Iivanainen A, Vuolteenaho R, Sainio K, Eddy R, Shows TB, Sariola H and Tryggvason K (1994) The human laminin β 2 chain (S-laminin): structure, expression in fetal tissues and chromosomal assignment of the LAMB2 gene, *Matrix Biol.* 14:489–497.
41. Noakes PG, Gautam M, Mudd J, Sanes JR and Merlie JP (1995) Aberrant differentiation of neuromuscular junctions in mice lacking s-laminin / laminin β 2, *Nature* 374:258–262.
42. Noakes PG, Miner JH, Gautam M, Cunningham JM, Sanes JR and Merlie JP (1995) The renal glomerulus of mice lacking s-laminin / laminin β 2: nephrosis despite molecular compensation by laminin β 1, *Nat. Genet.* 10:400–406.
43. Rosenzweig LJ and Kanwar YS (1982) Removal of sulfated (heparan sulfate) or unsulfated (hyaluronic acid) glycosaminoglycans results in increased permeability of the glomerular basement membrane to 125I-bovine serum albumin, *Lab. Invest.* 47:177–184.
44. Kanwar YS, Liu ZZ, Kashihara N and Wallner EI (1991) Current status of the structural and functional basis of glomerular filtration and proteinuria, *Semin. Nephrol.* 11:390–413.

45. Van de Lest CH, Versteeg EM, Veerkamp JH and van Kuppevelt TH (1995) Digestion of proteoglycans in porcine pancreatic elastase-induced emphysema in rats. *Eur.Respir.J.* 8:238–245.
46. Gadek J and Pacht ER (1990) The protease-antiprotease balance within the human lung: implications for the pathogenesis of emphysema, *Lung Suppl.* 168:552–564.
47. Kallunki P, Eddy RL, Byers MG, Kestilä M, Shows TB and Tryggvason K (1991) Cloning of human heparan sulfate proteoglycan core protein, assignment of the gene (HSPG2) to 1p36.1–p35 and identification of a BamHI restriction fragment length polymorphism. *Genomics* 11:389–396.
48. Dodge GR, Kovalszky I, Chu ML, Hassel JR, McBride OW, Yi HF and Iozzo RV (1991) Heparan sulfate proteoglycan of human colon: partial molecular cloning, cellular expression, and mapping of the gene (HSPG2) to the short arm of chromosome 1, *Genomics* 10:673–680.
49. Heintz B, Stöcker G, Mrowka C, Rentz U, Melzer H, Stickeler E, Sieberth HG, Greiling H and Haubeck HD (1995) Decreased glomerular basement membrane heparan sulfate proteoglycan in essential hypertension, *Hypertension* 25:399–407.
50. Bork P and Bairoch A (1995) *Trends Biochem. Sci.* 20, poster.

CHAPTER SEVEN

Functional analysis of human renal agrin

Functional analysis of human renal agrin

CHAPTER SEVEN

SUMMARY The presence of agrin in the glomerular basement membrane (GBM) suggests that, in addition to its role in the development of the neuromuscular junction, this heparan sulfate proteoglycan may have other functions in the kidney. To assess these functional properties, we produced 19 recombinant fragments of human kidney agrin as fusion proteins with glutathione S-transferase. The purified fusion proteins were used to localise the epitope of 25 monoclonal antibodies, raised against HSPG purified from human GBM and tubular basement membrane (TBM). Epitopes were found in the N-terminal through central region of the agrin core protein, a region near the ninth follistatin-like domain proving particularly immunogenic. Functional analyses of the fragments showed that the fifth follistatin-like domain had a relatively high plasmin-inhibiting activity. Furthermore, the N-terminal fragment AGR1 had laminin-binding activity. This activity was utilised to analyse agrin-laminin interactions in the GBM. AGR1 adhered to the GBM in human kidney cortex tissue and also to extracellular matrix produced by cultured human podocytes and glomerular endothelial cells. Agrin expression was exclusively detected in matrix produced by podocytes. The results indicate that agrin has multiple functions in the GBM, ranging from the incorporation of heparan sulfate to protease inhibition and cell-matrix interaction.

TO INDEX

INTRODUCTION

Agrin, known as a heparan sulfate proteoglycan (HSPG) is well-characterized as a component of the neuromuscular junction with a synapse-organizing function [1–3]. Much is known about structural-functional relationships in this regard. Agrin induces the clustering of acetylcholine receptor molecules on the postsynaptic membrane [4–6]. This activity is exclusive for neuronal agrin isoforms, and depends on differential splicing at the z site (called B in chick agrin) [7–10]. Muscle agrin isoforms also influence the differentiation of presynaptic structures, such as the formation of synaptotagmin clusters in the neuron [11]. Agrin is translocated to the extracellular matrix and immobilized there by its laminin-binding domain [12, 13].

Besides its role in synaptogenesis, agrin seems to have additional functions. For example agrin interacts with α -dystroglycan, a cell surface glycoprotein that is linked to the dystrophin-associated glycoprotein complex and the cytoskeleton [14–17]. The 212 kDa core protein contains many large domains that appear to be redundant for neuronal function, in particular the follistatin-like domains, laminin-like EGF repeats, serine/threonine-rich regions and SEA module. In fact, a 45 kDa C-terminal fragment of neuronal agrin is sufficient to induce clustering of acetylcholine receptors [7]. Also the role of the heparan sulfate (HS) residues linked to the central region of the core protein is unknown. These considerations suggest that additional functions of this multifunctional molecule are yet to be revealed.

The localization of agrin in non-neural tissues, including kidney, may contribute to the recognition of such functions [18–20]. We previously purified HSPG from human glomerular and tubular basement membrane (GBM and TBM) and generated a large panel of monoclonal antibodies (mAbs) [21, 22]. This HSPG appeared to be immunologically related to agrin and accumulates in high amounts in the GBM [23]. Since HSPGs are essential to maintain the

charge-selective permeability of the GBM during renal ultrafiltration [24–27], this suggests a crucial function for agrin's HS residues. In this study, we describe the expression of a large group of recombinant agrin fragments and demonstrate that the mAbs against GBM-HSPG recognize the agrin core protein. The recombinant proteins were also utilized to investigate the functions of agrin with special regard to the GBM, including inhibition of protease activity and binding to laminin. And finally, we describe the cellular origin of agrin expression in the human GBM.

MATERIALS AND METHODS

Production and characterization of recombinant fusion proteins

For synthesis of recombinant fragments of human agrin as fusion proteins with glutathione-S-transferase (GST) from *Schistosoma japonicum*, we used the pGEX expression system (Pharmacia Biotech, Roosendaal, The Netherlands). The borders of each recombinant agrin fragment were defined by engineering mutagenic primers so that a *Bam*HI- and an *Eco*RI restriction site were introduced at the 5'- and 3'- end of the corresponding PCR products (Table 1). Oligonucleotides were from Life Technologies (Breda, The Netherlands). Purified plasmids from the previously described clones Cs1, Cs2 and Cs4 were used as template DNA (GenBank AF016903) [28]. The PCR products were double-digested with *Bam*HI and *Eco*RI (Life Technologies), and ligated into the corresponding sites of the appropriate vector (pGEX-4T1, -4T2 or -4T3, each vector contains the multiple cloning site in a different reading frame). An alternative procedure was applied for the constructs AGR10 and AGR17. For AGR10, the internal 1.7 kb *Srf*I fragment of clone Cs1 was subcloned into the *Sma*I-digested, alkaline phosphatase-treated vector pGEX4T3. AGR17 was prepared by inserting the 2.1 kb *Not*I fragment of Cs1 into the alkaline phosphatase-treated *Not*I sites of the vector pGEX4T1. The resulting clones were screened for a correct orientation of the insert by restriction enzyme digestion analysis. To prepare AGR18, the 179 bp *Eco*RI-*Not*I restriction fragment of Cs1 was introduced into the corresponding sites of AGR10. For AGR19, the 2.1 kb *Not*I fragment from AGR17 was introduced into the *Not*I site of AGR18.

Biosynthesis of the recombinant agrin fragments was performed in batch cultures of *Escherichia coli* strains JM109 and BL21 following established procedures [29], except that the incubation temperature was 30°C which increased the solubility for many fusion proteins [30]. Cells were lysed in PBS containing 2% Triton-X100 and fusion proteins were purified by affinity chromatography to glutathione-conjugated Sepharose beads (Pharmacia). No protease inhibitors were used to avoid interference with functional assays. The cellular localization was analyzed by western blot detection of GST-like immunoreactivity in supernatants, cell lysates and insoluble fractions using an anti-GST mAb [29]. The yield of purified fusion proteins was determined by the Bradford method with bovine serum albumin (BSA) as standard. For molecular mass analysis, samples were analyzed by SDS-PAGE (T=12.5%, C=1%) under denaturing conditions. Molecular mass markers were from New England Biolabs. Predictions for molecular mass were calculated with the "Compute pI/MW" algorithm provided by the Swiss Institute of Bioinformatics (Geneva, Switzerland) [31].

Monoclonal antibodies and epitope mapping

A mAb against *S. japonicum* GST [29] was a kind gift from Dr. L. Uitto, Oulu, Finland. Anti-agrin mAbs were raised in mice against purified HSPG extracted from human GBM and TBM [21, 22]. We selected 25 mAbs that produced a linear staining of the glomerular capillaries in immunofluorescence, and recognized purified agrin in ELISA [22, 23]. These were named HAM1–25. To localize their epitopes, we assayed the immunoreactivity of each mAb towards all recombinant fusion proteins. Fusion proteins, along with BSA and GST as two negative

Table 1: Names and exact borders of the produced fusion proteins. Nucleotide sequences of the expression vectors are aligned above the encoded amino acids. Underlined residues indicate the restriction sites used for subcloning. Unrecovered restriction sites are dotted-underlined. The N-terminus of the fusion proteins are formed by glutathione-S-transferase (amino acids in normal face), fused to fragments of human agrin at the C-terminus (amino acids in bold). In-frame stop codons are located within 11 amino acids from the displayed C-terminal borders.

Name	GST/agrin fusion site	C- terminal border
AGR1	GTGGATCCACATGCCCGGAGC... R <u>G S T C P E</u>CGCCTGCTCAGCCGCATCGTGR L L S R I V
AGR2	GTGGATCCACATGCCCGGAGC... R <u>G S T C P E</u>GGCCCGTGTGACCAGAATTCCG P C D Q N S
AGR3	GTGGATCCTGTCAGGGCGCCC... R <u>G S C Q G A</u>AGTGCCAGGGTCGAGAATTCC ...Q C Q G R E F
AGR4	GTGGATCCTGCCCGGAGCCCT... R <u>G S C P E P</u>TGTGACCAGGCCCGAATTCCC D Q A P N S
AGR5	GTGGATCCCAGGCCCGTCCC... R <u>G S Q A P S</u>GCAAAGGACCCTGTGAATTCC ...R K G P C E F
AGR6	GTGGATCCTGTGACCGCTGCG... R <u>G S C D R C</u>GCTGGACCCTGCGAGAATTCCA G P C E N S
AGR7	GTGGATCCTGTGGAGATGCCG... R <u>G S C G D A</u>GCTCTGGCTCTGGGGAATTCC ...G S G S G E F
AGR8	GTGGATCCGGAGGCTCTGGCT... R <u>G S G G S G</u>TTACACTGTGCCAGAATTCCL H C A Q N S
AGR9	GTGGATCCGCTTCTGCGCCTG... R <u>G S A S A P</u>CCCAGCACTCACCCGAATTCCP S T H P N S
AGR10	ATTCCCGGGCAGGGCCGTGCG... N <u>S R A G P C</u>GCACCCGACGTGGCCCGGGTCA P D V A R V
AGR11	GTGGATCCCATGGCTCTTACG... R <u>G S H G S Y</u>GACTGTGAGCAGATGAATTCCD C E Q M N S
AGR12	GTGGATCCTCGTGTAAAGCCCG... R <u>G S S C K P</u>TGCTCACCTGTCCAGAATTCC ...M L T C P E F
AGR13	GTGGATCCTGTCCAGAGGCCA... R <u>G S C P E A</u>GCCTCCGTGACTGTGAATTCCA S V T V N S
AGR14	GTGGATCCGTGACTGTGACCA... R <u>G S V T V T</u>CGTCCGCCTTTGGTGAATTCC ...A S A F G E F
AGR15	GTGGATCCCCTGCACCCAGCC... R <u>G S P A P S</u>CCCGCCACCAAGGTGAATTCCP A T K V N S
AGR16	GTGGATCCTTCAGGGCACCCG... R <u>G S F R A P</u>GGGAGCCACGGCCAGAATTCCG A T A R N S
AGR17	AGCGGCCGCTGCAGGAGCACG... E <u>R P L Q E H</u>CCGTCAACACCAACGGGCTAG ...P V N T N G L
AGR18	ATTCCCGGGCAGGGCCGTGCG... N <u>S R A G P C</u>GGGGTGAGGCGGCCGCATCGTG V R R P H R
AGR19	ATTCCCGGGCAGGGCCGTGCG... N <u>S R A G P C</u>CCGTCAACACCAACGGGCTAG ...P V N T N G L

controls and purified human agrin as positive control, were coated during 16 h at 4°C in ELISA wells. Subsequently the wells were blocked with BSA for 1 h at 22°C, incubated with hybridoma supernatants (diluted 1:5 in PBS containing 0.2% Tween-20) for 1 h at 22°C. After washing 5 times with the same buffer, bound antibody was detected following standard methods using peroxidase conjugates [32].

Protease inhibition assays

The capability of human kidney agrin and recombinant agrin fragments to inhibit the activity of various proteases was investigated as follows. Reaction mixtures containing fluorogenic protease substrates were incubated with the corresponding protease and the potential inhibitor. Unless otherwise indicated, reactions were performed at 37°C in PBS containing 0.01% BSA

and liberated fluorescent product was measured at $\lambda_{\text{ex}}=340$ nm and $\lambda_{\text{em}}=440$ nm. The proteases and their substrates used were: trypsin from porcine pancreas (ICN) was incubated at a final concentration of 10 USP/ml with N α -benzoyl-L-Arg-7-AMC; elastase from porcine pancreas (Sigma) at 2.3 $\mu\text{g/ml}$ with N-succinyl-Ala-Pro-Ala-7-AMC at 25°C; collagenase type 2 (Worthington Biochemical Corp., Freehold, New Jersey, USA) with 7-MCA-Pro-Leu-Gly-Leu- β -(2,4-dinitrophenylamino)-Ala-Ala-Arg-amide in PBS containing 0.01% BSA and 1 mM CaCl₂ at $\lambda_{\text{ex}}=328$ and $\lambda_{\text{em}}=393$ nm, plasmin from porcine blood (Sigma) at 0.8 $\mu\text{g/ml}$ with Ala-Phe-Lys-7-AMC at 25°C, urokinase from human kidney cells (Sigma) with the same substrate as plasmin, and angiotensin converting enzyme (Sigma) at 3.7 mU/ml with *o*-aminobenzoyl-Gly-p-nitro-Phe-Pro in 100 mM Tris pH 8.3, 300 mM NaCl and 10 μM ZnSO₄ at $\lambda_{\text{ex}}=360$ and $\lambda_{\text{em}}=410$ nm. The aminopeptidase M substrate L-Leu-7-AMC (Sigma; at 25°C) and the renin substrate N-succinyl-Arg-Pro-Phe-His-Leu-Leu-7-AMC were incubated with crude kidney cortex extract, depleted of endogenous HSPG by anion exchange chromatography on a DEAE column in 50 mM Tris pH 6.8 containing 140 mM NaCl (the flow-through is devoid of HSPG). Reactions were allowed to proceed for 1 to 3 h (depending on the protease) in presence or absence of potential inhibitors. Full activity was defined as the amount of fluorescence units generated in absence of inhibitors. Zero activity was defined as the fluorescence after incubation in absence of protease. As potential inhibitors we added the peptides AGR3–AGR9 and purified agrin, and as a control GST. To allow mutual comparison the reaction volume was kept constant, all reactions were kept on ice during pipetting and mixing, and protease/substrate reaction mix was added from a single “master mix” to equal volumes of the potential inhibitors.

Localization of laminin-associated binding sites for agrin

The recombinant fusion protein AGR1 that contains the laminin-binding domain was used to visualize the distribution of laminin isoforms that may function as agrin binding sites. Cryosections from human kidney cortex tissue and coverslips with confluent glomerular cell monolayers were incubated with affinity-purified AGR1 (diluted to 200 $\mu\text{g/ml}$ in PBS) for 2 h at 22°C. No fixatives were used. After washing 3 times for 5 min with PBS, the sections and monolayers were incubated with the anti-GST mAb (hybridoma supernatant diluted 5-fold in PBS). This mAb does not produce endogenous staining of the sections or cells. After 1 h at 22°C and washing as above, the sections and monolayers were incubated for 1 h with a FITC-conjugated goat-anti-mouse antiserum (Dakopatts, Copenhagen, Denmark), washed again, mounted in Vectashield mounting medium (Brunschwig, Amsterdam, The Netherlands), and analyzed on a Leitz fluorescence microscope. To ensure the specificity of the observed binding we replaced the fusion protein by GST purified from the identical host strain carrying the parental plasmid. In another parallel control experiment, we omitted the primary antibody in the procedure. Furthermore we checked that binding could be inhibited by competition with soluble laminin (isolated from human placenta, Sigma, St. Louis, USA), which was mixed with the fusion protein at a final concentration of 200 $\mu\text{g/ml}$.

Primary culture of glomerular cells

Human glomerular endothelial cells (HGEC) were taken into primary culture as described in detail elsewhere [33]. In short, glomeruli were obtained from human cortex tissue by gradual sieving under sterile conditions. Endothelial cells were isolated from collagenase-digested glomeruli and cultured on gelatin-coated wells in M199 medium (Biowithaker, MD, USA) supplemented with 10% newborn calf serum (Gibco, Grand Island, NY, USA), 10% human serum (local bloodbank), 2 mM glutamine (ICN Biomedicals, Zoetermeer, The Netherlands), 100 U/ml penicillin, 100 mg/l streptomycin, 5 U/ml heparin (Leo Pharmaceuticals, Weesp, The Netherlands) and 150 mg/l crude endothelial cell growth factor from bovine brain [34]. Endothelial origin and purity of the cells was ascertained by a fenestrated morphology, the

presence of PECAM-1, C3b receptor, EN-4 antigen, V,E-cadherin, and Von Willebrand factor and the absence of α -smooth muscle actin and cytokeratin-8 [33].

Human podocytes were cultured from isolated glomeruli according to described procedures [35–37]. The culture medium was DMEM (Seromed Biochrom K.G., Berlin, Germany) with 15 mM HEPES (Sigma), 20% fetal calf serum (Hyclone Laboratories, Logan, UT, USA), and 100 U/ml penicillin and 100 mg/l streptomycin (Gibco). Identity and purity of the cells were confirmed by the presence of cytokeratin, CD10, TN10, BA-1, BA-2, J5 and the extracellular matrix components collagen type IV, fibronectin, laminin and HSPG. The Von Willebrand factor, TN9, C3b receptor, desmin, and collagen types I and III were absent as expected for podocytes. The cells also developed interdigitating microvilli, reminiscent of foot process structures [35, 36]. Both HGEC and podocytes were seeded onto gelatin-coated glass coverslips in 12-wells plates (Costar, Cambridge, MA, USA) and cultured for 8 days to allow the production of an extracellular matrix. The confluent monolayers were subjected to conventional immunofluorescence microscopy [32] and agrin-binding assays without the use of fixatives.

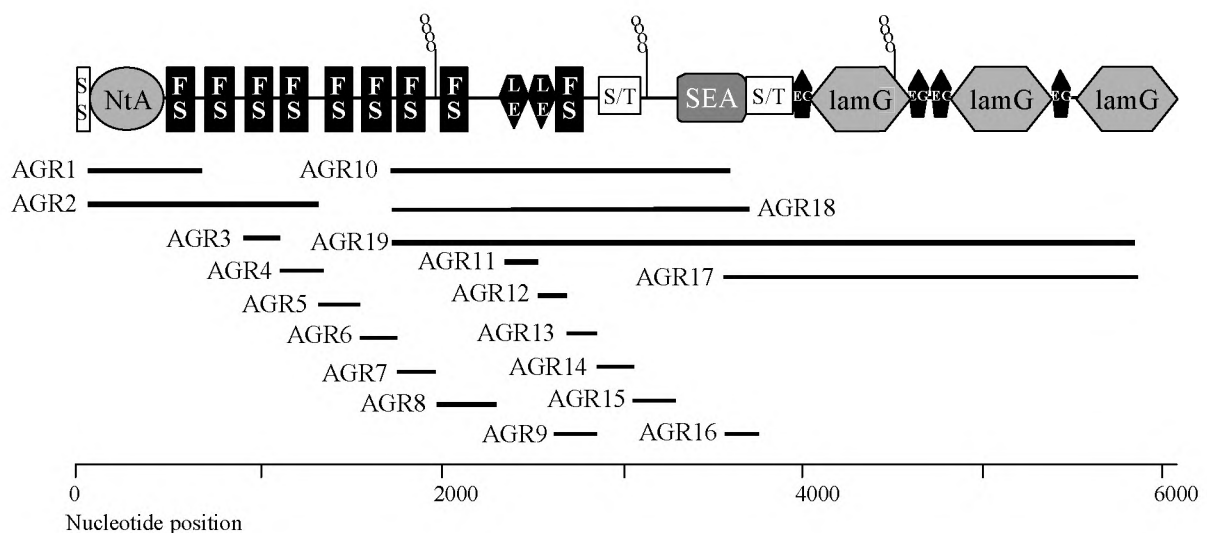


Figure 1: Schematic alignment of the fragments of human agrin produced as recombinant fusion proteins with full-length human agrin cDNA. SS: signal sequence; NtA: N-terminal agrin (laminin-binding) domain; FS: follistatin-like module; LE: laminin-III-like EGF repeat; S/T: serine/threonine-rich module; SEA: module first found in sperm protein, enterokinase and agrin; EG: EGF-like repeat; lamG: laminin-G-like module. The exact borders of each fragment are defined in Table 1.

RESULTS

Production of recombinant fragments of human agrin

An array of hybrid recombinant proteins was designed that consisted of GST from *S. japonicum* on the N-terminus and different fragments of human agrin on the C-terminal side. An overview of the produced fusion proteins is shown in Figure 1, and the exact borders of each clone are defined in Table 1. The fused GST polypeptide provides a tag for affinity purification. To characterize the recombinant fusion proteins, we first checked their cellular localization in small-scale pilot cultures. Fourteen fragments (the smaller ones) were synthesized in abundant amounts in the cytoplasm. Especially the larger fragments (AGR2, -10, -17, -18 and -19) accumulated in inclusion bodies, indicating that they were insoluble under the used conditions. Consistent with previous reports [30] their solubility was much

higher after biosynthesis at 30°C, allowing purification of the fusion proteins from the cell lysates.

The affinity-purified fusion proteins were analyzed by SDS-PAGE and their apparent molecular mass was compared with predicted values. Most fusion proteins migrated with the expected mobility compared to GST and to each other (Figure 2). In general, short fragments were more stable and displayed a major band at the expected height (e.g. AGR1, -4, -5, -6, -8, -9, -11, -13 and -15). Few relatively short fusion protein produced multiple bands, including AGR3, -6, -14 and -16. Larger fusion proteins were generally less stable and produced multiple additional bands (e.g. AGR2, -10, -17, -18 and -19). The additional bands were recognized by an anti-GST mAb in Western blot experiments, indicating that they represent degradation products of the full-length fusion proteins (data not shown). The functional and immunological analyses described in this study were performed with these preparations of affinity-purified fusion proteins.

Epitope localization of anti-agrin monoclonal antibodies

In a previous investigation, our laboratories generated a large panel of mAbs against HSPG isolated from the human GBM and TBM [21, 22]. Since agrin was recently identified as a predominant HSPG of the GBM [28], we analyzed if these antibodies recognized human agrin. Each mAb was screened for immunoreactivity towards the different recombinant fusion proteins in ELISA (Table 2). In this way, epitopes were mapped on regions of the core protein of human agrin. The central region of the molecule (AGR 9, -12 and -13) appeared to be especially immunogenic in mice. Also the N-terminal region contained epitopes recognized by this panel of antibodies, including the fragment AGR1 that was recognized by HAM-1. In contrast to this, no epitopes could be mapped in the C-terminal region included in AGR17. The reactivity of the mAbs raised against HSPG from the GBM and TBM with the

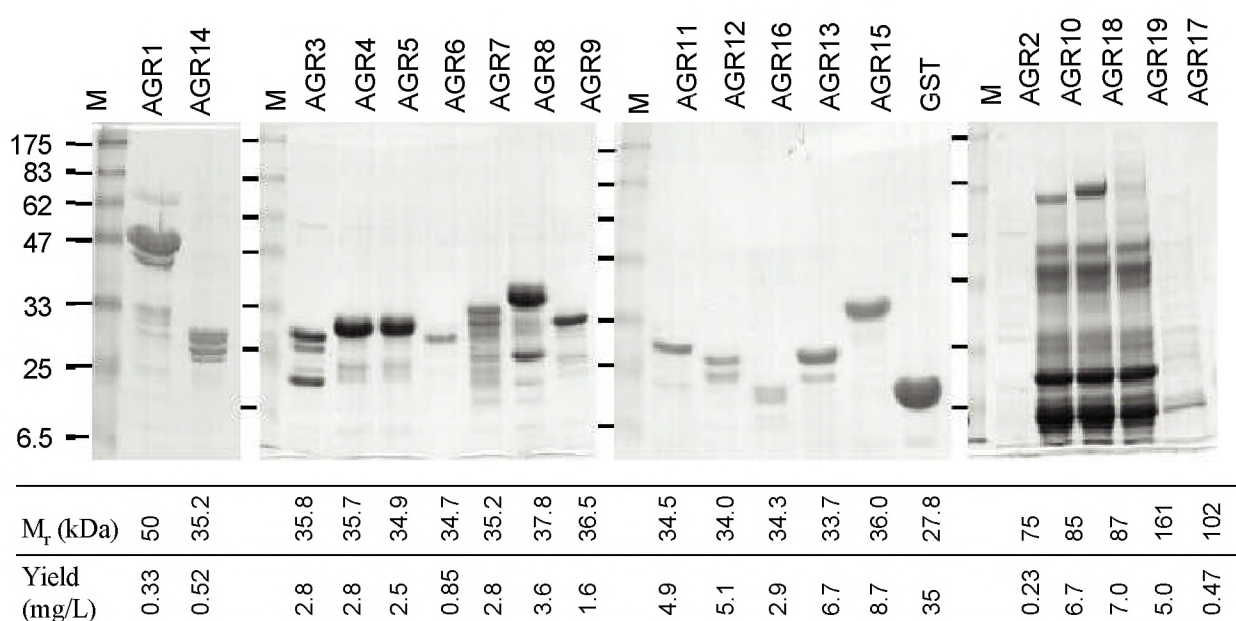


Figure 2: SDS-PAGE of recombinant fusion proteins and staining by Coomassie Brilliant Blue. Molecular mass markers are specified on the left (the 6.5 kDa marker is not present in the gel fragment shown on the right). The predicted molecular mass (in kDa) and obtained yield (in mg fusion protein per L of culture) are given for each fusion protein on the bottom.

recombinant fusion proteins confirms unequivocally that they are directed to the core protein of agrin.

Table 2: Immunoreactivity of monoclonal antibodies with recombinant fragments of human agrin in ELISA. To check the specificity of the mAbs, bovine serum albumin (BSA) and GST were included as negative controls. Purified agrin from human glomerular basement membranes was included as a positive control. ¹⁾ In case multiple overlapping fusion proteins were recognized, the smallest and therefore most informative fragment is given. ²⁾ Background signal was calculated as the mean optical density of all fragments that do not overlap the recognized fusion protein. ³⁾ Besides AGR9 this antibody also recognized AGR13, indicating that the epitope is located within the overlap of these fragments. ⁴⁾ Besides AGR9 this antibody also recognized AGR12, indicating that the epitope is located within the overlap of these fragments.

	BSA OD ⁴⁹²	GST OD ⁴⁹²	Agrin OD ⁴⁹²	Recognized fusion protein OD ⁴⁹²	Recognized fusion protein name ¹⁾	Background (mean ± SD) ²⁾ OD ⁴⁹²
HAM1	0.04	0.08	1.43	0.49	AGR1	0.08 ± 0.01
HAM2	0.04	0.05	0.85	2.67	AGR9 ³⁾	0.05 ± 0.01
HAM3	0.05	0.04	0.50	1.38	AGR10	0.06 ± 0.01
HAM4	0.04	0.04	1.76	3.20	AGR9 ³⁾	0.09 ± 0.15
HAM5	0.08	0.28	1.69	2.91	AGR9 ⁴⁾	0.21 ± 0.12
HAM6	0.05	0.06	1.75	3.52	AGR12	0.09 ± 0.06
HAM7	0.05	0.04	0.73	0.88	AGR15	0.05 ± 0.01
HAM8	0.04	0.04	0.97	0.27	AGR3	0.04 ± 0.01
HAM9	0.05	0.05	1.31	2.25	AGR12	0.05 ± 0.01
HAM10	0.06	0.06	0.66	1.20	AGR15	0.07 ± 0.03
HAM11	0.04	0.05	0.79	2.76	AGR9 ³⁾	0.05 ± 0.00
HAM12	0.12	0.06	0.86	2.58	AGR6	0.18 ± 0.34
HAM13	0.05	0.05	1.62	2.50	AGR9 ³⁾	0.13 ± 0.28
HAM14	0.04	0.05	1.98	1.25	AGR9 ³⁾	0.07 ± 0.02
HAM15	0.05	0.11	1.34	3.49	AGR10	0.15 ± 0.04
HAM16	0.04	0.05	1.17	0.80	AGR3	0.05 ± 0.01
HAM17	0.04	0.05	1.16	2.61	AGR9 ³⁾	0.05 ± 0.01
HAM18	0.04	0.05	1.08	3.04	AGR9 ³⁾	0.05 ± 0.01
HAM19	0.04	0.04	1.47	0.70	AGR3	0.07 ± 0.07
HAM20	0.04	0.04	0.91	2.87	AGR19	0.05 ± 0.02
HAM21	0.05	0.11	1.55	3.01	AGR10	0.12 ± 0.04
HAM22	0.04	0.05	1.62	0.18	AGR9 ³⁾	0.05 ± 0.01
HAM23	0.05	0.05	0.42	0.20	AGR10	0.07 ± 0.02
HAM24	0.07	0.08	1.11	2.58	AGR10	0.09 ± 0.04
HAM25	0.05	0.05	1.07	2.68	AGR9 ³⁾	0.04 ± 0.01
anti-GST	0.05	2.88	0.05			

Protease inhibition by individual follistatin-like domains

Based on primary structure predictions, the nine follistatin-like domains of the agrin molecule may function as protease inhibitors. Different concentrations of agrin purified from human kidney were tested for their ability to inhibit various proteolytic enzymes. We observed a dose-dependent inhibition of trypsin, plasmin and elastase activity (Figure 3). Collagenase, urokinase, renin, aminopeptidase M and the angiotensin converting enzyme were not inhibited (data not shown). To investigate protease-inhibiting functions in a domain-specific manner,

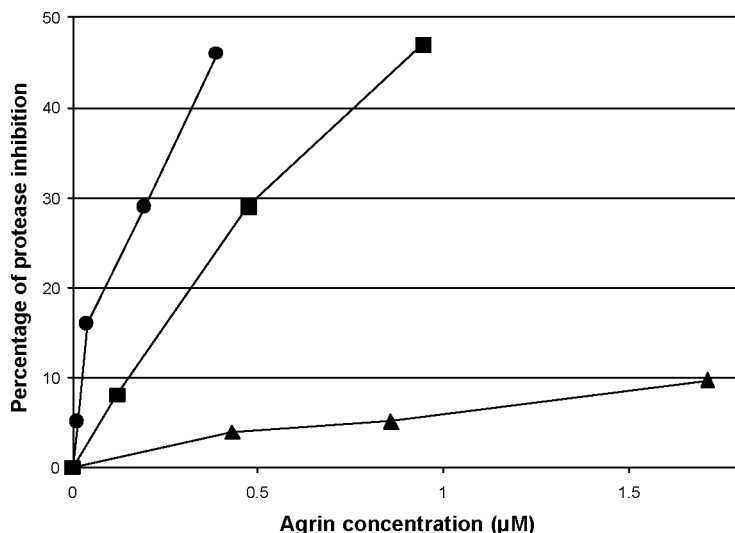


Figure 3: Protease inhibitory activity of agrin purified from human kidney. The decrease of protease activity is given as a percentage of the activity in absence of agrin. A dose-dependent inhibition of trypsin (circles), plasmin (squares) and elastase activity (triangles) was observed.

we next used the fusion proteins AGR3–AGR9 as potential inhibitors. For plasmin, the fusion protein AGR5 that contains the fifth follistatin-like domain displayed the highest inhibitory activity (data not shown). Other fragments did not cause inhibition. To achieve a plasmin inhibition of 5% the required concentration of AGR5 was 3.8 μM , whereas agrin was required at 0.08 μM . This difference could suggest an involvement of additional domains in plasmin inhibition, or a different tertiary structure of the recombinant fragment. For trypsin and elastase, the inhibitory effect could not be assigned to a distinct domain by this procedure.

Agtrin expression by glomerular cells in primary culture

Since agrin is expressed in the GBM along the full length of the capillary loops (Figure 4a), it is likely synthesized by either glomerular endothelial cells, podocytes, or both. To investigate the precise cellular origin of agrin, we used primary cultures of both cell types from human kidneys. A high purity and well-differentiated state of the two cell types was ascertained [33, 35, 36]. Cells grown to confluence produce an extracellular matrix, and we investigated the presence of agrin-like antigenicity herein by indirect immunofluorescence staining with the anti-agrin mAb HAM-6. This antibody recognizes fragment AGR12, located in the central region of the agrin core protein (Table 2). Podocytes produced readily detectable amounts of agrin (Figure 4b and c). In areas of relatively high cell density, large fibrillar structures were observed that stained strongly with mAb HAM-6. Antibodies directed towards other regions of the molecule (HAM-1, -5, -13 and -20) produced similar staining patterns (data not shown). Endothelial cells did not produce detectable amounts of agrin (data not shown). Despite this, they produced an extracellular matrix with binding sites for agrin as described below. The data suggest that podocytes are the main source of agrin in the GBM.

The GBM contains functional binding sites for fragment AGR1

Agtrin was demonstrated to bind laminin, and this interaction may be important for the immobilization of the proteoglycan within basement membranes [13]. We investigated if agrin-laminin binding also occurs in the GBM. To visualize the distribution of functional agrin-binding sites in the glomerulus we used the recombinant fusion protein AGR1. This fragment contains the laminin-binding domain, and showed affinity to laminin in ELISA (data

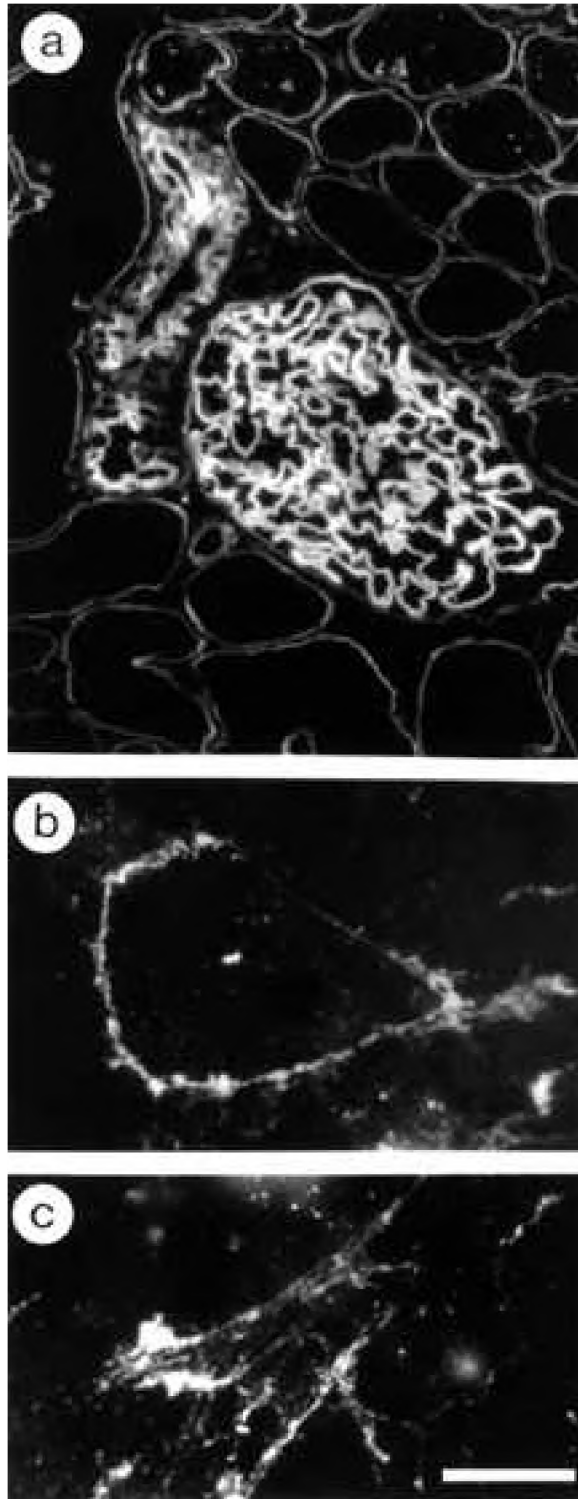


Figure 4: Immunofluorescence staining of agrin using the mAb HAM-6. *a*: On cryosections of human kidney cortex. *b* and *c*: On monolayers of human podocytes in primary culture (two typical areas are shown). Bar, 50 μ m.

not shown). The GST tag was used to detect binding. In this way we localized the binding sites for AGR1 in cryosections from human kidney cortex tissue, monolayers of human podocytes, and monolayers of human glomerular endothelial cells. In kidney cortex, AGR1 binding was detected in the GBM and the peritubular capillary walls (Figure 5*a*). Tubular basement membranes were also weakly stained. When soluble laminin from human placenta was added as a competitor, binding of the fusion protein was markedly reduced (Figure 5*b*). As a control, GST alone did not bind to renal cortex tissue (Figure 5*c*). The extracellular matrix produced by cultured human podocytes also contained binding sites for AGR1 (Figure 5*d-f*). The observed staining was more irregular than that of endothelial cells. In addition to a fibrillar staining of the extracellular matrix juxtaposing most cells (Figure 5*d*), some regions of the monolayers were covered with strongly stained sheet-like or fibrillar structures (arrowhead in Figure 5*d*, and Figure 5*e-f*). On cultured human endothelial cells, the AGR1-binding assay yielded an intense fluorescence in the extracellular matrix, following a granular and homogeneous pattern (Figure 5*g-h*). The cell membrane and cytoplasm were not stained. Again, incubation with GST as a control did not produce any staining (Figure 5*i*). In conclusion, the results demonstrate that the GBM contains laminin isoforms that bind agrin. These laminins are presumably produced by both the endothelial and visceral epithelial cell layer.

DISCUSSION

In this study we described the epitope localization of the first available mAbs known to recognize human agrin. The antibodies recognize both native (on tissue) and denatured (isolated) agrin, indicating that they bind linear epitopes rather than tertiary structures. The scattered epitope distribution enables to detect differences in the domain organization of agrin in different tissues.

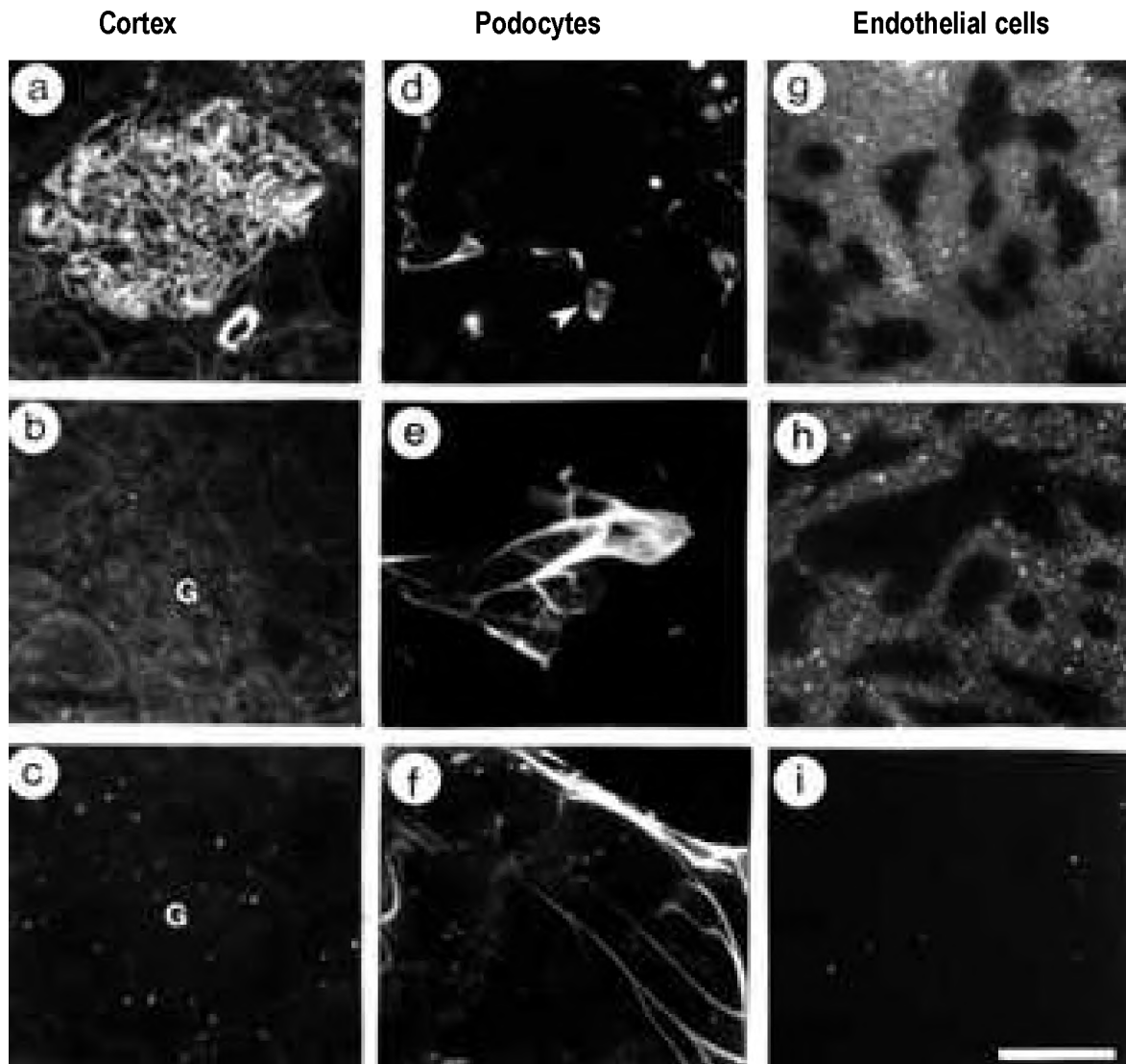


Figure 5: Detection of binding sites for the fusion protein AGR1 that contains the laminin-binding domain of human agrin. *a-c*: in human kidney cortex cryosections; *d-f*: on monolayers of human podocytes in primary culture; *g-i*: on monolayers of human glomerular endothelial cells in primary culture. *a*: In cryosections of human kidney cortex, AGR1 binds to the glomerular capillary wall and the basement membrane of renal venules. *b*: Same as *a*, but by addition of purified laminin as a competitor the staining was considerably reduced (G indicates a glomerulus). *c*: Same as *a*, but AGR1 was replaced by GST as a control. *d*: AGR1 binds to the extracellular matrix of podocytes in culture in a fibrillar pattern. In some regions this pattern assumes a sheet-like appearance (arrowhead). *e, f*: Same as *d*, illustrating two typical sheet-like structures in the podocytes extracellular matrix with binding sites for AGR1. *g, h*: In the extracellular matrix produced by glomerular endothelial cells in culture, AGR1 binds in a homogeneous granular pattern surrounding the cells. Two typical examples are shown. *i*: Same procedure and exposure as *g*, but with GST as a control. Bar = 50 μm .

For example, truncated agrin isoforms that lack a C-terminal region of the molecule were described to occur in the TBM [38]. Consistent with this, the mAbs used in this study reacted mostly with N-terminal and central regions of agrin.

Some of the mapped antibodies were applied in previous investigations in ignorance of the identity of the antigen. First, HAM-21 that recognizes AGR10 was shown to intensely stain the GBM in a linear homogeneous way by immunofluorescence microscopy [23]. The assumption that the involved antigen was agrin, is convincingly affirmed by the present results. Second, HAM-15 that also recognizes AGR10 was previously shown to stain the amyloid deposits in AL and AA amyloidosis with increased intensity [39]. Also the expanded mesangial matrix in focal segmental glomerulosclerosis, lupus nephritis, IgA nephropathy and membranoproliferative nephritis appears to produce increased amounts of agrin [39]. Moreover, the staining of glomerular capillaries by HAM-15 was previously reported to decrease under diabetic conditions [40]. The localization of the corresponding epitope on the central region of the agrin core protein places these results in a new perspective. Agrin may contribute to the decrease of GBM-HSPG known to occur in diabetic nephropathy [41–43]. In the future we will investigate agrin's role in the pathogenic mechanism of this diabetic complication in more detail.

Although purified agrin markedly inhibits trypsin activity in accordance with previous results [19], we could not allocate this action to distinct follistatin-like domains. The trypsin- and elastase-inhibiting activity could be associated with other or multiple regions of the agrin molecule. Alternatively, the inhibitory activities of individual domains may be underestimated or missed in this study due to limitations of the prokaryotic expression system. This may also explain the relatively low plasmin-inhibitory activity of the recombinant fusion protein AGR5 compared with agrin purified *ex vivo*. The specificity of the observed inhibition was confirmed by parallel controls, including GST purified by the same procedure and from the same host strain. We avoided the use of protease inhibitors during purification of the fusion proteins. Thus, we ascertained that the observed inhibition of plasmin by AGR5 is specific.

The distribution of agrin in the matrix of cultured podocytes resembles that of laminin [35]. The finding that agrin is produced by podocytes, but not endothelial cells is analogous to the expression pattern of perlecan. This HSPG, expressed in the GBM at a lower level than agrin was also shown to originate exclusively from podocytes [44]. This is in line with the general idea that podocytes contribute for a large part to GBM synthesis. Only a few exceptions were reported, e.g. nidogen is synthesized by all glomerular cell types [44]. The epithelial origin of agrin in the GBM further strengthens the established opinion that podocytes play a major role in the maintenance of the glomerular charge-selective ultrafiltration barrier. The majority of heparitinase-degradable polyanionic sites resides in the lamina rara externa of the GBM [42], and detachment of the podocyte foot processes from the GBM augments permeability for macromolecules [45, 46]. Our data suggest that podocytes are also primarily responsible for the production of HSPGs of the GBM.

Whereas agrin was previously shown to bind laminin-1 ($\alpha 1\beta 1\gamma 1$), -2 ($\alpha 2\beta 1\gamma 1$) and -4 ($\alpha 2\beta 2\gamma 1$), the GBM is particularly rich in laminin-11 ($\alpha 5\beta 2\gamma 1$) [3, 13, 47]. The interaction of the fusion protein AGR1 with the matrix produced by glomerular cells and the GBM *in vivo* demonstrates, that binding to laminin also occurs in the kidney. In addition to its affinity for laminin, renal agrin also interacts with α -dystroglycan, a peripheral cell surface glycoprotein that is associated with the dystrophin-associated glycoprotein complex [48, 49]. The splice composition of human kidney agrin supports α -dystroglycan binding in a heparin-independent way [28, 50, 51]. α -Dystroglycan was shown to be present in the epithelium of the developing nephron and remains present in the mature glomerular basement membrane [52]. Co-purification and co-immunoprecipitation of α -dystroglycan with kidney agrin showed that both components interact with high affinity [17]. Together there is now substantial experimental evidence that renal agrin forms a link between the cytoskeleton (via α -dystroglycan) and the GBM (via laminin).

In summary, the functions of agrin in the GBM appear to be manifold. Agrin contributes to the polyanionic charge of the glomerular ultrafiltration barrier, and we have identified podocytes as its primary cellular source. The anchorage of agrin within the GBM via its N-terminus suggests a potential role in cell-matrix interaction. The functional properties of agrin in the GBM should be analyzed in more detail. Of special interest is the interaction between agrin and α -dystroglycan, which may trigger intracellular signals in the podocyte. The availability of the cDNA clones, fusion proteins and region-specific mAbs presented in this study facilitate new approaches for this purpose. Furthermore, the possible involvement of agrin in various nephropathies associated with a decreased anionic charge of the GBM may be investigated.

ACKNOWLEDGEMENTS

This study was supported by grant C93.1309 from the Dutch Kidney Foundation and grant NWO/DFN940-10-009. The laboratory participated in the concerted action "Alterations in extracellular matrix components in diabetic nephropathy and other glomerular diseases", which is financially supported by the European Community with the Biomed I program (BMH1-CT92-1766). We acknowledge Dr. P.A. van Setten and Drs. M. te Loo for expert assistance in endothelial cell culture.

REFERENCES

1. Tsen G, Halfter W, Kroger S and Cole GJ (1995) Agrin is a heparan sulfate proteoglycan, *J. Biol. Chem.* 270: 3392–3399.
2. Cole GJ and Halfter W (1996) Agrin: an extracellular matrix heparan sulfate proteoglycan involved in cell interactions and synaptogenesis, *Perspect. Dev. Neurobiol.* 3: 359–371.
3. Denzer AJ, Brandenberger R, Gesemann M, Chiquet M and Ruegg MA (1997) Agrin binds to the nerve-muscle basal lamina via laminin, *J. Cell Biol.* 137: 671–683.
4. Glass DJ and Yancopoulos GD (1997) Sequential roles of agrin, MuSK and rapsyn during neuromuscular junction formation, *Curr. Opin. Neurobiol.* 7: 379–384.
5. Meier T, Masciulli F, Moore C, Schoumacher F, Eppenberger U, Denzer AJ, Jones G and Brenner HR (1998) Agrin can mediate acetylcholine receptor gene expression in muscle by aggregation of muscle-derived neuregulins, *J. Cell Biol.* 141: 715–726.
6. Ruegg MA and Bixby JL (1998) Agrin orchestrates synaptic differentiation at the vertebrate neuromuscular junction, *Trends. Neurosci.* 21: 22–27.
7. Gesemann M, Denzer AJ and Ruegg MA (1995) Acetylcholine receptor-aggregating activity of agrin isoforms and mapping of the active site, *J. Cell Biol.* 128: 625–636.
8. Gautam M, Noakes PG, Moscoso L, Rupp F, Scheller RH, Merlie JP and Sanes JR (1996) Defective neuromuscular synaptogenesis in agrin-deficient mutant mice, *Cell* 85: 525–535.
9. Cohen I, Rimer M, Lomo T and McMahan UJ (1997) Agrin-induced postsynaptic-like apparatus in skeletal muscle fibers *in vivo*, *Mol. Cell Neurosci.* 9: 237–253.
10. Meier T, Hauser DM, Chiquet M, Landmann L, Ruegg MA and Brenner HR (1997) Neural agrin induces ectopic postsynaptic specializations in innervated muscle fibers, *J. Neurosci.* 17: 6534–6544.
11. Campagna JA, Ruegg MA and Bixby JL (1997) Evidence that agrin directly influences presynaptic differentiation at neuromuscular junctions *in vitro*, *Eur. J. Neurosci.* 9: 2269–2283.
12. Denzer AJ, Gesemann M, Schumacher B and Ruegg MA (1995) An amino-terminal extension is required for the secretion of chick agrin and its binding to extracellular matrix, *J. Cell Biol.* 131: 1547–1560.
13. Denzer AJ, Schulthess T, Fauser C, Schumacher B, Kammerer RA, Engel J and Ruegg MA (1998) Electron microscopic structure of agrin and mapping of its binding site in laminin-1, *EMBO J.* 17: 335–343.
14. Gee SH, Montanaro F, Lindenbaum MH and Carbonetto S (1994) Dystroglycan- α , a dystrophin-associated glycoprotein, is a functional agrin receptor, *Cell* 77: 675–686.
15. Hopf C and Hoch W (1996) Agrin binding to

- α -dystroglycan. Domains of agrin necessary to induce acetylcholine receptor clustering are overlapping but not identical to the α -dystroglycan-binding region, *J. Biol. Chem.* 271: 5231–5236.
16. Meier T, Gesemann M, Cavalli V, Ruegg MA and Wallace BG (1996) AChR phosphorylation and aggregation induced by an agrin fragment that lacks the binding domain for α -dystroglycan, *EMBO J.* 15: 2625–2631.
 17. Gesemann M, Brancaccio A, Schumacher B and Ruegg MA (1998) Agrin is a high-affinity binding protein of dystroglycan in non-muscle tissue, *J. Biol. Chem.* 273: 600–605.
 18. Godfrey EW (1991) Comparison of agrin-like proteins from the extracellular matrix of chicken kidney and muscle with neural agrin, a synapse organizing protein, *Exp. Cell Res.* 195: 99–109.
 19. Biroc SL, Payan DG and Fisher JM (1993) Isoforms of agrin are widely expressed in the developing rat and may function as protease inhibitors, *Brain Res. Dev. Brain Res.* 75: 119–129.
 20. Barber AJ and Lieth E (1997) Agrin accumulates in the brain microvascular basal lamina during development of the blood-brain barrier, *Dev. Dyn.* 208: 62–74.
 21. Van den Heuvel LP, Van den Born J, Veerkamp JH, Van de Velden TJ, Schenkels L, Monnens LA, Schröder CH and Berden JH (1990) Heparan sulfate proteoglycan from human tubular basement membrane. Comparison with this component from the glomerular basement membrane, *Biochim. Biophys. Acta* 1025: 67–76.
 22. Van den Born J, Van den Heuvel LP, Bakker MA, Veerkamp JH, Assmann KJ and Berden JH (1994) Monoclonal antibodies against the protein core and glycosaminoglycan side chain of glomerular basement membrane heparan sulfate proteoglycan: characterization and immunohistological application in human tissues, *J. Histochem. Cytochem.* 42: 89–102.
 23. Groffen AJ, Ruegg MA, Dijkman H, Van de Velden TJ, Buskens CA, Van den Born J, Assmann KJ, Monnens LA, Veerkamp JH and Van den Heuvel LP (1998) Agrin is a major heparan sulfate proteoglycan in the human glomerular basement membrane, *J. Histochem. Cytochem.* 46: 19–27.
 24. Kanwar YS, Linker A and MG Farquhar (1980) Increased permeability of the glomerular basement membrane to ferritin after removal of glycosaminoglycans (heparan sulfate) by enzyme digestion, *J. Cell Biol.* 86: 688–693.
 25. Rosenzweig LJ and Kanwar YS (1982) Removal of sulfated (heparan sulfate) or nonsulfated (hyaluronic acid) glycosaminoglycans results in increased permeability of the glomerular basement membrane to 125 I-bovine serum albumin, *Lab. Invest.* 47: 177–184.
 26. Kanwar YS, Liu ZZ, Kashihara N and Wallner EI (1991) Current status of the structural and functional basis of glomerular filtration and proteinuria, *Semin. Nephrol.* 11: 390–413.
 27. Van den Born J, Van den Heuvel LP, Bakker MA, Veerkamp JH, Assmann KJ and Berden JH (1992) A monoclonal antibody against GBM heparan sulfate induces an acute selective proteinuria in rats, *Kidney Int.* 41: 115–123.
 28. Groffen AJ, Buskens CA, Van Kuppevelt TH, Veerkamp JH, Monnens LA and Van den Heuvel LP (1998) Primary structure and high expression of human agrin in basement membranes of adult lung and kidney, *Eur. J. Biochem.* 254: 123–128.
 29. Groffen AJ, Hop FW, Tryggvason K, Dijkman H, Assmann KJ, Veerkamp JH, Monnens LA and Van den Heuvel LP (1997) Evidence for the existence of multiple heparan sulfate proteoglycans in the human glomerular basement membrane and mesangial matrix, *Eur. J. Biochem.* 247: 175–182.
 30. Schein CH and Noteborn MH (1988) Formation of soluble recombinant proteins in *Escherichia coli* is favored by lower growth temperature, *Biotechnol.* 6: 291–294.
 31. Bjellqvist B, Basse B, Olsen E and Celis JE (1994) Reference points for comparisons of two-dimensional maps of proteins from different human cell types defined in a pH scale where isoelectric points correlate with polypeptide compositions, *Electrophoresis* 15: 529–539.
 32. Harlow E and Lane D (1988) Antibodies, a laboratory manual. Cold Spring Harbor Laboratory Press, Cold Spring Harbor, NY.
 33. Van Setten PA, Van Hinsbergh VW, Van der Velden TJ, Van de Kar NC, Vermeer M, Mahan JD, Assmann KJ, Van den Heuvel LP and Monnens LA (1997) Effects of TNF α on verocytotoxin cytotoxicity in purified human glomerular microvascular endothelial cells, *Kidney Int.* 51: 1245–1256.
 34. Maciag T, Cerundolo J, Ilesley S, Kelley PR

- and Forand R (1979) An endothelial cell growth factor from bovine hypothalamus: identification and partial characterization, *Proc. Natl. Acad. Sci. USA* 76: 5674–5678.
35. Van der Woude FJ, Michael AF, Muller E, Van der Hem GK, Vernier RL and Kim Y (1989) Lymphohaemopoietic antigens of cultured human glomerular epithelial cells, *Br. J. Exp. Path.* 70: 73–82.
 36. Van Det NF, Van den Born J, Tamsma JT, Verhagen NA, Van den Heuvel LP, Berden JH, Bruijn JA, Daha MR and Van der Woude FJ (1995) Proteoglycan production by human glomerular visceral epithelial cells and mesangial cells *in vitro*, *Biochem. J.* 307: 759–768.
 37. Van Det NF, Verhagen NA, Tamsma JT, Berden JH, Bruijn JA, Daha MR and Van der Woude FJ (1997) Regulation of glomerular epithelial cell production of fibronectin and transforming growth factor- β by high glucose, not by angiotensin II, *Diabetes*.46: 834–840.
 38. Raats CJ, Bakker MA, Hoch W, Tamboer WP, Groffen AJ, Van den Heuvel LP, Berden JH and Van den Born J (1998) Differential expression of agrin in renal basement membranes as revealed by domain-specific antibodies, *J. Biol. Chem.* 273: 17832–17838.
 39. Van den Born J, Van den Heuvel LP, Bakker MA, Veerkamp JH, Assmann KJ, Weening JJ and Berden JH (1993) Distribution of GBM heparan sulfate proteoglycan core protein and side chains in human glomerular diseases, *Kidney Int.* 43: 454–463.
 40. Tamsma JT, Van den Born J, Bruijn JA, Assmann KJ, Weening JJ, Berden JH, Wieslander J, Schrama E, Hermans J and Veerkamp JH (1994) Expression of glomerular extracellular matrix components in human diabetic nephropathy: decrease of heparan sulphate in the glomerular basement membrane, *Diabetologia*.37: 313–320.
 41. Goode NP, Shires M, Crellin DM, Aparicio SR and Davison AM (1995) Alterations of glomerular basement membrane charge and structure in diabetic nephropathy, *Diabetologia*.38: 1455–1465.
 42. Van den Born J, Van Kraats AA, Bakker MA, Assmann KJ, Dijkman HB, Van der Laak JA and Berden JH (1995) Reduction of heparan sulphate-associated anionic sites in the glomerular basement membrane of rats with streptozotocin-induced diabetic nephropathy, *Diabetologia*.38: 1169–1175.
 43. Van der Woude FJ and Van Det NF (1997) Heparan sulphate proteoglycans and diabetic nephropathy, *Exp. Nephrol.* 5: 180–188.
 44. Lee LK, Pollock AS and Lovett DH (1993) Asymmetric origins of the mature glomerular basement membrane, *J. Cell. Physiol.* 157: 169–177.
 45. Kanwar YS and Rosenzweig LJ (1982) Altered glomerular permeability as a result of focal detachment of the visceral epithelium, *Kidney Int.* 21: 565–574.
 46. Laurens W, Battaglia C, Foglieni C, De Vos R, Malanchini B, Van Damme B, Vanrenterghem Y, Remuzzi G and Remuzzi A (1995) Direct podocyte damage in the single nephron leads to albuminuria *in vivo*, *Kidney Int.* 47: 1078–1086.
 47. Miner JH, Patton BL, Lentz SI, Gilbert DJ, Snider WD, Jenkins NA, Copeland NG and Sanes JR (1997) The laminin α chains: expression, developmental transitions, and chromosomal locations of α 1–5, identification of heterotrimeric laminins 8–11, and cloning of a novel α 3 isoform, *J. Cell Biol.* 137: 685–701.
 48. Deyst KA, Bowe MA, Leszyk JD and Fallon JR (1995) The α -dystroglycan- β -dystroglycan complex. Membrane organization and relationship to an agrin receptor, *J. Biol. Chem.* 270: 25956–25959.
 49. Matsumura K, Yamada H, Saito F, Sunada Y and Shimizu T (1997) The role of dystroglycan, a novel receptor of laminin and agrin, in cell differentiation, *Histol. Histopathol.* 12: 195–203.
 50. O'Toole JJ, Deyst KA, Bowe MA, Nastuk MA, McKechnie BA and Fallon JR (1996) Alternative splicing of agrin regulates its binding to heparin α -dystroglycan, and the cell surface, *Proc. Natl. Acad. Sci. U. S. A.* 93: 7369–7374.
 51. Gesemann M, Cavalli V, Denzer AJ, Brancaccio A, Schumacher B and Ruegg MA (1996) Alternative splicing of agrin alters its binding to heparin, dystroglycan, and the putative agrin receptor, *Neuron*.16: 755–767.
 52. Durbeej M, Henry MD, Ferletta M, Campbell KP and Ekblom P (1998) Distribution of dystroglycan in normal adult mouse tissues, *J. Histochem. Cytochem.* 46: 449–457.

CHAPTER EIGHT

Urinary excretion of basic fibroblast growth factor by nephrotic children with focal segmental glomerulosclerosis

Urinary excretion of basic fibroblast growth factor by nephrotic children with focal segmental glomerulosclerosis

CHAPTER EIGHT

SUMMARY The pathogenesis of focal segmental glomerulosclerosis (FSGS) is accompanied by hypertrophy of glomerular epithelial cells. Basic fibroblast growth factor (bFGF) was previously shown to induce podocyte mitogenesis and dedifferentiation in rats, resulting in a FSGS-like nephropathy (Kriz et al., *Kidney Int.* 48:1435, 1995). This study was designed to evaluate the relevance of this mechanism in the clinical pathogenesis of FSGS. Thirty-four subjects were categorized in four groups according to their diagnosis: FSGS (n=13), minimal change disease (MCD; n=10), other nephropathies (n=4) and healthy controls (n=7). Four patients with FSGS produced strongly increased urinary bFGF concentrations up to 11.6 ng/mmol creatinine, whereas other patients of this group had normal excretion levels. Marked increases were exclusively found in urine samples with >5 g/l protein. Interestingly, the urinary bFGF concentrations detected in FSGS correlated in a linear way with proteinuria (correlation coefficient 0.98). In MCD, less pronounced increases (up to 2.2 ng/mmol) were found in three cases. Subjects from other groups showed no significant increase in urinary bFGF levels. Serum bFGF levels were within normal range in all subjects. Tubular dysfunction, as indicated by increased urinary concentrations of retinol-binding protein, was encountered in a few subjects but did not correlate with bFGF excretion. In biopsies from patients with FSGS and MCD, increased bFGF immunoreactivity was present in the glomerulus, where it was primarily associated with the capillary loops and Bowman's capsule. Together the results suggest that increased bFGF concentrations in the glomerulus may contribute to the pathogenesis of FSGS in the human.

TO INDEX

INTRODUCTION

Focal segmental glomerulosclerosis (FSGS) is a histological appearance occurring in patients with nephrotic syndrome, characterized by partial sclerotic lesions in some but not all glomeruli [1,2]. Glomeruli in the juxtamedullary zone are more frequently affected. The sclerotic lesions often display hyalinosis (acellular accumulations of lipid and glycoprotein material) and contain IgM, C3 and C4 deposits. When the affected segments are analyzed by electron microscopy, the glomerular basement membrane shows a thickened and laminated morphology. Podocytes become detached and show effacement of the foot processes. The mesangial matrix is expanded, containing accumulated laminin and collagen IV deposits. Foam cells may also be present in the capillary lumen. The pathological mechanism that causes these changes is not understood. Recurrence of the disease in approximately 20-25% of renal allografts suggests the involvement of a circulating factor [1, 3]. A polymorphism in the gene encoding angiotensin-converting enzyme was suggested as a hereditary risk factor for FSGS [4].

Several experimental animal models for FSGS have been generated by procedures which include nephrectomy, administration of adriamycin and puromycin aminonucleoside (PAN)

[5-8]. A common hallmark in the progression of these experimental animals to FSGS is the observed hypertrophy of glomerular epithelial cells [9]. This hypertrophy might be an attempt to restore the glomerular structure after mechanical or inflammatory injury. Interestingly, long-term subcutaneous administration of basic fibroblast-growth factor (bFGF) also provokes the development of FSGS in rats [10]. In an attempt to proliferate, the podocytes undergo mitosis but fail to complete cell division. As a result, an increased number of bi- and multinucleated podocytes appears. Many dysmorphic features occur, including pseudocyst formation, cell body attenuation, effacement and detachment of the foot processes. Denuded regions of the glomerular basement membrane adhere to the parietal epithelium of Bowman's capsule. Thus, this bFGF-induced experimental nephropathy shows characteristic features of FSGS [10].

Basic FGF is mostly expressed as an 18 kDa peptide, but 16, 20, 22 and 24 kDa variants also occur [11-15]. Although bFGF does not contain a classical signal peptide for extracellular targeting, an unknown export mechanism may exist [16-19]. Cell injury also induces the release of biologically functional bFGF [20-22]. Extracellular bFGF is activated by heparan sulfate proteoglycans that are immobilized in the glomerular basement membrane, mesangial matrix and on the cell surface [13, 23-27]. After binding a dimer complex recognizes the high-affinity receptor and triggers signal transduction [14, 28]. The cellular response of bFGF greatly differs between cell types. Endothelial cells are stimulated to migrate and proliferate [17, 29, 30]. Podocytes were demonstrated to show a mitogenic response, associated with morphological changes that suggest dedifferentiation (pseudocyst formation, multinucleation, foot process retraction and focal detachment from the GBM) [31, 32]. This may relate to the fact that differentiated podocytes are not mitotic. Mesangial cells normally do not show a mitogenic response, but after injury bFGF induces an increased proliferation [12, 21, 33]. In the present study we detected elevated concentrations of bFGF in the urine of patients with FSGS associated with massive proteinuria. The data suggest a possible role for bFGF in the pathogenesis of FSGS in the human.

SUBJECTS AND METHODS

Subjects and sample collection

Patients were asked to participate in this study and parental consent was ascertained. In total 34 subjects were categorized in four groups according to their diagnosis. FSGS patients (n=13) had a mean age of 10.8 years in the range 1-20 at sample collection (Table 1). Of two FSGS patients a biopsy but no urine sample was available; these patients are listed in Table 2. Subjects with minimal change disease (MCD; n=10) had a mean age of 7.9 years, range 2-14 years. Two of these patients were in remission (12, 13), three had a relapse (14-16) and two had their first period of nephrotic syndrome (17, 18). Of three patients (32-34), a kidney biopsy but no urine sample was available (Table 2). Subjects with other nephropathies than FSGS or MCD (n=4) had a mean age of 8.8 years, range 0-13 years. This group included patients with IgA nephropathy, systemic lupus erythematosus and mesangiocapillary glomerulonephritis type II. Healthy control subjects (n=7) had a mean age of 8.9 years in the range of 5-20 years, they received no medication and displayed no signs of renal abnormalities. Further information is given in Tables 1 and 2.

Fresh mid-stream urine samples were collected in sterile containers and immediately centrifuged for 10 min at 2000 x g. Creatinine and total urinary protein were quantitated in the supernatant by standard procedures. For quantitation of bFGF and retinol-binding protein (RBP), the supernatant was aliquotted and stored at -80°C freezer within 30 min after collection.

Table 1: Characteristics of patients and control subjects participating in this study. ¹FSGS: focal segmental glomerulosclerosis, MCD: minimal change disease, IgA: IgA nephropathy, SLE: systemic lupus erythematosus, MCGN2: mesangiocapillar glomerulonephritis type II. ²Abbreviations used are P (prednisone), C (cyclosporine). na, not analysed. Data of healthy control subjects (nr. 23–29) are not included in the table.

Subjects					Urine samples				Serum samples	
Patient nr.	Diagnosis ¹⁾	Age (y)	Sex (M/F) ²⁾	Medication	Total protein (g/l)	Creatinine (mM)	RBP (mg/l)	bFGF (ng/l)	Creatinine (μM)	bFGF (ng/l)
1a	FSGS	15	F	P+C	0.1	17.2	<0.30	0.9	68	0.4
1b	FSGS	15	F	P+C	0.5	19	<0.30	1.1	61	6.1
2	FSGS	12	F	P+C	6.8	20	<0.15	5.5	56	0
3	FSGS	10	M	P+C	10.1	7.2	11	6	141	na
4	FSGS	20	M	-	4.4	8.9	3.4	5	169	na
5a	FSGS	4	F	-	3.1	6.2	<0.15	2.3	45	na
5b	FSGS	4	F	C	1.5	5.4	<0.15	1.7	61	0.4
6	FSGS	12	M	C	1.1	12.3	<0.15	1.1	89	na
7	FSGS	10	F	-	7.4	3.9	14	15	na	0.3
8	FSGS	15	F	C	4.9	8.1	5.5	0.5	225	1.6
9	FSGS	11	F	-	15.3	8.1	<0.15	31.6	53	0
10	FSGS	11	M	-	1.7	1.2	0.9	3.4	64	1.8
11	FSGS	1	M	P+C	18.8	2.7	1.7	31.3	27	4.7
12	MCD	12	M	P+C	0	12	<0.15	4.5	66	0
13	MCD	10	M	P	0	8.1	<0.15	0.6	60	0.9
14	MCD	14	F	P	19.4	14.6	0.5	31.6	56	4.1
15	MCD	13	F	-	11.5	11.4	<0.15	0.6	na	na
16	MCD	5	F	P+C	5.5	5	0.3	8.5	52	na
17	MCD	2	F	-	14.8	1.8	<0.15	3.8	na	na
18	MCD	3	F	-	0.6	3.5	<0.15	2.2	na	na
19	IgA	13	M	-	0.3	20.6	<0.15	2.8	69	1.6
20	IgA	10	F	-	na	7.8	<0.15	0.6	na	na
21	SLE	12	M	P	1.7	7.4	<0.15	5.7	68	0.9
22	MCGN2	0	M	P	3.4	3.5	9	3.4	125	na

Serum samples were collected only when blood sampling was required for the patient. Five to 10 ml of blood sample was collected in absence of anticoagulants and allowed to clot for 30 min. After centrifugation for 10 min at 1500 x g, the supernatant was transferred to sterile polypropylene ampules. Creatinine and ureum were measured by standard methods. For bFGF assays, sera aliquots were stored at -20°C until analysis within 60 min after collection.

Quantification of bFGF concentrations in urine and serum

Quantitative determination of bFGF concentrations in urine samples and sera was performed with the “Quantikine” high-sensitivity kit (R&D systems, Minneapolis, MN, USA). Urine samples (200 μl) and serum samples (100 μl) were added to ELISA wells pre-coated with a monoclonal anti-human-bFGF antibody. After incubation for 3 h at 22°C, the wells were washed 6 times and incubated for 2 h at 22°C with an alkaline phosphatase-conjugated polyclonal antibody against human bFGF. After washing 6 times again NADPH was added as a substrate, converted into NADH and Pi by bound conjugate (60 min at 22°C). Subsequently, an amplification reaction was performed (30 min at 22°C) with INT-violet as a chromogenic substrate. The colored end product formazan was measured by optical density at 490 nm. All samples were assayed in duplicate, and the produced absorbances were compared with that of serial dilutions of recombinant human bFGF included on the same 96-wells plate (also in

duplicate). To determine the stability of bFGF during storage in urine, a 16 ng/l standard dilution of bFGF was incubated for 0, 2, 4, 8, 12, 24, 30 and 48 h at 4°C and 25°C respectively. Immediately thereafter, samples were placed in a -80°C freezer until analysis.

Measurement of retinol-binding protein in urine samples

RBP was quantitated by laser immunonephelometry using a Hyland Disc 120 nephelometer (Hyland, Nivelles, Belgium). 250 µl of the urine samples was mixed with 850 µl anti-RBP antiserum (Dakopatts, Copenhagen, Denmark) diluted 100-fold in 120 mM NaCl, 130 mM phosphate, 2.3% (w/v) polyethyleneglycol-2000, 2.3% (w/v) polyethyleneglycol-4000 and 0.025% sodium azide at pH 7.4. After overnight incubation at 22°C, light scatter of the samples was measured at a wavelength of 633 nm and an angle of 31°.

Immunostaining of bFGF in kidney biopsies

Biopsy specimens taken for pathohistological examination were available from storage in liquid nitrogen. For immunofluorescence, cryostat sections were fixed for 5 min in ethanol/acetic acid (19:1) at 4°C, washed twice with PBS during 5 min, and incubated for 60 min at room temperature with a mouse monoclonal anti-bFGF IgG (Upstate Biotechnology, Waltham, MA, USA) diluted 1:50 in PBS + 1% bovine serum albumin. The slides were then washed as above, incubated with a FITC-conjugated secondary antibody (sheep-anti-mouse, Cappel, Oss, The Netherlands) and washed again. After mounting in Vectashield medium (Brunschwig, Amsterdam, The Netherlands), the sections were examined using a Leitz fluorescence microscope.

Statistics

Based on their diagnosis, the subjects were regarded as four individual sample populations (FSGS, MCD, other nephropathies, and healthy controls). Mean values and standard deviations were calculated for each group. Student's t test was used to evaluate the significance of differences in bFGF excretion between groups. To evaluate a possible correlation of bFGF excretion levels with proteinuria, we performed linear regression and calculated Pearson's correlation coefficient for each subject group.

RESULTS

Assessment of urinary bFGF excretion

To determine the concentrations of bFGF in urine, we used a high-sensitivity immunoassay with a lower detection limit of 0.1 ng/l. A calibration line in the range of 0 - 32 ng/l bFGF showed a strict linear dependence on the concentration of bFGF (correlation coefficient was 0.9998). To ensure that the measurements were not biased by degradation effects, we checked the stability of bFGF in urine samples. We compared storage at 4°C and 25°C for up to 48 h. When urine samples are processed at 25°C, freezing within 3 h after collection is necessary to minimize degradation. After storage during 48 h at 25°C an approximately threefold decrease in the detected bFGF concentration was observed. In contrast, the detected concentration was undiminished after storage for 48 h at 4°C (data not shown).

The concentrations of bFGF detected in urine samples from all subjects ranged from 0.0 to 31.6 ng/l (Table 1). The bFGF/creatinine ratio was calculated (Figure 1). A previously published normal mean value for bFGF excretion by children is 0.34 ng/mmol creatinine (dotted line in Figure 1) [34]. As an upper limit for normal range we used 1.29 ng/mmol (normal mean value plus two standard deviations; dashed line in Figure 1). The urinary bFGF concentrations produced by patients with FSGS had a mean value of 1.91 ± 3.24 ng/mmol.

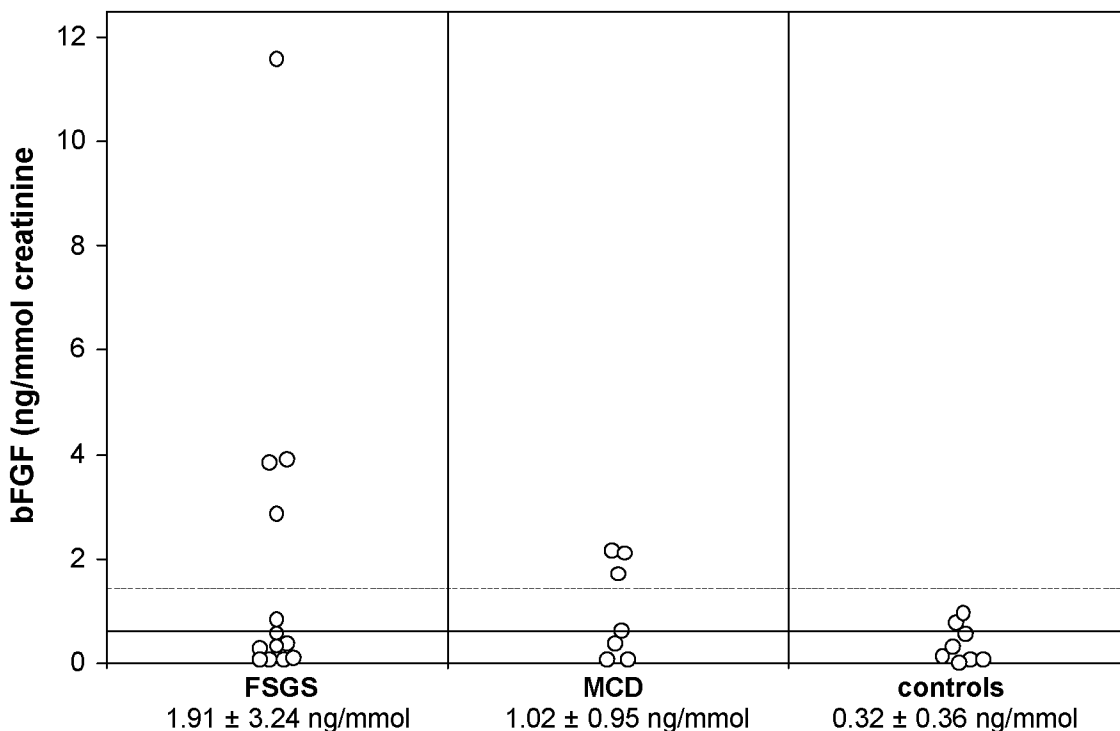


Figure 1: Comparison of urinary bFGF excretion by patients with FSGS (subjects 1–11), MCD (12–18) and control subjects (19–29). Values are given as ng of bFGF per mmol of creatinine to correct for urine concentration. Dotted line indicates normal mean, dashed line the upper limit for normal range in children [34].

This increase was significant ($P=0.05$). Excretion levels in the group of subjects with MCD were above-normal in three cases, and the mean value was 1.02 ± 0.95 ng/mmol. Mean bFGF excretion by healthy subjects and patients with other nephropathies than FSGS or MCD was 0.32 ± 0.36 ng/mmol, which corresponds well with previously reported normal mean values [34–36].

Interestingly, markedly increased urinary bFGF values were exclusively detected in association with high (>5 g/l) proteinuria. As shown in Figure 2, the dispersion of the paired values suggests a linear correlation between bFGF excretion and the extent of proteinuria. This was confirmed by linear regression on the paired values in the FSGS group, resulting in a correlation coefficient of 0.98 (the slope was 1.7 ng bFGF / g protein). The correlation between bFGF excretion and proteinuria suggests a role for bFGF in the pathogenesis of proteinuria.

Assays to determine the mechanism of increased bFGF excretion

Various mechanisms are conceivable to explain the increased bFGF excretion. Glomerular permeability may not influence bFGF excretion, because this small molecule can pass the filtration barrier freely. Does the bFGF excretion arise from its increased concentration in the circulating plasma? To address this question, we first analyzed the concentrations of bFGF in the sera of subjects (Table 1). No significant increase was found in any of the subject groups. The mean concentration of bFGF in serum from FSGS patients was 1.7 ± 2.2 ng/l ($n=9$), which is comparable with the normal mean value described in the test kit, 2.45 ng/l ($n=52$).

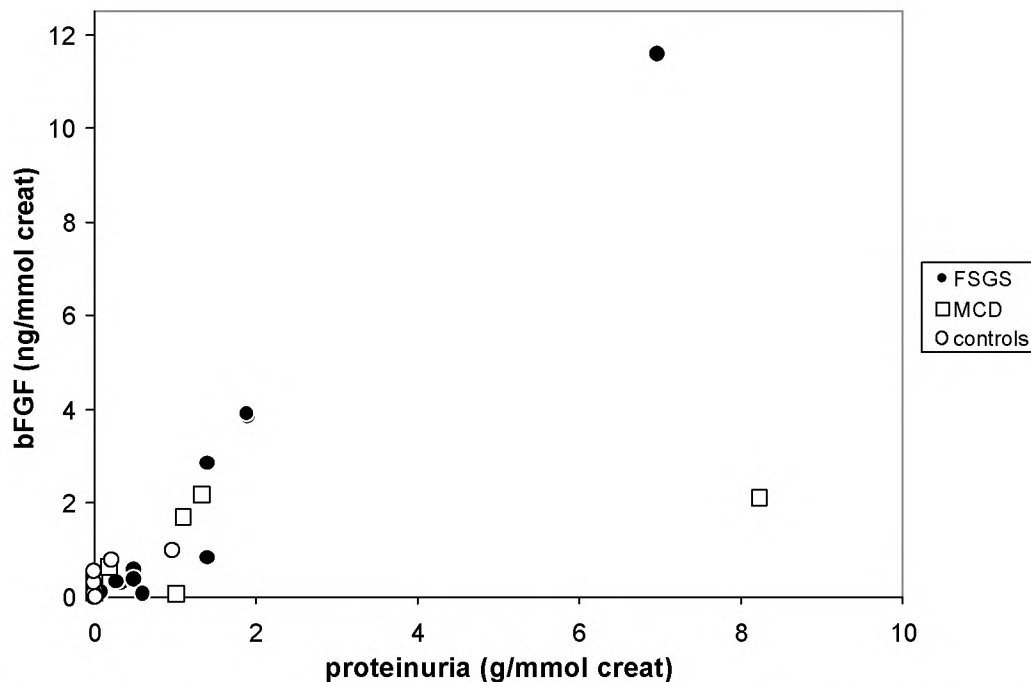


Figure 2: Relation between urinary bFGF concentrations and proteinuria in patients with FSGS, MCD, other nephropathies and subjects from the control group. In patients with FSGS, above-normal bFGF concentrations displayed a linear correlation with the degree of proteinuria (correlation coefficient 0.98).

Alternatively, the urinary bFGF values could reflect a deficiency in tubular reabsorption. To investigate this possibility we screened all subjects for tubular dysfunction. Retinol-binding protein (RBP) provides a good marker for tubular dysfunction, because this 22 kDa protein has a fractional tubular reabsorption near 100% in healthy individuals [37]. Retinol-binding protein is stable in urines with pH>5 [38, 39]. Normal ranges of RBP excretion are age-dependent [40, 41]. The RBP concentrations in urines from our subjects (Table 1) were compared with the proposed upper limits for normal subjects [41]. Four subjects with FSGS (nr. 3, 4, 7 and 8) produced increased urinary RBP levels. Of these, patient 7 also had increased bFGF excretion. The measured bFGF concentration in the urine from this patient may therefore be influenced by reduced tubular uptake. Patients 3, 4 and 8 had normal urinary bFGF concentrations. Patients 9, 10, 11, 14, 16 and 17, who produced high urinary bFGF concentrations, clearly displayed normal tubular function. Thus, no correlation between bFGF release and RBP excretion was present. Although we cannot exclude a bias in bFGF detection for patient 7, the above results indicate that the observed bFGF excretion is not the consequence of tubular dysfunction. The low levels of bFGF in the serum of all subjects, and the exclusion of tubular dysfunction as a cause for bFGF excretion, suggest that bFGF is most likely released in the urogenital system of patients with FSGS.

Immunological detection of bFGF in focal segmental glomerulosclerosis

To localize the sites of bFGF release in FSGS, we stained kidney biopsy specimens using a monoclonal antibody against bFGF. The same procedure was performed for sections of minimal change nephrotic syndrome and normal kidney. The staining of individual biopsies was interpreted by visual scoring as listed in Table 2.

In the normal kidney, anti-bFGF staining in the glomeruli was very weak (Figure 3A) which corresponds well with previous observations [42]. The tubules of normal kidney showed a marked staining with anti-bFGF antibodies. In glomeruli from patients with MCD and FSGS

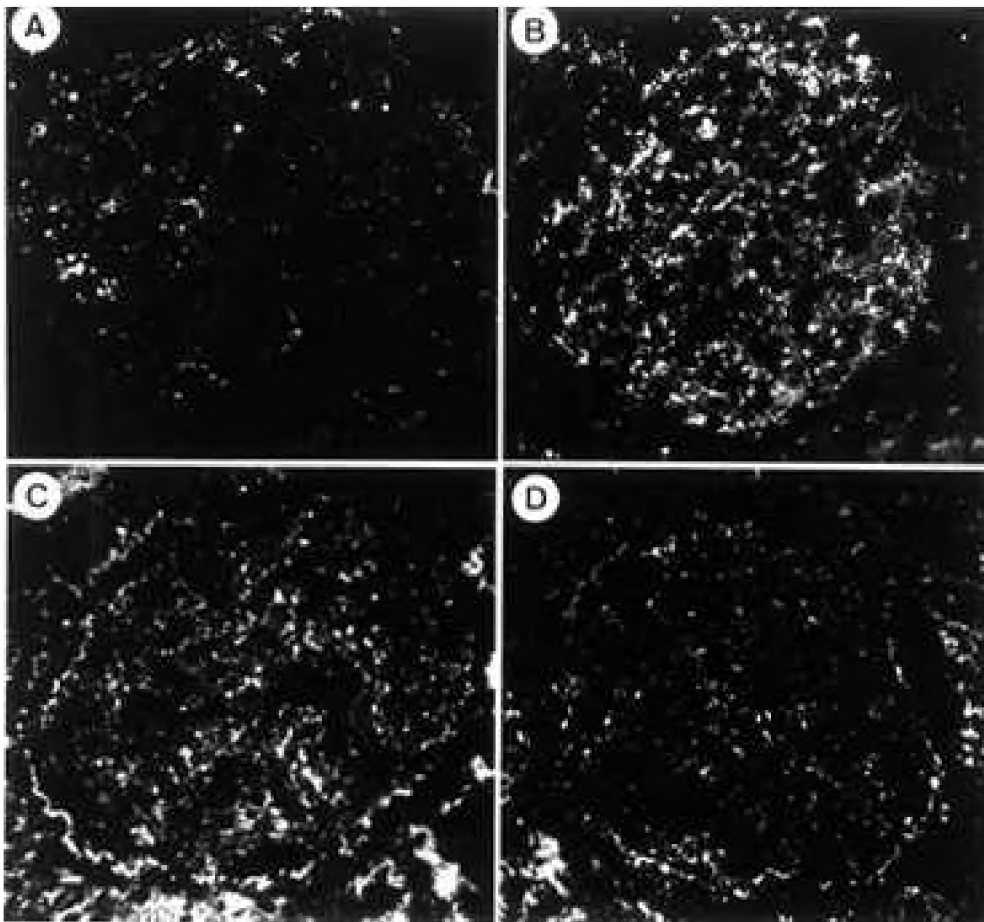


Figure 3: Indirect immunofluorescence staining of bFGF in kidney cortex tissue. (A) Patient with normal kidney, (B) patient nr. 31 with FSGS, (C) patient nr. 34 with minimal change nephrosis, and (D) patient nr. 9 with FSGS. Magnification 400x.

(Figures 3B and 3C) an increased staining was evident, with a degree that varied between individual subjects. Figure 3D represents a typical staining of a biopsy from a patient with FSGS. The staining pattern followed an irregular pattern along the capillaries. Tubular anti-bFGF staining showed a slight increase in biopsies from patients with MCD and FSGS compared to normal controls. We found that tubular anti-bFGF staining was dependent on the fixation temperature used. Compared with the sections that were fixed at 4°C (Figure 3), sections fixed at -20°C showed a less intense staining of bFGF in the tubuli (not shown). The glomerular staining was independent of the fixation temperature (data not shown). In some cases the Bowman's capsule also expressed substantial amounts of bFGF (e.g. Figure 3D). Interestingly, this latter biopsy originates from a FSGS patient who also produced high concentrations of urinary bFGF (Table 1). Urine samples of patients relating to the other shown sections were unavailable. The immunological detection of bFGF in glomeruli of patients with FSGS and MCD is in line with the increased urinary bFGF concentrations found in these nephropathies.

DISCUSSION

The increased urinary excretion of bFGF in 3 out of 4 patients with FSGS was not caused by defective tubular reabsorption. Besides these cases, a large subset of the FSGS patients

Table 2: Typical anti-bFGF staining intensity in glomeruli and tubules from six subjects with FSGS and three with MCD. From patient 3, a second biopsy was taken after recurrence of the disease in a renal allograft (FSGS-R). Visual scoring indicates changes in bFGF expression as follows: = normal intensity; + slight increase; ++ moderate increase; +++ strong increase compared to normal kidney. ¹⁾Abbreviations are listed in Table 1.

Patient nr.	Diagnosis ¹⁾	Age (y)	Sex	Medication ²⁾	Anti-bFGF staining intensity Glomeruli	Tubules
0	normal			-	=	=
3a	FSGS	9	M	-	+	+
3b	FSGS-R	11	M	P+C	+	+
4	FSGS	11	M	-	++	+
9	FSGS	8	F	P	++	+
30	FSGS	15	F	P	++	+
31	FSGS	12	M	C	+++	=
32	MCD	4	M	P	++	+
33	MCD	7	M	P	+	+
34	MCD	9	M	P	+++	+

displayed urinary bFGF values in the normal range. It is possible that a bFGF-independent mechanism of pathogenesis induces FSGS in these patients. Alternatively, a small increase in filtered bFGF may remain undetected through effective reabsorption.

Above-normal bFGF excretion was not detected only in FSGS, but also in three patients with MCD. Nevertheless a key role of bFGF in the pathogenesis of MCD is unlikely. Patients with MCD respond well to corticosteroid therapy and episodes of high proteinuria are relatively short. Since bFGF excretion correlated with proteinuria, we speculate that in MCD the influence of bFGF is only temporarily present and disappears when the patient is in remission. In contrast, proteinuria of FSGS patients is persistent and a long-term influence of bFGF is conceivable.

The presence of bFGF immunoreactivity in glomeruli of patients with FSGS is in agreement with the increased bFGF transcription in glomeruli from rats with progressive PAN-induced glomerulosclerosis [43]. The immunoreactivity seems to be mainly associated with the glomerular capillaries, suggesting that podocytes could be influenced by bFGF. The immunoreactivity was also associated with Bowman's capsule in some patients. This structure is particularly rich in perlecan, a receptor of bFGF [14, 44]. The finding that tubular anti-bFGF staining was dependent on the fixation procedure, was also reported by others [45]. In contrast to previous findings in Thy1.1-induced glomerulopathy in rats [33], we did not observe prominent staining in mesangial areas.

The glomerulus contains both the low- and high affinity receptors necessary for a bFGF-induced mitogenic response. The low-affinity receptors, heparan sulfate proteoglycans, are abundantly present in the glomerular basement membrane and mesangial matrix [44, 46, 47]. High-affinity receptors expressed in glomeruli were studied for the composition of their ligand-specificity-determining region, the second half of their third immunoglobulin-like domain [48–50]. This region is encoded by either exon IIIb or IIIc, determined by alternative splicing. For fibroblast growth factor receptor 2 it was shown, that the IIIc splice variant binds both aFGF and bFGF, whereas the IIIb variant recognizes only aFGF and FGF-7. The glomerulus contains exclusively mRNA that encodes type IIIc receptors [50]. This suggests that the high affinity receptors expressed in glomeruli recognize bFGF very well. Thus bFGF may influence the function of the podocyte, the cell type considered to be responsible for the

development of FSGS. The modulation of bFGF-induced glomerular hypertrophy could theoretically provide novel therapeutic tools for the clinical management of FSGS. Of special interest in this regard are low-molecular-weight heparin species or sulfated malto-oligosaccharides [51], and neutralizing antibodies or peptide antagonists [52] which can block the activity of bFGF.

In conclusion, this study suggests that increased glomerular bFGF may be involved in at least some forms of FSGS. The relation between urinary bFGF excretion and urinary protein content suggests that this growth factor could contribute to the pathogenesis of proteinuria.

ACKNOWLEDGEMENTS

This study was supported by grant C93.1309 from the Dutch Kidney Foundation. We acknowledge Dr. I. Klasen and Mrs. C.M. de Kat Angelino for expert technical assistance in the quantification of urinary retinol-binding protein, and we thank all participants of this study.

REFERENCES

1. Cameron JS (1996) The enigma of focal segmental glomerulosclerosis. *Kidney Int* 50 Suppl 57: S119–131.
2. Schwartz MM, Korbet SM. (1993) Primary focal segmental glomerulosclerosis: pathology, histological variants, and pathogenesis. *Am J Kidney Dis* 22: 874–883.
3. Savin VJ, Sharma R, Sharma M, et al. (1996) Circulating factor associated with increased glomerular permeability to albumin in recurrent focal segmental glomerulosclerosis. *N Engl J Med* 334: 878–883.
4. Lee DY, Kim W, Kang SK, Koh GY, Park SK (1997) Angiotensin-converting enzyme gene polymorphism in patients with minimal-change nephrotic syndrome and focal segmental glomerulosclerosis. *Nephron* 77: 471–473.
5. Floege J, Alpers CE, Burns MW, et al. (1992) Glomerular cells, extracellular matrix accumulation, and the development of glomerulosclerosis in the remnant kidney model. *Lab Invest* 66: 485–497.
6. Yoshida Y, Fogo A, Ichikawa I (1989) Glomerular hemodynamic changes vs. hypertrophy in experimental glomerular sclerosis. *Kidney Int* 35: 654–660.
7. Desassis JF, Raats CJ, Bakker MA, van den Born J, Berden JH (1997) Antiproteinuric effect of ciclosporin A in adriamycin nephropathy in rats. *Nephron* 75: 336–341.
8. Diamond JR, Karnovsky MJ (1986) Focal and segmental glomerulosclerosis following a single intravenous dose of puromycin aminonucleoside. *Am J Pathol* 122: 481–487.
9. Meguid El Nahas A (1992) Growth factors and glomerular sclerosis. *Kidney Int* 41 Suppl. 36: S15–20.
10. Kriz W, Hahnel B, Rosener S, Elger M. (1995) Long-term treatment of rats with FGF-2 results in focal segmental glomerulosclerosis. *Kidney Int* 48: 1435–1450.
11. Maier JA, Rusnati M, Ragnotti G, Presta M (1990) Characterization of a Mr 20,000 basic fibroblast growth factor-like protein secreted by normal and transformed fetal bovine aortic endothelial cells. *Exp Cell Res* 186: 354–361.
12. Francki A, Uciechowski P, Floege J, von der Ohe J, Resch K, Radeke HH (1995) Autocrine growth regulation of human glomerular mesangial cells is primarily mediated by basic fibroblast growth factor. *Am J Pathol* 147: 1372–1382.
13. Bikfalvi A, Klein S, Pintucci G, Quarto N, Mignatti P, Rifkin DB (1995) Differential modulation of cell phenotype by different molecular weight forms of basic fibroblast growth factor: possible intracellular signaling by the high molecular weight forms. *J Cell Biol* 129: 233–243.
14. Aviezer D, Hecht D, Safran M, Eisinger M, David G, Yayon A (1994) Perlecan, basal lamina proteoglycan, promotes basic fibroblast growth factor-receptor binding, mitogenesis, and angiogenesis. *Cell* 79: 1005–1013.
15. Perantoni AO, Dove LF, Karavanova I (1995) Basic fibroblast growth factor can mediate the

- early inductive events in renal development. *Proc Natl Acad Sci USA* 92: 4696–4700.
16. Mignatti P, Morimoto T, Rifkin DB (1991) Basic fibroblast growth factor released by single, isolated cells stimulates their migration in an autocrine manner. *Proc Natl Acad Sci USA* 88: 11007–11011.
 17. Seghezzi G, Patel S, Ren CJ, et al. (1998) Fibroblast growth factor-2 (FGF-2) induces vascular endothelial growth factor (VEGF) expression in the endothelial cells of forming capillaries: An autocrine mechanism contributing to angiogenesis. *J Cell Biol* 141: 1659–1673.
 18. Healy AM, Herman IM (1992) Density-dependent accumulation of basic fibroblast growth factor in the subendothelial matrix. *Eur J Cell Biol* 59: 56–67.
 19. Mignatti P, Morimoto T, Rifkin DB (1992) Basic fibroblast growth factor, a protein devoid of secretory signal sequence, is released by cells via a pathway independent of the endoplasmic reticulum-Golgi complex. *J Cell Physiol* 151: 81–93.
 20. McNeil PL, Muthukrishnan L, Warder E, D'Amore PA (1989) Growth factors are released by mechanically wounded endothelial cells. *J Cell Biol* 109: 811–822.
 21. Floege J, Burg M, Hugo C, et al. (1998) Endogenous fibroblast growth factor-2 mediates cytotoxicity in experimental mesangio-proliferative glomerulonephritis. *J Am Soc Nephrol* 9: 792–801.
 22. Muthukrishnan L, Warder E, McNeil PL (1991) Basic fibroblast growth factor is efficiently released from a cytosolic storage site through plasma membrane disruptions of endothelial cells. *J Cell Physiol* 148: 1–16.
 23. Vlodavsky I, Fuks Z, Ishai-Michaeli R, et al. (1991) Extracellular matrix-resident basic fibroblast growth factor: implication for the control of angiogenesis. *J Cell Biochem* 45: 167–176.
 24. Guillonnet X, Tassin J, Berrou E, Bryckaert M, Courtois Y, Mascarelli F (1996) *In vitro* changes in plasma membrane heparan sulfate proteoglycans and in perlecan expression participate in the regulation of fibroblast growth factor 2 mitogenic activity. *J Cell Physiol* 166: 170–187.
 25. Aviezer D, Iozzo RV, Noonan DM, Yayon A. (1997) Suppression of autocrine and paracrine functions of basic fibroblast growth factor by stable expression of perlecan antisense cDNA. *Mol Cell Biol* 17: 1938–1946.
 26. Joseph SJ, Ford MD, Barth C, et al. (1996) A proteoglycan that activates fibroblast growth factors during early neuronal development is a perlecan variant. *Development* 122: 3443–3452.
 27. Turnbull JE, Fernig DG, Ke Y, Wilkinson MC, Gallagher JT (1992) Identification of the basic fibroblast growth factor binding sequence in fibroblast heparan sulfate. *J Biol Chem* 267: 10337–10341.
 28. Brickman YG, Ford MD, Small DH, Bartlett PF, Nurcombe V (1995) Heparan sulfates mediate the binding of basic fibroblast growth factor to a specific receptor on neural precursor cells. *J Biol Chem* 270: 24941–24948.
 29. Presta M, Maier JA, Ragnotti G (1989) The mitogenic signaling pathway but not the plasminogen activator-inducing pathway of basic fibroblast growth factor is mediated through protein kinase C in fetal bovine aortic endothelial cells. *J Cell Biol* 109: 1877–1884.
 30. Rogelj S, Klagsbrun M, Atzmon R, et al. (1989) Basic fibroblast growth factor is an extracellular matrix component required for supporting the proliferation of vascular endothelial cells and the differentiation of PC12 cells. *J Cell Biol* 109: 823–831.
 31. Takeuchi A, Yoshizawa N, Yamamoto M, et al. (1992) Basic fibroblast growth factor promotes proliferation of rat glomerular visceral epithelial cells in vitro. *Am J Pathol* 141: 107–116.
 32. Floege J, Kriz W, Schulze M, et al. (1995) Basic fibroblast growth factor augments podocyte injury and induces glomerulosclerosis in rats with experimental membranous nephropathy. *J Clin Invest* 96: 2809–2819.
 33. Floege J, Eng E, Lindner V, et al. (1992) Rat glomerular mesangial cells synthesize basic fibroblast growth factor. *J Clin Invest* 90: 2362–2369.
 34. Bägli DJ, Van Savage JG, Khoury AE, Carr M, McLorie GA (1997) Basic fibroblast growth factor in the urine of children with voiding pathology. *J Urol* 158: 1123–1127.
 35. Kaplan F, Sawyer J, Connors S, et al. (1998) Urinary basic fibroblast growth factor. A biochemical marker for preosseous fibroproliferative lesions in patients with fibrodysplasia ossificans progressiva. *Clin Orthop* 346: 59–65.
 36. Chow NH, Chang CJ, Yeh TM, Chan SH, Tzai TS, Lin JS (1996) Implications of urinary basic fibroblast growth factor excretion in

- patients with urothelial carcinoma. *Clin Sci* 90: 127–133.
37. Bernard A, Viau C, Ouled A, Lauwerys R (1987) Competition between low- and high-molecular-weight proteins for renal tubular uptake. *Nephron* 45: 115–118.
 38. Tomlinson PA (1992) Low molecular weight proteins in children with renal disease. *Pediatr Nephrol* 6: 565–571.
 39. Donaldson MDC, Chambers RE, Woolridge MW, Whicher JT (1989) Stability of α 1-microglobulin, β 2-microglobulin and retinol binding protein in urine. *Clin Chim Acta* 179: 73–78.
 40. Smith GC, Winterborn MH, Taylor CM, Lawson N and Guy M (1994) Assessment of retinol-binding protein excretion in normal children. *Pediatr Nephrol* 8: 148–150.
 41. Lehrnbecher T, Greissing S, Navid F, Pfüller H, Jeschke R. (1998) Albumin, IgG, retinol-binding protein, and α 1-microglobulin excretion in childhood. *Pediatr Nephrol* 12: 290–292.
 42. Hughes SE, Hall PA. (1993) Immunolocalization of fibroblast growth factor receptor 1 and its ligands in human tissues. *Lab Invest* 69: 173–182.
 43. Nakamura T, Ebihara I, Fukui M, et al. (1993) Messenger RNA expression for growth factors in glomeruli from focal glomerular sclerosis. *Clin Immunol Immunopathol* 66: 33–42.
 44. Groffen AJ, Ruegg MA, Dijkman H, et al. (1998) Agrin is a major heparan sulfate proteoglycan in the human glomerular basement membrane. *J Histochem Cytochem* 46: 19–27.
 45. Hanneken A, Baird A. (1992) Immunolocalization of basic fibroblast growth factor: dependence on antibody type and tissue fixation. *Exp Eye Res* 54: 1011–1014.
 46. Van den Heuvel LP, van den Born J, Veerkamp JH, et al. (1990) Comparison of heparan sulfate proteoglycans from equine and human glomerular basement membranes. *Int J Biochem* 22: 903–914.
 47. Groffen AJ, Hop FW, Tryggvason K, et al. (1997) Evidence for the existence of multiple heparan sulfate proteoglycans in the human glomerular basement membrane and mesangial matrix. *Eur J Biochem* 247: 175–182.
 48. Yayon A, Zimmer Y, Shen GH, Avivi A, Yarden Y, Givol D (1992) A confined variable region confers ligand specificity on fibroblast growth factor receptors: implications for the origin of the immunoglobulin fold. *EMBO J* 11: 1885–1890.
 49. Johnson DE, Lu J, Chen H, Werner S, Williams LT (1991) The human fibroblast growth factor receptor genes: a common structural arrangement underlies the mechanisms for generating receptor forms that differ in their third immunoglobulin domain. *Mol Cell Biol* 11: 4627–4634.
 50. Ford MD, Cauchi J, Greferath U, Bertram JF (1997) Expression of fibroblast growth factors and their receptors in rat glomeruli. *Kidney Int* 51: 1729–1738.
 51. Foxall C, Wei Z, Schaefer ME, et al. (1996) Sulfated malto-oligosaccharides bind to basic FGF, inhibit endothelial cell proliferation, and disrupt endothelial cell tube formation. *J Cell Physiol* 168: 657–667.
 52. Floege J, Burg M, Hugo C, Gordon KL, Van Goor H, Reidy M, Couser WG, Koch KM, Johnson RJ (1997) Endogenous fibroblast growth factor-2 mediates cytotoxicity in experimental mesangioproliferative glomerulonephritis. *J Am Soc Nephrol* 9: 792–801.

CHAPTER NINE

Survey of results and indications for future research

Samenvatting in het Nederlands

List of original papers

Curriculum vitae

Dankwoord

Survey of results and indications for future research

BACKGROUND AND AIMS OF THE STUDY

Heparan sulfate proteoglycans (HSPGs) are important components of the glomerular basement membrane (GBM) as they contribute to the selectivity of renal clearance of proteins. This activity is based on the anionic charge of their heparan sulfate (HS) side chains, that diminishes the permeability of the GBM for negatively charged molecules in the blood plasma (e.g. most proteins). There is convincing evidence that absence of HS in the GBM results in a nephrotic syndrome (albuminuria, hypoproteinemia and edema). In line with this, many researchers have investigated the role of HSPGs in the development of various nephropathies associated with a nephrotic syndrome. The first identified HSPG that occurs in basement membranes, perlecan, was the subject of most of these studies. The objective of the study described here was to analyze the functional role of perlecan, to investigate whether additional HSPG molecules other than perlecan could be present in the GBM, and to investigate how HSPGs may be involved in various nephropathies.

A MODEST ROLE FOR PERLECAN IN THE GBM

To investigate the functional properties of perlecan, recombinant fragments (containing domains I and different parts of domain II) were produced in *Escherichia coli* (bacteria), *Pichia pastoris* (yeast) and *Spodoptera frugiperda* (insect cells). Based on primary structure predictions, domain I was proposed to be responsible for heparan sulfate attachment. Domain II does not contain sites for attachment. In insect cells, the perlecan fragment was produced as a chondroitin sulfate proteoglycan (chapter 2). This demonstrates the functionality of the glycosaminoglycan attachment sites in the SEA module. Furthermore this indicates that this domain can be alternatively glycosylated dependent on the cell type in which it is synthesized. Interestingly, chondroitin sulfate carrying perlecan isoforms also occur in cartilage matrix. Domain II is similar in structure to the low-density lipoprotein receptor. We therefore investigated if the recombinant perlecan fragments showed affinity to lipoprotein fractions of human serum (chapter 3). The affinity of the various fragments differed: the glycosaminoglycan-free peptides produced in *E. coli* and *P. pastoris* bound to apolipoprotein-B-containing lipoproteins, while the chondroitin sulfate-containing peptide from *S. frugiperda* showed no detectable binding. This provides the first *in vitro* evidence that domains I and II of the core protein may act as a lipoprotein receptor. The data further suggest that the glycosylation characteristics of perlecan modulate its lipoprotein-binding activity. If this mechanism is of physiological importance, it may contribute to the adhesion of lipoproteins to the subendothelial matrix in blood vessels.

The recombinant proteins were also used to generate a well-defined monoclonal antibody against human perlecan, named 95J10. This antibody was used to investigate the distribution of perlecan immunoreactivity by immunofluorescence and immuno-electron microscopy. Although abundantly present in Bowman's capsule and the tubular basement membranes, perlecan was absent in many regions of the GBM. This suggests a more modest role for perlecan in renal ultrafiltration than was initially assumed. Different results obtained with previously prepared monoclonal antibodies demonstrated that additional HSPG species are present in the GBM (chapter 4).

AGRIN AS A MAJOR HSPG OF THE GBM.

A major HSPG component of the GBM was identified as agrin, known as a mediator during development of the neuromuscular junction (chapter 5). In immuno-electron microscopy, anti-agrin antibodies produced an intense linear homogenous staining of the GBM. Anti-agrin antisera recognized HSPG purified from the GBM. By northern hybridization, agrin transcription levels were compared between multiple human tissues. Of all tissues the highest agrin mRNA levels were detected in adult kidney and lung. Given its potential relevance for GBM permselectivity, we cloned and sequenced the cDNA that encodes human renal agrin (chapter 6). The sequence comprises 7032 base pairs and encodes a mature protein of 212 kDa with several potential HS attachment sites and a laminin-binding domain. As far as can be predicted, two sites are particularly favorable for substitution with HS. Sites of alternative splicing (designated *c*, *x*, *y* and *z*) were devoid of inserts except the *x* site where a 9-amino acid insert was present.

Nineteen recombinant fragments of human agrin, distributed along the core protein, were engineered and expressed as fusion proteins in *E. coli*. Previously raised MAbs against human GBM HSPG were tested for immunoreactivity towards these constructs. In this way, the epitopes of 25 antibodies were mapped to regions of the agrin core protein (chapter 7). Then the anti-agrin MAbs were used to stain the extracellular matrix produced by human podocytes and human glomerular endothelial cells in primary culture. The results suggest that agrin is exclusively synthesized by podocytes.

Since agrin was shown to bind to laminin in the neuromuscular junction, we asked whether these molecules could also interact in the GBM. The fusion protein AGR1, that contained the laminin-binding domain, displayed laminin-binding activity *in vitro*. AGR1 also bound to the extracellular matrix of kidney cortex tissue and of cultured glomerular cells. This indicates that laminin-binding is likely a mechanism by which agrin is anchored within the GBM (chapter 7).

THE POTENTIAL ROLES OF HSPGS IN RENAL DISEASE

Regarding the limited expression of perlecan in the GBM, it is not surprising that we found no indications for a causal role of perlecan in the development of nephropathies. In contrast, agrin may be involved in such processes. Previous studies reported a relative decrease of GBM HSPG in diabetic nephropathy. By localizing the epitope of the antibody used in these studies, it has now become clear that agrin is involved in these changes.

In other nephropathies (e.g. in minimal lesions and renal manifestations of Denys-Drash Syndrome) a reduced HS content was previously shown to be associated with a normal expression of the core protein. These alterations may therefore be related to disturbances in the synthesis, modification or degradation of HS.

Not only do HSPGs contribute to GBM anionic charge, they also function as storage sites and activators of various growth factors. Among these is basic fibroblast growth factor (bFGF). Glomerular cells respond to bFGF by cell proliferation. Long-term exposure of glomerular podocytes to bFGF was previously shown to induce their dedifferentiation and damage, resulting in a nephropathy that resembled focal segmental glomerulosclerosis (FSGS). To investigate if a similar mechanism could occur during the clinical pathogenesis of FSGS, bFGF concentrations were measured in urine and serum from patients with various nephropathies (chapter 8). In four patients with FSGS and severe proteinuria, a marked increase in urinary bFGF excretion was found. Other patients with FSGS had normal urinary bFGF concentrations. The results suggest that increased glomerular bFGF concentrations may contribute to the pathogenesis of FSGS in the human.

CONCLUSIONS

The results presented in this thesis together support the following conclusions:

- Domain I of human perlecan can also be glycosylated with chondroitin sulfate (chapter 2)
- Domains I and/or II of the core protein of human perlecan can bind apoB-containing lipoproteins and this activity is influenced by its glycosylation (chapter 3)
- The GBM contains at least two different HSPG molecules: agrin and perlecan (chapter 4 and 5)
- Perlecan is absent from the GBM in many regions of the capillary loop (chapter 4)
- Agrin is a major HSPG of the GBM (chapter 5)
- Human agrin consists of a 212 kDa core protein and supports glycosylation by the presence of a SEA module and two especially favorable sites for HS attachment (chapter 6).
- Human renal agrin is expressed by podocytes and binds to the GBM via its laminin-binding domain (chapter 7).
- Human renal agrin inhibits the proteases trypsin, plasmin and elastase (chapter 7)
- The influence of basic fibroblast growth factor on podocytes may be involved in the development of proteinuria in FSGS (chapter 8)

INDICATIONS FOR FUTURE RESEARCH

The results from this study offer new perspectives for investigating the functions of HSPGs and the structure of the GBM. Here, possible future approaches are discussed in relation to the current status of knowledge in this field.

Our data suggested a low expression of perlecan in the GBM, and therefore a limited role in determining permselectivity. The affinity of its core protein for lipoproteins could be of importance especially in the subendothelial matrix of the vascular system, and this possible function deserves further attention. First, the physiological relevance of the described interactions should be assessed by *in vivo* experiments. Subsequently it is important to understand how heparan sulfate residues attached to domain I influence the affinity of lipoproteins for perlecan. Investigation of these issues may contribute to an increased understanding of the mechanisms involved in the retention of atherogenic lipoproteins in the subendothelial matrix.

The high expression of agrin in the GBM suggests that it contributes importantly to the maintenance of the charge-selective permeability in ultrafiltration. This hypothesis may be investigated by a targeted elimination of the HS attachment sites of agrin in mutant mice. In relation to this, the number of HS residues on the human agrin core protein and the location of their attachment sites should be confirmed experimentally. The attachment of two to three HS chains was already demonstrated for recombinant chick agrin by rotary shadowing electron microscopy. It is however uncertain if human agrin is glycosylated in the same way. Another topic for future investigation is the temporal regulation of agrin transcription and expression during nephrogenesis. Regulatory mechanisms that influence agrin expression in the kidney are largely unknown. The promoter area of the agrin gene should be characterized to identify the potentially involved transcription factors. Completion of the Human Genome Project will provide novel clues in this respect. Furthermore, it would be interesting to know if the cloned agrin isoform (with the splice composition $C_0X_9Y_0Z_0$) is the only isoform expressed in the glomerulus. And how does alternative splicing at site x influence the functions of agrin?

The functional properties of renal agrin should be analyzed in more detail. The cDNA clones, recombinant fusion proteins and region-specific monoclonal antibodies described in this study facilitate new approaches for this purpose. Of special interest are the interactions of agrin with α -dystroglycan and integrin. These cell-matrix interactions, besides providing a link between

the cytoskeleton and the basement membrane, have the potential to trigger signal transduction processes.

A subject of great interest is the possible involvement of agrin in various nephropathies where a decrease in polyanionic sites of the GBM occurs. These include the minimal change nephrotic syndrome and diabetic nephropathy. It would be interesting to know how HSPG expression and glycosylation are influenced by the circulating factors that induce minimal change lesions and focal segmental glomerulosclerosis.

Samenvatting in het Nederlands

ACHTERGROND EN DOELSTELLING VAN HET ONDERZOEK

De nieren hebben een onmisbare functie in het menselijk lichaam: ze zijn onder andere verantwoordelijk voor het zuiveren van het bloed en het produceren van de urine. Het is hierbij belangrijk dat nuttige bestanddelen van het bloed zo goed mogelijk worden behouden, terwijl schadelijke zoveel mogelijk worden uitgescheiden. De eerste stap in dit scheidingsproces vindt plaats in de glomerulaire basaalmembraan (GBM). De GBM fungeert als een filter tussen het bloed aan de ene, en de voorurine aan de andere kant. Doordat de bloeddruk in de nieren hoog is, komen alle stoffen die het filter kunnen passeren in de voorurine terecht. Andere delen van de nier verfijnen deze grove scheiding nog. Zo ontstaat uiteindelijk de urine.

De selectieve doorlaatbaarheid van de GBM is van groot belang voor een goede werking van de nieren. Bij afwijkingen hierin kunnen verschillende nierziekten ontstaan. Wanneer bijvoorbeeld eiwitten uit het bloed weglekken, ontstaat oedeem (zwellings van lichaamsdelen). Om zulke nierziekten te kunnen begrijpen en behandelen, wordt sinds lange tijd onderzocht hoe de doorlaatbaarheid precies wordt geregeld. Al in 1980 heeft men ontdekt dat de GBM moleculen bevat die de doortocht van eiwitten bemoeilijken. Deze moleculen heten heparansulfaatproteoglycanen (HSPG's). HSPG's bestaan deels uit eiwit en deels uit suikerketens (heparansulfaat) die sterk negatief geladen zijn. De aanwezigheid van HSPG's in de GBM zorgt ervoor dat de meeste eiwitten in het bloed –die eveneens negatief geladen zijn– worden afgestoten en dus in het bloed blijven. Wanneer de heparansulfaatketens afwezig zijn ontstaat dan ook een eiwitlek.

Onze groep slaagde er in het verleden in om het HSPG uit de GBM van menselijke nieren te zuiveren. Dit preparaat werd gebruikt om antistoffen tegen het HSPG te maken (in het laboratorium een belangrijk hulpmiddel om het HSPG zichtbaar te kunnen maken). Ondanks deze vorderingen bleef de precieze identiteit van het HSPG-molecuul lange tijd onbekend. In 1988 ontdekte men een HSPG genaamd perlecan, dat drie heparansulfaatketens draagt en inderdaad voorkomt in basaalmembranen. Toch werd tot op heden niet aangetoond dat perlecan de doorlaatbaarheid van de GBM bepaalt.

Het hier beschreven onderzoek richt zich op de HSPG-samenstelling van de GBM. De vraagstelling was driedig. Welke functies heeft perlecan? Komen er nog andere HSPG's voor in de GBM en zo ja, welke? En tenslotte: zijn HSPG's betrokken bij het ontstaan van nierziekten?

EEN BESCHIEDEN ROL VAN PERLECAN IN DE GBM

Om de functies van perlecan te kunnen onderzoeken is natuurlijk perlecan nodig. Om dit in handen te krijgen werd gebruik gemaakt van de recombinant-DNA-technologie. Delen van het erfelijke materiaal (het DNA) dat voor de productie van menselijk perlecan zorgt, werden hierbij in bacterie-, gist- en insectencellen geplaatst. Normaal gesproken bestaat perlecan uit vijf verschillende delen, domeinen genoemd. Bij dit onderzoek werd alleen het DNA dat codeert voor domein I en II naar de gastheercellen overgebracht. Op grond van de structuur van het perlecan bestonden al vermoedens voor een mogelijke functie van deze twee domeinen: domein I was waarschijnlijk betrokken bij de aanhechting van de suikerketens van het HSPG, domein II leek veel op een eiwit dat belangrijk is in het lipoproteïnenmetabolisme (de omzetting van vet-eiwitcomplexen die in het bloed voorkomen). De door recombinant-DNA-technologie verkregen perlecan-fragmenten werden gebruikt om te onderzoeken of deze vermoedens terecht waren.

Het perlecanfragment dat door insectencellen werd geproduceerd, bleek in het bezit te zijn van suikerketens (hoofdstuk 2). De structuur van de gevormde suikerketens verschilde echter

van heparansulfaat. Het bleek een variant te zijn: chondroitinesulfaat. Ook in het menselijk lichaam zijn perlecanvarianten aangetroffen die in het bezit waren van chondroitinesulfaat, bijvoorbeeld in kraakbeen. Het celtype dat perlecan maakt, beïnvloedt waarschijnlijk de structuur van de suikerketens. Door verschillen in suikeraanhechting zou perlecan in het ene weefsel andere functies uit kunnen oefenen dan in het andere.

Vervolgens werd de mogelijke functie van domein II van perlecan onderzocht. Hieruit bleek dat perlecan mogelijk een rol speelt bij de binding van lipoproteïnen (hoofdstuk 3). De perlecanfragmenten gemaakt door bacterie- en gistcellen, die niet voorzien waren van suikerketens, bleken in staat te zijn om lipoproteïnen te binden. Het door insectencellen gemaakte perlecanfragment vertoonde deze activiteit niet. De binding van lipoproteïnen aan perlecan is dus mogelijk, en deze functie wordt beïnvloed door de aanwezigheid van de suikerketens. Indien deze wisselwerking ook in het lichaam plaatsvindt, is dit vooral van betekenis voor de binding van lipoproteïnen in de bloedvaten.

Behalve voor bovenstaande studies werd een perlecanfragment ook gebruikt om een nieuwe antistof, genaamd 95J10, te maken dat het menselijke perlecan herkent. Door de manier waarop 95J10 opgewekt is, staat onomstotelijk vast dat deze antistof perlecan herkent. Dit maakte het mogelijk om te achterhalen op welke plaatsen van de nier perlecan precies aanwezig is. Verassend genoeg bleek de GBM slechts zeer weinig perlecan te bevatten, en in grote delen ervan is het zelfs geheel afwezig. Dit betekent dat perlecan niet verantwoordelijk kan zijn voor het regelen van de doorlaatbaarheid van de GBM; het kan hoogstens een kleine bijdrage leveren. Gezien de grote hoeveelheid HSPG's moet er dus nog een tweede HSPG in de GBM bestaan (hoofdstuk 4).

AGRINE: EEN BELANGRIJK HSPG IN DE GBM

Op grond van bovenstaande resultaten werd een zoektocht gestart naar de identiteit van een tweede HSPG in de GBM. Hierbij dienden het opgezuiverde HSPG uit de GBM en de ertegen opgewekte antilichamen als een belangrijk hulpmiddel. De zoektocht eindigde bij agrine. Agrine stond al geruime tijd bekend als een onderdeel van basaalmembranen, in het bijzonder op de plaats waar zenuwuiteinden in contact staan met de skeletspiercellen (de neuromusculaire overgang). Onlangs werd ontdekt dat agrine heparansulfaatketens draagt en dus een HSPG is. Naar aanleiding hiervan werd onderzocht of agrine toevallig ook voorkomt in de basaalmembranen van de nier. Het bleek sterk vertegenwoordigd in de GBM, gelijkmatig verdeeld over de volle breedte en lengte. Het totaal aantal agrinemoleculen was vele malen groter dan het aantal perlecanmoleculen. Deze bevindingen wijzen op een mogelijk zeer belangrijke rol van agrine in de selectieve doorlaatbaarheid van de GBM (hoofdstuk 5).

Daarom werd de structuur van het erfelijke materiaal (het cDNA), dat de code van het menselijke agrine draagt, vervolgens ontrafeld (hoofdstuk 6). Dit levert meer inzicht op in de structuur van menselijk agrine. Zo bleek dat menselijk agrine een eiwit met een massa van 212 kilodalton bevat, waaraan tenminste twee heparansulfaatketens kunnen worden gehecht. De beschikbaarheid van het cDNA biedt nieuwe mogelijkheden voor onderzoek. Een van deze mogelijkheden is het meten van de activiteit van het agrinegen, transcriptie genaamd. Van de 44 geteste weefsels werd duidelijk de hoogste transcriptie gemeten in de nieren en de longen. De hoge transcriptieniveaus kwamen inderdaad overeen met de ophoping van agrine in deze weefsels.

Om onomstotelijk te bewijzen dat het HSPG uit de GBM echt identiek is aan agrine, werd getoetst of de tegen GBM HSPG opgewekte antilichamen het zuivere agrinemolecuul herkennen. Dit gebeurde door recombinant-DNA-technologie. Fragmenten van het DNA dat codeert voor agrine werden overgebracht naar bacteriën, zodat stukken van het agrinemolecuul konden worden geproduceerd, geogst en gezuiverd. De antilichamen vertoonden een sterke reactie met delen van het agrinemolecuul. Het ene antilichaam

herkende een andere plek op het molecuul dan het andere antilichaam. Zo'n herkenningsplaats heet een epitoom. Van 25 antilichamen werd zo het epitoom gelocaliseerd (hoofdstuk 7). Agrine is dus aanwezig in de GBM. Maar hoe komt het er terecht en hoe blijft het er? De GBM wordt op de meeste plaatsen geflankeerd door twee soorten cellen: endotheelcellen en podocyten. Beide celtypen werden afzonderlijk van elkaar gekweekt en getest op agrine-productie. Agrine bleek uitsluitend door de podocyten te worden gemaakt. Waarschijnlijk is dat in de nier ook het geval. Vervolgens wordt agrine in de GBM verankerd via laminine, een integraal onderdeel van de basaalmembraan. Dit lijkt veel op wat er gebeurt bij de neuromusculaire overgang; ook daar hecht agrine zich aan laminine.

NIEUWE INZICHTEN IN HET ONTSTAAN VAN NIERZIEKTEN

De nieuwe inzichten in de HSPG-samenstelling van de GBM suggereren dat perlecan waarschijnlijk geen belangrijke rol speelt bij het ontstaan van een eiwitlek. Een betere kandidaat is agrine. Bij nierafwijkingen die bij sommige diabetici ontstaan, is eerder aangetoond dat de hoeveelheid HSPG in de GBM afneemt. De bij dat onderzoek gebruikte antistoffen blijken nu het agrinemolecuul te herkennen. Agrine is dus waarschijnlijk betrokken bij veranderingen in de GBM die plaatsvinden tijdens het ontstaan van diabetische nierziekte.

In andere nierziekten (bijvoorbeeld "minimale lesies") blijft het agrine-eiwit onveranderd aanwezig in de GBM, terwijl de hoeveelheid heparansulfaat wél afneemt. In deze gevallen spelen mogelijk enzymen die betrokken zijn bij de opbouw, modificatie en afbraak van heparansulfaat een rol.

Naast het regelen van de doorlaatbaarheid van de GBM vervullen HSPG's nog meer belangrijke functies. Zo binden ze aan het celoppervlak en activeren ze groeifactoren als basische fibroblast-groeifactor (bFGF). Podocyten reageren op bFGF door te gaan groeien en delen. Bij langdurige blootstelling aan bFGF raken ze beschadigd, wat een nierziekte oplevert. Het ziektebeeld lijkt veel op een ziekte met de naam "focale segmentale glomerulosclerose" (FSGS), waarvan de precieze oorzaak onbekend is. Om te kijken of deze ziekte door hetzelfde mechanisme ontstaat, werden de concentraties van bFGF in urine en bloed van patiënten met FSGS gemeten. Patiënten met een ernstige vorm van FSGS produceerden urine met verhoogde concentraties bFGF. Controlepersonen en patiënten met een milde vorm van FSGS hadden normale waarden. Deze bevindingen suggereren een mogelijke rol van bFGF bij de ontwikkeling van deze ziekte (hoofdstuk 8).

CONCLUSIES UIT DIT ONDERZOEK

De resultaten van dit onderzoek leiden tot onder andere de volgende conclusies:

- Domein I van het menselijke perlecan kan naast heparansulfaat ook chondroitinesulfaat dragen (hoofdstuk 2).
- Het eiwitdeel van perlecan kan lipoproteïnen binden (hoofdstuk 3). Dit gebeurt via het gedeelte dat domein I en II bevat. Deze activiteit wordt beïnvloedt door de aanwezigheid en samenstelling van de suikerketens (hoofdstuk 3).
- Er komen ten minste twee verschillende HSPG's voor in de GBM: agrine en perlecan (hoofdstuk 4 en 5).
- De hoeveelheid perlecan in de GBM is slechts zeer beperkt (hoofdstuk 4).
- Agrine is een belangrijk HSPG van de GBM (hoofdstuk 5). Van alle geteste weefsels komt het meeste agrine-mRNA voor in de volwassen nier en long (hoofdstuk 6).

- Het menselijke agrine-eiwit heeft een massa van 212 kilodalton en ondersteunt de aanhechting van heparansulfaat door de aanwezigheid van een zgn. SEA-module en geschikte aanhechtingsplaatsen voor suikerketens (hoofdstuk 6).
- Het menselijke agrine wordt gemaakt door podocyten en kan zich via laminine aan de GBM vasthechten (hoofdstuk 7).
- Agrine remt de activiteit van trypsine, plasmine en elastase (hoofdstuk 7).
- De afgenomen HSPG-concentratie in de GBM, die eerder werd waargenomen bij diabetische nierziekte, is (deels of geheel) te verklaren door een afname van agrine-concentratie (hoofdstuk 7).
- De invloed van bFGF op podocyten zou in de mens betrokken kunnen zijn bij de ontwikkeling van FSGS (hoofdstuk 8).

BEKNOPTE AANWIJZINGEN VOOR TOEKOMSTIG ONDERZOEK

De resultaten van dit onderzoek bieden meer inzicht in de functies van HSPGs en de samenstelling van de GBM. Agrine speelt waarschijnlijk een grotere rol in het bepalen van de ladingsafhankelijke doorlaatbaarheid van de GBM dan perlecan. Het is daarom belangrijk om te onderzoeken of er een verband is tussen veranderingen in de agrineproductie en de ontwikkeling van verschillende nierziekten waarbij een eiwittekort optreedt, zoals de diabetische nierziekte. Zulke veranderingen zouden zowel in de suikerketens als in het eiwitdeel plaats kunnen vinden.

In verband hiermee is het relevant om te onderzoeken hoe de productie van agrine wordt beïnvloed door fysiologische parameters. Aangezien agrine alleen lijkt te worden geproduceerd door gedifferentieerde podocyten, is de opheldering van mechanismen die dedifferentiatie van de podocyt bewerkstelligen zeer interessant. Nieuwe methoden voor het kweken van podocyten onder gedifferentieerde en gedifferentieerde omstandigheden bieden veelbelovende mogelijkheden om zulke vraagstellingen te onderzoeken.

Of de heparansulfaatketens van agrine onmisbaar zijn voor het reguleren van de doorlaatbaarheid van de GBM, kan worden beoordeeld door het gericht aanbrengen van mutaties in zogenaamde transgene muizen. Het is nog niet bewezen welke aanhechtingsplaatsen voor suikerketens ook daadwerkelijk benut worden in het menselijke agrine. Om dit te onderzoeken kunnen naast het toepassen van gerichte mutaties elektronenmicroscopische technieken worden gebruikt. Ook rijst de vraag hoe de agrineproductie verandert tijdens de ontwikkeling van de nier in het embryo en na de geboorte.

Om meer inzicht te werven in de functies van agrine in de GBM is het belangrijk om te weten met welke moleculen het een wisselwerking heeft. Bekende voorbeelden zijn α -dystroglycan, integrine en laminine. Het zou interessant zijn om te weten welke effecten de binding van agrine met het celoppervlak teweegbrengt.

Tenslotte is het niet uitgesloten dat de GBM, naast agrine en perlecan, nog andere HSPG-soorten bevat. Er bestaan aanwijzingen voor het bestaan van zo'n HSPG, dat een eiwitdeel van 22 kDa zou bevatten. De identiteit van dit molecuul en de mogelijke rol ervan in het functioneren van de nier verdient zeker de aandacht.

List of original papers

Groffen AJA, Buskens CAF, Tryggvason K, Veerkamp JH, Monnens LAH and Van den Heuvel LPWJ (1996) Expression and characterization of human perlecan domains I and II synthesized by baculovirus-infected insect cells. *Eur. J. Biochem.* 241:827-834.

Groffen AJA, Hop FWH, Tryggvason K, Dijkman H, Assmann KJM, Veerkamp JH, Monnens LAH and Van den Heuvel LPWJ (1997) Evidence for the existence of multiple heparan sulfate proteoglycans in the human glomerular basement membrane and mesangial matrix. *Eur. J. Biochem.* 247:175-182.

Groffen AJ, Ruegg MA, Dijkman H, Van de Velden TJ, Buskens CA, Van den Born, J, Assmann KJ, Monnens LAH, Veerkamp JH and Van den Heuvel LP (1998) Agrin is a major heparan sulfate proteoglycan in the human glomerular basement membrane. *J. Histochem. Cytochem.* 46:19-27.

Groffen AJA, Buskens CAF, Van Kuppevelt TH, Veerkamp JH, Monnens LAH and Van den Heuvel LPWJ (1998) Primary structure and high expression of human agrin in basement membranes of adult lung and kidney. *Eur. J. Biochem.*, 254:123-128.

Raats CJI, Bakker MAH, Hoch W, Groffen AJA, Van den Heuvel LPWJ, Berden JHM and Van den Born J (1998) Differential agrin expression in renal basement membranes revealed by domain-specific monoclonal antibodies. *J. Biol. Chem.* 273: 17832-17845.

Groffen AJA, Veerkamp JH, Monnens LAH and Van den Heuvel LPWJ (1999) Recent insights in the structure and functions of heparan sulfate proteoglycans in the human glomerular basement membrane. *Nephrol. Dial. Transplant.* (in press).

Groffen AJA, Buskens CAF, Demacker PNM, Veerkamp JH, Monnens LAH and Van den Heuvel LPWJ (in preparation) Lipoprotein binding by the core protein of human perlecan.

Groffen AJA, Yard B, Van den Born J, Berden JHM, Van der Woude F, Eigenhuijsen J, Buskens CAF, Veerkamp JH, Monnens LAH, Van den Heuvel LPWJ (1999) Functional analysis of human renal agrin. *J. Biol. Chem.* (in press).

Groffen AJA, Monnens LAH, Oude Nijhuis C, Dijkman H, Veerkamp JH and Van den Heuvel LPWJ (submitted) Urinary excretion of basic fibroblast growth factor by nephrotic children with focal segmental glomerulosclerosis. Submitted for publication in *Nephrol. Dial. Transplant.*

Curriculum vitae

Op 14 maart 1970 ben ik geboren te Zevenaar. Het grootste deel van mijn jeugd bracht ik echter in Waalwijk door, waar ik ook het basisonderwijs heb gevolgd. In 1988 behaalde ik het VWO-examen aan het Willem van Oranje College te Waalwijk. In hetzelfde jaar begon ik met de studie moleculaire wetenschappen aan de Landbouwniversiteit te Wageningen. Deze studie voltooide ik met drie praktijkperioden van elk 6–7 maanden. Het eerste afstudeervak (bacteriële genetica aan de vakgroep Microbiologie te Wageningen) werd begeleid door dr. J. Nölling en prof. W.M. de Vos. Vervolgens werkte ik op de vakgroep Virologie te Wageningen onder begeleiding van dr. J. Martens en prof. R.W. Goldbach. Als derde liep ik een stage op de afdeling Getherapie (tegenwoordig IntroGene B.V.) van het TNO te Rijswijk onder supervisie van dr. J.J. Boesen en prof. D. Valerio. In januari 1994 studeerde ik af.

Van 1994 tot 1998 werkte ik als assistent in opleiding aan het laboratorium Kindergeneeskunde aan de Faculteit der Medische Wetenschappen van de Katholieke Universiteit te Nijmegen onder directe begeleiding van dr. L.P.W.J. van den Heuvel. De resultaten van het promotie-onderzoek vormen de inhoud van dit proefschrift. De beginfase van dit onderzoek bracht ik van maart tot december 1994 door in het laboratorium van prof. K. Tryggvason te Oulu, Finland.

Vanaf januari 1999 ben ik als postdoc-onderzoeker werkzaam op de afdeling Cellulaire en Moleculaire Neurobiologie van het Rudolf Magnus Instituut aan de [Universiteit van Utrecht](#).

Dankwoord

Aan de totstandkoming van dit proefschrift hebben veel mensen een bijdrage geleverd, zowel op het werk als daarbuiten. Ook al is de onderstaande lijst verre van volledig, toch wil ik graag enkele personen met name bedanken.

Bert, als begeleider heb jij me veel geleerd. Het klikte al vanaf het begin goed tussen ons, en bij het bediscussiëren van te volgen strategieën zaten we nagenoeg altijd op dezelfde golflengte. Ik beschouwde onze band dan ook meer als een vriendschappelijke dan zakelijke relatie. Prof. Monnens en Prof. Veerkamp, ook u wil ik graag bedanken voor uw belangrijke bijdrage aan de inhoud van dit onderzoeksproject. Niet alleen uw ervaring en kennis van zaken, maar ook uw enthousiaste belangstelling voor de voortgang van dit project heeft mij zeer gemotiveerd.

Prof. Tryggvason, I am very grateful for the opportunity to work in your department during the first nine months of this research project. Your excellent group formed a unique environment to achieve a good start of the research and become familiar with extracellular matrix biology at the same time. Of this group, I would like to direct my gratitude especially (but not exclusively) to Antti Iivanainen, Ulrich Bergmann, Xu Zhang, Ari Tuuttila and Helena Vornanen, whose valuable support extended beyond the lab.

Carin Buskens, jouw betrokkenheid bij het onderzoek was goud waard. Je zorgvuldige en zelfstandige manier van werken vormt een belangrijk ingrediënt van dit proefschrift. Bij deze wil ik je hiervoor nog eens bedanken. Henri Dijkman, ook jouw werk is duidelijk terug te vinden in dit boekje. Je bedrevenheid in immunofluorescentie- en electronenmicroscopie is de kwaliteit van dit proefschrift ten goede gekomen. Ook gaat mijn dank uit naar Thea en Elly, die me bij tijd en wijlen hebben bijgestaan. Petra en Maroeska, wanneer er weer glomeruli gezeefd of endotheelcellen gekweekt moesten worden waren jullie altijd behulpzaam. Bedankt.

Alle collega's van het "DNA-lab" ben ik dankbaar voor de altijd prettige sfeer. Ik noem alleen Henk, Henny, Iwan, Jan, Léonard, Maarten, Marjan, Nathalie, Ralf, Roel, Sandra en Sandy. Maria en Frans, ook jullie wil ik bedanken voor jullie steun. Erik, Hanneke en Richard, als er nog eens ijs ligt gaan we zeker weer een tocht schaatsen. Markus, I greatly appreciated our many social talks that lightened work even in the small hours. Ook de "spiergroep" (met name Anton, Diana, Wim, Marloes, Liesbeth, Christine en Ans) wil ik graag bedanken voor de fijne samenwerking, evenals de collega's van de afdeling Antropogenetica (Willy, Manno, Joop, Frans en vele anderen).

De samenwerking met de afdelingen Biochemie, Nefrologie, Reumatologie, Pathologie en Algemene Interne Geneeskunde droeg bij aan de goede infrastructuur waarin dit onderzoek kon plaatsvinden. Toin van Kuppevelt en alle anderen van de afdeling Biochemie ben ik zeer dankbaar voor de fijne samenwerking, en de mogelijkheid om jullie werkbesprekingen bij te wonen. Van de afdeling Nefrologie dank ik onder anderen Prof. Berden, Jaap van den Born, Ilse Raats en Marinka Bakker voor de intensieve samenwerking, en voor de grote hoeveelheid interesse die jullie voor het onderzoek toonden. Tijdens de "proteoglycanen-werkbesprekingen" namen jullie deel aan talrijke waardevolle discussies. Dit geldt ook voor Prof. van den Berg en Peter van de Kraan van de afdeling Reumatologie. Prof. Assmann, behalve als lid van de manuscriptcommissie was u ook behulpzaam bij het interpreteren en beschrijven van weefsel distributies, waarvoor ik u bij deze gelegenheid wil bedanken. Pierre Demacker, je talrijke nuttige aanwijzingen maakten het mogelijk om lipoproteïnen in deze studie te betrekken. De manier waarop je over het onderzoek meedacht waardeer ik bijzonder, alsmede je snelle en grondige correcties.

Niet minder belangrijk was de inzet van de studenten die ieder hun aandeel aan dit werk hebben geleverd: Karin, Frank, Jochem en Claudi. Jullie toewijding en enthousiasme leverden naast goede resultaten ook een boel gezelligheid op.

Prof. Nurcombe and Sharon Joseph, thank you very much for your help and hospitality. Although the obtained results are not included in this thesis, they certainly contributed to the final result. Prof. Ruegg and Alain Denzer, thank you for your support which was both fruitful and pleasurable. I sincerely hope that our collaboration will be sustained in the future. Ook Prof. Van der Woude en Benito Yard wil ik danken voor de geboden gastvrijheid en medewerking tijdens de eindfase van dit onderzoek.

Alvorens dit proefschrift af te sluiten wil ik mijn ouders bedanken voor hun onvoorwaardelijke steun en interesse. En tenslotte dank ik jou, Jolanda: je hebt me als geen ander duidelijk gemaakt dat het leven meer biedt dan alleen agrine en perlecan.